Ministry of Higher Education and Science
University of Babylon
College of Science
Department of Applied Geology

Petrophysical and Stratigraphic Analysis of Mishrif Formation in Eridu Oilfield, Southern Iraq

Submitted to the College of Science
University of Babylon
in partial fulfillment of the
Requirements for the degree
of Master in Science in Geology

By
Shahad Laith Abbas Saeed
B.Sc. Applied Geology, University of Babylon
2020

Supervised by

Prof.Dr. Amer Atyah Alkhalidy **Prof.Dr. Hamid Ali Alsultan**

2023 A.D **1444A.H**

بِسْمِ اللَّهِ الرَّحْمَنِ الرَّحِيمِ

نٓ وَالْقَلَمِ وَمَا يَسْطُرُونَ (١) مَا أَنتَ بِنِعْمَةِ رَبِّكَ

بِمَجْنُونٍ (٢) وَإِنَّ لَكَ لَأَجْرًا غَيْرَ مَمْنُونٍ (٣) وَإِنَّكَ

لَعَلَى خُلُقٍ عَظِيمٍ (٤) فَسَتُبْصِرُ وَيُبْصِرُونَ (٥) بِأَيِّكُمُ

الْمَفْتُونُ (٦) إِنَّ رَبَّكَ هُوَ أَعْلَمُ بِمَن ضَلَّ عَن

سَبِيلِهِ وَهُوَ أَعْلَمُ بِالْمُهْتَدِينَ (٧)

صدق الله العظيم

سورة القلم الآية من ١ الى ٧

SUPERVISORS CERTIFICATION

We certified that this thesis **(Petrophysical and Stratigraphic Analysis of Mishrif Formation in Eridu Oilfield, Southern Iraq)** had been prepared under my supervision, in the Department of Applied Geology, College of Science – University of Babylon in partial Fulfillment of the Requirements for the degree of Master in Geology.

Signature:

Name: Amer Atyah Alkhalidy

Title: Professor.

Address: Department of Applied Geology- College of Science –University of Babylon.

Date: / /2023

Signature:

Name: Hamid Ali Ahmed Alsultan

Title: Professor.

Address: Department of Applied Geology- College of Science –University of Babylon.

Date: / /2023

APPROVED BY THE HEAD OF DEPARTMENT OF APPLIED GEOLOGY

In view of the available recommendation, I forward this thesis for debate by examining committee.

Signature:

Name: Mohanad Rasim Al-Owaidi

Title: Assist Professor.

Address: Head of Department of Applied Geology / College of Science – University of Babylon.

Date: / / 2023

Certification of the Examining Committee

We certified that this thesis **" Petrophysical and Stratigraphic Analysis of Mishrif Formation in Eridu Oilfield, Southern Iraq "** and has examined the student (**Shahad Laith Abbas Saeed**) in its content and that, were prepared under our supervision at College of science as partial fulfillment for the degree of Master in Geology.

Signature

Title: Professor

Dr. Amer Jassim Salman

College of Science/University of Babylon

Data: / / 2023

(Chairman)

Signature

Title: Professor

Dr. Maher Mandeel Mahdi

College of Science/University of Basrah

Data: / / 2023

(Member)

Signature

Title: Assist Professor

Dr. Mohanad Rasim Al-Owaidi

College of Science/University of Babylon

Data: / / 2023

(Member)

Signature

Title: Professor

Dr. Amer Atyah Alkhalidy

College of Science/University of Babylon

Data: / / 2023

(Supervisor)

Signature

Title: Professor

Dr. Hamid Ali Alsultan

College of Science/University of Babylon

Data: / / 2023

(Supervisor)

Signature/

Professor Dr. Mohammed Hadi Shinen Alshammeri

Dean

College of Science / University of Babylon

Dedication

بسم الله الرحمن الرحيم
(قل اعملوا فسيرى الله عملكم ورسوله والمؤمنون)
صدق الله العظيم

إلى من كلله الله بالهيبة والوقار.. إلى من علمني العطاء بدون انتظار.. إلى من أحمل أسمه بكل افتخار..

(والدي العزيز)

الى بسمة الحياة وسر الوجود إلى من كان دعائها سر نجاحي وحنانها بلسم جراح..

(امي الغالية)

إلى صاحبة القلب الطيب والنوايا الصادقة

(اختي الحبيبة)

كما أهدي ثمرة جهدي لأستاذي الكريمين **الدكتور: عامر عطية الخالدي والدكتور حامد علي السلطان** اللذين كلما تظلمت الطريق أمامي لجأت إليهما فأناروه لي وكلما دب اليأس في نفسي زرعوا فيا الأمل لأسير قدما وكلما سألت عن معرفة زودوني بها وكلما طلبت كمية من وقتهم الثمين وفروه لي بالرغم من مسؤولياتهم المتعددة.

إلى كل أساتذة قسم علم الأرض التطبيقي؛

وإلى كل من يؤمن بأن بذور نجاح التغيير هي في ذواتنا وفي أنفسنا قبل أن تكون في

أشياء أخرى...

ولا انسا الأصدقاء...إلى من تحلو بالإخاء وتميزوا بالوفاء والعطاء إلى ينابيع الصدق الصافي إلى من معهم سعدت، وبرفقتهم في دروب الحياة الحلوة والحزينة سرت إلى من كانوا معي على طريق النجاح والخير إلى من عرفت كيف أجدهم وعلموني ألا أضيعهم

(أصدقائي وصديقاتي الأعزاء)

shahad

Acknowledgements

Firstly, I would like thanks, to "God" and to Our Messenger "peace and blessing be upon him" and Ahl al-Bayt "peace be upon them" for helped me to fulfill this study.

Thanks, to the Department of Geology at College of Science/Babylon University through the aid and provided a scientific reference that were used to supported this study. I am grateful to my supervisor***, Prof. Dr. Amer Atyah Alkhalidy and Prof. Dr. Hamid Ali Alsultan,*** who has been very supportive for me through providing comments, constructive.

I would also like to express my gratitude to ***Prof. Dr. Hasan Majdi***, chancellor of the AL-Mustaqbal University College, for his continuous support of my academic career. All thanks and gratitude to his Excellency.

I would like thanks to the Ministry of oil represented by the Dhi-Qar oil company, especially ***Mr. Mohammed Ismai and Mr. Firas kerem adail***. I would like thanks to the Ministry of oil especially ***Dr. Ali Duair Al-Musaw***. I want to thanks oil Exploration Company Especially ***Mr. Abdulsalam Mohammed***

shahad

Abstract

Six oil wells were selected in this study, which included Mishrif Formation in the Eridu oilfield (Late Cenomanian - Early Turonian) in southern Iraq, which is considered one of the main reservoirs in the field to study the microfacies, the modal processes affecting them, the sedimentary environments, the different types of porosity, and the evaluation of petrophysical properties.

Six major microfacies were diagnosed the Mishrif Formation, these are Mudstone, Wackestone, Packstone, Grainstone, Boundstone, and Rudstone and twelve submicrofacies include: Bioclastic Packstone submicrofacies with rich Echinodermat, Coral and Rudist fragment and high Dolomitization, Rudstone submicrofacies with large Rudist fragment and vug porosity , Boundstone submicrofacies with very large coral, Plankton Foraminiferal Packstone submicrofacies with *Globigerinelloides* and Calcispheres, Bioclastic Wackestone to Packstone submicrofacies with dolomite and calcareous algae, Peloidal Packstone with coral, pillites, pieces of Rudist and Separate-Vug pore, Bioclastic Packstone to Grainstone submicrofacies, Peloidal to Bioclastic Packstone submicrofacies, Benthonic Foraminiferal Mudstone submicrofacies, Rudist fragmented Mudstone. These microfacies were deposited in restricted, shoal, shallow open marine, rudist Biostrum, and deep marine environments.

The petrophysical characteristics of the formation (shale volume, porosity of all kinds and water saturation) were calculated and studied using the (Tichloge ve.15) program using the available logs such as (gamma ray, density, neutron, self-potential, sonic, caliber and resistance). Mishrif Formation into four units from top to bottom (CR-I, MA, CR-II and MB), where the reservoir units have high porous in most wells separated by hard rocks with little

porosity. As for water saturation, its percentage was high in hard rocks, the percentage of residual and mobile hydrocarbons were high in the MB unit and for some wells only, and were low in the MA unit.

In this study, structural maps were drawn and a three-dimensional geological model was built for the distribution of petrophysical properties, which included total porosity, effective porosity, and water saturation, as well as the distribution of facies for the Mishrif formation. In the trend wells (ER-1,4 and7) where the facies specifications improve and the oil saturation is high in these wells compared to the other wells of the study.

At the end of the study, a stratigraphic analysis was carried out in the light of the sedimentary environments that were distinguished by knowing the microfacies of the wells that contain a core, where five sedimentary cycles were distinguished (A, B, C, D. E) and two main surfaces boundary were identified (SB1, SB2) based on the association behaviors of the facies within the boundaries of the sequence layers and paths (HST and TST)

List of Contents

List of Figures

List of Tables

plates

NOMNCLATURE

ER-1	**Eridu Well-1**
ER-2	**Eridu Well-2**
ER-3	**Eridu Well-3**
ER-4	**Eridu Well-4**
ER-6	**Eridu Well-6**
ER-7	**Eridu Well-7**
Fig	**Figure**
m	**Meter**
CPI	**Computer Processing Interpretation**
NE	**North-East**
SW	**South-West**
SMF	**Standard Microfacies**
AP	**Arabian Plate**
SP	**Self-potential log**
GR	**Gamma ray log**
PHIE	**Effective porosity**
PHIT	**Total porosity**
SW	**Water saturation**
Sox	**Water saturation of the washed area**
Rt	**Resistivity of uninvaded zone**
Rw	**Resistivity of formation water**
BVW	**Bulk volume of water of uninvaded zone**
BVXO	**Bulk volume of water of flushed zone**
SGR	**Spectral gamma ray**
CR-I	**Cape Rock**
MA	**Upper Mishrif Reservoir**
CR-II	**Cape Rock**
MB	**Mishrif Reservoir**
VSH	**Volume of shale**
SB	**Sequence boundaries**
MFS	**Maximum Flooding surface**
TS	**Transgressive surface**
LST	**Lowstand systems tracts**
TST	**Transgressive systems tract**
HST	**Highstand System Tract**

Chapter One

Introduction

1.1 Preface

The Cretaceous rocks in Iraq and the Middle East represent a distinguished location within the stratigraphic column, so the formations of this period represent rocks with good oil potential, some of them are source rocks that generate hydrocarbons, and others are oil reservoirs.

This study came to complement the previous studies in the Eridu oilfield which is one of the new fields in southern Iraq. The Mishrif Formation is one of the formations of the sedimentary cycle Late Cenomanian–Early Turonian and one of the most important reservoirs in the Mesopotamian Basin in central and southern Iraq (Al-Naqib, 1967).

Many studies had been carried out on all geological aspects of the Mishrif Formation in various fields in southern Iraq, but these deposits are still at an early stage of development in many fields, such as Eridu oilfield.

Nine wells were drilled in the Eridu oilfield by the Russian company (LUKOIL), forming Mishrif, based on the approval obtained from the Ministry of Oil., Eridu-1, was drilled in 2016, and drilling reached the final depth 3168 meters within the Yamama formation, and oil production was established from the reservoirs of the Mishrif and Yamama Formations. In addition to the presence of oil evidence within the formations of Khasib, Shuaiba and Ratawi.

1.2 Aims of the Study

1. Description the stratigraphic and lithological of the Mishrif Formation in the wells studied.
2. Determining the microfacies and sedimentary environments of the Mishrif Formation of wells that contain cores and predicting their extensions in the study area by comparing the facies description and the behavior of the logs (GR and Sonic) for field wells that do not contain cores, and determine digenesis processes that effect on the Mishrif Formation.

3. Calculation of petrophysical parameters by using geophysical well logs in Studying Reservoir Properties of Mishrif Formation.
4. Building a 3D geological model using the Petrel ve.18 program to know the distribution of petrophysical properties and the vertical variation within the formation.
5. Studding the sequence stratigraphic analysis to clarify the effect of local tectonism and eustasy on the development of the succession.

1.3 Study Area

The Eridu oilfield is located in the southern part of Iraq within the administrative borders of Al-Muthanna Governorate, approximately 35 km southeast of Samawah, and 60 km west of Nasiriyah. Surrounding the Eridu field are fields and structures such as the Nasiriyah, Subaa, Luhais, Samawah fields, and structures such as Diwan and Ur.

Together these units represent a single carbonate sequence from the Mid-Cretaceous in the Mesopotamian Basin. The Mishrif Formation is a carbonate formation that extended widely into the Arabian Gulf. The Mishrif Formation in central Iraq reflects the continuous deposition of shallow shelf carbonates during periodic sea level rises, which resulted in deeper downward depositional events (Jassim and Goff, 2006).

1.4 Tectonic and Structural Setting

The Mishrif Formation in Iraq was deposited under the action of tectonic movement and eustasy. The Mishrif Formation corresponds to the Albian-Early Turonian supersequence IV of the Iraqi Cretaceous sequence-stratigraphic framework, the large sequence AP8 deposited on the passive margin of the Arabian plate (Sharland *et al*. ,2001).

Each of these subzones may be identified by structural highs and lows with different trends that were created during the deformation of the northern Tethyan border of the Arabian Plate between the Cenomanian and Early

Turonian (Jassim and Goff, 2006). Negative gravity residuals are found under a number of supergiant oilfield formations, including Zubair, Rumaila, and Nahr Um, indicating that salt diapirism is the source of numerous structures in southern Iraq (Jassim and Goff, 2006; Aqrawi et al., 2010). Early Jurassic time is when some of these structures first started to emerge (Al-Sakini, 1992; Sadooni and Aqrawi, 2000).

The study area is located within the Mesopotamian belt, which is divided into the Zubair, Tigris, and Euphrates tectonic subzones (Buday and Jassim, 1987). Geological evidence for this subdivision, which demonstrates increased subsidence rates, can be found in the thick Mishrif Formation that runs along the Euphrates subzone. During the Cenomanian–Early Turonian deformation of the Arabian Plate's northern Tethyan boundary, structural highs and lows with various trends distinguish each of these subzones (Jassim and Goff, 2006).

The Zagros belt is considered the first zone. This belt, which forms the eastern and northern boundaries of the Mesopotamia Basin, exhibits extensive tectonic deformation as a result of the collision of the Arabian and Iranian plates. The platform that marks the second zone and is where the Eridu oilfield is situated is what defines the Mesopotamia basin from the west (Buday,1980).

The Mesopotamian Foredeep is where the Eridu oil field is located. Located between the stable continental component (Inner Platform) and the western Zagros fold-thrust belt to the northeast, it is the final surviving piece of the Zagros foreland basin that stretches southeast to its marine counterpart, "The Arabian Gulf." It has a lot of submerged structures, including ones that are actively undergoing neotectonic movement. The Mesopotamian Foredeep is divided into the Al-Jazira and Basra subzones in the north and south, respectively, depending on its diverse mobility and activity (Fouad, 2012), figure (1-2).

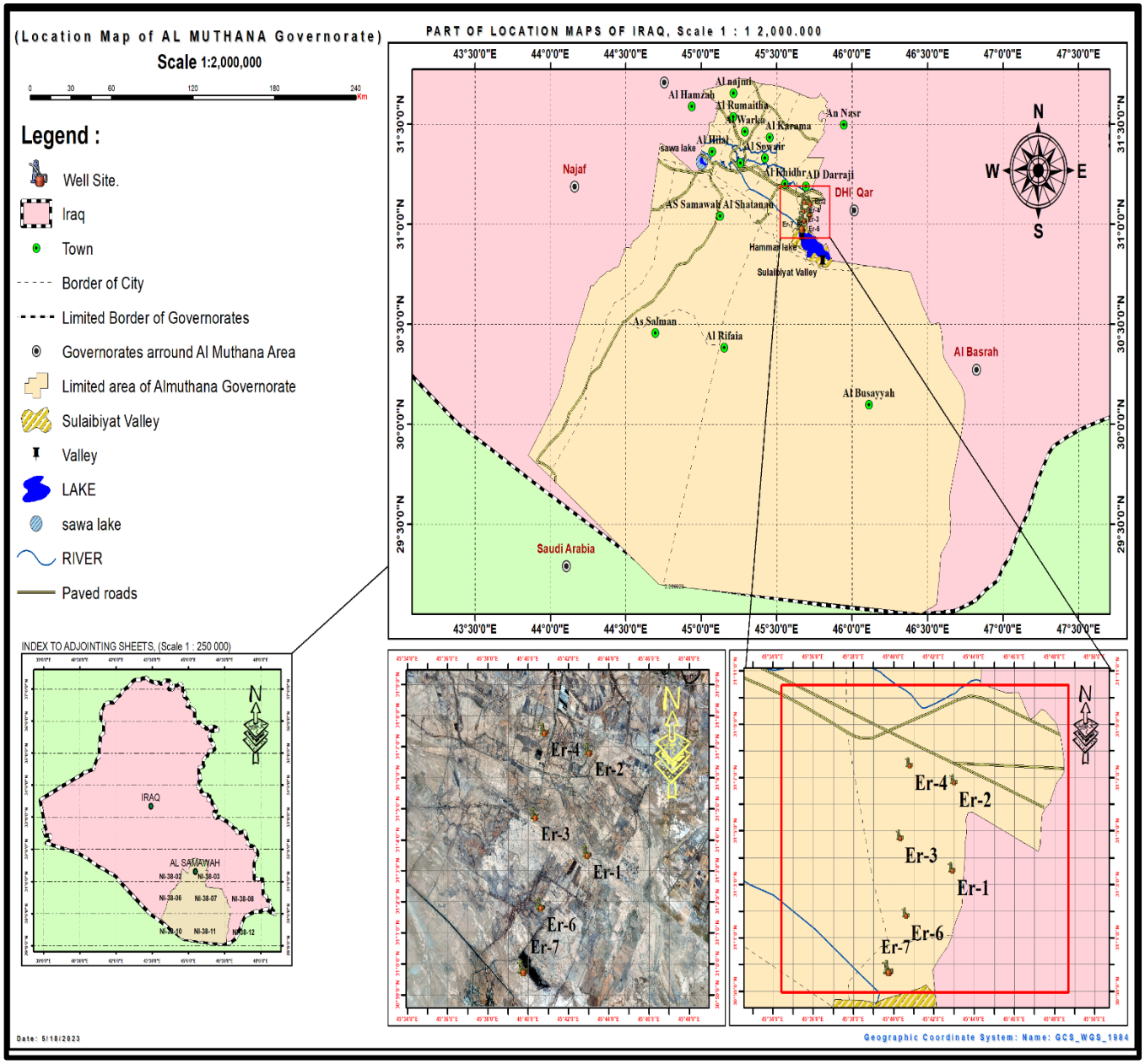

Figure (1-1) Map of the study area showing the Eridu oilfield location.

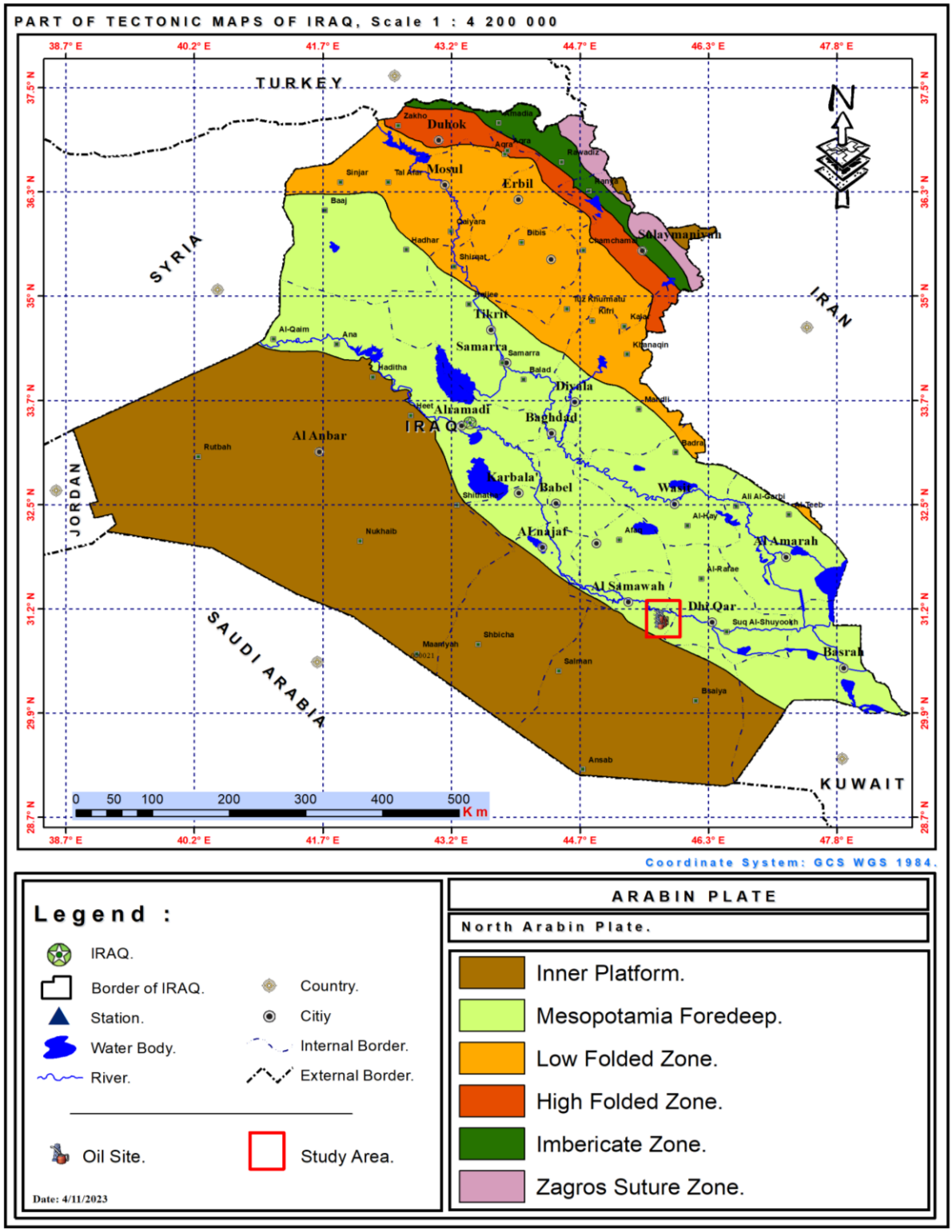

Figure (1-2) Tectonic map of Eridu oil field southern Iraq modified after (Fouad, 2012)

1.5 Stratigraphy of Mishrif Formation

The Mishrif Formation was deposited in the Early Cenomanian cycle, the second depositional cycle of strata previously known as the Middle Cretaceous, in the Mesopotamian Basin and southern and central Iraq. Buday (1980) divided the sequence into two sedimentary cycles. The Cenomanian-Early Turonian cycle begins with the deposition of the Rumaila Formation during the period of marine advance in the cycle and is topped by the deposition of the Rumaila Formation, which consists of limestone and chalky, graduating in turn upwards to the Mishrif Formation during the period of marine decline in the Late Cenomanian- Early Turonian. The gradient, in turn, leads upwards to the Khasib Formation containing high evaporates, which overhangs the Mishrif Formation. Awadees *et al*., (2018) divided the Cenomanian – Early Turonian mega-sequence into seven 4th-order genetic - mega sequences, each containing 5th-order lithofacies cycles.

Where the Mishrif Formation takes its stratigraphic position between the Khasib Formations from above and is bordered by the Rumaila Formation from the bottom, where the contact between them is unconformity, it may sometimes be difficult to distinguish between the rock units of these two formations. It should be noted that the anhydrite facies of the Kifil Formation symmetrically cover the facies of the Mishrif Formation in some wells in southern and central Iraq, which in turn represents the last stage of marine retreat and the end of the sedimentary cycle, (Figure 1-3).

The first to describe the Mishrif Formation is Rabanit (1952) where it is described in the Type section of Zb-3 within the upper part of what was called the Khutiah Formation within (the Wesea Group) which includes the Ahmadi, Rumaila and Mishrif Formations.

The largest significant oil resource in the Mesopotamian Basin is the Mishrif Formation, which is Late Cenomanian in age (van Bellen *et al*., 1959). The AP9/AP8 megasequence boundary is located at the top of the Mishrif Formation truncation (Sharland *et al*., 2001).

Where the Early Turonian period was characterized by a remarkable activity of land movements that led to a marine retreat, which in turn worked on the gathering of Breccia indicating the existence of a surface incompatible between the two formations of Mishrif and the Kifil above it (Ditmar and Iraqi-Soviet Team, 1980) the upper part of the Massad Formation is equivalent to the formation of Mishrif in the Rutba region (Dunning, 1959) and in the northwest of Iraq, it is equivalent to the formation of Gerber and Merge Mir formations (Chattonl and Hart,1961), but in neighboring countries it is equivalent to a group of formations that coincide with it in sedimentation in Iran and the regions of the Arabian Gulf and Syria, as it is equivalent to Magwa Formation in Kuwait (Powers,1968) and Natih Formation in Oman (Scott et al.,1994) and the two formations of Al-Khatia and Rumaila in the north of the Emirates.

The Mishrif facies overlap with the Wasia group in Saudi Arabia and it is in the form of two units, part of which is equivalent to the formation of the Mishrif and is called the lower Mishrif (Powers, 1968) In Iran, the formation is equivalent to the upper part of Sarvak Formation (James and Wynd, 1965). In both Qatar and Bahrain, there is the Mishrif formation, and it is also called the Mishrif formation.

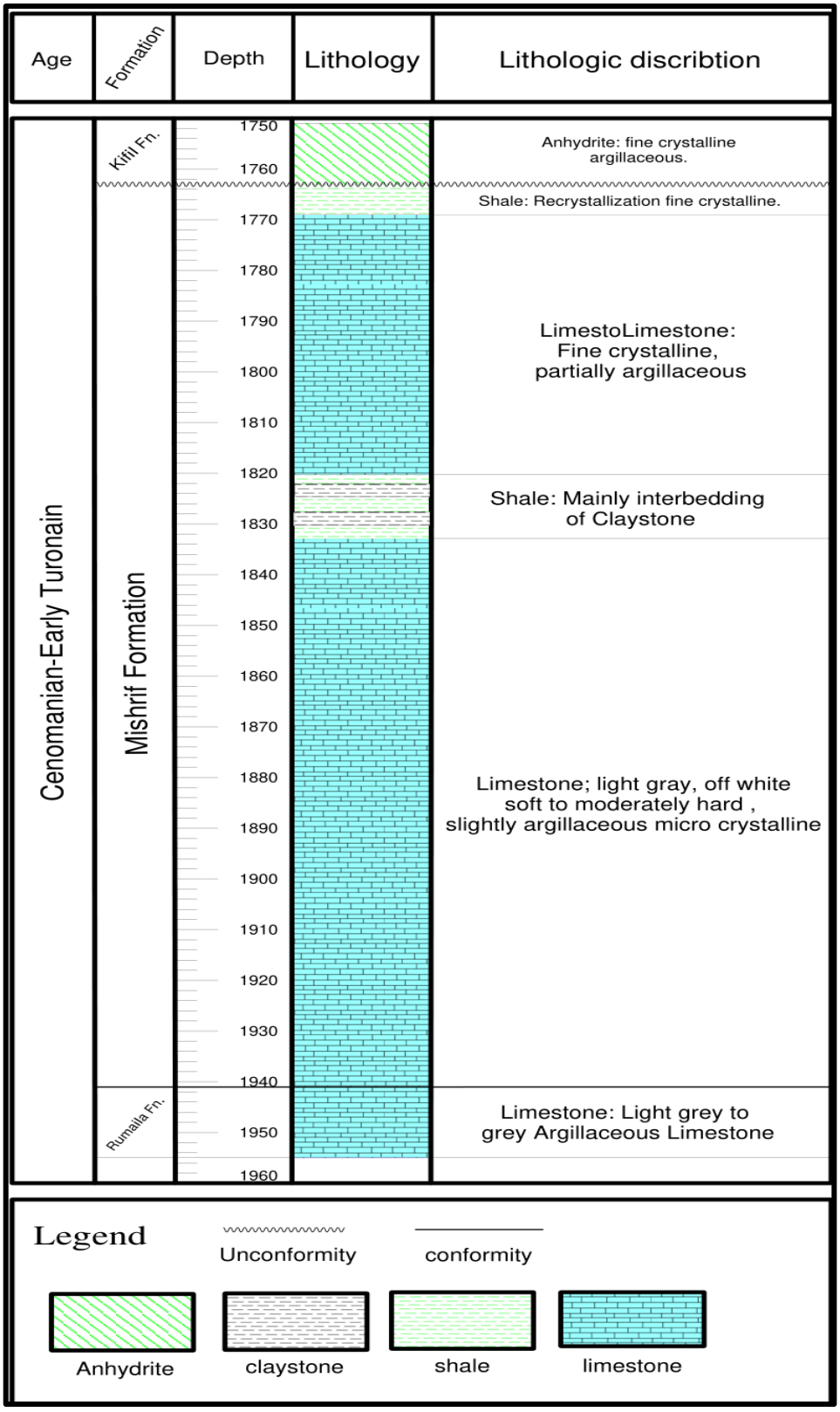

Figure (1-3) Stratigraphic column showing the lithology of Mishrif Formation in ER-4 well.

1.6 Methodology

1.6.1 Field work

Collecting rock samples from the Mishrif Formation under study Oil Wells from the laboratories of the Oil Exploration Company of the Ministry of Oil Figure (1,4).

1.6.2 Laboratory work

123 thin sections were prepared in the rock thin sections workshop at the Department of Applied Geology at the University of Babylon., Figure (1,5). Table (1.1)

1.6.3 Office work

1. It included the collection of preliminary information from the final reports of the wells of the study area, and the wells containing the probes and the probe data required for the study were identified, preparing the information, and analyzing the probes of the open wells of the study wells, which included each of the sensors (Spontaneous potential (SP), Gamma Ray Log , Density Log (RHOB), Neutron log (NHI), Sonic log (DTC) (At Well Measurement Caliper log Electrical Resistance Resistivity micro resistivity logging as well as the use of several programs in petrophysical analysis and chart stratigraphic and rock sections such as Tichloge ve.15 program.
2. Petrophysical measurements and equations used for interpretation Calculation of total and effective porosity and shale volume, interpretation of logging.
3. Using the application of microfacies analysis to interpret the stratigraphic analysis and determine the sedimentary environment of Mishrif Formation.
4. Diagrams were made between the various logs through the Tichloge ve.15 program.
5. For the purpose of creating a 3D geological model for a reservoir, Petrel 2018 software has been used. For the construction of this kind of model,

there are several processes that start with the essential data. These facts include: -

- Well heads: Position of each well in the Eridu oilfield, in particular the northern, eastern, and (RTKB).
- Well tops: measured depth for each well and defined all unites for formation in the Eridu oilfield.
- Well logs: These comprise the reservoir's parameters (PHIT, PHIE, and SW), as well as the CPI value imported into Petrel ve.18 from Tichloge V. 15.
- Mishrif Top and unit structure maps that were scanned in 2015 using the surfer program after being taken from a geological report. The flow work diagram in figure shows the process (4-1).

Figure (1-4) Laboratory work: It consists in preparing the thin sections of the core samples from exportation company

Table (1-1): The heights and thicknesses of the Mishrif Formation in the Eridu oil field according to the global coordinate system (U.T.M. WGS 1984) and number of core available for it

Well. ID	Top(m)	Bottom(m)	Thickness(m)	X(m)	Y(m)	Core simple	cutting simple
ER-1	1695.8	1885	189.2	568188	3436483	42	__
ER-2	1744.5	1898	153.5	568294	3442598	39	__
ER-3	1717.9	1879.5	161.6	564069	3438718	43	__
ER-4	1763	1941	178	573411	3442721	__	20
ER-6	1734.5	1889	154.5	564786	3443762	__	15
ER-7	1649.9	1841.5	191.6	563247	3429508	__	25

Figure (1-5) Laboratory work: It consists in preparing the thin sections of the core samples at university of Babylone

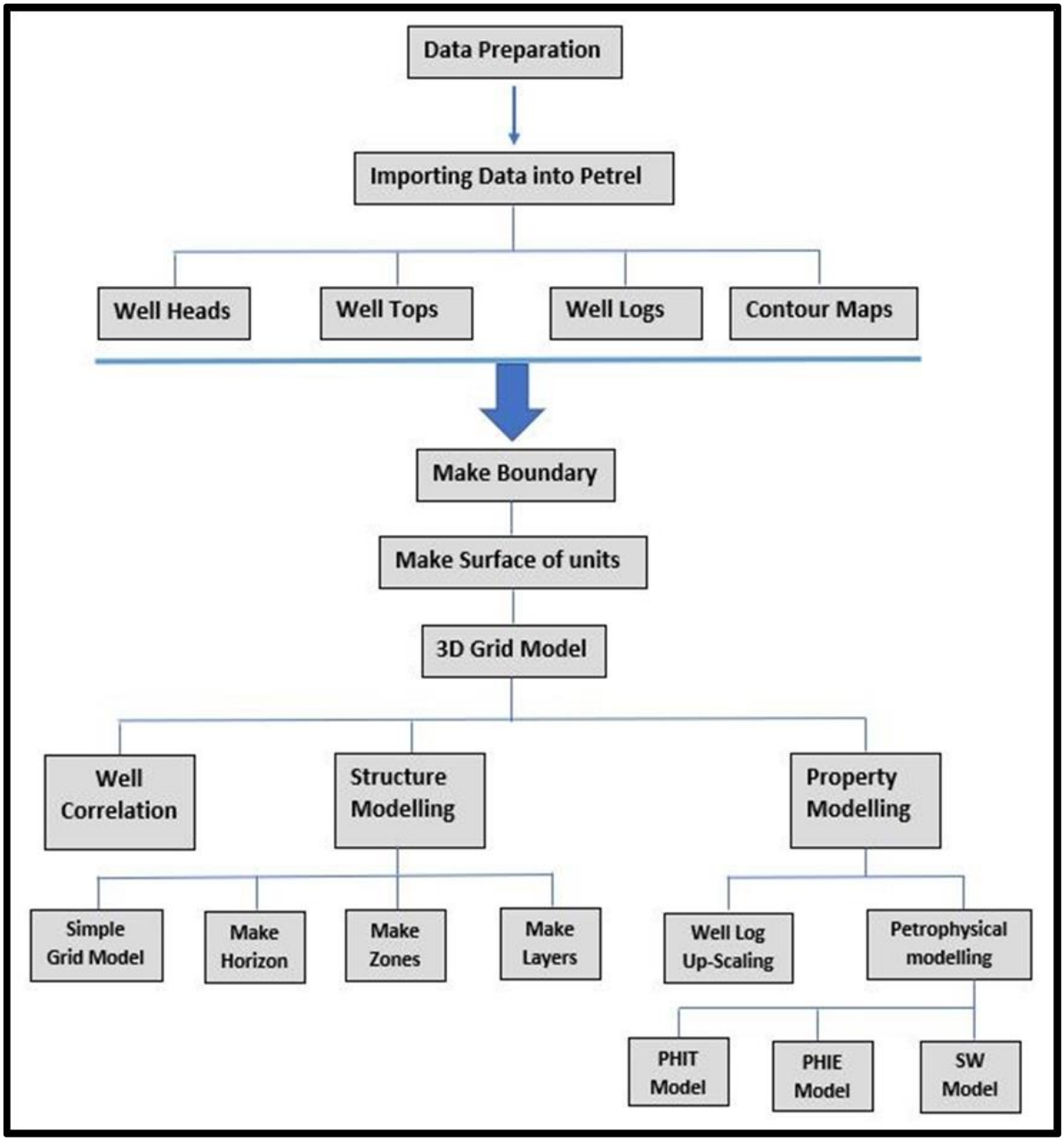

Figure (1-6) 3D geological model work flow diagram

1.8 Previous studies

Smout (1956) and Fox (1957) they used the term "Mishrif" after the study of Rabaint (1952).

Gaddo (1971) Studied the petrography and paleoenvironment of the Mishrif Formation and divided its environment into five environments.

Aqrawi et al. (1998) Discussed the sequence stratigraphy and facies of the Mishrif Formation in Iraq.

Al- Jumaily (2001) Studied the facies and depositional environments of Mishrif Formation in selected oil fields in south of Iraq.

Van Buchem et al. (2002) Used the same outcrops (Adam Foothills) with subsurface data to construct a more detailed model.

Al-Jawad (2005) Studied the Reservoir Properties of the Mishrif Formation in selected wells from North Rumaila and South Rumaila and West Qurna Fields.

Al-Attiyah (2009) conducted a reservoir geological study to form Mishrif Formation in selected wells from southern Iraq.

Al-Baldawi, (2012) studied the characterization of carbonate reservoirs and he built a 3D geological model of Mishrif Formation in six wells of Amara oil field and he made a petrographic and micro facies study.

Jaefar (2012) conducted a study to build a geological model for Mishrif Formation in the Buzurgan field.

Mahdi, et.,al (2013) Sedimentological characterization of the Mid-Cretaceous Mishrif Formation resesrvoir in southern Mesopotamian Basin, Iraq.

Al-Shabender (2014) studied a sequential geoscience workflow (geophysical, petrophysical evaluation, and modeling) of the Cenomanian early –Toronian carbonate succession of Mishrif Formation in Buzurgan oil- field, South-Eastern of Iraq.

Saqer (2014) recognized four main microfacies within Mishrif Formation in Tuba oil field, interpreted the well logs and built the reservoir geological model.

Jaed (2016) the Mishrif Formation in the Gharaf oil field was studyed for reservoir characterisation and a 3D petrophysical modeling.

Al-Mosawy (2014) studied an advanced well logging analysis and reservoir heterogeneity modeling of Mishrif Formation in southeast Missan governorate.

Mohammed *et al*., (2021) reservoir characterization of the Middle Cretaceous Mishrif Formation in the Buzurgan oilfield, Southern Iraq

Al-Maliky (2022) Geological model of Mishrif formation in selected wells of Zubair Oil field in Southern Iraq.

Badr (2022) Reservoir Evaluation and Geological model for Mishrif Formation in Nasiriyah and Eridu Oil-Fields, Southern Iraq.

Al-Mashhdani (2023) Reservoir Evaluation and Geological model for Mishrif Formation in Nasiriyah and Eridu Oil-Fields, Southern Iraq.

Chapter Two

Petrography and Microfacies Analysis

2.1 Introduction:

The succession of the Mishrif Formation was subjected to a facies analysis through the study of microfacies because of its special importance in giving a clear view of the sedimentary environments and diagenetic processes of any calcareous formation. A sedimentary facies is defined as a rocky body with certain lithological characteristics, such as granular size, mineral composition, sedimentary structures, etc., that distinguish it from other facies.

Therefore, the current study tended to study the microfacies under the microscope to show the type of microfacies, the effective transformational processes, and to identify the sedimentary environments and the facies discovered in this study were traced vertically using well logs (Sonic and Gamma ray). The classifications used in this study is the Dunham classification (1962), Wilson (1975), and Flugel (2010), for its ease of application on the facies of the study area and for its usefulness in showing different types of sedimentary texture depending on the clay or granular support. Their characteristic skeletal and non-skeletal grain types in Mishrif Formation. Skeletal grains are one of the most important and widespread constituents of the Mishrif Formation. They consist of whole fossilized organism's foraminifera, bioclasts, or fragments encased in varying degrees of abrasiveness (Booge, 2009).

A large number of thin section were examined by polarizing light microscopy from cores ER-1, ER-2, and 3, where 123 thin section were examined.

2.2 Petrography of carbonate rock

Petrography is the geological description of rocks supported by microscopic examination of thin sections. Detailed studies of diagenetic properties and changes in porosity distribution in thin. Although many carbonate classification

schemes are available (and most are very useful), the scheme used in this study the "Dunham classification system".

(Dunham ,1962) classification of carbonate rocks, as modified by (Embry and Klovan ,1971), is based on sedimentary structure, whether the rocks are supported by a matrix (mud) or a framework (grains). The limestone units of the Mishrif Formation are classified according to this classification (Figure 2-1). The lithofacies composition of the Mishrif Formation is essential in identifying and subdividing the microfacies of these units. They include matrix (micrite) and various skeletal and non-skeletal particles.

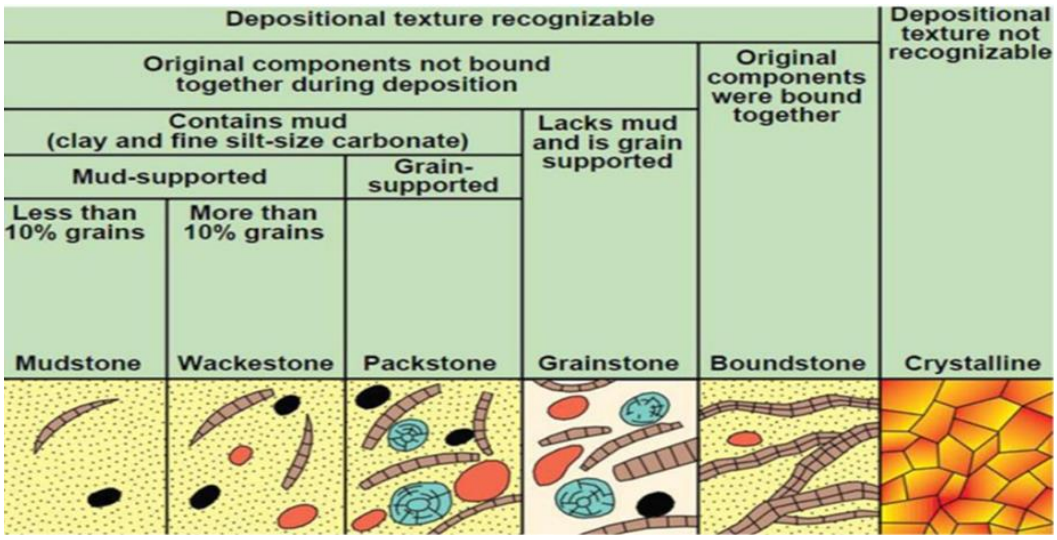

Figure (2-1) Dunham classification (1962).

2.2.1 Skeletal Grains

Skeletal grains are one of the most important and widespread constituents in the Mishrif Formation. They consist of whole fossilized organism's foraminifera, bioclasts, or fragments encased in varying degrees of hardness (Booge, 2009). The most important and widely distributed skeletal particles in the limestone of the Mishrif Formation are rudist, foraminifera and calcareous algae.

2.2.1.1 Rudists

Rudists were common throughout the Cretaceous. Diversity decreased in Early Aptian and Late Cenomanian, and increased significantly in Early Maastrichtian (Flugel, 2004). In recent years, oil and gas scientists have achieved particularly outstanding results in the search for oil and gas, helping to more clearly define the Cretaceous succession and its evolution in various paleogeographical domains. Rudist and their derived bioclasts play an important role as the main fossil constituents of many sedimentary reservoirs found in Cretaceous carbonate rocks (Cestari and sartario, 1995).

Rudist represents an important fossil index and contributes to the construction of the Mishrif strata. It is clearly visible in the ER-1 well. Fragments ranging from small to large were found. (plates 2-2.D and 2-4. C)

2.2.1.2 Foraminifera

Benthic foraminifera are the main constituents of the rocks of the Mishrif Formation and are present in front and back reefs as well as in slope and shoal environments. It frequently occurs with corals, algae, *Textularia* sp., (plats 2-1. D) *Nezzazata* sp., (plats 2-1. A) Milliode. are examples of common benthic foraminifera found in the thin sections analyzed. Planktonic foraminifera were abundant in the upper Mishrif Formation, and they were restricted to specific depths within the formation as the depositional environment deepened such us, *Globigerinelloides* sp., *Heterohelix* sp. and *Hedbergella* sp. (plates 2-1. A and D, 2-2. A, 2-2. B and C), (Flugle,2010).

2.2.1.3 Calcareous algae

Calcareous algae represent a large and diverse assemblage of aquatic photosynthetic plants, ranging from tiny micron-sized plankton to giant benthic marine plants tens to meters long. The Mishrif Formation is rich in calcareous algae, especially green algae. (plates 2-3. A)

2.2.1.4 Coral

Corals are very common in the Mishrif succession and, together with rudest, have made an important contribution to the construction of the Mishrif carbonate platform. The emergence of corals was almost related to the high effect of recrystallization and cementation, destroying the porosity within the corals (plates 2-7. D).

2.2.2 Non-skeleton

Non-skeletonized grains are those that do not appear to have been derived from microbial skeletal material. They are less dominant in the Mishrif Formation, represented by spheroids and Peloids. (Boogs, 2009)

2.2.2.1 Peloids

Peloid is in the form of spherical or oval particles and is widely used in most studies. It is composed of microcrystalline calcite with a diameter of 0.2-1 mm and internal structures of other shapes (Tuker, 1990; Flugel, 1982), and is distributed in shallow coral reefs and silt mounds on carbonate ledges in tropical and subtropical seas (Flugel, 2004), they have multiple origins and may be the result of bioclastic aversive processes or bioclastic feces (plates 2-8. A and C).

2.3 Fine-Grained Carbonate Matrix (Groundmass)

The floor consists mainly of fine-crystalline calcite called micrite, which is small crystals whose diameter does not exceed 4 microns and often appears opaque under the microscope. If its diameter exceeds 5 microns, it is called sparry calcite. The (Micrite) is deposited in an environment with calm sedimentation energy, while sparry Calcite is deposited in an environment with high sedimentation energy (Flugel, 1982)

2.3.1 Micrite

The bottom of the fine-grained carbonate matrix (groundmass) is mainly composed of fine-grained calcite called micrite, which are small crystals no larger than 4 microns in diameter and usually appear opaque under the

microscope. When its diameter exceeds 5 microns, it is called sparry calcite. Soil is one of the most important indicators to determine the strength of subsidence energy. Micrite mud is deposited in an environment with calm subsidence energy (Flugel, 1982). Microcrystalline calcite is referred to as "Micrite". The term currently refers to rocks composed of fine-grained calcite crystals and in situ-generated grains or aggregates of fine-grained, pre-existing carbonate material. (plat 2-2. C)

2.3.2 Sparite

Besides carbonate grains and micrite, the third major constituent of limestone is sparry calcite. Sparring calcite crystals are larger (0.02-0.1 mm) (Booge, 2009). The origin of spar is the recrystallization of micrite-sized calcite crystals during recrystallization, or as a one-step process of aragonite precursor cementation and calcification (Flugel, 2004)

2.4 Microfacies of Mishrif Formation

The thin section of Mishrif Formation was studied and examined, and the main microfacies were distinguished based on the classification of (Dunham,1962).

Six major microfacies were diagnosed the Mishrif Formation, Mudstone, Wackestone, Packstone, Grainstone, Boundstone, and Rudstone associated with twelve submicrofacies include: Bioclastic Packstone submicrofacies with rich Echinodermat, Coral and Rudist fragment and high dolomatiztion, Rudestone submicrofacies with large Rudist fragment and vug porosity , Boundstone submicrofacies with very large coral, Plankton Foraminefral Packstone submicrofacies with Globigerinelloides sp. and Calcispheres, Bioclastic Wackestone to Packstone submicrofacies with dolomite and calcareous algae, Peloidal Packstone with coral, pillites, pieces of Rudist Bioclastic Packstone to Grainstone submicrofacies, Peloidal to Bioclastic

Packstone submicrofacies, Benthonic Foraminiferal Mudstone submicrofacies, Rudist fragmented Mudstone. The important microfacies that identified are:

2.4.1 Mudstone Microfacies

This facies was observed in all wells of the Eridu oilfield, and it mainly consists of lime mud, as the environment in which this type of facies is deposited is characterized by the calmness of the movement of sea currents (Dunham, 1962), and therefore it is an unsuitable environment for the growth of organisms, the production and formation of granules, and it is free of fossils .The existence of this facies was observed mainly in the environment of the restricted and when it contains planktonic foraminifera, its environment is deep marine. Submicrofacies include benthonic foraminiferal mudstone (plate 2-2, fig. B), rudist fragmented mudstone wackestone (plate 2-2. D) and bioclastic mudstone (plate 2-6. C) (Figs. 2-3,2-4 and 2-5)

2.4.1.1 Benthonic Foraminiferal Mudstone

This facies is characterized by the presence of a percentage of fossils that do not exceed (10%), which includes smull fragment of *Nezzazat*.This secondary facies was diagnosed in the Eridu 1 well of Mishrif formation (1702m, 1758 m) and in the Eridu 2 well of Mishrif formation (1847m, 1936 m) and in the Eridu 3 well within the depths (1818m, 1888m) . (plate 2-2. B) (Figs. 2-3,2-4 and 2-5).

2.4.1.2 Rudist fragmented Mudstone toWackestone

This facies is characterized by the presence of echinodes , large rudist fragment with intrafossils porosity. These secondary facies have been identified in the Eridu 1 well, at different depths .This facies are deposited within the environment ristrected marine. Comparing this facies with the standard facies

suggested by (Wilson 1975), it was found to be similar to the (SMF-24) facies. and within the range (FZ-8). (plate 2-2. D) (Figs. 2-3,2-4 and 2-5).

2.4.1.3 Bioclastic mudstone

This facies is characterized by the presence algae and fine grins of pellets.This secondary facies was diagnosed in the Eridu 3 well of Mishrif formation. Comparing this facies with the standard facies suggested by (Wilson 1975), it was found to be similar to the (SMF-20) facies. and within the range (FZ-8). (plate 2-6. C) (Figs. 2-3,2-4 and 2-5).

2.4.2 Wackestone Microfacies

This facies was observed in all wells of Eridu oilfield, its floor consisted of micrite, and it contained very few percentages of the benthic Foraminifera genera Textularia sp. sp. Pseudolituonella sp in addition to the soft living fragments and living pieces of echinoderms and the scarcity of the benthonic Foraminifera genera, especially in the lower part of the formation of some wells, and this facies are sometimes graded in proportion to the facies of packstone. Submicrofacies include bioclastic wackestone (plate 2-9. D), fossiliferous wackestone to packstone (plate 2-6. D), planktonic wackestone (plate 2-7. A) and bioclastic wackstone to packstone (plate 2-9. A). The presence of this facies was observed in the shallow open marine , restricted and deep marine environments, depending on the biological content of the facies. (Figs. 2-3,2-4 and 2-5).

2.4.2.1 Bioclastic Wackestone

This facies is distinguished by its high level of life fragments and inclusions. The floor of this facies consists of micrite. This facies are deposited within the environment shallow open marine in the wells of this study, for which the rock slides were studied. Comparing this facies with the standard facies suggested

by (Wilson 1975), it was found to be similar to the (SMF-9) facies. and within the range (FZ-7). (plate 2-9. D) (Figs. 2-3,2-4 and 2-5).

2.4.2.2 Fossiliferous Wackestone to packstone

This facies consists of structural granules, which are immersed in a micrite floor, where the structural components are the benthic foraminifera in addition to the presence of dissolution that was distinguished in the Eridu 2 well. Comparing this facies with the standard facies suggested by (Wilson 1975), it was found to be similar to the (SMF-9) facies. and within the range (FZ-7). (plate 2-6. D) (Figs. 2-3,2-4 and 2-5).

2.4.2.3 Planktonic wackestone

This facies commonly consists of an abundance of planktonic foraminifera represented by genera of (*Globigerinelloides* sp., *Heterohelix* sp. and *Hedbergella* sp.) and a smaller percentage of bio-fragments and rhudist as well as benthic foraminifera. The floor of this facies consists of micrite in most of the segments of this facies. Comparing this facies with the standard facies suggested by (Wilson ,1975), it was found to be similar to the (SMF-3) facies. and within the range (FZ-1 and FZ-3). (plate 2-7. A) (Figs. 2-3,2-4 and 2-5).

2.4.2.4 Bioclastic wackstone to Packstone

This facies consists mainly of structural granules and non-skeletal granules, where it was found that the structural components are benthic foraminifera and planktonic foraminifera as well as biological alge , echinoderma and rudist pieces. Comparing this facies with the standard facies suggested by (Wilson 1975), it was found to be similar to the (SMF-5) facies. and within the range (FZ-4). (plate 2-9. A) (Figs. 2-3,2-4 and 2-5).

2.4.3 Packstone Microfacies

This facies contained a small percentage of mud, and its content gradually increased in the proportions of living fragments and pieces of echinoderms from the previous facies, as it also contained pieces of rudest. Depending on the biological content of the facies, where it was observed that it was deposited mainly in the environment of the shallow open marine , deep marine and shoal . Submicrofacies include planktonic packstone (plate 2-9. B), peloidal packstone (plate 2-1. B), peloidal to bioclastic packstone (plate 2-8. C) and bioclastic packstone to grainstone (plate 2-8. D) (Figs. 2-3,2-4 and 2-5).

2.4.3.1 Planktonic Packstone

This facies is distinguished by its high level of life fragments ,Echinoderma,calssisfere and small fragmented of planktonic foram . The floor of this facies consists of micrite. This facies are deposited within the environment shallow open marine. Comparing this facies with the standard facies suggested by (Wilson 1975), it was found to be similar to the (SMF-2) facies. and within the range (FZ-2). (plate 2-9. B) (Figs. 2-3,2-4 and 2-5).

2.4.3.2 Peloidal Packstone

This facies contains mainly peloid, in addition to pieces of echinoderms and foramnefral , characterized by being well sorted due to the high energy of the waves, and characterized by the presence of high porosity. When comparing this facies with standard facies, it falls within the (SMF-14) facies in the (FZ-6) range, indicative of the shoal environment. (plate 2-1. B) (Figs. 2-3,2-4 and 2-5).

2.4.3.3 Peloidal to Bioclastic Packstone

This facies abundantly consists of pelletes, as well as the presence of biogenic crumps and pieces of foraminifera and rudest. This type of secondary facies is formed under a special environment represented by sedimentary energy and the medium wave movement responsible for the washing of clay materials and the micrate base. The specifications of this microfacies were compared with the standard (Wilson,1975) facies, and it was found that they are comparable to the standard (SMF-16) facies, which fall within the (FZ-7) facies represented by the environment of the shallow open marine. (plate 2-8. C) (Figs. 2-3,2-4 and 2-5).

2.4.3.4 Bioclastic Packstone to Grainstone

This facies is characterized by the dominance of packstone stacked on top of each other in a sparite floor, and the presence of macrite is less, as the granules form a high percentage of this structure within a floor that is often made of sparse calcite. Biological fragments constitute a high percentage of the components of this facies. Certain types of granules may prevail over other types, as in the previous ones from the aforementioned main facies, so the secondary facies were named depending on the dominant granules in them. This facies can be considered as the environment (Shoals) and environments with high energy. When comparing this facies with standard facies, it falls within the (SMF-11) facies in the (FZ-6) range. (plate 2-8. D) (Figs. 2-3,2-4 and 2-5).

2.4.4 Grianstone Microfacies

This facies was observed in some wells of the oilfield, the grounds of which consist of Sparite. The facies contained pieces of rudest and echinoderms, as well as peloids . This facies was deposited in the environment of shallow open

marine , deep marine and shoal. Submicrofacies include piloidal grainstone (plates 2-8.A). (Figs. 2-3,2-4 and 2-5).

2.4.4.1 Piloidal grainstone

This facies is characterized by the predominance of non-skeletal granules represented by peloid resulting from the micratiztion process to which the skeletal granules are exposed. It also includes crumpes, biological fragments and Echinoderma, which constitute a high percentage of the components of this facies, in addition to a few bottom planctonic foraminifera and some rarely benthonic foraminifera. The ground of this facies is composed of fine sparite resulting from the process of new formation of fine sparite, noting that the grains of this facies range from large to medium in size. The specifications of this microfacies were compared with (Wilson's ,1975) standard facies, and it was found to be comparable to the standard (SMF-16) facies, which fall within the facies range (FZ-6) represented by the environment of the Shoal and the shallow open marine. (plates 2-8.A) (Figs. 2-3,2-4 and 2-5).

2.4.5 Rudstone Microfacies

This facies was observed mainly in the Eridu 1 well, and to a lesser extent in the Eridu 2 well. Depending on the comparison between the wells, it is considered mainly visible in wells 4 and 7, and it consisted of small and large pieces of rudist in addition to coral. This facies was observed in the environment of the shoal , shallow open marine and rudist biostrum. (plate 2-7.D) (Figs. 2-3,2-4 and 2-5).

2.4.6 Boundstone Microfacies

This facies was observed mainly in the Eridu 1 well, and depending on the comparison between the wells, it is considered mainly visible in wells 4 and 7 and consisted of rudist structures and some pieces of coral. These structures

were affected by solubility forming a secondary porosity of the type (Growth Framework porosity).

This facies was observed in the environment of the rudist biostrum. The two facies of the rudestone and the boundstone are considered among the most important formation facies in the oilfield because they contain large porous voids resulting from the dissolution process that allow the presence of oil in them in large quantities. (plate 2-7.C). (Figs. 2-3,2-4 and 2-5).

2.5 Diagenetic processes

Diagenesis is the totality of the chemical, physical, and biological processes that rocks go through between the time of deposition and the time of metamorphism (Tucker, 1982). Without directly involving crustal movement, all those alterations in sediment at the earth's surface that occur at low temperatures and pressure are examined (Taylar, 1964 in Land, 1967).

Understanding the processes and products of carbonate rock diagenesis is crucial to the exploration and optimal development of hydrocarbon reservoirs in carbonate rocks (Longman, 1980). Diagenesis can start from the seafloor (syngenetic or eogenetic alteration), continue through deep burial (mesogenetic alteration), and extend to subsequent uplift (telognetic alteration). It can mask information about key features and also leave behind basic information about post-depositional setting history, pore water composition and temperature. It can also reduce or increase porosity (Scholle and Ulmer- Scholle, 2003).

2.5.1 Dissolution

The dissolution process improves the reservoir specifications by dissolving the rocks and the components they contain depending on the mineralogy of the dissolved parts and the degree of saturation of the interfacial water with calcium carbonate and the depth of these deposits in addition to being affected by temperature and carbon dioxide pressure. The effect of this process varies according to the size of the crystals, which are proportional Reversible with

him (Flugel, 2004) forming different types of porosity, as calcareous rocks are among the rocks most affected by this process, as the solutions work to dissolve the minerals and shells of fossils that make up these rocks. (plats2-3. C)

2.5.2 Compaction

Compaction represents the mechanical and chemical reactions that occur due to increased silt loading and increased temperature and pressure conditions during maintenance. A suture is a suture thread whose surface is usually covered with an insoluble material such as clay or organic debris. Sutures are usually parallel to the sediment, but may also occur as bedding at different angles, thus generating reticular or nodular confinement patterns (Ahr, 2008) (plate 2-8, fig.C). Stylolites were observed in muddy deep marine facies and the most of them have irregular configuration associated with calcite-cemented grains, which were commonly occurred along the stylolite surfaces indicating their late origin (plate 2-9. C).

2.5.3 Recrystallization

This refers to changes in crystal size, crystal shape, and crystal lattice orientation without changes in mineralogy (Flugel, 2004). This process affects the evolution of some parts of micrite to microsparite. This process was characterized in the lower parts of the Mishrif Formation within the studied wells.

2.5.4 Dolomitization

Dolomitization is the conversion of limestone to dolomite, which takes place when magnesium carbonate replaces the initial calcium carbonate by the action of magnesium-bearing water (Flugel, 2004). When compaction and cementation processes are absent, late diagenetic dolomatiztion enhances the porosity of the rocks, improving reservoir quality, (Moore, 2004). Within the studied wells, dolomitization was identified in the upper and middle parts of the Mishrif Formation (plates 2-4. A and C)**.**

2.5.5 Cementation

According to Flugel (1982), the process is defined as the process of chemical precipitation of calcium carbonate from a saturated solution present in the primary pores between the structural grains or the secondary cracks created by the solution during dissolution, resulting in the growth of calcite crystals, Affect the coagulation and solidification of sediments, reduce porosity. (Flugel, 1982) divided cement into two main phases, namely:

1. The first phase: It is represented by cement formed during the early stages of the Diagenetic processes, where it is called (cement - A) and consists of fine, fibrous crystals composed of either the mineral Aragonite or high-magnesium calcite is deposited in shallow or deep marine environments with limited sedimentation as well as in coastal.
2. The second phase: It is represented by the cement formed during the late stages of the Diagenetic processes, which is called (Cement B). General type after hardening of the sediment and its provisions.

The obvious result of this process is in the Lower part in the Mishrif Formation. Among the most important types of cement that were distinguished in some of the cavities and chambers of fossils and in some cracks and fractures of the facies of the study area are the following:

2.5.5.1 Equivalent granular cement

This cement consists of transparent calcite crystals, fully to half-faceted and almost identical in size, as its crystals are characterized by their small size and abundance, as this type of cement is developed from saturated to The calcium carbonate deposited during the process hydrates near the surface and then begins to gradually grow toward the center of the cavity, forming specific types of micro pores between the crystals (Flugel, 1982). This cement is commonly found in the Wackestone and Packstone facies as cement filling the

intercrystalline voids as it exists in some facies of the formation in diffuse form and fills some structures and some bio fractures (plates 2-4. B)**.**

2.5.5.2 Blocky Cement

It occurs as fully to half-faceted and large calcite crystal blocks. It is usually shed at a later stage of the metamorphic process (Flugel, 1982). Some crystals may be the result of Druze cement crystals growing at the expense of other crystals (Blatt et al., 1980). This type of cement is found in the cavities and chambers of some fossils. (plates 2-3. B)**.**

2.5.5.3 Druzy mosaic cement

Cement used in fractures, molds, and intergranular pores for void filling and pore lining. Drusy cement crystals have a shape of equant, elongated, and anhedral to subhedral. Its size is commonly less than (10 um). The fabric characteristic by increase of crystal size toward the center of the void. Drusy cement may forms near-surface meteoric and within burial environments, (Flugel, 2010). (plates 2-2. A)**.**

2.5.5.4 Radiaxial Cement

Large calcite crystals are characterized by undulose extinction often turbid and cloudy, inclusion-rich. The crystalline size ranges from medium to coarse. Occasionally extending several millimeters in length and varying in diameter from 30 to 300 microns. The ratio of length/width in the crystal is 1:3 to 1:10. (plates 2-8. B)**.**

2.5.6 Micritization

This process Micritization results in fine-grained precipitation. However, decomposition has been included here as a very early action because it causes changes in previously formed sediments. The most important type of biological modification of sediments results from the grazing activities of organisms. Drilling by algae, fungi, and bacteria is a particularly important process for the modification of structural materials and carbonate grains (Boogs, 2009). In the

upper part of the Mishrif Formation and to a lesser degree in the lower part, this process (Micritization) was identified. (plates 2-6. B)**.**

2.6 Porosity in Carbonate Rocks

The pore system in carbonate rocks is much more complex than in siliciclastic (Choquette and Pray, 1970; Lucia, 2007). This complexity is a result of the overwhelming biological origin of carbonate deposits and their chemical reactivity. In carbonate sediments, the shape of the grains and the presence and sorting of porosity within grains have a major impact on porosity. The presence of pore space in the shells and spheres that make up the carbonate sediment grains increases porosity beyond that expected from intergranular porosity alone (Dunham, 1962).

Although there is no simple relationship between porosity and structure, it can be seen by inspection that as the grain size decreases and the grain packing becomes tighter, the pore size grains decreases. Porosity also decreases with denser packing, resulting in a correlation of intergranular pore size with grain size, gradation, and intercrystalline porosity. The size and volume of pore space in grains is related to the type of sediment and its post-deposition history (Lucia, 2007).

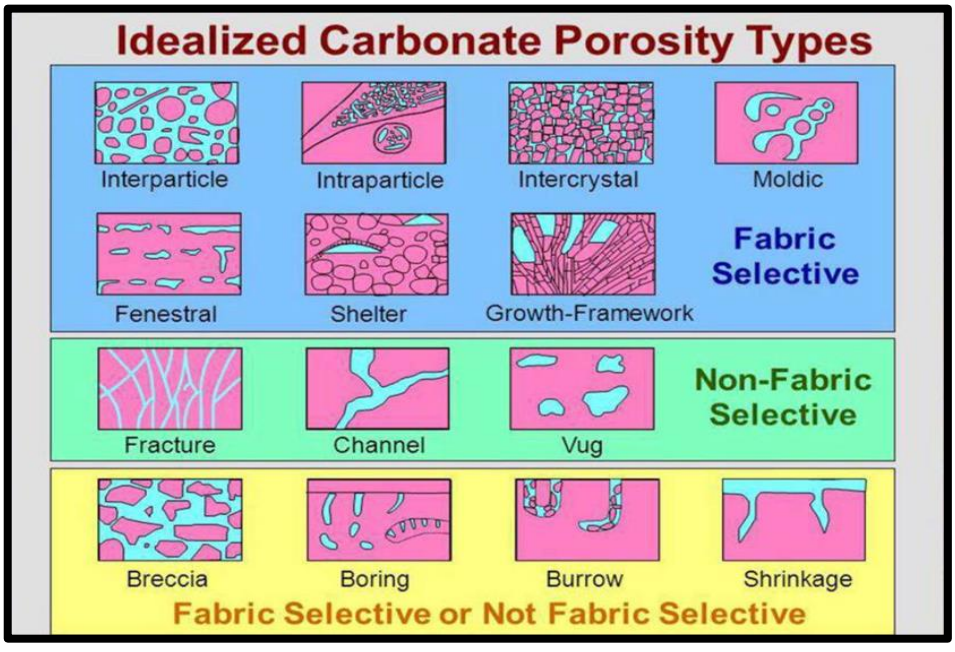

Figure (2-2) Types of pores in carbonate rocks (Choquette & Pray,1970)

2.6.1 Primary Porosity

Primary porosity is a material-selective porosity that forms during pre-depositional stages, such as intragranular pores in foraminifera, and during deposition, such as scaffold growth and intergranular porosity (Flugel, 2010).

2.6.1.1 Intragranular (Intraparticle) porosity

Intragranular porosity is found within the grains, especially in the framework grains. The effectiveness of this porosity often depends on the overall structure of the rock within the grain, (Tucker and Wright, 1990) (plates 2-5. D)**.**

2.6.1.2 Intergranular (Interparticle) porosity

Pore space exists between grains (Booge, 2009), but there is also secondary porosity created by the partial dissolution of aragonite peloid cortices. (Flugel, 2010) (plates 2-3. D)**.**

2.6.2 Secondary porosity

The two main forms of secondary porosity were non-fabric selective and fabric selective (Flugel, 2010). Any time following deposition during the diagenesis process, secondary porosity occurs. Dissolution, which creates secondary porosity and can happen at any point throughout the burial process, can considerably improve reservoir performance.

2.6.2.1 Fabric Selective Porosity

1. Mold when granules are selectively removed by solutions; porosity is created (e.g. peloid or fossils). This calls for a characteristic distinction between the matrix or cements and the solubility of grains in terms of microstructure framework or mineral composition. Mold may also develop in burial environments, although it is more common for them to grow in meteoric-phreatic rocks with mixed mineralogy, (Flugle,2010). (plates 2-6. A)**.**

2. Intercrystalline porosity Fabric selective porosity between almost equal-sized crystals is frequent during the early and late diagenesis phases of dolomitization and recrystallization, (Flugel, 2010)

2.5.2.2 Non fabric selective Porosity

1. The dissolved voids known as vug porosity are larger than the nearby crystals or grains (Ahr,2008). Pores of varying sizes, ranging from millimeters to meters, are created at early and late diagenesis by uneven dissolution that slashes through grains and/or cement boundaries. Dissolution may start in a mold pore or between two particles, (Flugel, 2010). (plates 2-5. A).
2. Channel porosity often develops along cracks when limestone within under saturated waters dissolves. The length of this elongate hole is 10 times greater than its diameter, (Tucker and Wright,1990). (plates 2-5. B).
3. Fracture porosity is formed by the components of the rock structure, and fractures that often occur due to tectonic deformation, collapse or solution collapse accompanied by evaporation, or dissolution of limestone, are what cause the occurrence of porosity. It is very diffuse and may significantly increase the effective porosity of limestone several times. (Tucker and Wright, 1990). (plates 2-5. C).

2.7 Depositional Environment and Facies Association

A depositional environment is defined as a specific portion of the Earth's surface "geographical environment in which sediments are deposited, characterized by complex physical, chemical, and living conditions that distinguish them from other environments (Selley, 1982).

Facies are associated with each facies the overlapping of others, their vertical and lateral succession is the result of lateral changes in the depositional environment, so what is the difference. Except those sediments, especially carbonate rocks, are affected by depositional environmental conditions, such as

water energy, salinity, temperature and other factors. As well as the influence of climate, these factors play a fundamental role in the generation and distribution of carbonate rock deposits. It can be seen from the above that the depositional environment of the core-containing borehole can be identified by delineating the core and preparing rock thin sections to identify the primary and secondary microfacies, and then linking these microfacies with the depositional environment for identification (Alsultan *et al*., 2021).

Five association facies were distinguished: Deep Marine, Shallow open marine, Rudist biostrum, Shoal and Restricted marine. Each of these Facies represents a different sedimentary environment.

And due to the unavailability of rock core for all study wells, a comparison was made between the wells that contain rock core and wells that do not contain core. Thus, the sedimentary environments of Mishrif Formation units were determined in all study wells in Figs. 2-6,2-7 and 2-8.

Well log analyzes were established and performed for the boreholes referenced in Figs. 2-3,2-4 and 2-5. The following is a description of the main depositional environment of the Mishrif Formation in the Eridu oilfield:

2.7.1 Facies Association: Deep marine Environment

The facies of this environment consist of the Mudstone and Wackestone containing the fragments of the neighborhoods located between the facies of the open sea and the facies of the shoal environment. The facies of this environment are characterized by a small thickness and intermittent extension. The facies of this environments are Planktonic Foraminiferal Packstone, Bioclastic Wackestone to Packstone, Fossiliferous Wackestone with dissolution and the carrying planktonic foraminifera such us Calcispheres, Echinoderms, *Globigerinelloides, Heterohelix, Hedbergella* and Bioclastic Packstone (Figs. 2-3,2-4 and 2-5).

2.7.2 Facies Association: Shallow Open Marine Environment

It represents a transitional environment between the facies of the Mishrif Formation, as sediments abound in the deep regions. Among the microfacies characteristic of this sedimentary environment are the Bioclastic Packstone, Peloidal to Bioclastic packstone, Peloidal packstone facies, and the carrying benthonic foraminifera such us *Textularia, Nezzazata*, Milliode and bioclastic fragments. It is distinctively downslope and seaward of the rudist biostrum habitat. Mostly bioclastic wackestone and packstone make up its texture.

A particular form of bioclastic may regionally predominate at different stages within the succession, particularly the rudist bioclastic, which appear as well-worn (sand-size or coarser) angular or tabular grains. The bioclastic range in size from silt to sand and, in some circumstances, are even coarser. Benthonic foraminifera like *Dicyclina* and *Praealveolina*, calcareous green algae, coral and coralline algae, echinoderms, and *gastropods* are some of the more significant fossils. Less often found were brachiopods and pelagic foraminifera.

The shallow open marine facies association was formed on the foreslope portion of the Mishrif carbonate platform, and its sediments are mostly made up of bioclasts that were created when rudist biostrum were destroyed by tidal currents or storms. In the Mishrif Formation, the shallow open marine facies is one of the more prevalent facies in the wells studied (Figs. 2-3,2-4 and 2-5).

2.7.3 Facies Association: Shoal Environment

The shoal environment is characterized by significant tidal current and wave activity near the seaward border of the carbonate substrate. Deposition depths are less than (5-10) meters above wave-base in this environment (Tucker, 1985). This environment is characterized by the facies of Grainstone to Packstone rich in pieces of bioclastic fragments, and the facies of Peloidal Packstone (Flugel, 1982). (Figs. 2-3,2-4 and 2-5).

2.7.4 Facies Association: Rudest Biostrum Environment

The facies of this environment are characterized by the presence of large sized pieces of rudest fragments deposited in facies ranging from Rudstone with a few algae and corals. The facies of the Boundstone facies it has a high initial porosity affected by the secondary dissolution process leading to the development of primary porosity. (Figs. 2-3 and 2-5).

2.7.5 Facies Association :Restricted marine environment

Benthic foraminiferal mudstone constitutes the main body of this facies relationship, *Nezzazata, Textularia* and many more benthic foraminifera are diverse. Other fossils found include coral fragments and red coral fragments. The matrix is basically fine mudstone, in some cases containing a large amount of argillaceous material. (Flugel, 1982) (Figs. 2-3,2-4 and 2-5).

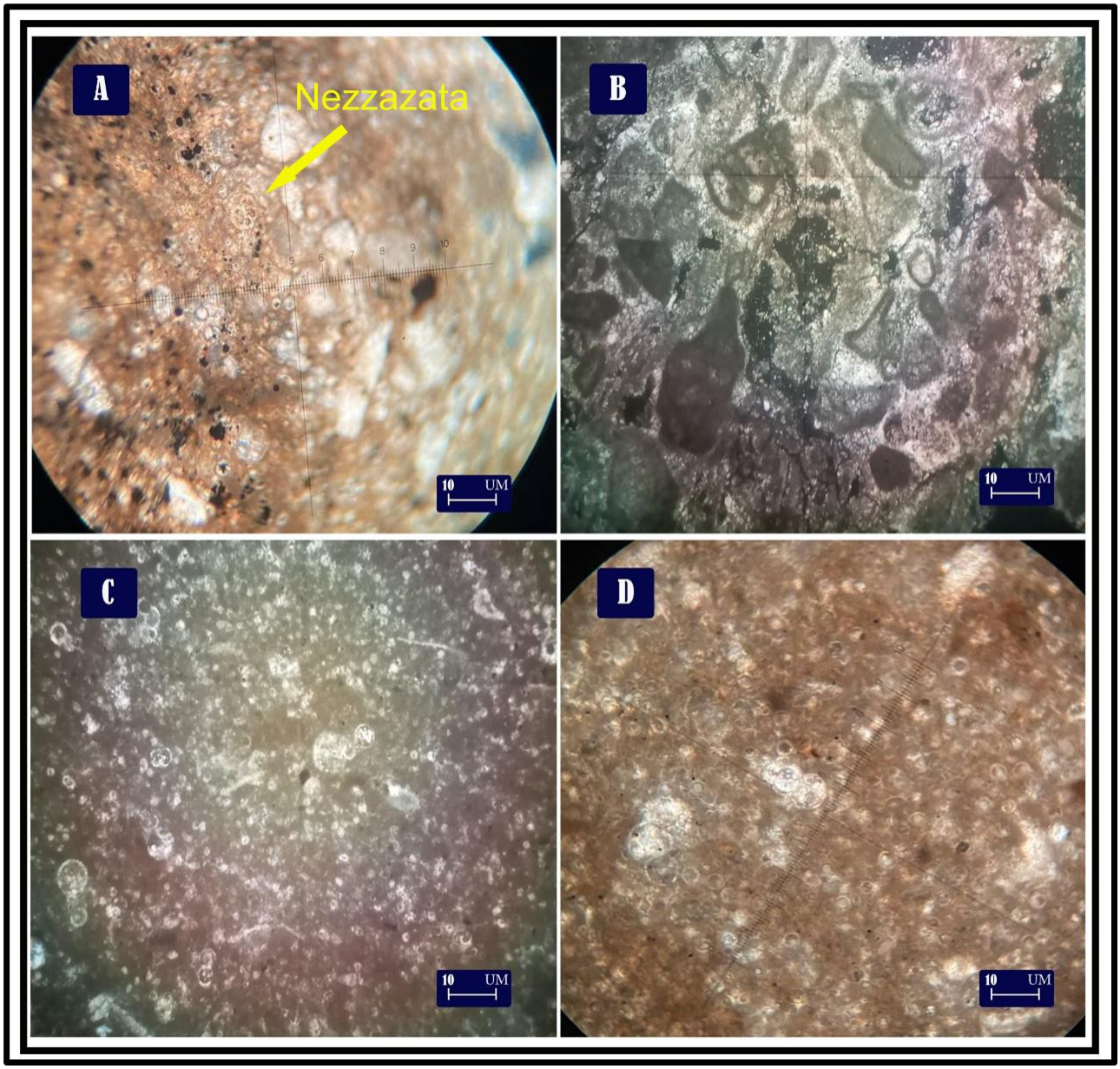

Plate 2.1

A; *Nezzazata sp.* (ER-2 depth 1881.81m)

B; Peloidal packstone (ER-2 depth 1888.8m)

C; Calcispheres (ER-2 depth 1909.3m)

D; *Globigerinelloides sp.* and *Heterohelix sp.* with planktonic foram (ER-3 depth 1882m

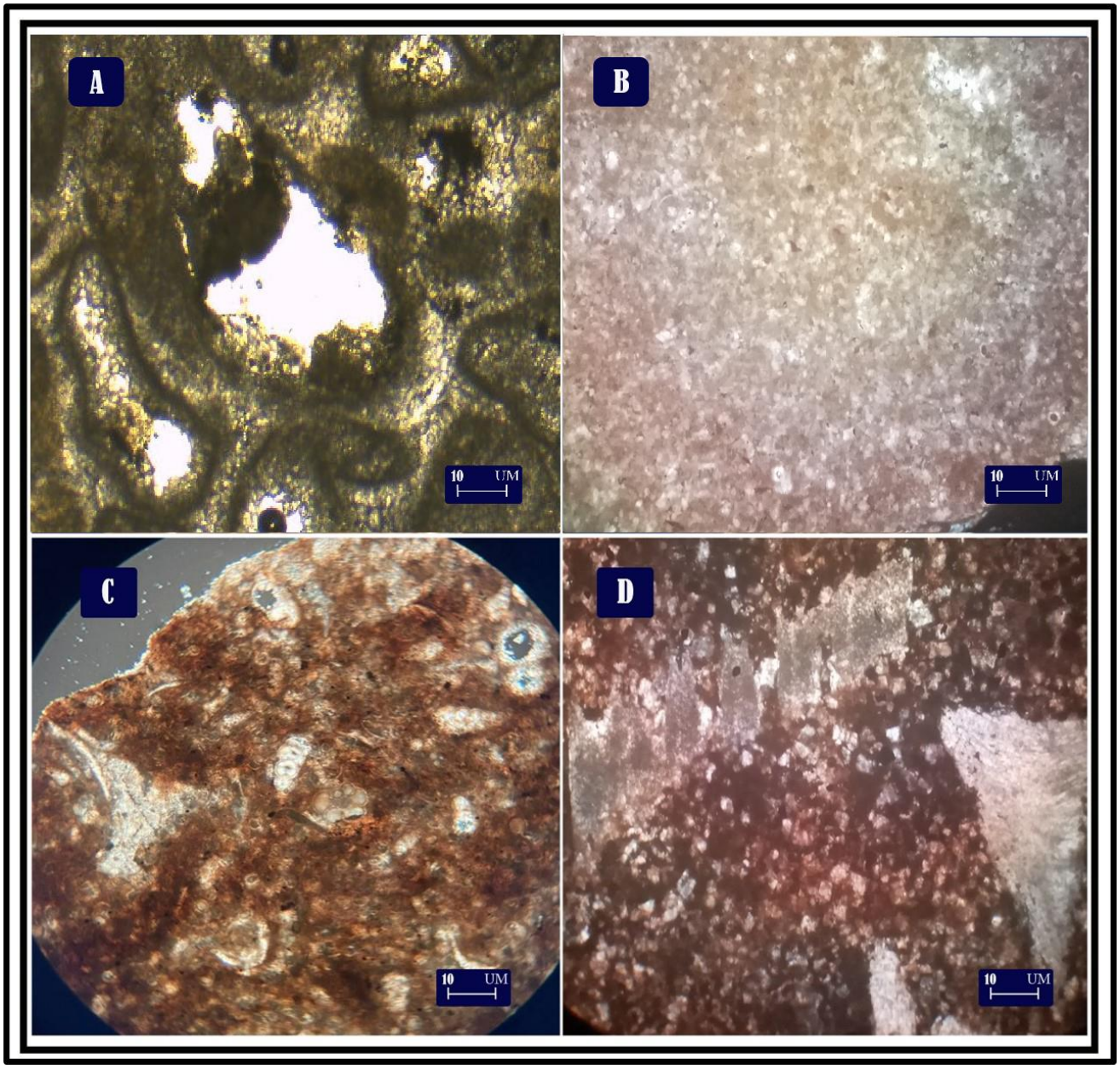

Plate 2.2

A; Drusy cement (ER-1 depth 1839.71m)

B; Benthonic foraminiferal mudstone (ER-2 depth 1847.95m)

C; *Textularia sp.* (ER-3 depth 1877.7m)

D; Rudest fragmented mudstone to wackestone with intrafossils porosity (ER-2 depth 1866.30 m)

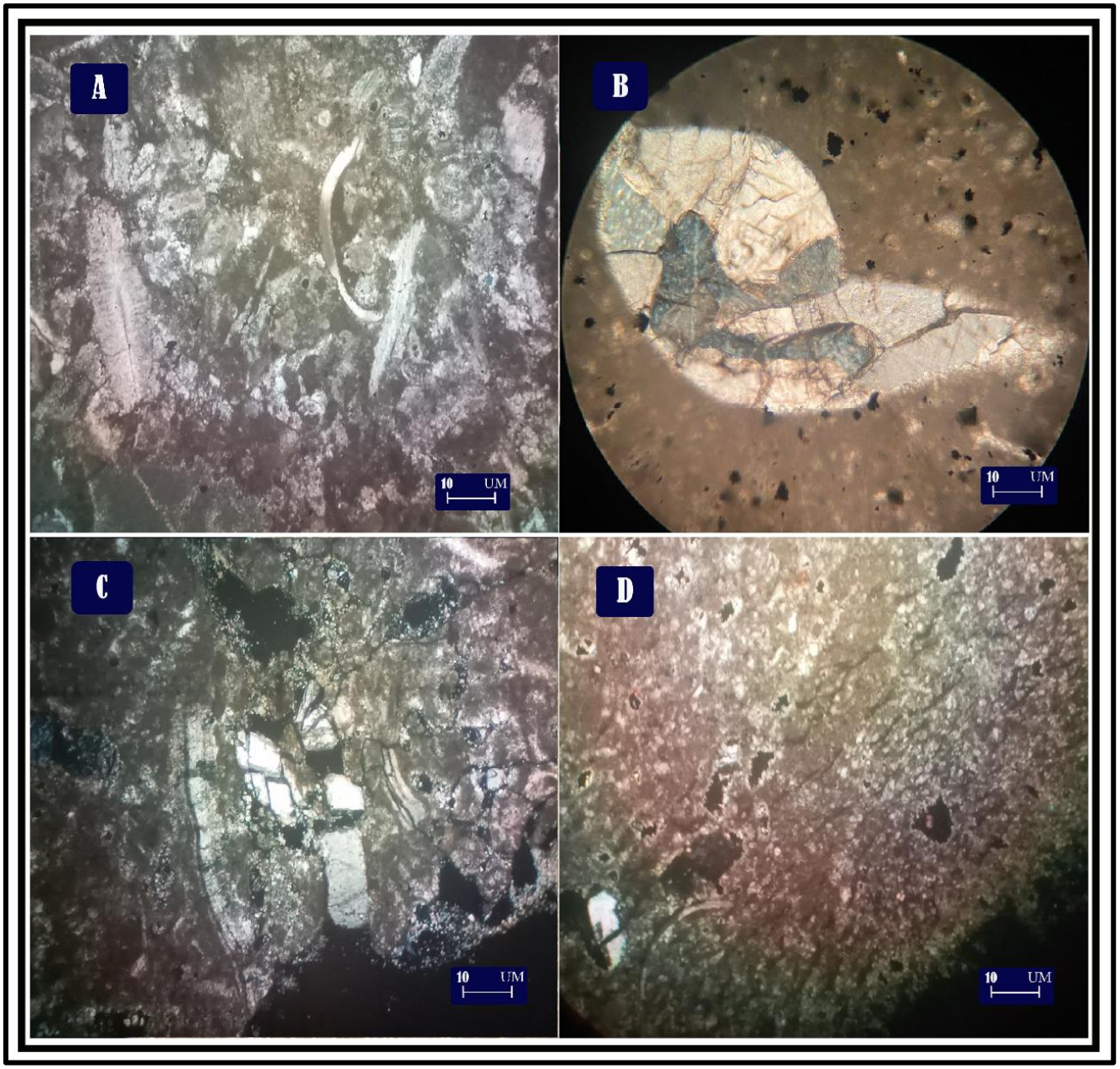

Plate 2.3

A; Echinoderm and calcareous alga (ER-2 depth 1891.90 m)

B; Blocky cement (ER-3 depth 1850.73m)

C; Dolomatiztion (ER-2 depth 1838.95 m)

D; intergranular porosity (ER-2 depth 1850 m)

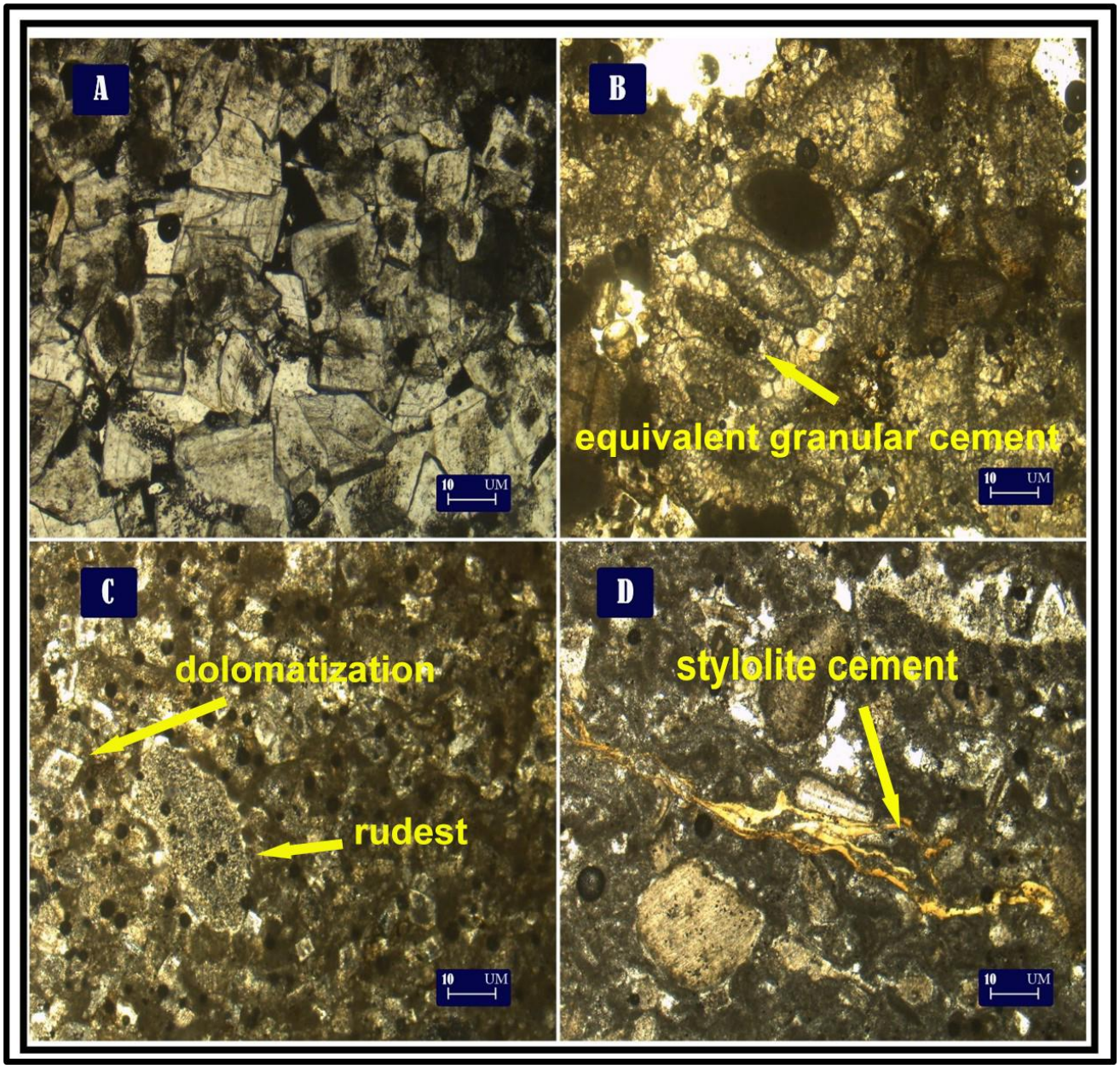

Plate 2.4

A; Dolomatiztion (ER-1 depth 1783.95 m)

B; Equivalent granular cement (ER-1 depth 1777.10 m)

C; Dolomatiztion with rudest fragment (ER-1 depth 1790.95 m)

D; Stylolite cement (ER-1 depth 1792.50 m)

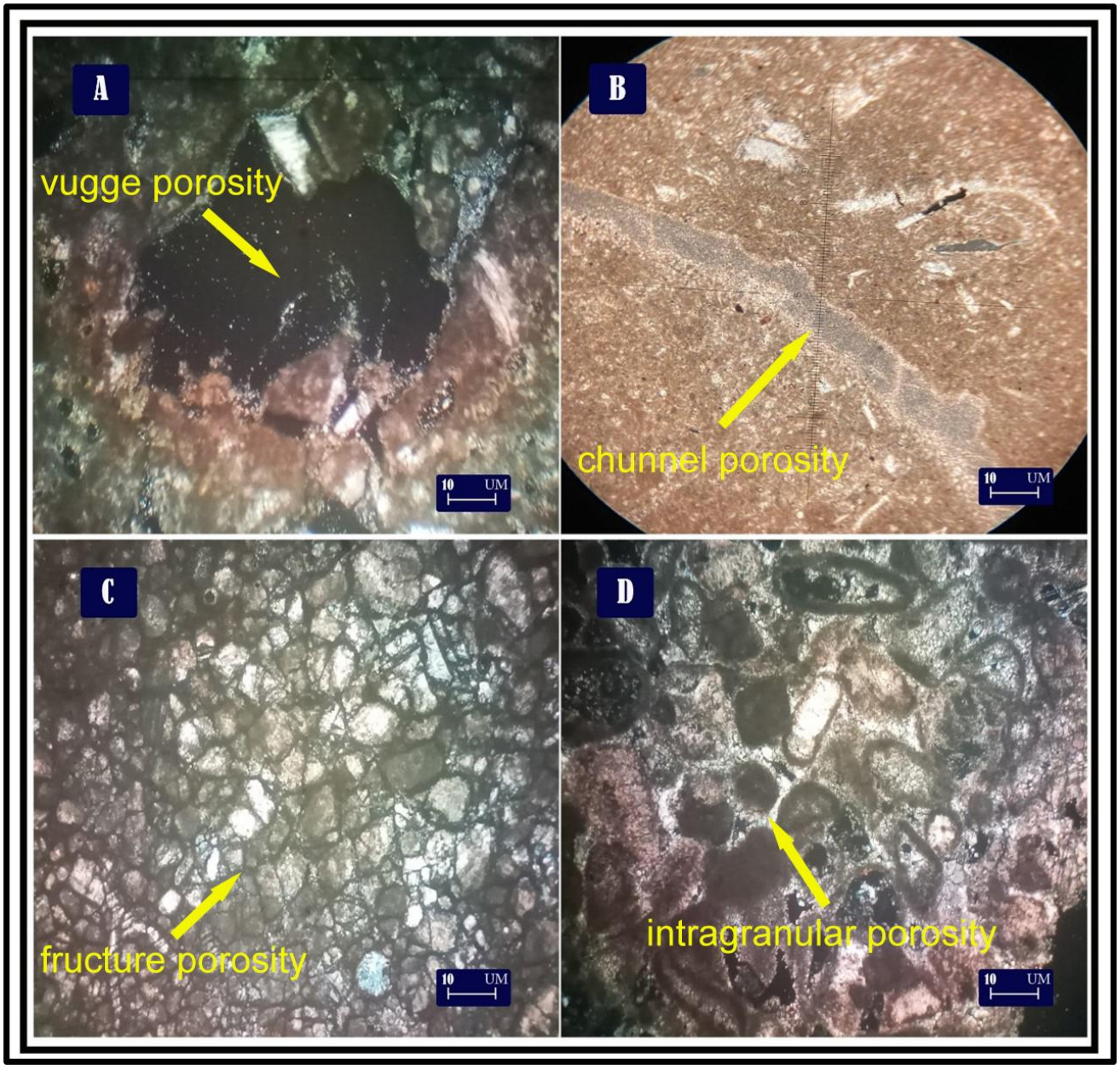

Plate 2.5

A; Vug porosity (ER-2 depth 1837.05 m)

B; Chunnel porosity (ER-3 depth 1845.05 m)

C; Fracture porosity (ER-2 depth 1909.30 m)

D; intergranular porosity (ER-2 depth 1843.40 m)

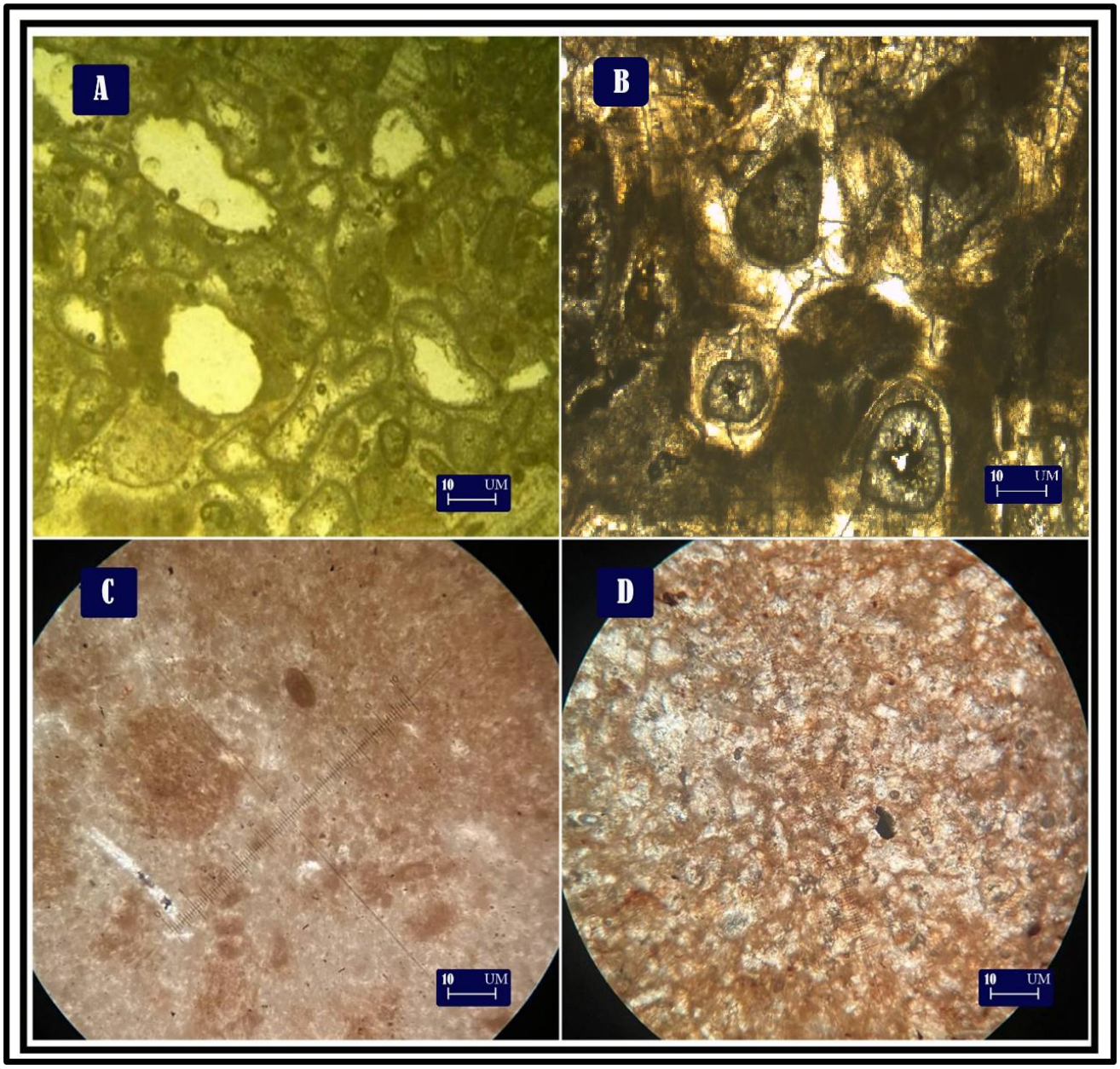

Plate 2.6

A; Moulid porosity (ER-1 depth 1780.5 m)

B; Micritization (ER-1 depth 1773.95 m)

C; Bioclastic mudstone with fine grins of pellets (ER-3 depth 1839.73 m)

D; Fossiliferous Wackestone to packstone (ER-3 depth 1871.24 m)

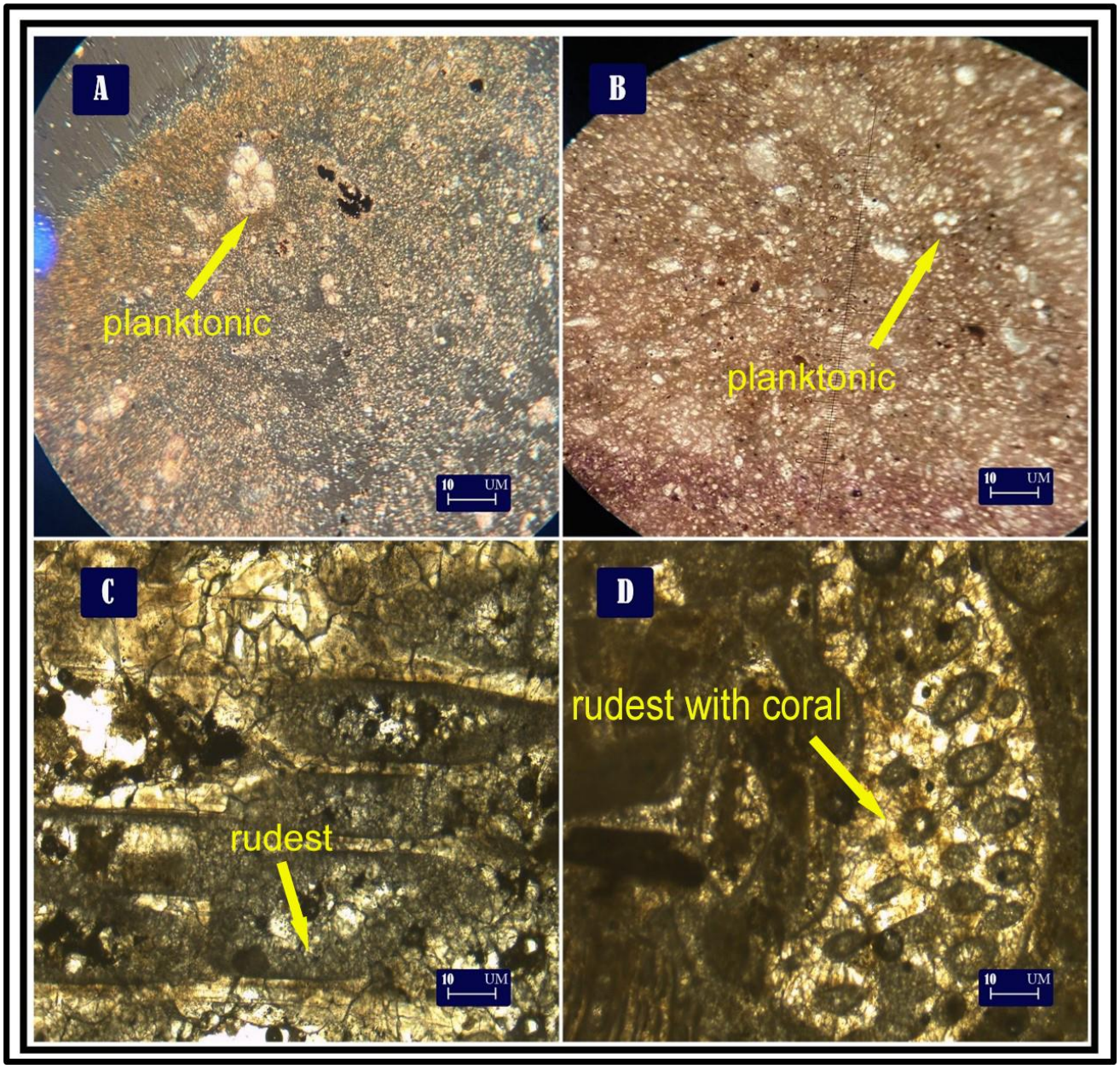

Plate 2.7

A; Planktonic Wackestone (ER-3 depth 1812.05 m)

B; Bioclastic packstone with small fragment of planktonic (ER-3 depth 1861.20 m)

C; Boundstone with rudest fragment (ER-1 depth 1808.90 m)

D; Rudstone with very fine grain of coral (ER-1 depth 1800 m)

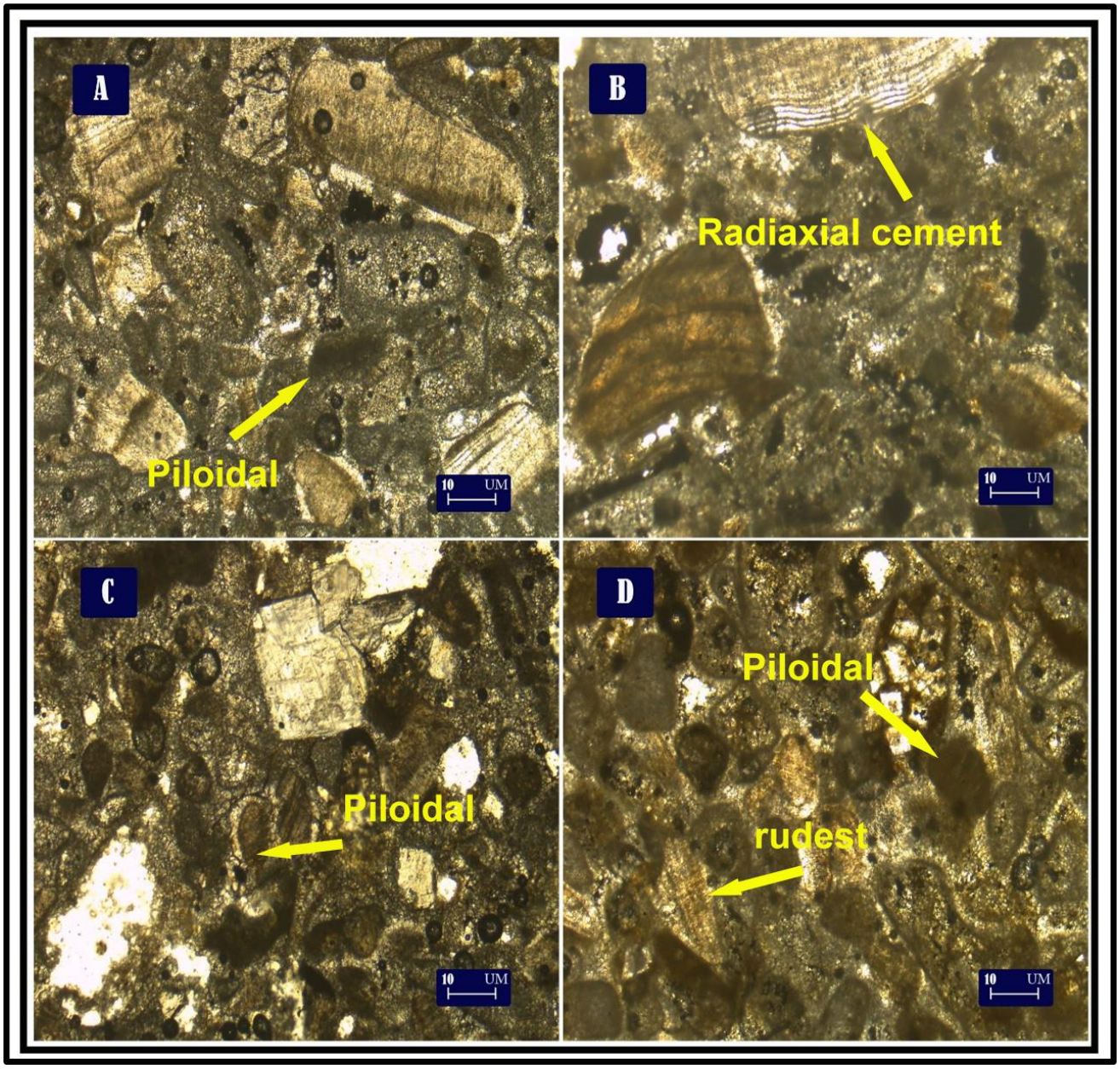

Plate 2.8

A; piloidal grainstone with rudest fragment (ER-1 depth 1790.95 m)

B; Radiaxial Cement into rudest (ER-1 depth 1786.50 m)

C; peloidal to bioclastic packstone (ER-1 depth 1780 m)

D; Bioclastic packstone to grainstone with high peloidal, coral and rudest fragment (ER-1 depth 1782 m)

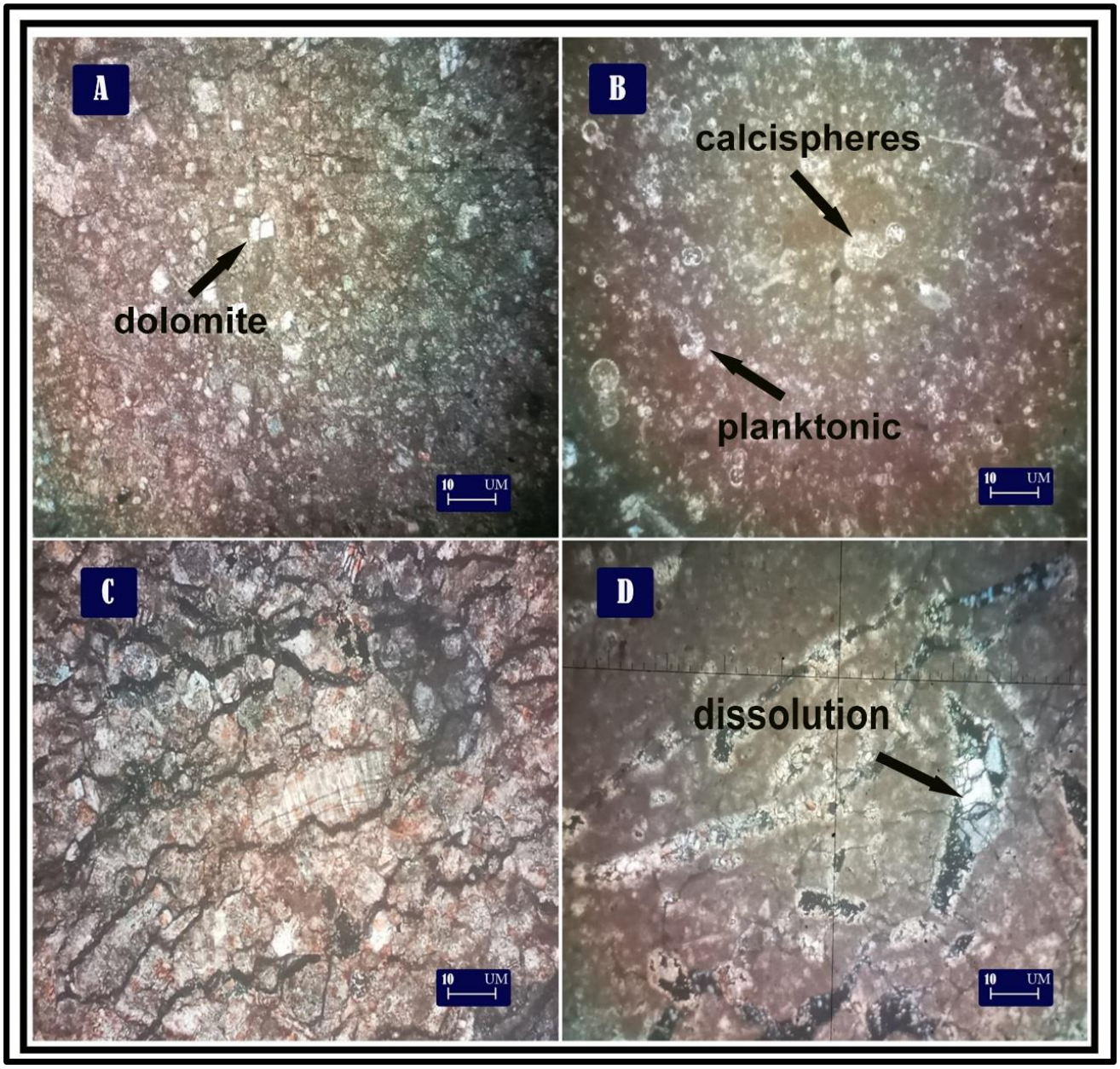

Plate 2.9

A; Bioclastic Wackestone to packstone with fragment of dolomite (ER-2 depth 1855.40 m)

B; planktonic packstone (ER-2 depth 1909.30 m)

C; Bioclastic mudstone with compaction (ER-2 depth 1831.50 m)

D; Bioclastic Wackestone with dissolution (ER-2 depth 1837.05 m)

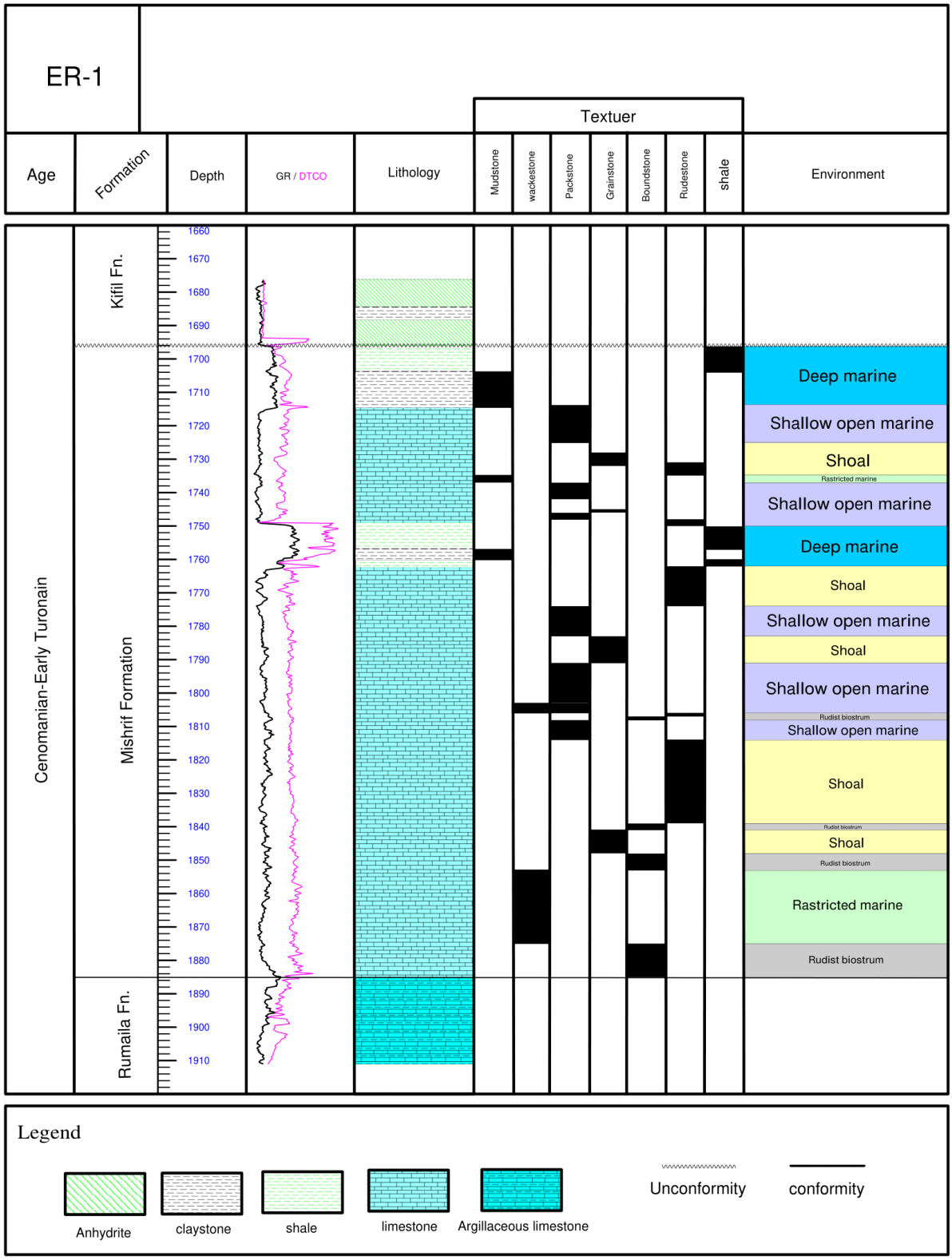

Figure (2-3) Microfacies succession and depositional environment of Mishrif Formation in well ER-1

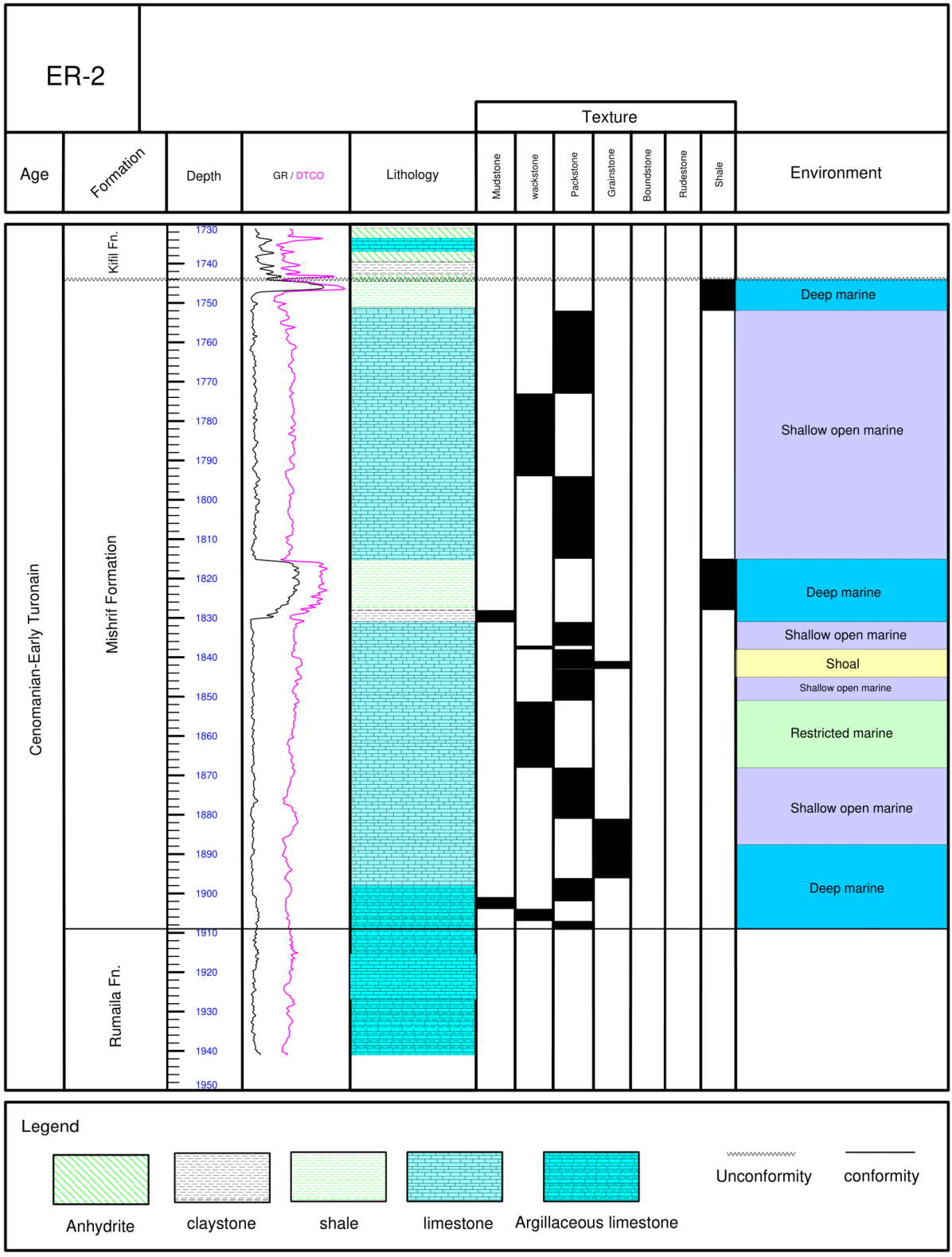

Figure (2-4) Microfacies succession and depositional environment of Mishrif Formation in well ER-2

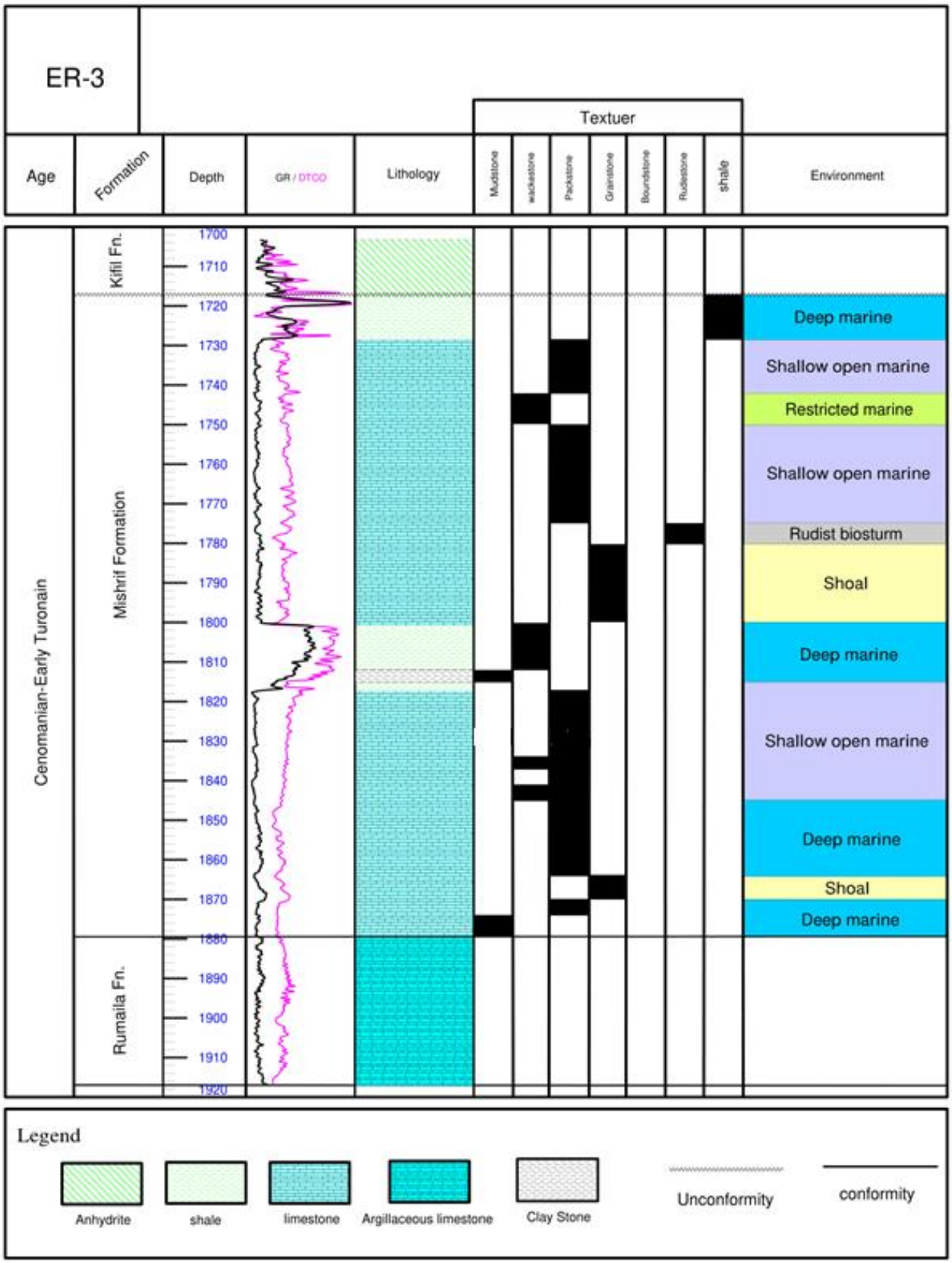

Figure (2-5) Microfacies succession and depositional environment of Mishrif Formation in well ER-3

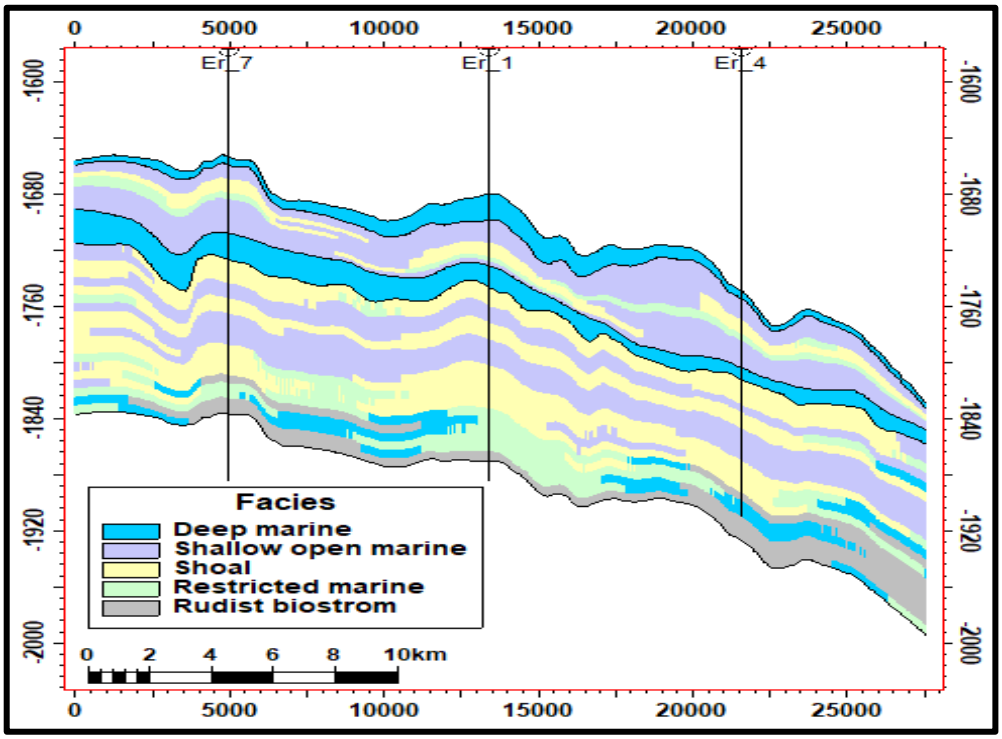

Figure (2-6) A cross section showing the sedimentary environments of the Mishrif Formation units for wells (7,1,4)

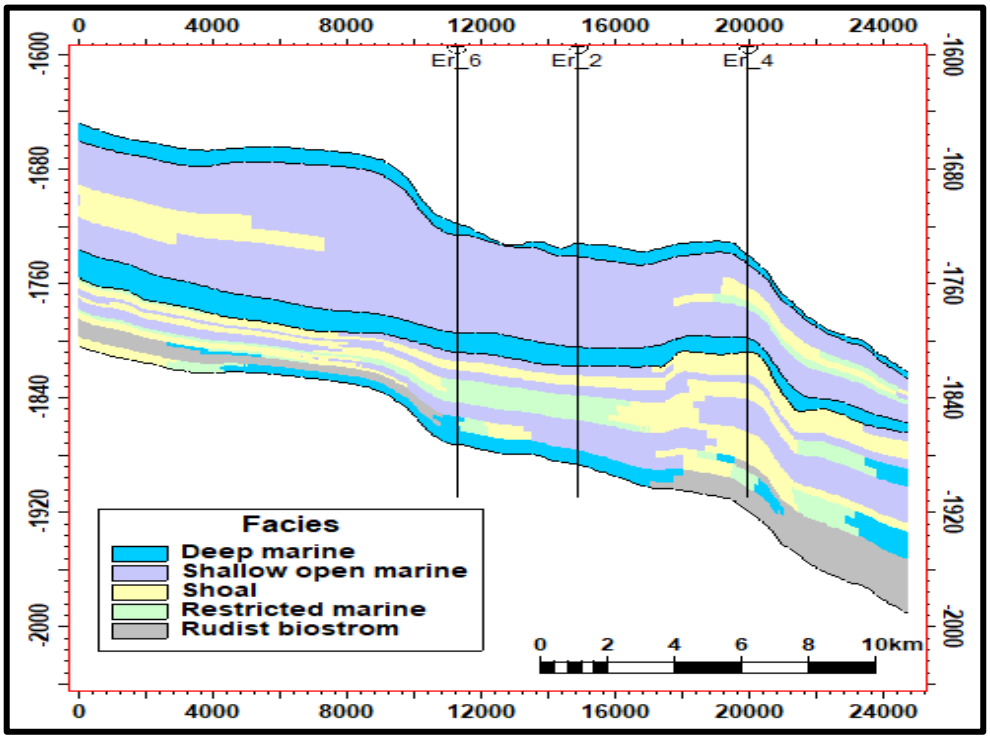

Figure (2-7) A cross section showing the sedimentary environments of the Mishrif Formation units for wells (6,2,4)

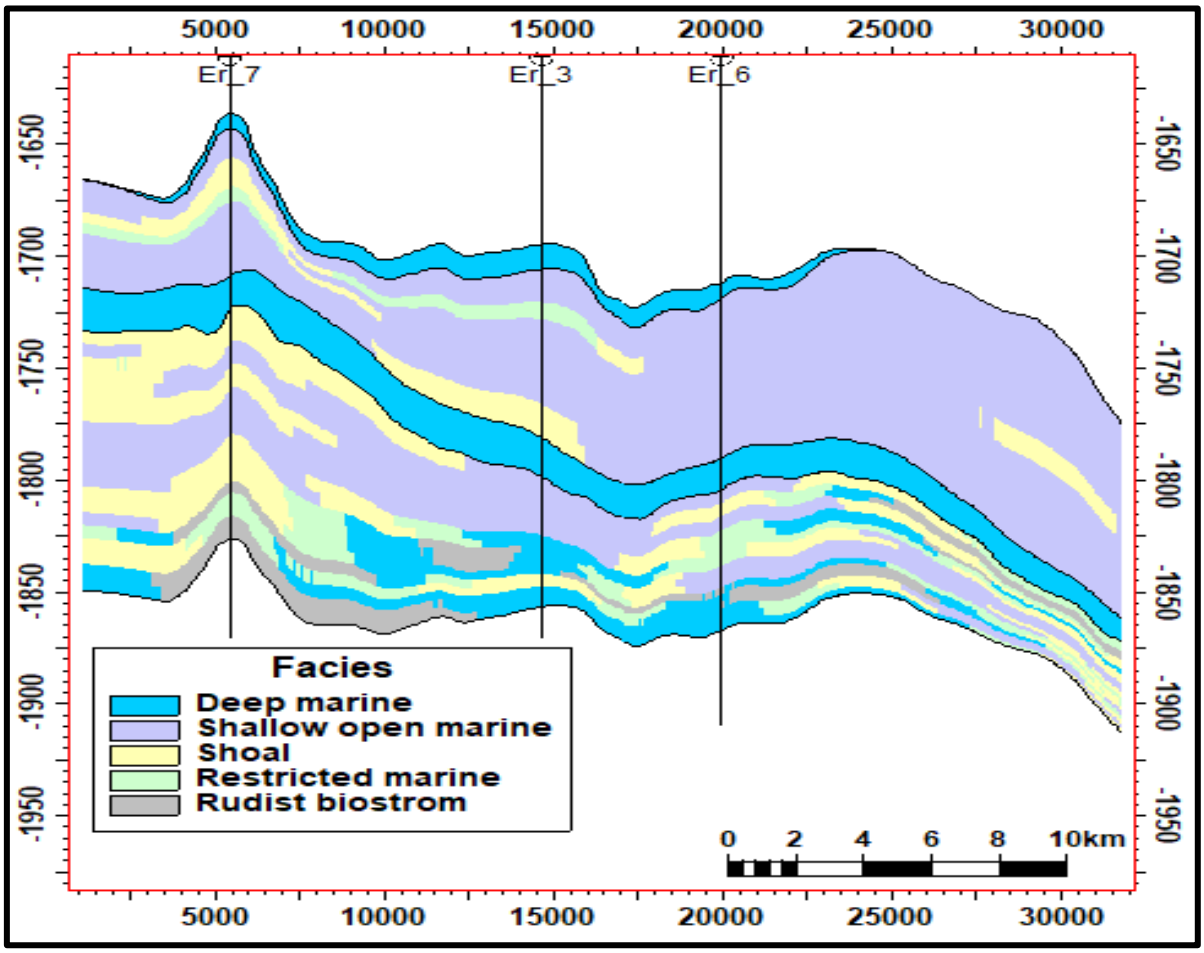

Figure (2-8) A cross section showing the sedimentary environments of the Mishrif Formation units for wells (7,3,6)

Chapter Three
Well Log Interpretation

3-1 Introduction

In this chapter, the various well logs of the study area were studied, especially with regard to the open wells, from which all the petrophysical characteristics that help in evaluating the reservoir units and then evaluating the performance of the reservoir for production were concluded. The wells of ER-1, ER-2, ER-3, ER-4, ER-6 and ER-7were also studied for the formation of the Mishrif Formation through the Tichloge ve.15 program. Table (3-1)

The ultimate aim of well log interpretation is, however, the evaluation of potential productivity of porous and permeable formations encountered by drilling. Successful logging program, along with core analysis, can supply data for the determination of the physical properties, define the lithology, identify the productive zones and accurately describe their depth and thicknesses, distinguish between oil and gas, and permit a valid qualitative and quantitative interpretation of reservoir characteristics. These petrophysical properties cannot be measured directly and, therefore, they must be inferred from the measurements of other parameters of the reservoir rocks, such as resistivity, density, and interval transit time, spontaneous potential, and natural radioactivity well-logs.

Table (3-1) tops of reservoir and cap units for Eridu oilfield

Well. ID	kifil	CR-I	MA	CR-II	MB	Rumaila
ER-1	1676.2	1695.80	1714.30	1749	1762.30	1885
ER-2	1731	1744.5	1752	1815.3	1828.72	1898
ER-3	1703.30	1717.90	1728.40	1800.70	1817.30	1879.5
ER-4	1751	1763	1769	1820.3	1832.90	1941
ER-6	1719.60	1734.5	1741	1810	1825	1889
ER-7	1639.20	1649.90	1657.60	1721.80	1739.2	1841.5

3-2 Qualitative interpretation

Qualitative interpretation is done by studying the behavior of the curves of the open well logs used in the current study. Through the (SP) log, the permeable and impermeable layers are determined, as well as determining the thickness of the layers. Since the deviation of the SP log depends on the contrast in salinity between the drilling mud infiltrate and the formation water, so it gives a negative deviation in the case of the mud filter less salinity than the formation water, while it gives a positive deviation when the formation water is fresh (Schlumberger, 1989). Since the study formation is under great depths and its water content is salty, the (SP) deviates in a negative left direction against the permeable layers and towards the hale base line against the impermeable layers.

As for the (GR) log, which measures the content of shales in the formation, this is because the radioactive elements tend to be concentrated in mud and shales, while clean formations have a low concentration of radioactive elements (Schlumberger, 1989), we notice through the behavior of the (GR) log in wells Study area: The Mishrif Formation is considered one of the clean formations because the log's readings are few in some areas of the cover rocks that contain a percentage of shale.

The well log, Caliper logs, can also be used to determine the permeable areas in the formation, as this log is used to measure the diameter and shape of the well with depth. Through the change in the reading of the log, it is possible to identify the areas of collapse and the occurrence of cavities (caving), especially against the layers of the shale.

As for the neutron log, it is used in qualitative and quantitative interpretations, mainly in giving an image of the formation pores and determining their porosity directly. And since the neutron log is designed to specifically sense the hydrogen present in the formation (Cubitt, 2015), therefore, it is possible to depend on this log to determine the porous areas in

the formation by recording high readings against the layers containing oil or water, since these fluids contain a high amount of hydrogen. A resistivity log can also be used to confirm the type of fluid that fills the pores. While the log records a low reading in front of the gas-containing layers in the pores of the rocks because it contains a small amount of hydrogen compared to oil and water. Among its other applications, and in partnership with the density log, is the determination of the rockiness in the formation of the Mishrif, which is represented by calcareous limestone with the overlapping of dolomitic limestone at some depths.

As for resistivity logs, which are a function of the type of rock fluid (Asquith and Krowski 2004), resistivity logs are used to determine the watER-bearing and hydrocarbon-bearing regions, that is, they are used to indicate the permeable regions. (Figs 2-3,2-4 and 2-5)

3-3 Borehole Environment

A tool that is attached to a wireline or cable is lowered into a borehole to measure the reservoir's parameters. Drilling mud with an oil or water base, air, or both, may be used to fill the borehole. Drilling mud intrudes into the rock around the borehole during the drilling operation, which has an impact on logging measures and the flow of fluids into and out of the formation. While logging and analyzing logs, each of these considerations must be made. Understanding the well-log environment and the following elements is crucial, including the uninvaded zone, flushed zone, invaded zone, mud cake, and mud filtrate (Hilliburton, 2001).

The rock-fluid system, which is affected when a hole is bored into a formation, changes in the area around the borehole. The drilling fluid contaminates the borehole and the rock around it, which has an impact on the logging measures (Asquith &Krygowski, 2004). Figure displays a few of the more significant symbols (3-1).

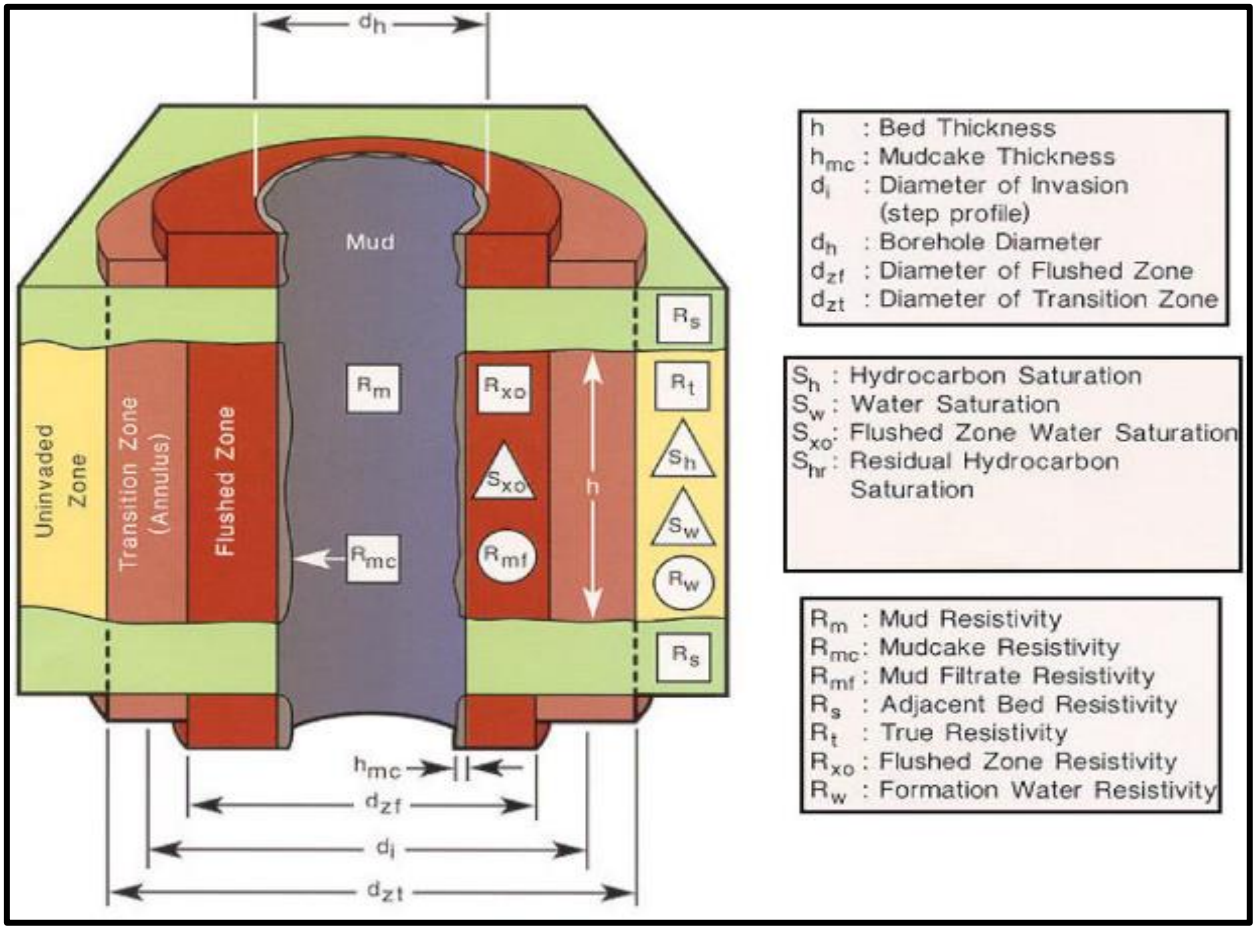

Figure (3-1) Borehole environment (Hilliburton,2001)

Probe behavior and qualitative interpretation in the study wells:

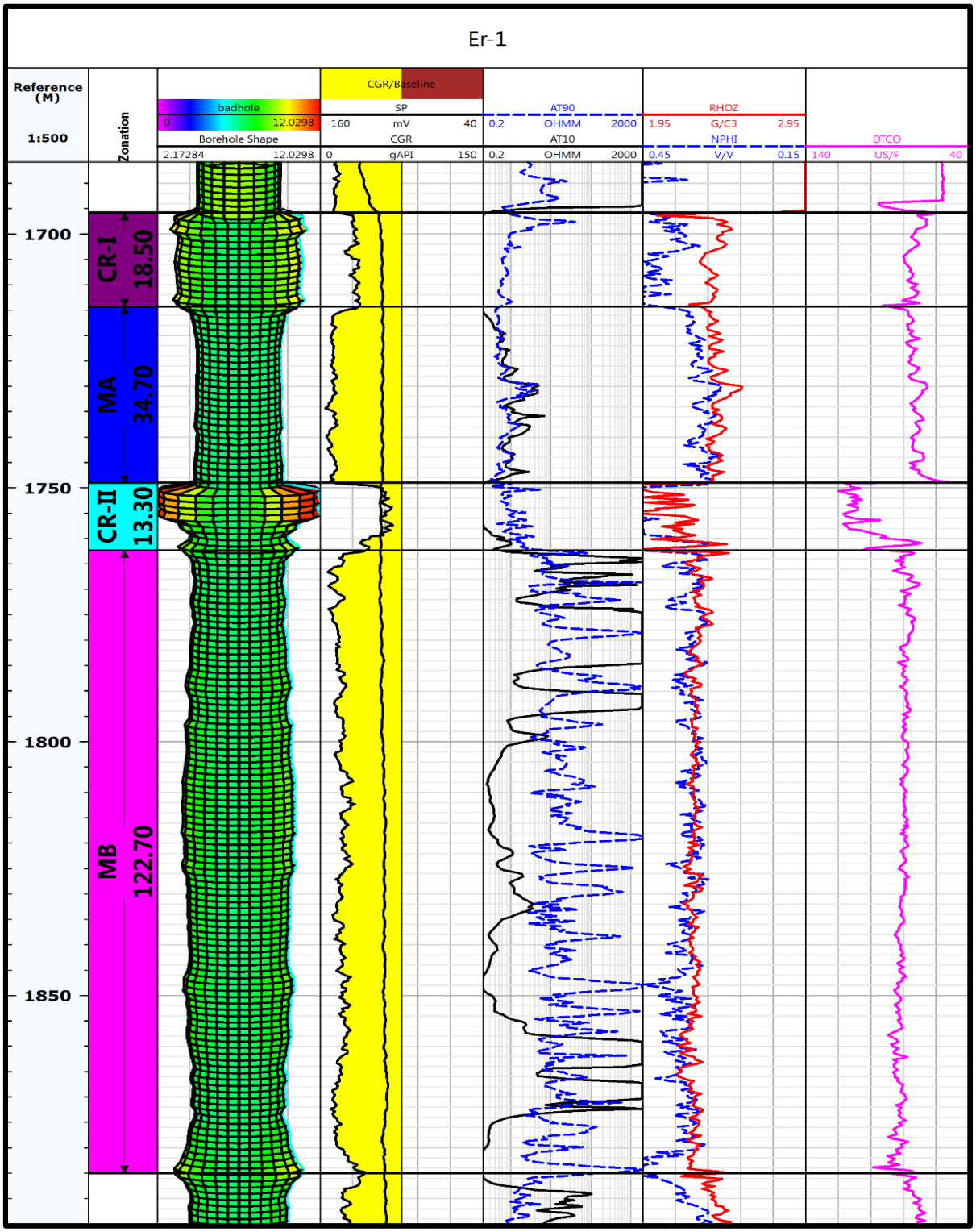

Figure (3-2) Qualitative interpretation of Mishrif Formation in the for well ER-1

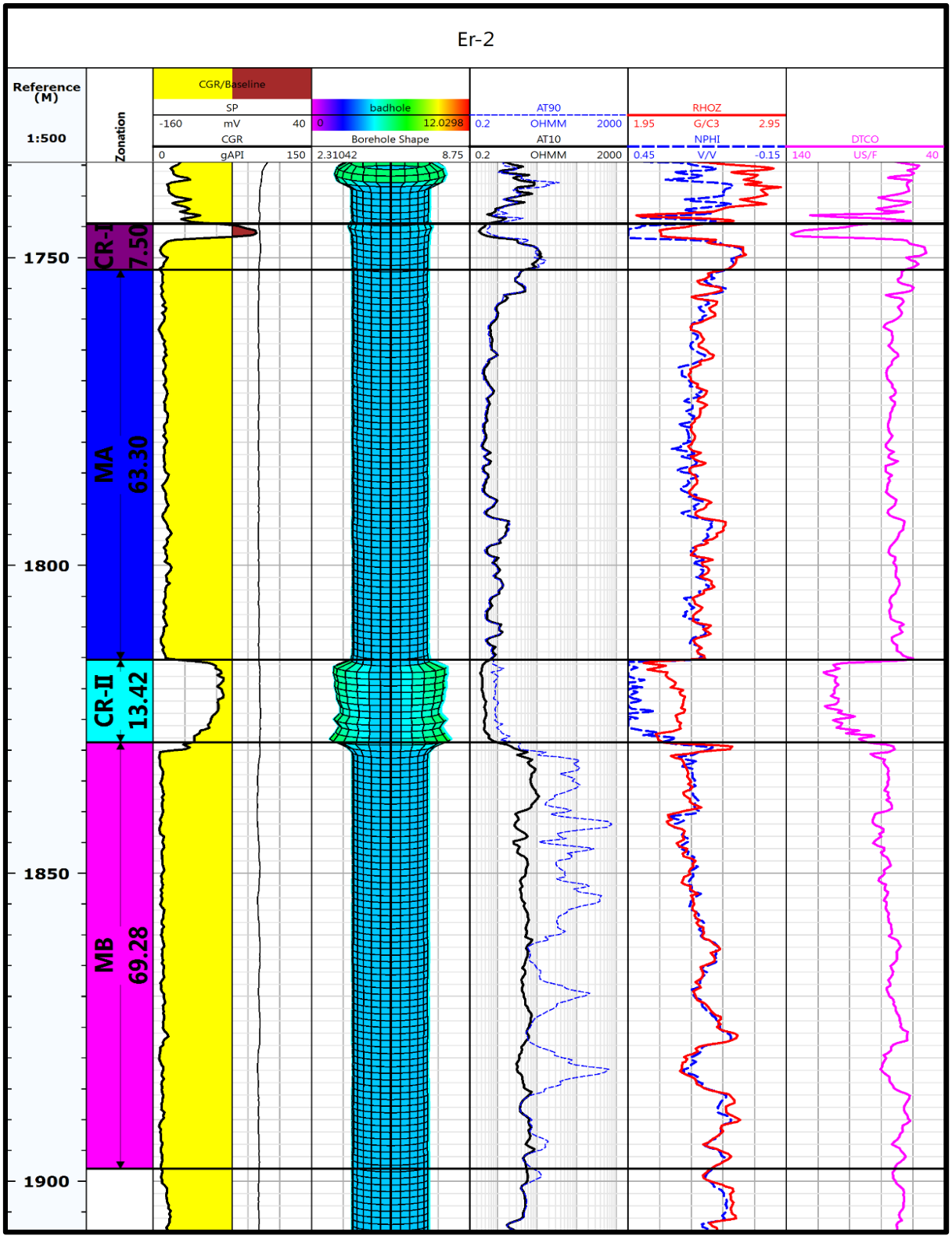

Figure (3-3) Qualitative interpretation of Mishrif Formation foe well ER-2

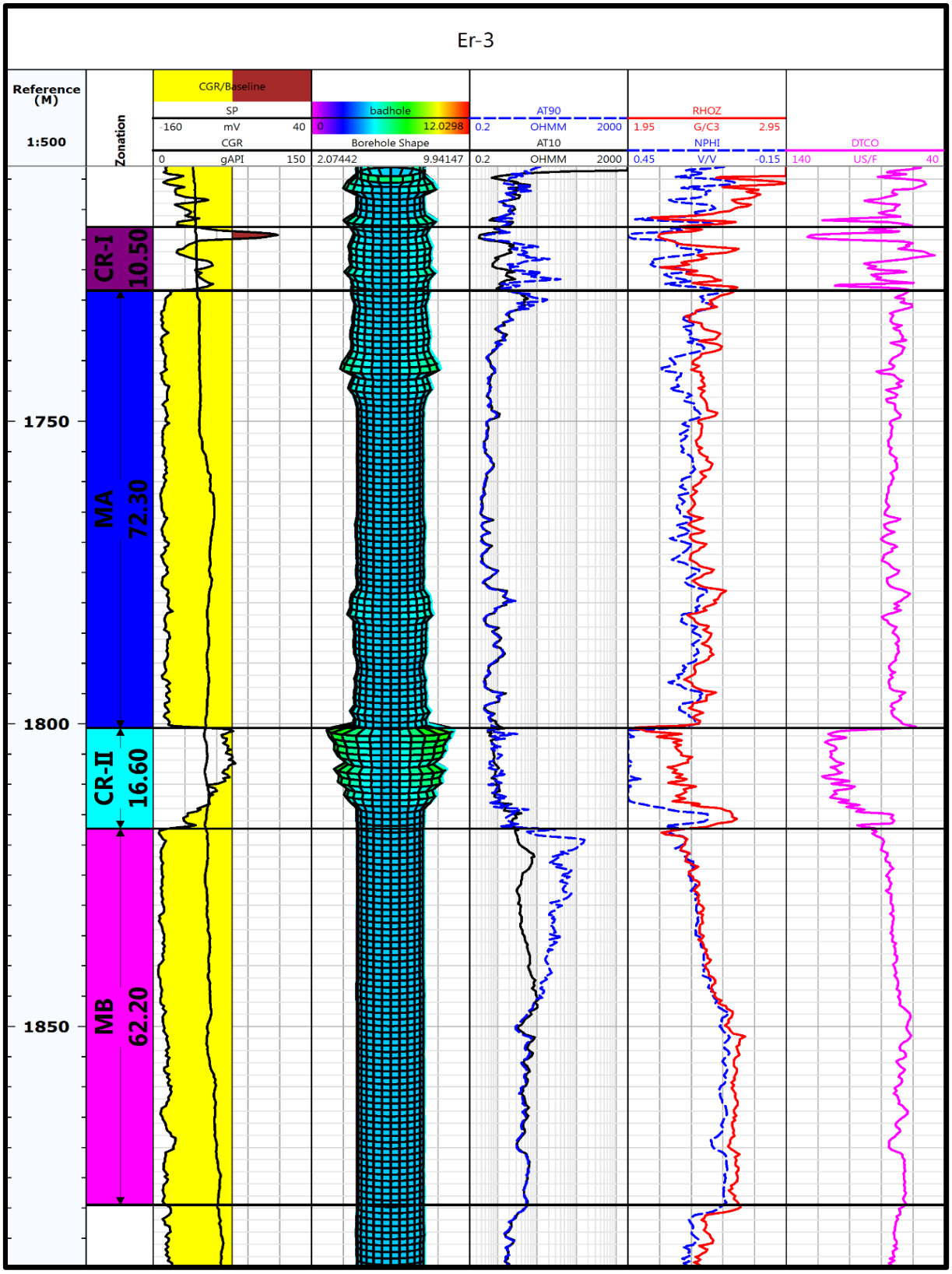

Figure (3-4) Qualitative interpretation of Mishrif Formation for well ER- 3

3-4 Quantitative interpretation includes

3-4-1 Determining the volume of oil shale

The presence of shale rocks in the formation affects the petrophysical properties of the reservoir such as total and effective porosity and water saturation. Therefore, it is necessary to calculate the volume of shale in the formation. It was calculated through the (GR) log, which is the best in calculating the volume of oil shale due to its sensitivity to fine radioactive materials concentrated in shale rocks. Shale Volume Determination (Asquith and Krygowski, 2004)

$$V_{Sh} = 0.33 \times (2^{(2 \times IGR)} - 1) \qquad (3\text{-}1)$$

The log size, gamma radiation coefficient (IGR) must be calculated by the following equation: (Asquith and Krygowski, 2004)

$$I_{GR} = \frac{GR_{Log} - GRmin}{GR_{mix} - GRmin} \qquad (3\text{-}2)$$

I_{GR} = gamma ray index.

GR_{log}= gamma ray reading by log *(API).*

GR_{min}= minimum gamma (clean sand or carbonate).

GR_{max}= maximum gamma ray (shale).

And depending on the volume of oil shale extracted from equation (1-2) for each well, areas free of oil shale were determined in which the value of (V_{Sh}) is less than (10), and areas containing oil shale (not clean) then the value of (V_{Sh}) is greater than or equal to (10%).

3-4-2 Calculating Porosity

Calculating Porosity is the most important characteristic of a reservoir rock as it is a measure of the hydrocarbon storage capacity (Lucia 2007). There are several ways to calculate it, either by analyzing the underlying data or through investigation data.

3-4-2-1 Neutron log Porosity:

The neutron log is used in qualitative and quantitative interpretations, mainly in giving an image of the formation pores and determining their porosity directly. And since the neutron log is designed to specifically sense the hydrogen present in the formation (Cubitt, 2015), therefore, it is possible to rely on this log to determine the porous areas in the formation by recording high readings against the layers containing oil or water, since these fluids contain a high amount of hydrogen. A resistivity log can also be used to confirm the type of fluid that fills the pores. While the log records a low reading in front of the gas-containing layers in the pores of the rocks because it contains a small amount of hydrogen compared to oil and water. Among its other applications, and in partnership with the density log, is the determination of the rockiness in the formation of the Mishrif, which is represented by calcareous limestone with the overlapping of dolomitic limestone at some depths.

As for resistivity logs, which are a function of the type of rock fluid, resistivity logs are used to determine the watER-bearing and hydrocarbon-bearing regions, that is, they are used to indicate the permeable regions.

The neutron log directly measures the porosity of the shale-free depths. As for the shale-containing depths, the (Tiab and Donaldson ,2004) equation was used:

$$\emptyset_{Nc} = \emptyset_{N} - (\emptyset_{N(sh)} \times V_{sh}) \qquad (3\text{-}3)$$

$\emptyset_N$: porosity derived from neutron Log

$\emptyset_{Nc}$: porosity derived from neutron Log and corrected by the effect of the shale

$\emptyset_{N(sh)}$: Neutron porosity of the adjacent shale

Vsh: is the shale volume

3-4-2-2 Sonic Log Porosity:

A sonic log is a type of porosity log that estimates the time it takes for a compression sound wave to travel through the foot of a formation. One or more sound transmitters and two or more receivers form a sound recording device. Borehole compensation equipment is used in the modern sound protocol (BHC). These devices significantly reduce the disturbing effects of borehole size variations and errors caused by sonic tool tilt. (Schlumberger, 1972). The reciprocal of the compression sound velocity in feet per second is the interval time (Δt), in microseconds per foot. Interlayer transit time (At) is affected by lithology and porosity. Therefore, the matrix velocity of the formation (Table 3-2) (Badr, 2022)

Through the sonic log, the porosity was calculated as in the equation (Wyllie et al. 1958), which uses shale-free depths in (Clean Zone)

$$\emptyset_S = 1 - \frac{\Delta tlog - \Delta tma}{\Delta tf - \Delta tma} \qquad (3\text{-}4)$$

Where:

$\emptyset_S$: porosity derived from Sonic Log

Δt_{log}: The transmission distance of the sonic wave from the sonic log is measured (μsec / ft)

Δt_{ma}: The transition interval of the vector through the matrix (μsec / ft) by using the table (3.2) (Schlumberger, 1972).

Δt_f: The transition time interval of the wave through the fluid and is measured depending on the type of mud if the mud is salty (185μsec / ft) and if the mud is fresh (189μsec / ft)

Table (3-2): Sonic velocity and interval time for different matrices. These constants are used in the sonic porosity formula above (Schlumberger, 1972).

Lithology/Fluid	Matrix Velocity ft/sec	Δt_{matrix} or Δt_{fluid} (Wyllie) µsec/ft (µsec/m)	Δt_{matrix} (RHG) µsec/ft(µsec/m)
Sandstone	18,000 -19,500	55.5 - 51.0 (182 - 186)	56(184)
Limestone	21,000 -23,000	47.6 (156)	49(161)
Dolomite	23,000 -26,000	43.5 (143)	44(144)
Anhydrite	20,000	50.0 (164)	
salt	15,000	66.7 (219)	
Casing(iron)	17,500	57.0 (187)	
Freshwater mud filtrate	5,280	189 (620)	
Saltwater mud filtrate	5,980	185 (607)	

3-4-2-3 Density log porosity:

Density is measured in grams per cubic centimeter g/cm3 and is indicated by the Greek letter ρ. Two separate density values are used by the density log: the bulk density (ρ_b or RHOB) and the matrix density (ρ_{ma}). The bulk density is the density of the entire formation (solid and fluid parts) as measured by the logging tool. The matrix density is the density of the solid framework of the rock.

Porosity is derived from the bulk density of clean liquid-filled formations when the matrix density ρma and the density of the saturating fluids ρf are known (Asquith and Krygowski, 2004): Porosity can also be calculated using the density log, which is one of the porosity logs. Wiley's equation (Wiley et al., 1958):

$$\emptyset_D = \frac{(\rho ma - \rho b)}{(\rho ma - \rho f)} \qquad (3\text{-}5)$$

$\emptyset_D$ = porosity measured from Density log.

ρ_{ma} = Density of the dry rock (g/cm^3)

ρ_f = Density of fluid (g/cm^3)

ρ_b = The total density of formation is taken from the log reading and measured in units (g/cm^3).

Taking into account that the porosity of the fill is equal to 2.71 (g/cm^3) because in this study the formation is limestone, and a value equal to 1 (g/cm^3) for fresh water or 1.1 (g/cm^3) for salt clay.

3-4-3 Neutron-Density cross plot for lithology identification

Neutron- Density crossplots help determine the lithology of pure lithology's such as sandstone, limestone, or dolomite, which are oil- or water-filled formations. If the formation is heterogeneous, such as for dolomitically cemented sandstone, density-neutron crossplot analysis can be misleading (Hartmann and Beaumont, 1999).

Neutron- Density multi-crossing plots for many wells, marked with red dots, showing the best match for the set of points Figures (3-5) to (3-7), most of which lie on the limestone curve in units of (CRI, MA, CRII and MB), which are the main components of Mishrif Formation lithology. There are fewer points distributed on the dolomite and sandstone curves in Eridu oilfield.

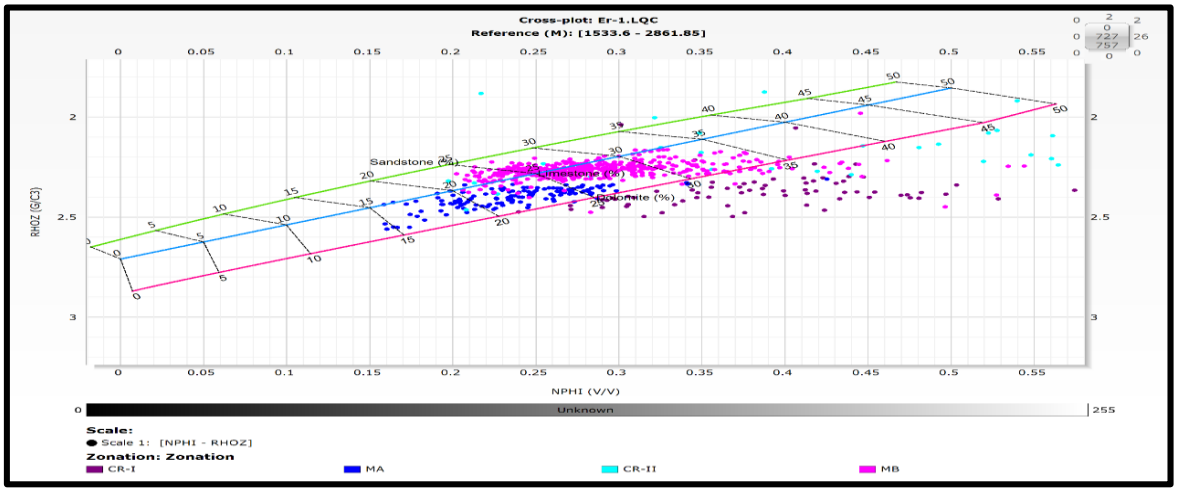

Figure (3-5) Shows the crossplot of Neutron log and Density log for well ER-1

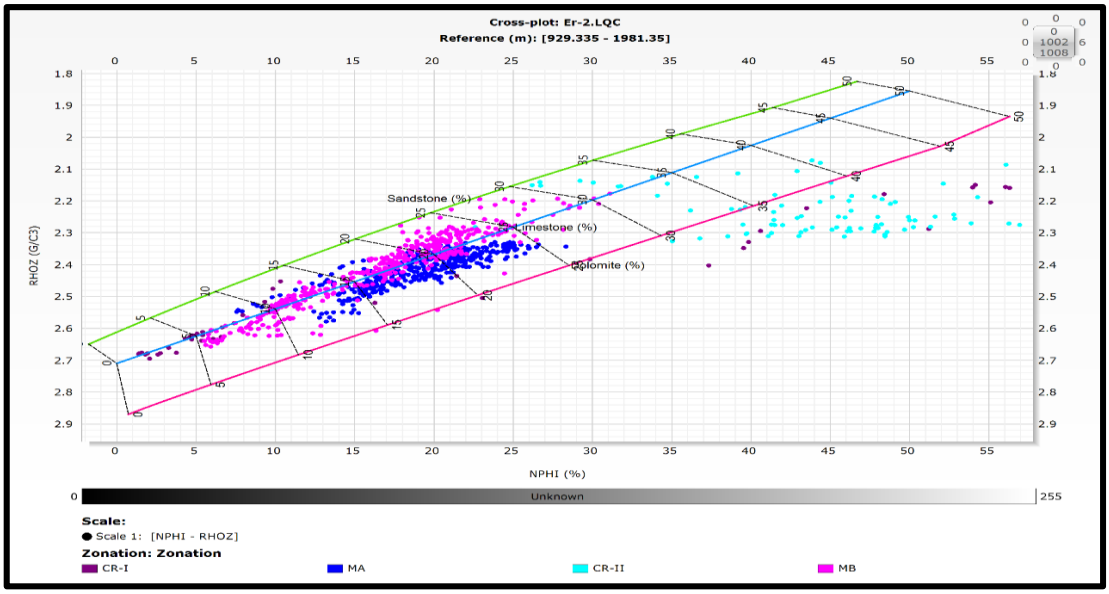

Figure (3-6) Shows the crossplot of Neutron log and Density log for well ER-2

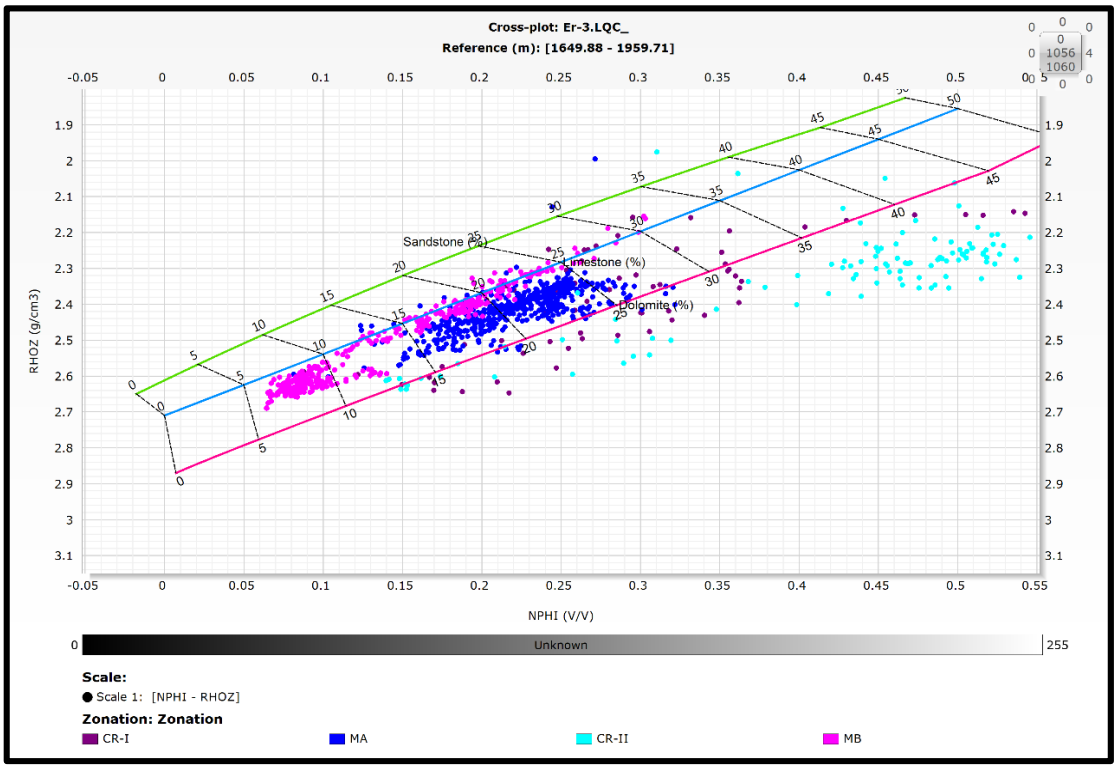

Figure (3-7) Shows the crossplot of Neutron log and Density log for well ER-3

3-4-5 Determination porosity

Porosity is defined as the ratio of the pore volume (or void space) to the total volume (volume) of a reservoir rock as a percentage. Pore volume is the total volume of all pore spaces in a given reservoir rock (Dandekar, 2013). This important reservoir rock property has been symbolized and expressed mathematically as follows:

$$\emptyset = \frac{pore\ volume}{total\ or\ bulk\ volume} \qquad (3\text{-}6)$$

3-4-5-1Total porosity

The total porosity (PHIT) was calculated using the equation (Schlumberger, 1997): It is possible to determine the total porosity through density and neutron logs for depth periods containing less than (10) the percentage of shale rocks using the (Schlumberger, 1997) equation:

$$\emptyset_T = \frac{\emptyset N + \emptyset ND}{2} \qquad (3\text{-}7)$$

$\emptyset_T$: The total porosity, calculated from the density and neutron logs, for the oil and gas carrier regions.

Table (3-3) The classification of porosity according to (Leverson, 1972)

Type of porosity	%
Negligible	**0-5**
Poor	**5-10**
Fair	**10-15**
Good	**15-20**
Very good	**20-25**

3-4-5-2 Effective porosity

The pore volume associated with a reservoir or void space that facilitates fluid flow or penetration. Isolated pores and pore volume occupied by water adsorbed on clay particles or other particles are not included in the effective porosity. Total porosity is the total amount of free space in a rock, whether or not it facilitates fluid flow. Usually, the effective porosity is smaller than the total porosity (Schlumberger, 1998).

Effective porosity (PHIE) is calculated by subtracting the volume filled with clay and bound water from the total porosity, which is always less than or equal to the total porosity depending on the amount of shale (Cannon, 2016).

$$\emptyset_{E} = \emptyset_{T} \times (1 - V_{SH}) \qquad (3\text{-}8)$$

$\emptyset_T$: The total porosity

$\emptyset_E$: The effective porosity

V_{sh}: Volume of shale

3-4-5-3 Secondary porosity:

Porosity that develops inside a reservoir after deposition is known as secondary porosity. Secondary porosity index (SPI) measurements show that the secondary porosity in the Mishrif reservoir is too small or insignificant, vuggy or fracture secondary porosity (Bowen, 2003).

$$SPI = \emptyset_{T} - \emptyset_{sonic} \qquad (3\text{-}9)$$

After the deposit of sediments, geological processes (diagenesis) produce the secondary porosity (Tiab and Donaldson, 2004). It comprises fracture gaps developed in fractured reservoirs or vugular spaces produced in carbonate rocks by the chemical process of leaching (Ezekwe, 2010).

While having somewhat higher values in some Mishrif Formation intervals, the overall porosity continues to be the greatest. These periods of increased secondary porosity indicate that dolomitization and dissolution, two digenesis processes, have an impact on the porosity of the Mishrif Formation.

3-4-6 Determination of Archie's parameters using Pickett's method

Pickett's (1966) suggested a method that depends on a cross plot between resistivity vs. porosity to calculate (m) and/or (a) from well logs. The following logic describes this method. According to Pickett (1966):

$$R_t=\frac{a}{\emptyset^m}\times\frac{R_w}{S_w^n} \qquad (3\text{-}10)$$

Where,

S_w: is the water saturation (fraction),

R_w: is the water resistivity (ohm-m),

$\emptyset^m$: is the porosity (fraction)

R_t: Resistivity of uninvaded zone (ohm-m), and, a, n, and m: Archie's parameters (dimensionless).

In a watER-bearing zone $S_w = 1$; Equation (3-11) is an equation of a straight

line on log-log plot, where m is the slope and (a.Rw) is the intercept at $\emptyset$=1. As R_w is known from other sources, (a) may be easily found.

$$\log R_t = -mlog(\emptyset) + \log(a \times R_w) - n\log(S_w) \qquad (3\text{-}11)$$

In a watER-bearing zone $S_w = 1$; thus Eq. (3-12) may be reduced to:

$$\log R_t = -mlog(\emptyset) + \log(a \times R_w) \qquad (3\text{-}12)$$

Archie's parameters obtained by Pickett's plot for Wells ER-1, ER-2, Er,3, ER-4, ER-6 and Er,7 (a=1, m=1.94, n=2) either value (Rw=0.027). The figures (3-8, 3-9,3-10 and 3-11) show the results of pickett plot in all study wells.

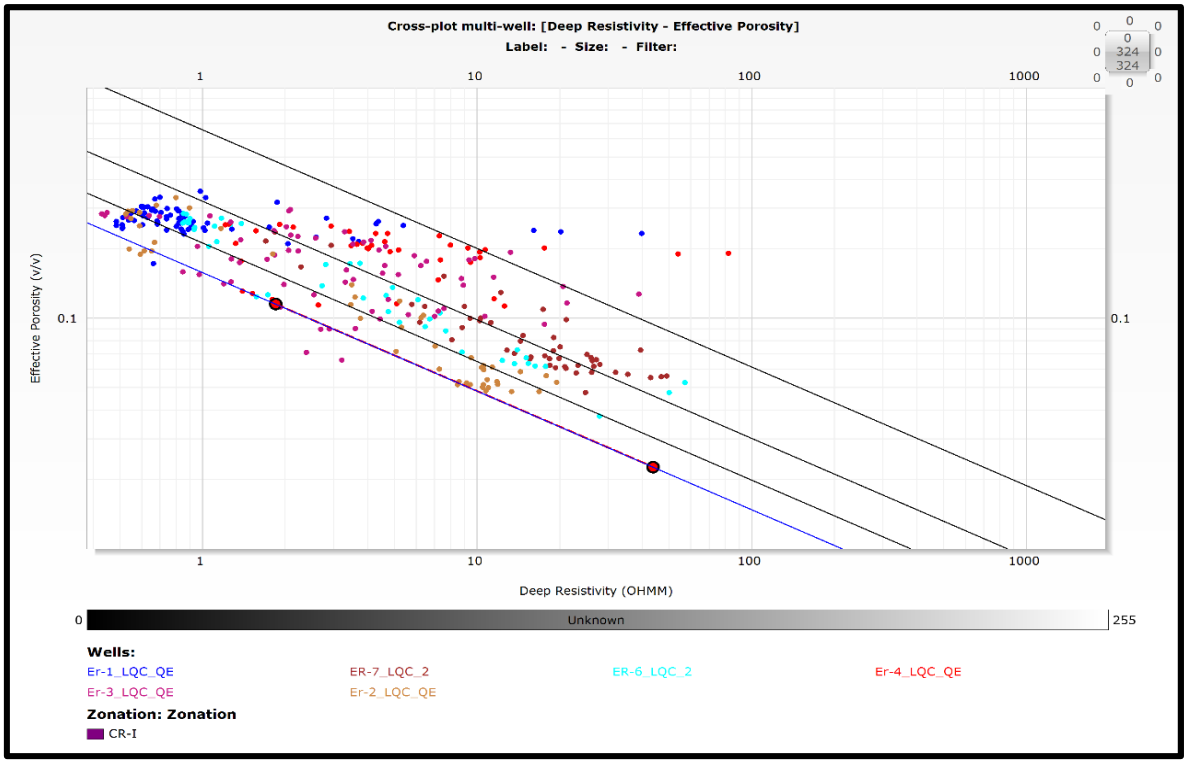

Figure (3-8) Shows the crossplot of Deep Resistivity and Effective Porosity in all wells of the study unit (Cr-I)

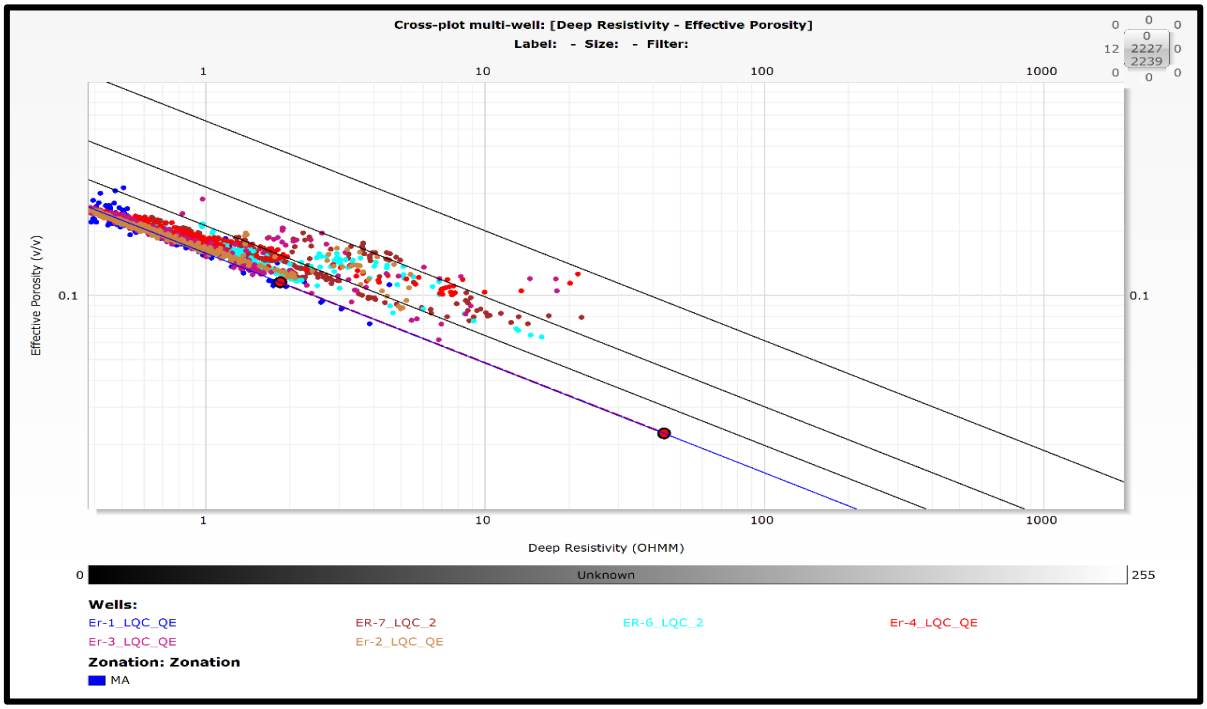

Figure (3-9) Shows the crossplot of Deep Resistivity and Effective Porosity in all wells of the study unit (MA)

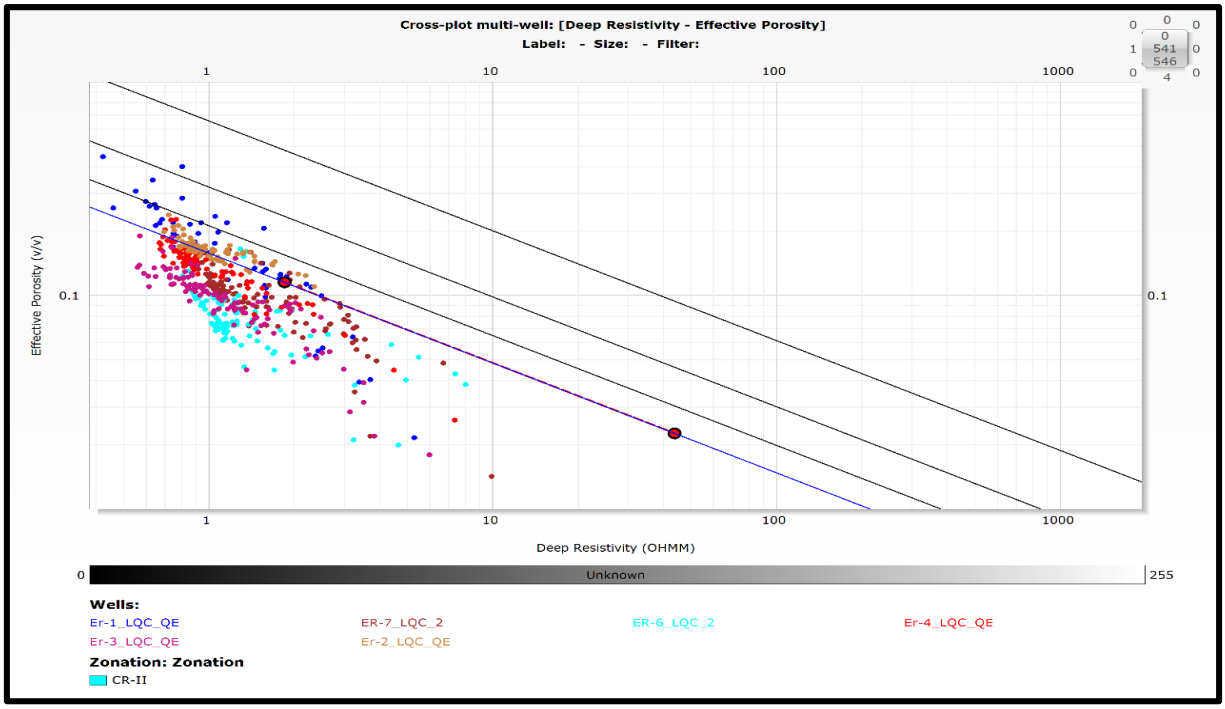

Figure (3-10) Shows the crossplot of Deep Resistivity and Effective Porosity in all wells of the study unit (CR-II)

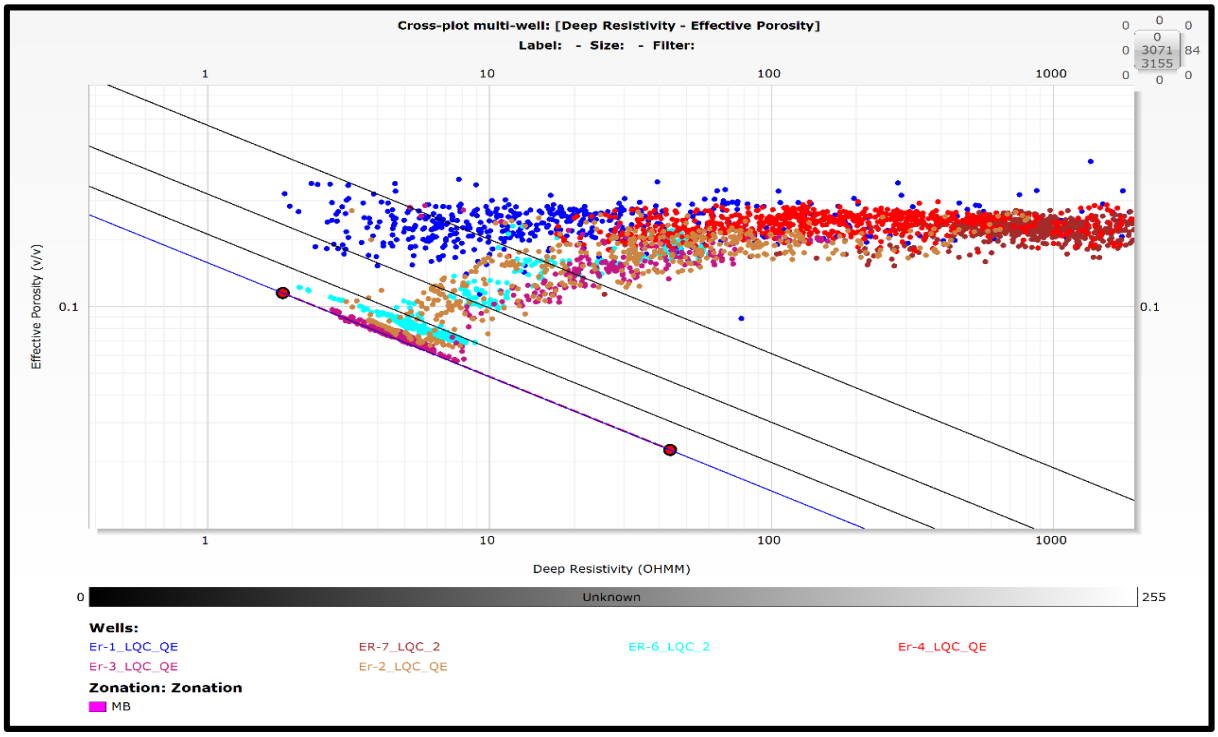

Figure (3-11) Shows the crossplot of Deep Resistivity and Effective Porosity in all wells of the study unit (MB)

3-4-7 Determination of fluid saturation:

Porosity and liquid saturation are the main reservoir properties used to estimate hydrocarbon reserves. Given the heterogeneity of most deposits, continuous plots of these attributes as a function of depth are essential for accurate assessment (AL-Mosawy, 2014)

Saturation was mainly calculated by differentiating between the different fluid components (water and hydrocarbons). After determining water saturation that is the most important step in well analysis for hydrocarbon movement. Water saturation in the uninvaded area at depths where the shale content is less than (10) was determined using Archie's equation (1942).

$$S_w = \left(\frac{FxRw}{R_t}\right)^{\frac{1}{n}} \qquad (3\text{-}13)$$

S_W: Water saturation of the uncontaminated area with the drilling mud infiltrate

F: Formation factor.

R_w: Resistivity of water formation.

$R_{t:}$ True formation resistivity.

n: Saturation exponent (assumed to be 2.0)

When the porosity and formation water are compromised by the drilling mud filter, the mud filter will replace the formation water, and accordingly, the water saturation in the flashed zone of the (Archie equation) is determined by replacing the resistance of the formation water (R_w) with the resistance of the drilling mud filter (R_{mf}). and the true configurable resistance (R_t) by the resistance in the washed range recorded from the shallow resistance log reading (R_{xo})

$$S_{xo} = \left(\frac{F \times Rmf}{R_{xo}}\right)^{\frac{1}{2}} \quad (3\text{-}14)$$

$S_{ox:}$ Water saturation of the washed area (contaminated by drilling mud filtrate)

In order to apply the Archie's equations, it is necessary to clarify how to determine their variables:

3-4-7-1 Calculating the formation factor (F)

Between Archie's (1942) that the resistance of the saturated formation (100%) water (R_{o}) is linked to the resistance of the formation water (R_w) through a constant called the formation coefficient (F)

$$R_{o} = F \times R_w \quad (3\text{-}15)$$

Archie also showed that the formation coefficient (F) is related to the formation porosity through the following equation To calculate the formation factor (F) :

$$F = \frac{a}{\emptyset^m} \quad (3\text{-}16)$$

Where:

m: Cementation factor

a: Tortuosity factor

3-4-7-2 Bulk Volume Analysis (BVW and BVXO)

Total water in the contaminated range (BV_{xo}) and non-polluted (BV_w) using the two equations below Schlumberger (1998):

$$BV_W = S_W \times \emptyset_T \quad (3\text{-}17)$$

$$BV_{XO} = S_{XO} \times \emptyset_T \quad (3\text{-}18)$$

Where:

BV_W = bulk volume of water of uninvaded zone

BV_{XO} = bulk volume of water of flushed zone

S_W = water saturation of uninvaded zone

S_{XO} = water saturation in the flushed zone

$\emptyset$ = porosity

A relationship between the total volume of water and the porosity in the carbonate rocks Table (3-5) (Asquith and Krygowski, 2004)

Table (3-5) It shows the BVW values of carbonates as a general guide to the types of porosity

Type of porosity	Bulk volume water (BVW)
Vuggy	**0.005-0.015**
Vuggy and intercrystalline (intergranular)	**0.015-0.025**
Intercrystalline	**0.025-0.04**
Chalky	**0.05**

3-5 Application of Elan Model

According to available data and Quanti's model results, the mineral and fluid components of Mishrif Formation that used in this model are selected as the following:

- Illite
- Quartz
- Calcite
- Dolomite
- Invaded water
- Uninvaded water

• Invaded oil

• Uninvaded oil

The reconstruction log for well ER-1, ER-2and ER-3 was illustrated in the figure (3-12, 3-13, 3-14). Track 1 shows the difference and matching ratio between the gamma ray log (GR) and the reconstruction gamma ray (Gr-QE), bulk density, neutron porosity, sonic log, invaded zone resistivity, and uninvaded zone resistivity, which were shown respectively in the next track to show the difference between both logs. The final track sees the percentage error of the Quanta-Elan track.

3-6 Spectrometry Log Analysis

The potassium (K), uranium (U), and thorium (Th) components of the natural gamma rays produced by a formation are separated using the natural gamma ray spectral log (Th). KUT logs are another name for these logs. The contents of KTH, U, Th, and K may also be obtained from a natural gamma-ray spectrometry log in addition to the total gamma-ray of production. The information acquired may be applied to the study of sedimentary environment and formation features. The thorium, potassium, and uranium content of the rock will be revealed in this case by the natural gamma ray spectral log. The rock is not shale if uranium is abundant and thorium and/or potassium are low. The porosity and rock type are then determined using other data, such as sonic, density and neutron.

3-6-1 The Clay Minerals Analysis:

Using typical POTA-THOR crossplots, the clay minerals were inferred from the spectral gamma ray (SGR) (Stephen, 2001). Figure (3-12) to (3-14) POTA-THOR maps a cross-section of Mishrif Illite-montmorillonite mixed layer clay and montmorillonite are the two primary clay minerals, with a little amount of

glauconitic and chlorite. The crossplots below can be used to see a variety of possible mineral pairings.

3-6-2 Analysis of the sedimentary environment

The SGR spectral gamma ray can be used to study the sedimentary environment by measuring the ratio of thorium to uranium (Th/U) (Ehrenberg, 2000). If the environment is one of continental deposition, oxidation, and weathering zone, Th/U > 7. Th/U 7 if the formation is gray shale or sea sediment. Th/U is less than 2 when the deposit is carbonate or marine black shale. As the most important Eridu formation, Mishrif is a limestone reservoir Th/U is less than 2 in a superstructure formation figure (3-12, 3-13, 3-14). which determines that the sediment is carbonate .

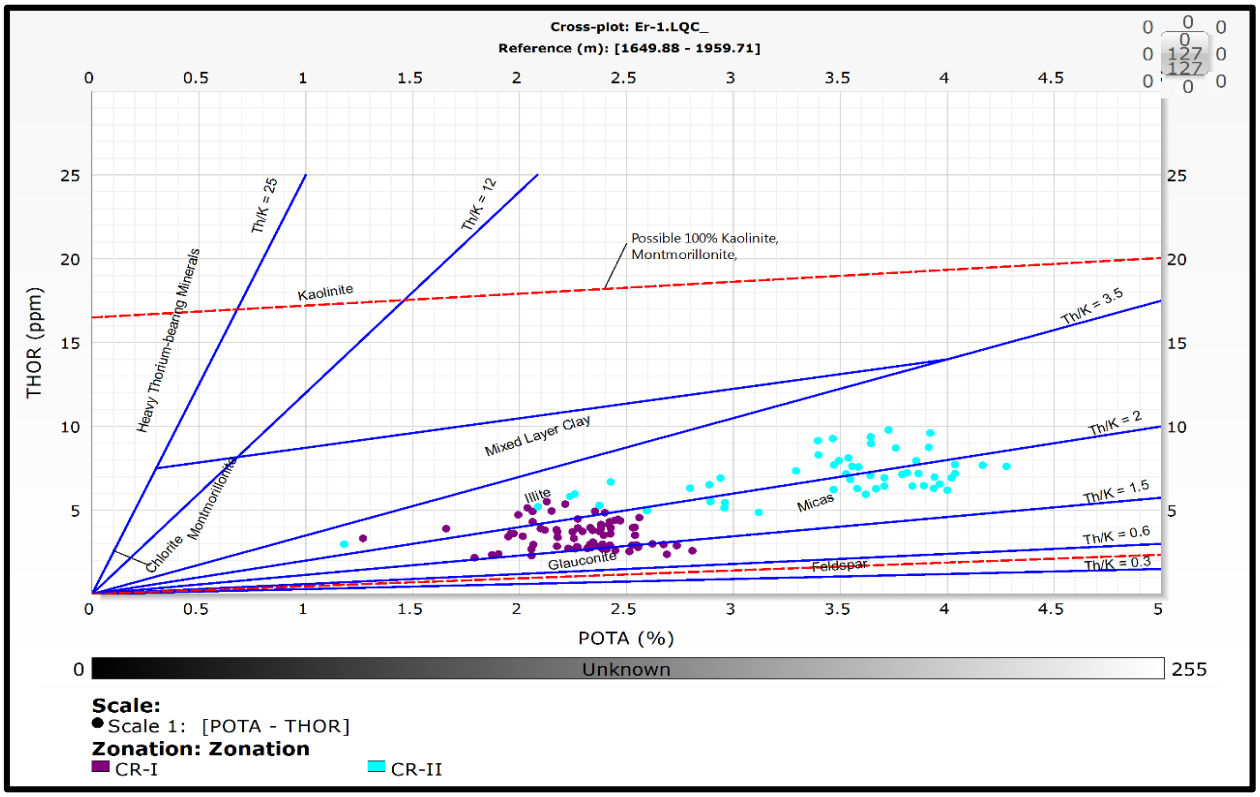

Figure (3-12) Shows the crossplot of Potassium- Thorium in ER-1 well

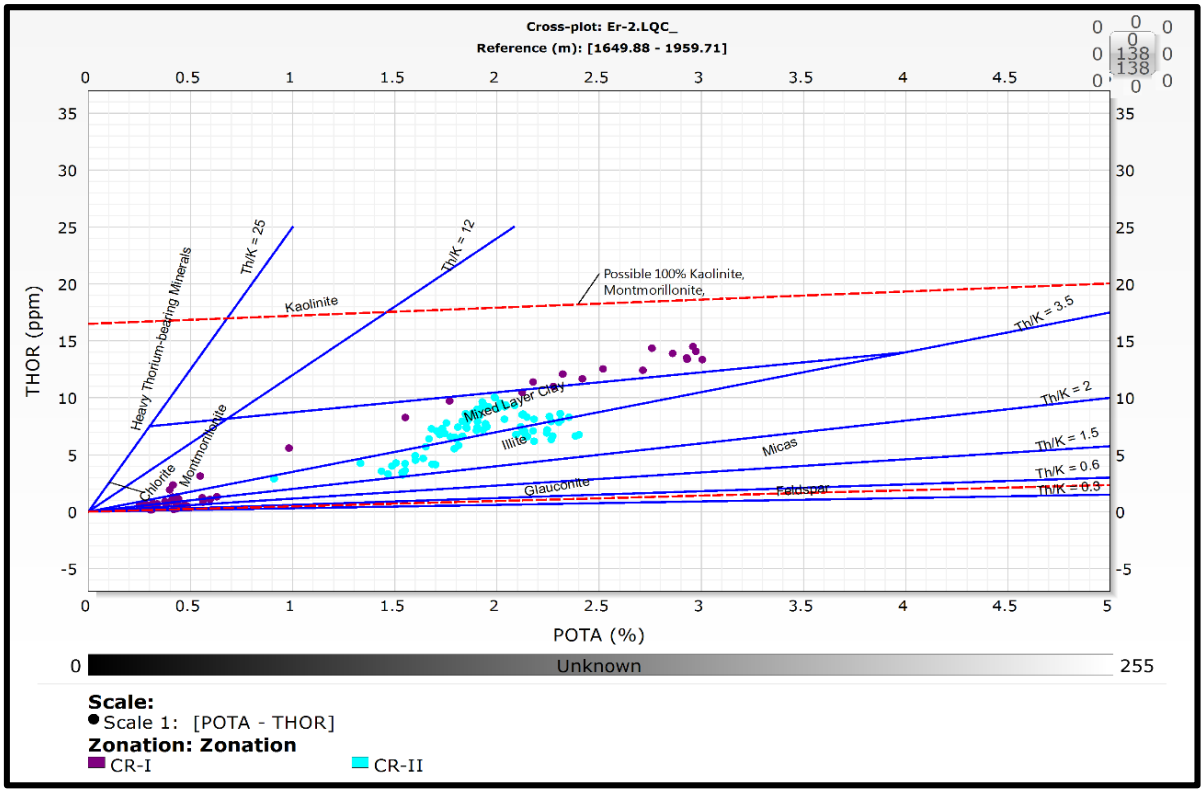

Figure (3-13) Shows the crossplot of Potassium- Thorium in ER-2 well

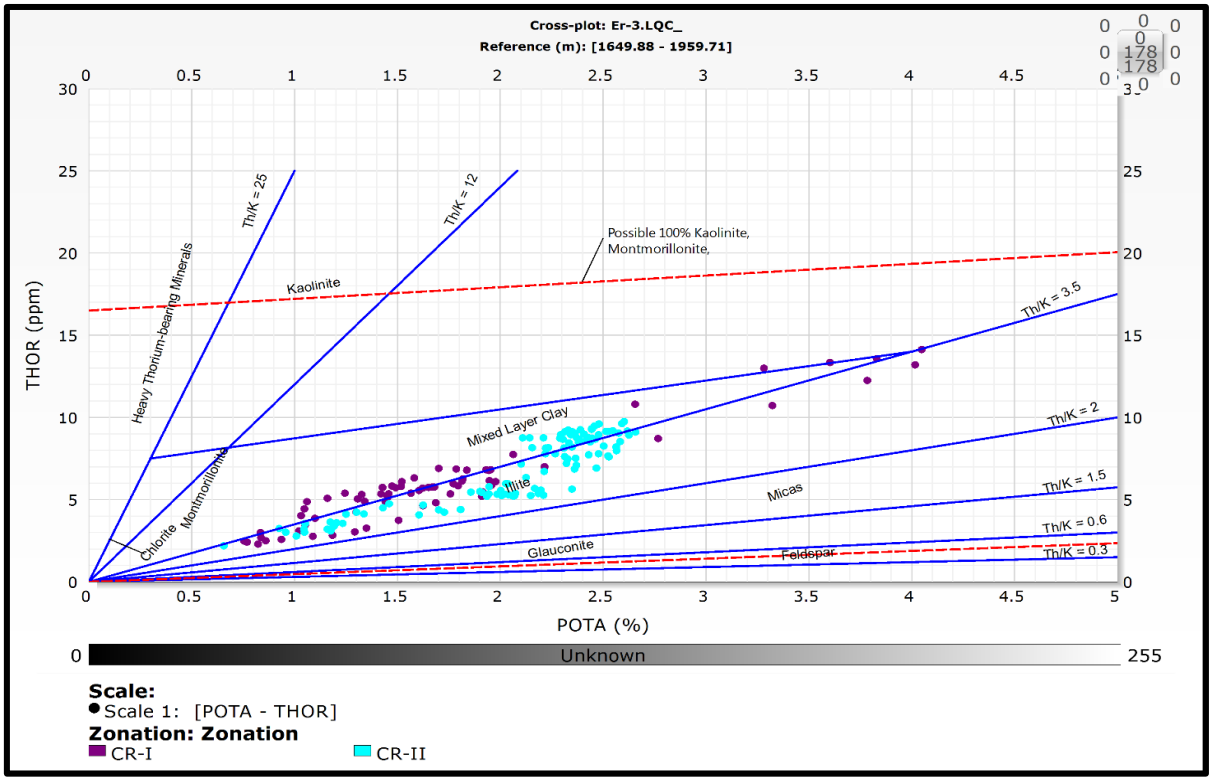

Figure (3-14) Shows the crossplot of Potassium- Thorium in ER-3 well

3-7 Reservoir units for the formation of the Mishrif

Based on the results of computer processing interpretation (Tichlog ve.15) to determine the petrophysical properties, the formation was divided into main reservoir units separated by (non-reservoir units) buffer units. As follows:

- Cape Rock (CR-I)
- Upper Mishrif Reservoir (MA).
- Cape Rock (CR-II)
- Mishrif Reservoir (MB).

The most important parameters used in the interpretation process are shale volume (VSH), effective porosity (PHIE), total porosity (PHIT), water saturation (SW), total water volume (Sxo): water saturation in the flushed zone and (BVXO) the total water volume in the uninvaded zone (BVW) All these factors affect the quality and quantity of oil in each reservoir unit, as the greater the porosity and the less water saturation, the more productive the unit will be, as all these factors affect the quality and quantity of oil in each reservoir unit, where the higher the porosity and the less water saturation the unit will be more productive.

3-7-1 Cap rocks (CR-I):

This unit has a thickness of around (6-19) meters in the Eridu oilfield wells, and it is composed of limestone shale rocks with basic reservoir characteristics. This unit exists in all study wells and shows the Mishrif Formation rock cover.

All 6 wells are having a porosity range between (0.09-0.28) for Eridu oilfield and water saturation ranges between (0.52-0.78) for Eridu oilfield.

3-7-2 Upper Mishrif Reservoir (mA).

It has a thickness of (35-72) meters in the Eridu oilfield wells, and it is composed of limestone, with minor clay content in certain wells and pure in

others. During which time weak oil evidence and oil stains occurred in Eridu-2, and the results of the analysis and interpretation of the probes revealed that it contained reservoir water in the Eridu oilfield.

a porosity ranges between (0.17-0.20) for Eridu, and water saturation ranges between (0.87-0.98) for Eridu oilfield.

3-7-3 Cap rocks (CR-II)

The thickness of this unit is around (13-20) meters in the wells of the Eridu oilfield, and it is composed of limestone rocks with a high shale percentage, with extremely poor reservoir properties. This unit can be found in all of the study's wells. This unit exemplify by porosities ranges between (0.16 and 0.25) and water saturation ranging (1.00) for Eridu oilfield

3-7-4 Lower Mishrif Reservoir (MB).

The thickness of this unit is around (62-123b) meters in the wells of the Eridu oilfield, this part of the formation is determined between the rocks of the Rumaila Formation, which is located below it, and ma layer that lies above it, in terms of the thickness of the wells in this unit of the Eridu oilfield, it will be similar to the previous unit in terms of increase and decrease**.** The highest value of porosity is in the wells ER-1 ,ER-4 and ER-7(0.24,0.24,0,22), and the lowest value in the wells ER-3 and 6 (0.11) but the water saturation highest value in the well ER-3 and 6 (0.63,0.62), the lowest value in the well ER-7 (0.03). This unit is considered the most important component in Mishrif Formation and is considered to have good characteristics for the reservoir.

figure (3-15, 3-16 and 3-17) represent the representation of (CPI) the interpretation of the probes and the petrophysical calculations of the reservoir units of the Mishrif Formation in the study wells and Tables (3-6) to (3-11) Interpretation value of Mishrif Formation in wells ER-1, ER-2, ER-3, ER-4, ER-6 and ER-7

Table (3-6) Interpretation value of Mishrif Formation in well ER-1

Well NA.	ER-1	MD	BVW	BVXO	PHIE	PHIT	SW	SXO	VSH
CR-1	MIN	1695.80-1714.30	0.00	0.17	0.17	0.23	0.10	1.00	0.00
	MAX		0.22	0.35	0.35	0.35	0.48	1.00	0.83
	AVG		0.16	0.27	0.27	0.28	0.61	1.00	0.17
MA	MIN	1714.30-1749	0.07	0.07	0.07	0.08	0.65	0.40	0.00
	MAX		0.26	0.32	0.32	0.33	1.00	1.00	0.26
	AVG		0.19	0.18	0.20	0.20	0.98	0.91	0.04
CR-II	MIN	1749-1762.30	0.02	0.02	0.02	0.12	1.00	1.00	0.00
	MAX		0.44	0.44	0.44	0.46	1.00	1.00	0.98
	AVG		0.18	0.18	0.18	0.25	1.00	1.00	0.66
MB	MIN	1762.8-1885	0.00	0.00	0.09	0.11	0.01	0.01	0.00
	MAX		0.12	0.46	0.46	0.46	0.54	1.00	0.41
	AVG		0.04	0.15	0.24	0.24	0.19	0.60	0.07

Table (3-7) Interpretation value of Mishrif Formation in well ER-2

Well NA.	ER-2	MD	BVW	BVXO	PHIE	PHIT	SW	SXO	VSH
CR-1	MIN	1744.5-1752	0.03	0.04	0.05	0.05	0.46	0.64	0.00
	MAX		0.20	0.22	0.33	0.40	1.00	1.00	0.76
	AVG		0.08	0.10	0.13	0.15	0.78	0.90	0.22
MA	MIN	1752-1815.3	0.07	0.08	0.09	0.09	0.54	0.60	0.00
	MAX		0.25	0.25	0.25	0.25	1.00	1.00	0.05
	AVG		0.19	0.19	0.19	0.19	0.97	0.98	0.00
CR-II	MIN	1815.3-1828.72	0.11	0.11	0.11	0.15	1.00	0.38	0.03
	MAX		0.24	0.20	0.24	0.32	1.00	1.00	0.77
	AVG		0.16	0.16	0.16	0.22	1.00	1.00	0.58
MB	MIN	1828.72-1898	0.00	0.05	0.07	0.07	0.02	0.26	0.00
	MAX		0.09	0.17	0.27	0.27	1.00	1.00	0.27
	AVG		0.04	0.08	0.16	0.16	0.32	0.54	0.04

Table (3-8) Interpretation value of Mishrif Formation in well ER-3

Well NA.	ER-3	MD	BVW	BVXO	PHIE	PHIT	SW	SXO	VSH
CR-1	MIN	1717.90-1728.40	0.00	0.07	0.07	0.10	0.18	0.55	0.00
	MAX		0.20	0.24	0.30	0.36	1.00	1.00	0.72
	AVG		0.08	0.14	0.18	0.20	0.54	0.83	0.42
MA	MIN	1728.40-1800.70	0.03	0.06	0.06	0.07	0.32	0.58	0.00
	MAX		0.26	0.26	0.28	0.28	1.00	1.00	0.25
	AVG		0.19	0.19	0.20	0.20	0.96	0.98	0.02
CR-II	MIN	1800.70-1817.30	0.00	0.00	0.00	0.08	1.00	1.00	0.19
	MAX		0.19	0.19	0.19	0.25	1.00	1.00	0.97
	AVG		0.10	0.10	0.10	0.18	1.00	1.00	0.76
MB	MIN	1817.30-1879.5	0.01	0.05	0.06	0.06	0.07	0.30	0.00
	MAX		0.10	0.10	0.28	0.29	1.00	1.00	0.14
	AVG		0.05	0.07	0.11	0.11	0.63	0.76	0.06

Table (3-9) Interpretation value of Mishrif Formation in well ER-4

Well NA.	ER-4	MD	BVW	BVXO	PHIE	PHIT	SW	SXO	VSH
CR-1	MIN	1763-1769	0.01	0.11	0.11	0.11	0.09	0.95	0.00
	MAX		0.14	0.25	0.25	0.28	1.00	1.00	0.39
	AVG		0.07	0.19	0.19	0.20	0.43	1.00	0.10
MA	MIN	1769-1820.3	0.03	0.10	0.10	0.10	0.28	1.00	0.00
	MAX		0.25	0.25	0.25	0.25	1.00	1.00	0.02
	AVG		0.19	0.20	0.20	0.20	0.93	1.00	0.00
CR-II	MIN	1820.3-1832.90	0.03	0.03	0.03	0.08	1.00	1.00	0.00
	MAX		0.23	0.23	0.23	0.27	1.00	1.00	0.88
	AVG		0.14	0.14	0.14	0.22	1.00	1.00	0.74
MB	MIN	1832.90-1941	0.00	0.11	0.17	0.17	0.01	0.45	0.00
	MAX		0.04	0.17	0.30	0.30	0.28	0.90	0.18
	AVG		0.01	0.13	0.24	0.24	0.06	0.57	0.04

Table (3-10) Interpretation value of Mishrif Formation in well ER-6

Well NA.	ER-6	MD	BVW	BVXO	PHIE	PHIT	SW	SXO	VSH
CR-1	MIN	1734.5-1741	0.00	0.04	0.04	0.05	0.40	0.54	0.00
	MAX		0.12	0.19	0.28	0.36	0.78	1.00	0.74
	AVG		0.17	0.11	0.15	0.19	0.55	0.81	0.34
MA	MIN	1741-1810	0.04	0.06	0.06	0.07	0.53	0.62	0.00
	MAX		0.25	0.25	0.25	0.25	1.00	1.00	0.27
	AVG		0.18	0.18	0.18	0.18	0.94	0.97	0.01
CR-II	MIN	1810-1825	0.02	0.02	0.02	0.07	1.00	1.00	0.00
	MAX		0.17	0.17	0.17	0.21	1.00	1.00	0.96
	AVG		0.08	0.08	0.08	0.16	1.00	1.00	0.79
MB	MIN	1825-1889	0.02	0.07	0.07	0.07	0.11	0.35	0.00
	MAX		0.11	0.12	0.23	0.23	0.91	1.00	0.14
	AVG		0.06	0.08	0.11	0.11	0.62	0.81	0.03

Table (3-11) Interpretation value of Mishrif Formation in well ER-7

Well NA.	ER-7	MD	BVW	BVXO	PHIE	PHIT	SW	SXO	VSH
CR-1	MIN	1649.90-1657.60	0.02	0.05	0.05	0.05	0.33	0.51	0.00
	MAX		0.13	0.15	0.24	0.24	0.72	1.00	0.21
	AVG		0.04	0.07	0.09	0.09	0.52	0.88	0.02
MA	MIN	1657.60-1721.80	0.03	0.07	0.07	0.07	0.44	0.65	0.00
	MAX		0.24	0.24	0.24	0.24	1.00	1.00	0.14
	AVG		0.15	0.17	0.17	0.17	0.87	0.97	0.02
CR-II	MIN	1721.80-1739.2	0.00	0.00	0.00	0.03	1.00	1.00	0.00
	MAX		0.19	0.16	0.16	0.24	1.00	1.00	0.93
	AVG		0.10	0.09	0.10	0.17	1.00	1.00	0.69
MB	MIN	1793.2-1841.5	0.00	0.04	0.11	0.12	0.01	0.18	0.00
	MAX		0.03	0.08	0.27	0.27	0.28	0.55	0.16
	AVG		0.00	0.06	0.22	0.22	0.03	0.27	0.03

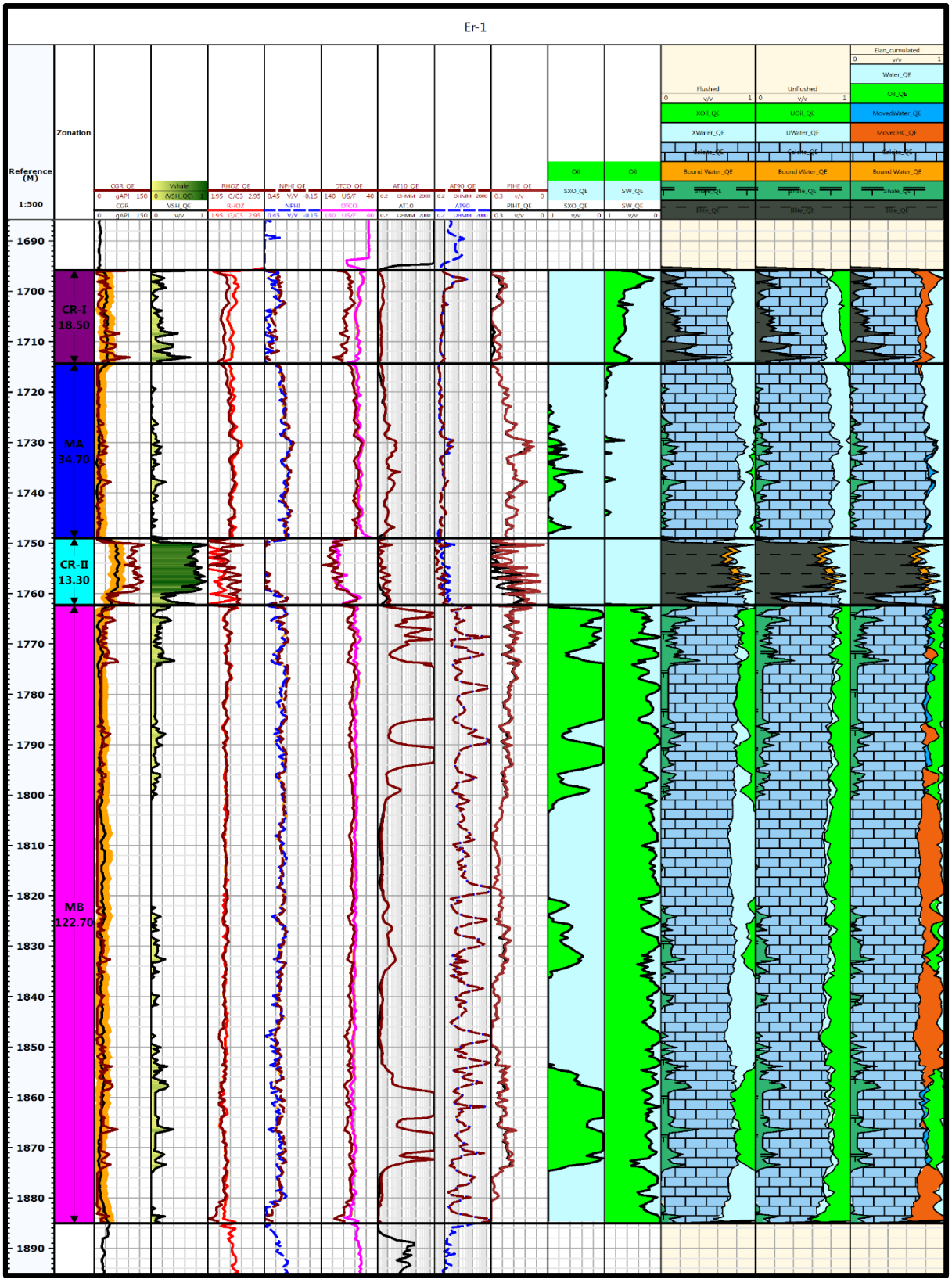

Figure (3-15) Petrophysical calculations for Mishrif Formation for well ER- 1

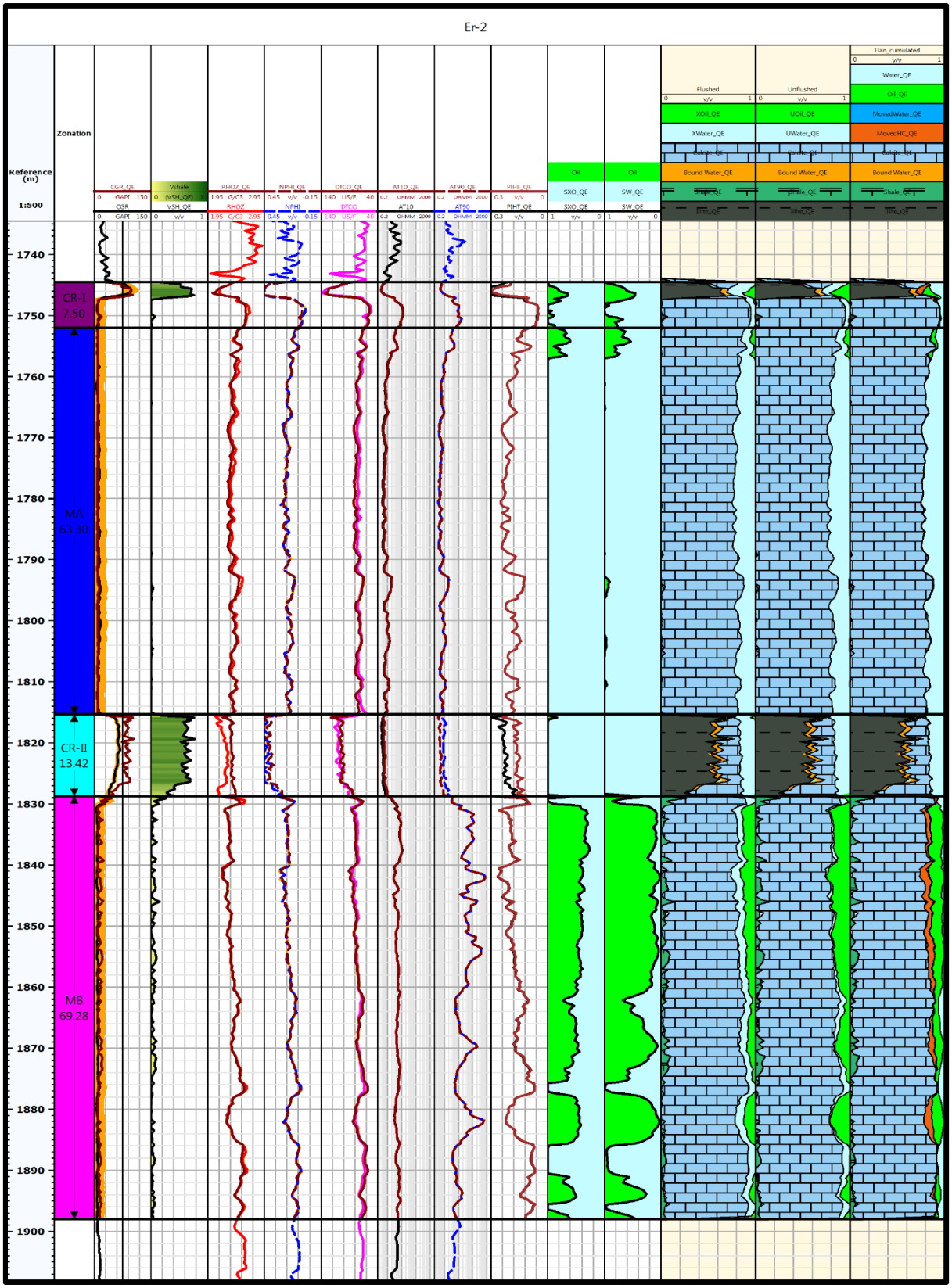

Figure (3-16) Petrophysical calculations for Mishrif Formation for well ER-2

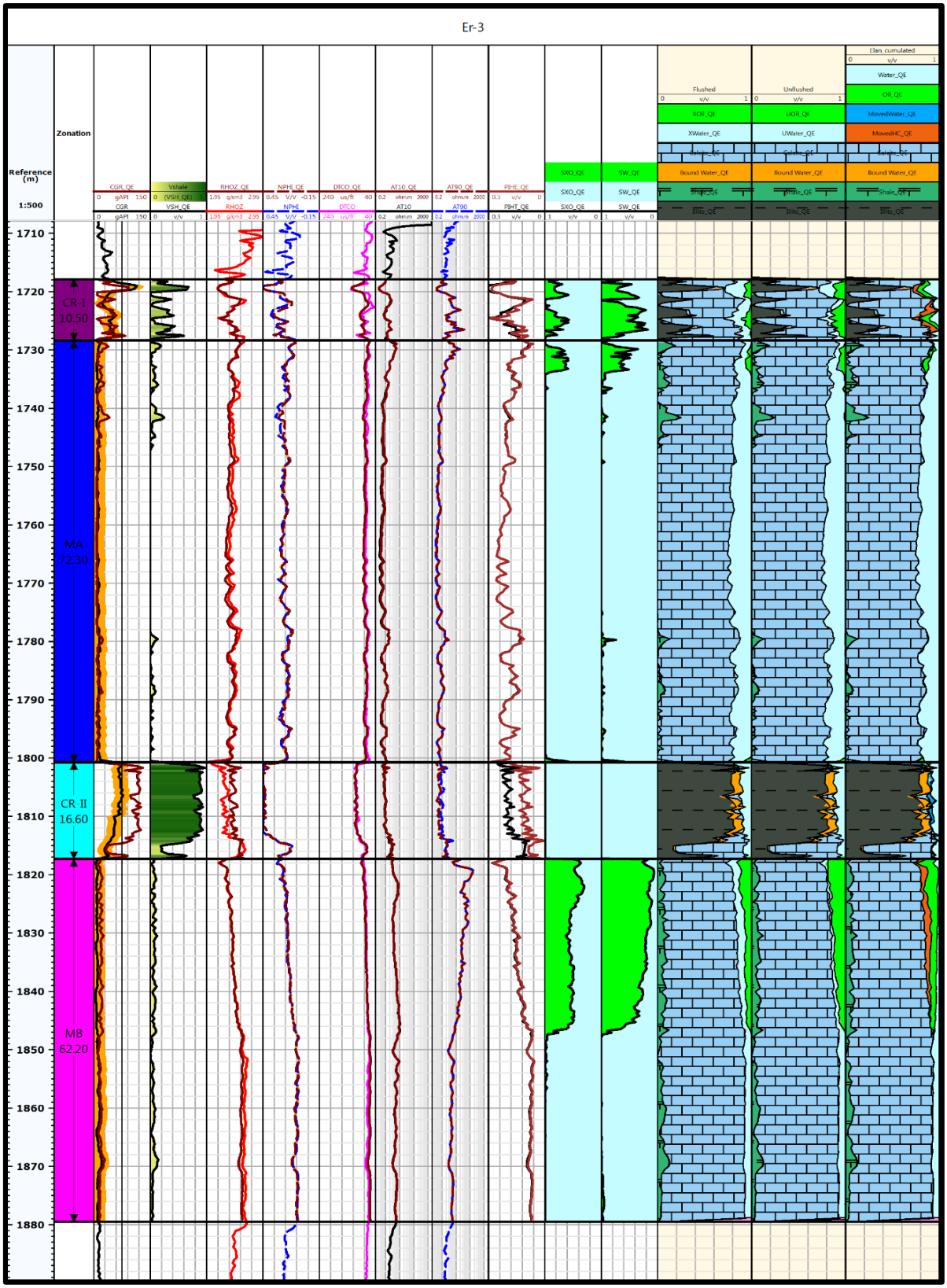

Figure (3-17) Petrophysical calculations for Mishrif Formation for well ER-3

Chapter Four
Sequence Stratigraphy

4.1 Introduction

It was vital to develop a science that compiles all of this information while also taking into consideration time. The concept of stratigraphy, which is concerned with studying the geological history of stratified rocks by dividing the rocky record and distributing rocks during time and space, is therefore the most organized and comprehensive concept of stratigraphy, and it came about as a result of the principle of convergence of evidence.

Sequence stratigraphy is the separation of sedimentary basin fill into genetic packages that are chronostratigraphic markers that characterize periods of relative sea level changes.

These genetic packages are connected by unconformities and their correlated conformities (Emery and Myer, 1996). According to (Van Wagoner et al,.1988), sequence stratigraphy is the study of rock connections within a chronostratigraphic framework of cyclic genetically linked strata.

Through the use of and integrating numerous types of data, such as seismic data, well data, and outcrop data, and taking into consideration several geologic disciplines, it has become a useful tool or strategy in petroleum exploration and reservoir characterization. The method was frequently used in shallow water carbonates as well as siliciclastic systems. The development of contemporary sequence stratigraphic ideas can be attributed to the work of Slows (1962, 1963) and (Wheeler ,1959). The need and value of linking time synchronous surfaces across geological sections were understood. They paved the path for seismic stratigraphy by incorporating chronostratigraphic into stratigraphic analysis.

These sequences depict several occurrences of deposition that took place in relation to the rising and dropping of the sea level (Mitchum et al., 1977). The combination of tectonics, eustasy, and climate led to the stratigraphic signatures and stratum patterns in the sedimentary rock record (Emery and Myers, 2003).

Sequence stratigraphy's strength resides in its capacity to forecast facies within a chronostratigraphic limited framework of depositional sequence

confined by unconformities (Haq *et al*., 1987). Applying stratigraphic series ideas to stratigraphic successions can be done in one of two ways. The first method entails creating age models using the world cycle chart published by (Haq *et al*.,1987) as a foundation.

The inclusion of the identification of predicted lithological succession brought on by relative sea level variations is tasteful. To create a stratigraphic structure that is useful for reservoir characterization, the application is more pertinent than the first was (Kerans and Tinker, 1997). It may be summed up in a few stages, as those (Van Buchem *et al*.,1996,2002) employed.

4.2 Concepts of Sequence Stratigraphy

Sequence stratigraphy is based on the assumption that sedimentary succession may be broken down into unconformity-bounded units (sequences) that emerge over the course of a single cycle of sea level fluctuation. A sequence can be divided into more manageable pieces (called system tracts). These reflect several phases of a single sea level cycle and are genetically related. In sequence stratigraphy, the term "sequence" refers to a stratigraphic unit made up of genetically related strata that are fairly conformable, with unconformities or their accompanying conformities at the top and bottom (Mitchum *et al*., 1977). The surfacies of marine floods and their associated surFacies serve to define the generally conformable or bed sets that are genetically connected beds in the parasequence (Van Wagoner *et al*., 1988).

System tracts are formed of one or more Parasequence, which are asymmetrical sedimentary cycles representing growth of the sedimentary succession during a few hundred thousand years.

4.3 Accommodation

Jervey (1988) defined accommodation as "the space available for potentially accumulating sediment and it is measured by the distance between base level and the depositional surface." It is the result of three variables working together (Figure 4-1).

Which are:

- The sea surface (eustasy: global sea level measured from a datum such as the center of the earth)
- The seafloor (tectonics)
- Changes in rates of sediment accumulation

Accommodation = eustasy + subsidence + compaction

Therefore, basin subsidence and eustatic increases in the global sea level are the two factors that govern the establishment of accommodation space.

Basin inversion, eustatic sea level rises, and a higher rate of sediment input are the three factors that reduce the amount of available area for housing (Sharland, 2001).

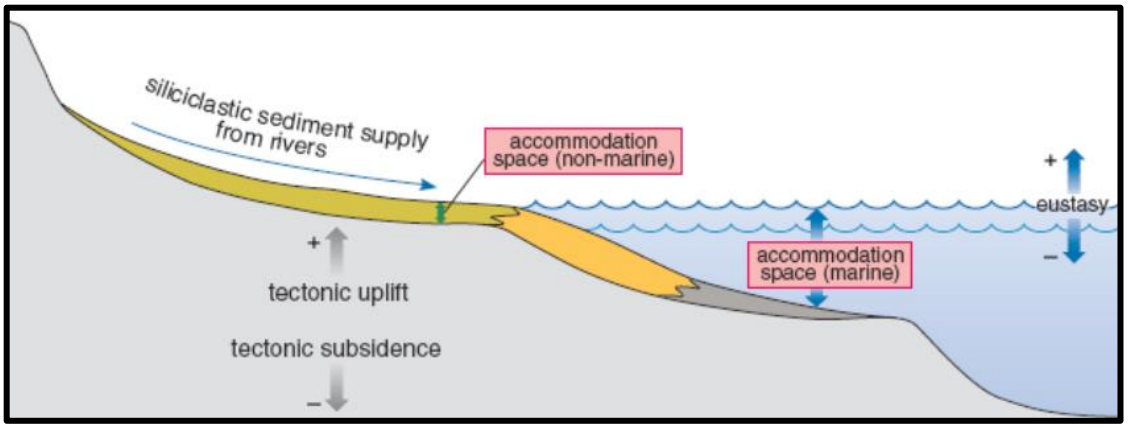

Figure (4-1) Sediment accommodation space and its relationship to eustatic sea level and tectonic uplift and subsidence (Jervey,1998).

4.4 Key surface

The depositional sequences of the Study Formation were correlated and subdivided using a variety of stratigraphic surfaces. The maximum flooding surfaces, transgressive surface, and sequence boundaries were those.

4.5 Sequence boundaries (SB)

The definition of the sequence boundary by (Vail *et al*.,1977), which is wide and gives opportunity for further elaboration figure (4-2), is an unconformity or correlative conformity that separates conformable succession of strata. There are three different kinds of sequence boundaries: Type 1, Type 2, and Type 3.

If the pace of eustatic fall clearly exceeds the rate of subsidence, exposing the platform and fore slope, type 1 (SB1) sequence boundary develops (Sarg, 1988). If the rate of eustatic fall is less than or equal to the rate of subsidence, exposing the inner-platform and shoal area, a type 2 (SB2) sequence boundary is created (Sarg, 1988). When sea levels rise faster than the system can aggrade, type 3 (SB3) sequence boundaries occur, and transgression system tracts with substantial marine hiatuses overlie the previous highstand tract.

4.5.1 Maximum Flooding surface (MFS)

According to Glalloway (1989), the Maximum Flooding Surface (MFS) is the boundary between the maximum transgression and regressive strata. The surface designates the transgression of the shelf's shelf at its maximum flooding or Chapter Four Sequence stratigraphy, and it divides the transgressive systems tracts from the highstand systems tract figure (4-2). According to Helland and Gjelberg (1994), the Maximum Flooding frequently delineates the boundary between coarsening and fining upward cycles and is utilized to connect these cycles for deepening and shallowing in the geological section. (MFS) have a rich and varied fossil assemblage that frequently includes pelagic marker species, according to (Sharland,2001).

4.5.2 Transgressive surface (TS)

The Transgressive surface separates the lowstand systems tract from the transgressive systems tract figure (4-2), It is characterized by in situ reworking and winnowing of sediment (Emery and Myers, 1996).

5.6 Systems Tracts

System tracts are characteristic units that may be used to further break down the sequence. According to Brown and Fisher (1977), they are a connection between contemporaneous depositional systems. Their internal geometry and boundary characteristics are what define them (Emery and Myers, 2003). According to Posamentier *et al.* (1988), systems are classified as a combination of modern depositional systems defined by strata geometry of bounding

surfaces, sequence location, and stacking pattern of internal parasequences, and are thought to be connected to a specific eustatic curve segment figure (4-2)

4.6.1 Lowstand systems tracts (LST)

The deposition that occurred during the relative sea level decrease and the early period of the succeeding relative sea level rise, which occurs before the commencement of transgression, are indicative of this basal subdivision of a series (Van Wagoner et al. 1988). Basin floor fans and slope fans deposition grading to the lowstand wedge depict the LST. figure (4-2)

4.6.2 Transgressive systems tract (TST)

The landward shift in deposition settings, which is a reflection of an increase in relative sea level, is traced by the transgressive systems tract. The transgressive surface serves as the unit's bottom, while the maximum-flooding surface serves as its top. Accommodation outweighs sediment intake, resulting in an a retrogradational facies-stacking pattern. The deposits of the transgression system tracts are most developed landwards of the underlying off lap break; they onlap the transgressive surface of the merged sequence boundary in a landwards direction and downlap on it in a basin wards manner (Mclaughlin, 2005). figure (4-2)

4.6.3 Highstand System Tract (HST)

According to Emery and Myers (1996), the most recent tract in the sequence of types one and two forms during the last phases of sea level rise and is characterized by rapid sedimentation rates. According to (Catuneanu,2002), figure (4-2), these two tracts' sedimentation was initially characterized by staking patterns (aggradation), which later gave way to progradation patterns. figure (4-2)

4.7 Carbonate response to sea level changes

Carbonate geometry, Facies, and digenesis are all impacted by relative sea level displacement (Kendal et al., 1991). The following factors can represent whether the relative sea level increase is quick or slow:

Give up: Complete halt to carbonate manufacturing.

- Back-step: carbonate deposition ceases producing at the basin margin and retreats to a new position back across the shelf.
- Catch-up: carbonate accumulation is initially unable to keep pace with the sea level rise but then aggrades to sea level.
- Keep up: carbonate accumulation match sea level rise.
- Prograde: carbonate accumulation is greater than the needed to match sea level rise, so causing the platform margin to advance in a seaward direction.

Carbonate response to sea level fall is reflected by:

- Deep-water slop and basin fans deposition, if the basin remains deep deposit the fall.
- Shelf -margin wedges when the adjacent basin becomes shallow enough to maintain shallow water carbonate deposition.

When the fall isolates a basin of deposition, replacement by evaporates.

The interior platform is exposed. Figure (4-3)

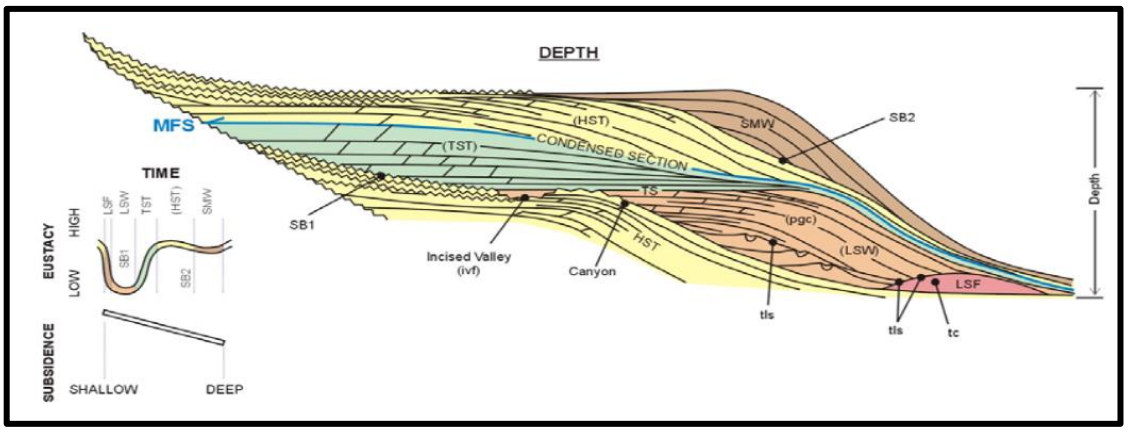

Figure (4-2) System tracts and sequence boundaries (after Van Wagoner *et al.*)

4.8 Carbonate sequences

According to Sarg (1988), four key factors tectonic subsidence, eustacy, the volume of deposited sediments, and climate control facies patterns in carbonate rocks.

They work together to create relative sea level changes that are visible in the stratigraphic succession as units of shallowing, deepening, and down stepping. These units produced the highstand, transgressive, and lowstand systems tracts of siliciclastic and carbonate sequences (Handford and Loucks, 1993).

Most carbonate sedimentation has been reported in the (TST) and (HST). The carbonate deposition in the lowstand system tract (LST) is restricted to narrow areas and is characterized by abundant siliciclastic input and exposure surface of carbonate platform.

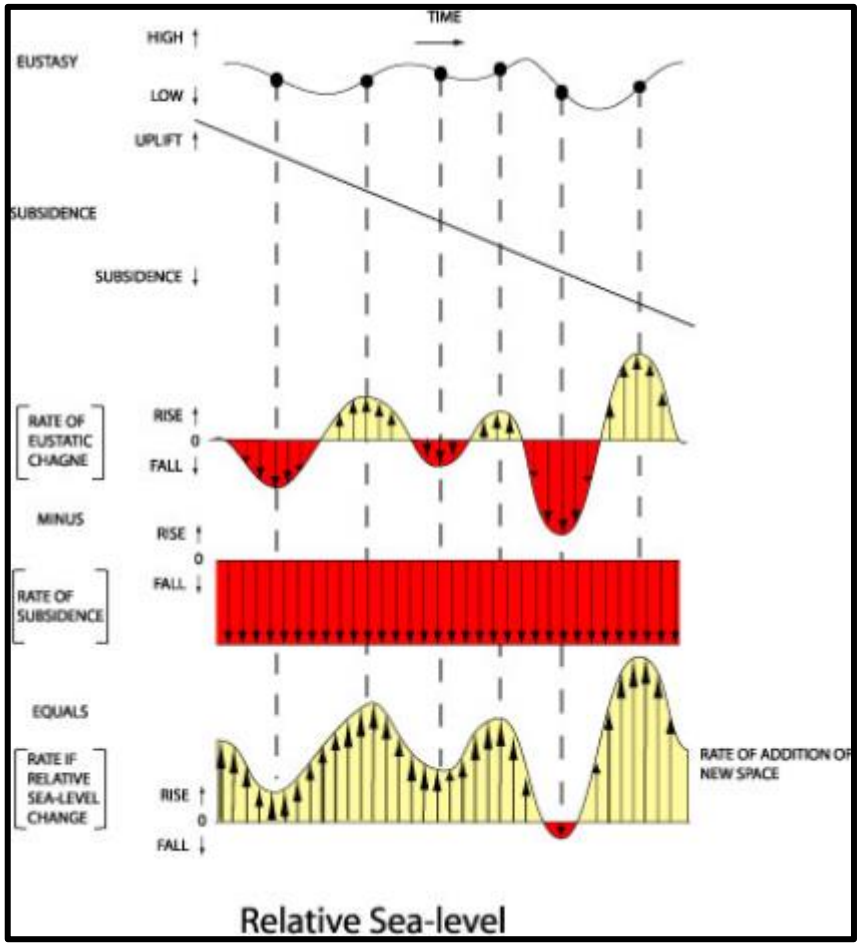

Figure (4-3) Carbonate depositional response to sea level changes (Posamentier&Jervey&Vail,1988)

4.9 Sequence Development

According to (Scott *et al.*,1994), depositional cycles are sedimentary deposits that, independent of date and provenance, reflect changing

environmental circumstances. These deposits must be recognized by the physical and biological information they carry.

Changes in eustasy, tectonism, climate, and other processes occurring within depositional settings impose these cycles or sequences over a range of timescales (1st = longest term, 6th = shortest term). Figure (4-4)

The most crucial phase in the building and analysis of the sequence stratigraphic model is the selection of a datum or datum from which to" hang "the available interpretive data (Kerans and Tinker, 1997).

In this study, the choice of dates was based on the considerable generalization of (Kerans and Tinker ,1997); some of them may be relevant to mention:

- According to the stratigraphic interval of interest, the choice of date should be change.
- There are very few (if any) stratigraphic marked beds stored and/or kept flat.
- The stratigraphic interpretation process is iterative, in that usually an initial correlation pass is made with a single datum, and then other datums are added to achieve a final interpretation. Usually, multiple dates are required to explain the stratigraphic structure.
- A reasonable choice of date can be made for the shales.
- If erosion non-conformities.

The succession of the Mishrif Formation consists of five third order cycles (A, B, C, D and E) representing successive intervals of relative sea level rises and stillstand. The nature of cycle asymmetry and thicknesses suggest that the tectonic component is the main controlling factor on cycle development in highly subsiding basin. figure (4-5, 6 and 7).

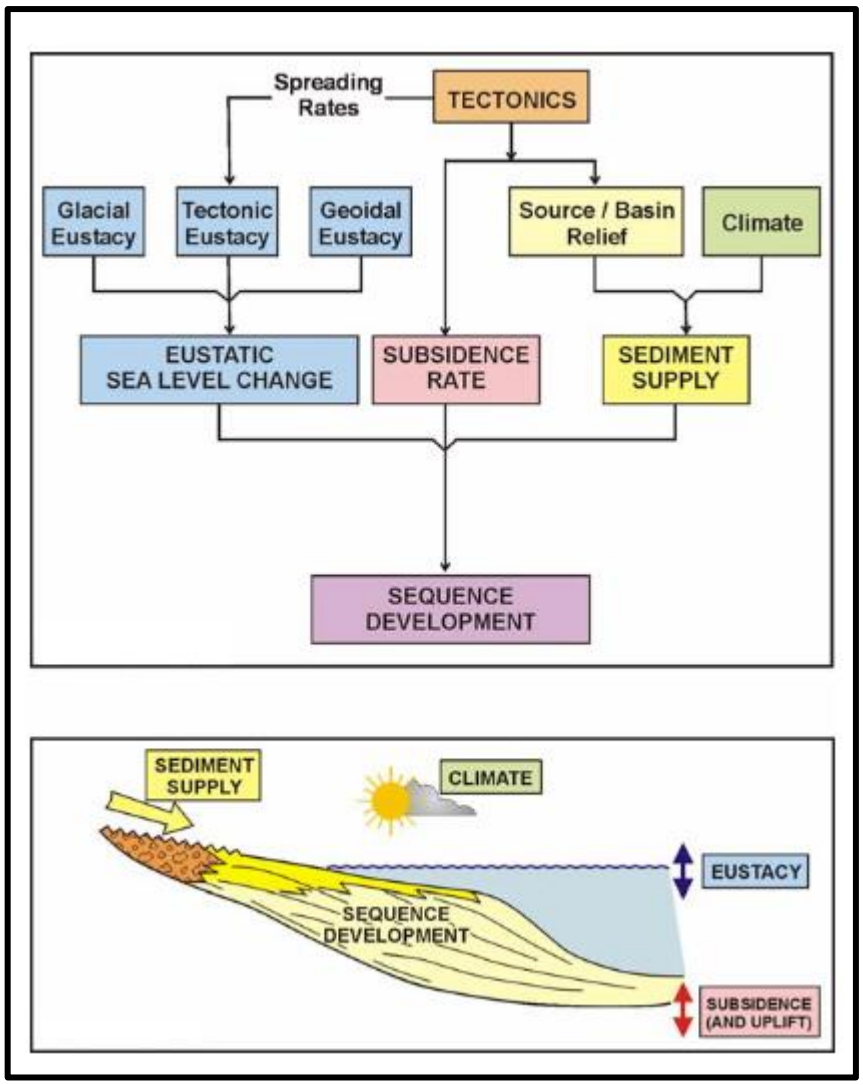

Figure (4-4) An interplay of four main controlling factors influence sequence stratigraphic (Adapted from Vail, 1987)

4.9.1 Sequence development of Mishrif Formation at Eridu-1 well

The Mishrif succession in Eridu-1 is represented by five third order asymmetrical cycles and recognizes by alternation of the transgressive systems tract (TST) and highstand system tracts (HST). The lower contact of the studied sequence with the Rumaila Formation is the gradual contact, which represents a transitional period that separates a marine progression consisting of limestone and chalk of the Rumaila Formation, and thus they gradually progress upward to the Mishrif Formation during the period of marine fall, figure (4-5).

Cycle A represents the Highstand System Tract (HST), which is a continuation of the sedimentary cycle extending from the sedimentation of the

Rumaila Formation and represents the beginning of the marine fall and transition from the deep Rumaila sediments towards the sedimentation of the shallow open marine of the Mishrif Formation. The Highstand System Tract is composed of bioclastic packstone, rudstone with large rudist fragment, mudstone to Wackestone, peloidal Wackestone to packstone and mudstone with benthonic foraminifera Textularia, Nezzazata and Milliode with fragmented of coral and algae it represented by shoal, rudist Biostrum and restricted marine.

Cycle B (TST) consists rudstone with rudist fragment, boundstone with coral, bioclastic packstone and wackestone it is represented by shallow open marine and rudest biostrum. The cycle B (HST) is composed of piloidal grainstone it represented by shoal.

Cycle C (TST) consists bioclastic packstone it is represented by shallow open marine. The cycle C (HST) is composed of rudstone it represented by shoal.

Cycle D (TST) consists planktonk packstone and benthonic foraminiferal mudstone it is represented by shallow open marine and deep marine. The cycle D (HST) is composed of rudstone and peloidal grainstone it represented by shoal and restricted marine.

The cycle E (TST) consists bioclastic packstone microfacies, peloidal grainstone microfiches, bioclastic Wackestone microfacies and bioclastic mudstone to Wackestone microfacies, it is it is represented by shoal and restricted marine, the HST) is composed of. The cycle E (HST) is composed of peloidal packstone with rudist fragment and peloidal packstone to grainstone which consist mainly of tiny equally size Peloids with some benthic foraminifera, *Textularia, Nezzazata* and Milliode, it is represented by shoal. This cycle ended at (SP1) over by Kifil formation.

4.9.2 Sequence development of Mishrif Formation at Eridu-2well

The fourth third order asymmetrical cycles that make up Eridu-2 for Mishrif succession are used to identify it through the alternation of transgressive and highstand system tracts (TST and HST). Figure (4-6) shows that the studied sequence gradually advances upward to the Mishrif Formation during the period of marine fall from its lower contact with the Rumaila Formation, which represents a transitional period separating a marine progression made up of the Rumaila Formation's limestone and chalk.

Cycle A represents the Highstand System Tract (HST), which is a continuation of the sedimentary cycle extending from the sedimentation of the Rumaila Formation and represents the beginning of the marine fall and transition from the deep Rumaila sediments towards the sedimentation of the shallow open marine of the Mishrif Formation. Planktonic Foraminiferal Packstone such us Calcispheres, Echinoderms, *Globigerinelloides, Heterohelix*, *Hedbergella* and Bioclastic Packstone, Benthic foraminiferal mudstone it represented by deep marine, shallow open marine and restricted marine. The cycle A (TST) consists Bioclastic Packstone, Piloidal to Bioclastic packstone, Piloidal packstone facies, and the carrying benthonic foraminifera such us *Textularia, Nezzazata*, Milliode and bioclastic fragments it is represented by shallow open marine.

Cycle B (TST) consists rudstone with bioclastic packstone it is represented by shallow open marine. The cycle B (HST) is composed of piloidal grainstone it represented by shoal.

Cycle C (TST) consists peloidal to bioclastic packstone, shale and mudstone it is represented by shallow open marine and deep marine. The cycle C (HST) is composed of peloidal packstone and bioclastic wackestone it represented by shallow open marine.

The cycle D (TST) consists Planktonic Foraminiferal Packstone, Bioclastic Wackestone to Packstone, Fossiliferous Wackestone with dissolution and the

carrying planktonic foraminifera such us Calcispheres, Echinoderms, *Globigerinelloides*, *Heterohelix*, *Hedbergellait* is it is represented by deep marine. The cycle D (HST) is composed of bioclastic Wackestone and bioclastic packstone it is represented by shallow open marine. This cycle ended at (SP1) over by Kifil formation.

4.9.3 Sequence development of Mishrif Formation at Eridu-3 well

Transgressive and highstand system tracts (TST and HST) are utilized to distinguish the five third order asymmetrical cycles that make up Mishrif succession in Eridu-3. During the period of marine fall from its lower contact with the Rumaila Formation, which represents a transitional period separating a marine progression made up of the limestone and chalk of the Rumaila Formation, Figure (4-7) demonstrates how the studied sequence gradually advances upward to the Mishrif Formation.

Cycle A represents the Highstand System Tract (HST), which is a continuation of the sedimentary cycle extending from the sedimentation of the Rumaila Formation and represents the beginning of the marine fall and transition from the deep Rumaila sediments towards the sedimentation of the shallow open marine of the Mishrif Formation. Cycle A (HST) is composed of bioclastic Packstone with Planktonic Foraminiferal such us Calcispheres, Echinoderms, Globigerinelloides, Heterohelix, Hedbergella, bioclastic Wackestone to packstone and bioclastic mudstone it is represented by deep marine. The cycle A (TST) consists fossiliferous Wackestone to packstone and bioclastic packstone with peloid it is represented by shallow open marine.

Cycle B (TST) consists planktonk packstone it is represented by deep marine. The cycle B (HST) is composed of piloidal packstone it represented by shallow open marine.

Cycle C (TST) consists bioclastic mudstone to wackestone it is represented by deep marine. The cycle C (HST) is composed of peloidal grainstone it represented by shoal.

Cycle D (TST) consists rudstone and bioclastic packstone it is represented by shallow open marine and rudist biostrum. The cycle D (HST) is composed of rudstone and bioclastic wackestone it represented by restricted marine.

The cycle E (TST) consists Planktonic Wackestone, Bioclastic mudstone and bioclastic packstone it is represented by deep marine. it is represented by deep marine and shallow open marine. This cycle ended at (SP1) over by Kifil formation.

4.10 Basin development

- **First stage: -** this stage was represented the deposition in the basin of Rumaila Formation and continued to deposition the lower part of Mishrif Formation within the deep marine environment. The end of this basin (Rumaila basin) was represented by the shallow open marine associated facies in the studied area.

  The highstand sequence distinguished by deposition the deep marine Facies and the shallow open marine as two cycle. The first stage was finished by deposition of the shoal facies in all studied area to marked a sequence boundary type Il (prograde stage A).

- **Second stage: -** during this stage the basin was developed from the shoal to rudest biostrum dominated facies with slow sea level rise. The deposition of the open marine associated facies within the rudest biostrum-shoal sequence marked the mfs surface. The final step of this stage was shown the shallowing up-ward by overlaying the shallow open marine association facies upon the rudest biostrum and shoal. At the end of deposition this sequence, the restricted facies were spread in the studied area to formed the prograde stage B as sequence boundary type II.

- **Third stage: -** the sea level was raised in the southwest direction as open sea association facies, while to the northeast the restricted facies was dominated. This sequence appeared the shoal facies underlay the open

sea facies marked the mfs surface to start the final high stand deposition overly the restricted facies. This stage is representing the prograde stage D for the Mishrif Formation, where ended the deposition to mark the unconformable surface (SBI) with Kifil Formation.

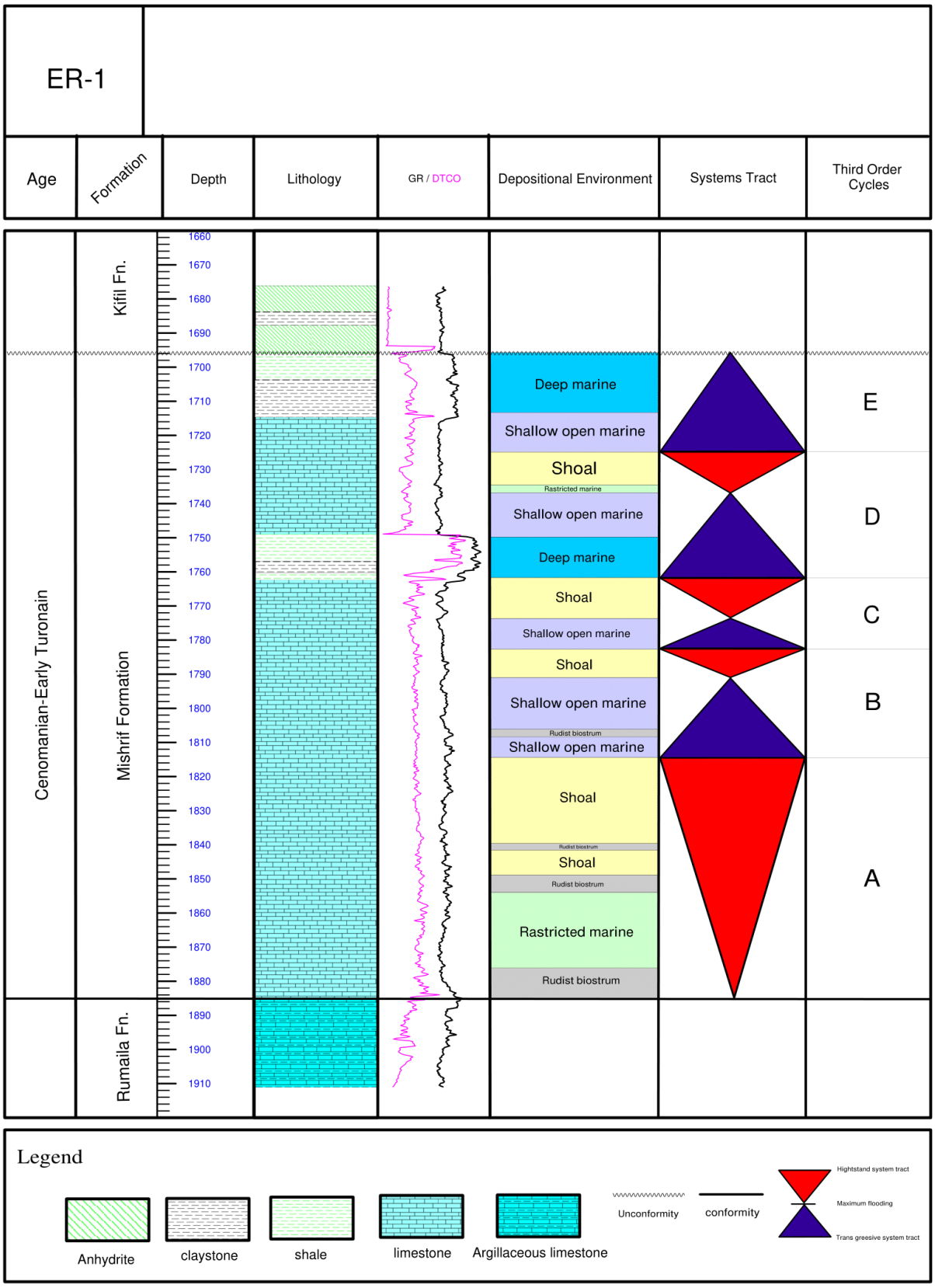

Figure (4-5) Sequence stratigraphic analysis of Mishrif Formation in well ER-1

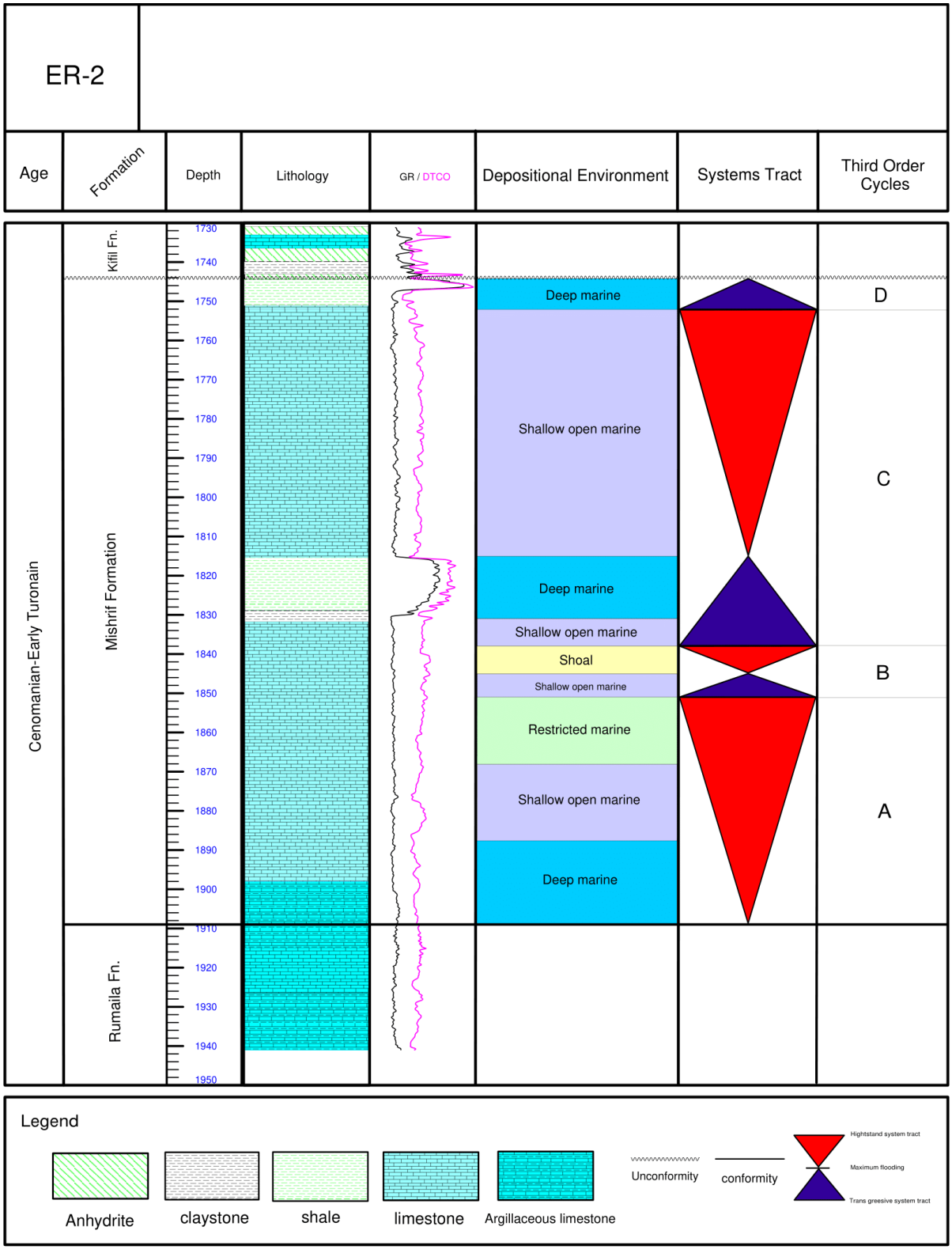

Figure (4-6) Sequence stratigraphic analysis of Mishrif Formation in well ER-2

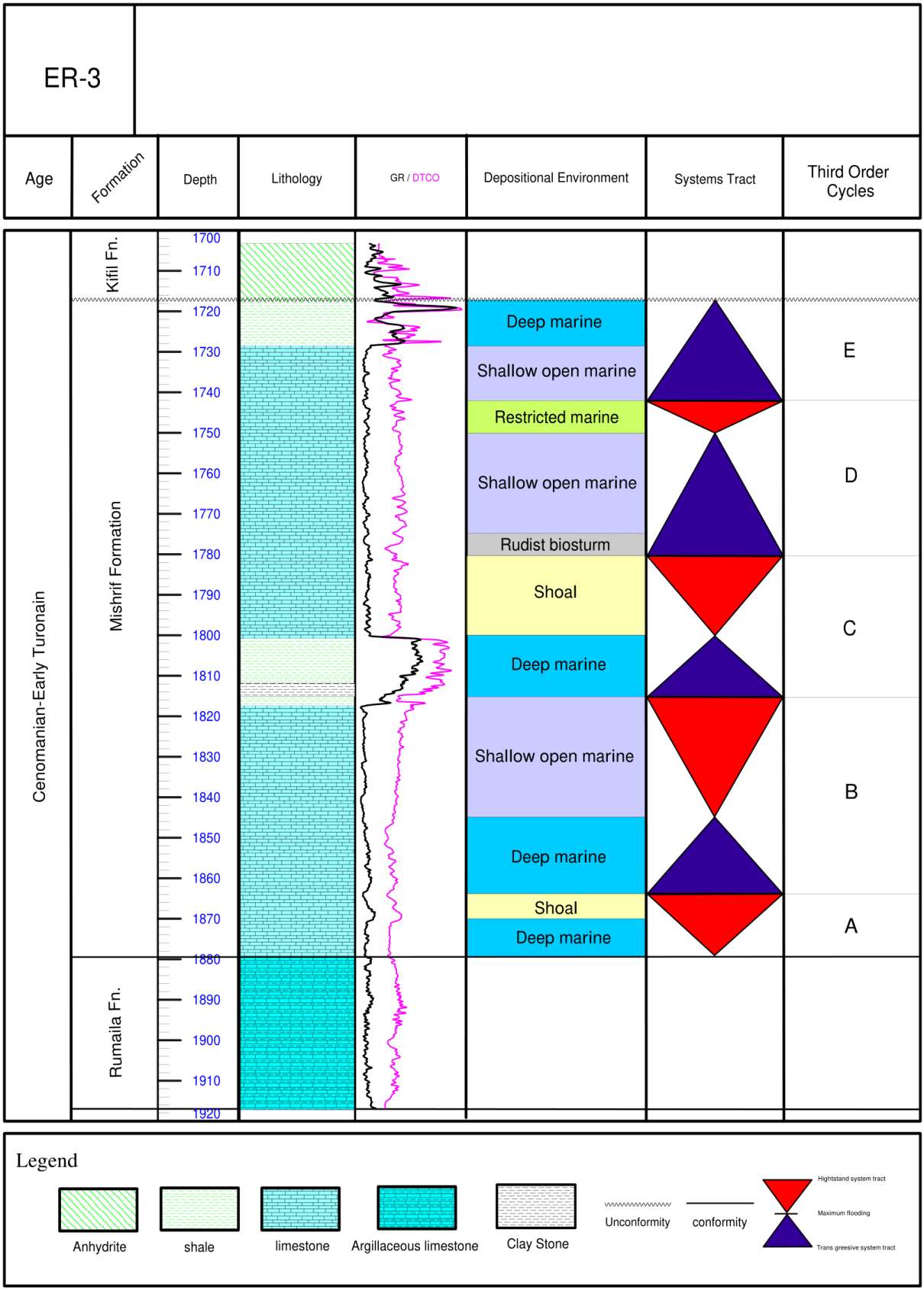

Figure (4-7) Sequence stratigraphic analysis of Mishrif Formation in well ER-3

Chapter Five
3D Geology Model

5.1 Introduction

The majority of operations fields use 3D geological models to obtain the most accurate descriptions of subsurface reservoir attributes and quantities through data on reservoir characteristics. In order to determine the distribution of these features, it is necessary to comprehend and cover the majority of geological features with respect to porosity, water saturation, kinds of rocks and barriers (faults and folds). Structure modeling, stratigraphic modeling, Petrophysical modeling, and lithological modeling are the four key steps of a geological model. The complicated applications and methods. Improved hydrocarbon bearing zone quantification required high-resolution geological models and more accurate data collection. (Doyle and Sweet,1995).

Creating a 3D Petrophysical model for a reservoir in the Eridu field is mostly illustrated in this chapter. Basic data that may be utilized in 3D geological models often comprises sources, types of data, sizes, and then numerous steps to describe how geologic modeling is conducted.

5.2 Model Design

To create the geological model for the reservoir in the Eridu oilfield, Petrel 2018 software was chosen. Petrel software offers a wide range of tools for modeling, interpretation, and the construction of accurate subsurface models. Petrel really takes into account the most recent software modeling created by Schlumberger. The data base was created using the Petrel program, which included specific information needed to finish this investigation. The primary data source input into Petrel contains geology and petrophysical data, which enables visualization of simulator results in 3D and 2D for optimal reservoir exploitation. (Schlumberger,2008).

5.3 Data Import

This project will use a variety of data kinds to create a 3D geological model, which must be export to the Petrel software. These data types include well heads, well tops, and well logs, which will be used to digitize structural maps.

4.3.1 Well Heads

each well's 3D topographic position (Eastern, Northern). The well heads include the well's location and the path's measured depth.

5.3.1 Well Tops

In order to indicate the depth of each zone of the Mishrif Formation, well tops are points along the course of each well.

5.3.2 Well Logs

The Mishrif Formation's raw data and findings are included in the well logs together with CPI (Porosity, Water Saturation), Neutron, Density, Sonic, and Resistivity measurements.

5.4 Structure Contour Map

Surface data may be used to create a contour map that is connected with well tops. After digitizing a geological report with surfer software, a structural map for geologic units in reservoirs was created that took well tops and the top of the Mishrif Formation into consideration. The Mishrif Formation units were then built on top of well tops in accordance with the trend of the Mishrif top map.

5.5 Vertical wells correlation

The distribution of petrophysical parameters (Porosity and water saturation), as well as the extents and thickness of various lithological units in reservoirs, may be shown via well correlation ideas (Schlumberger, 2008). (Figures 5-1 and 5-2).

In the great majority of log correlation investigations, the following calculated logs are used:

- Clay volume (Vcl).
- Effective Porosity (PHIE).
- Water saturation (S_w).

Some basic logs also make good correlation as:

- Caliper
- Variation between Neutron (φ_D) and Density (φ_N) porosity.
- Variation between R_t and R_{xo} (deep and shallow resistivity)

5.6 Structural Model

To incorporate and explain unique geologic characteristics inside the geomodel, structural modeling might be employed. Geologic construction mapping typically forms the basis of structural modeling, assuming it is accessible.

The three procedures that make up structural modeling are pillar gridding, creating horizons, and layering zones. Using a single amount of data, each of these stages was implemented in turn to create 3D grids.

For the Mishrif formations, five contour maps have been created. These units (CR-I, MA, CR-II, MB, and Rumaila) are based on the well tops of each well that was used in the Eridu oilfield. A 3D structural contour map for the Mishrif Formation is shown in figure (5-3), and other units are shown in figure (5-4 to 5-8) These structural maps illustrate a stratigraphic trap, or Rudest accumulation, particularly in the MB unit around the ER-7, ER-1, and ER-4 wells, with anticlines that have their axes in the same directions as the wells and the area's major slope running from west-south and west to north-east and east.

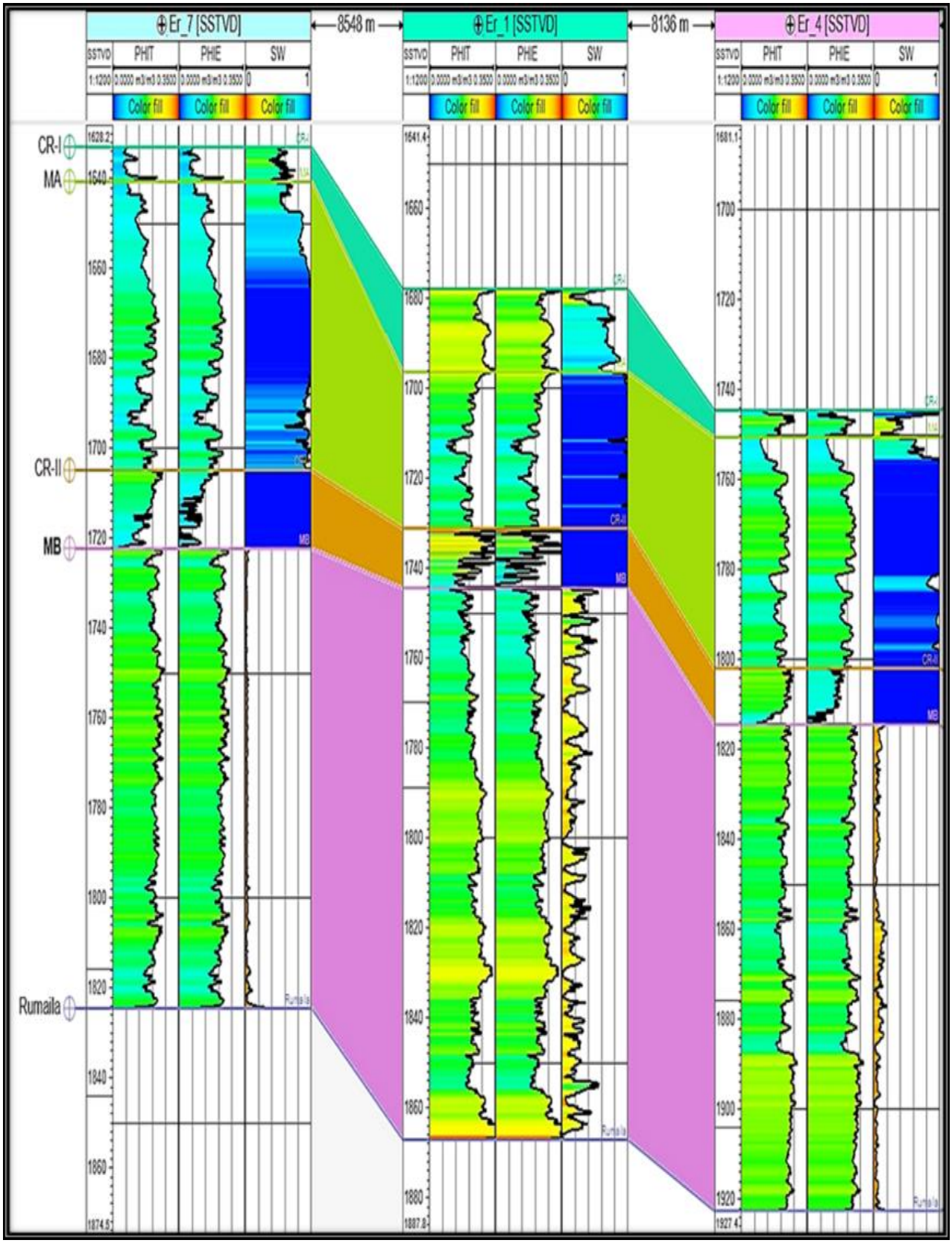

Figure (5-1) Vertical Cross section in direction N-S shows correlation of Mishrif Formation in Eridu oilfield in wells (ER-1, ER-4 and ER-7).

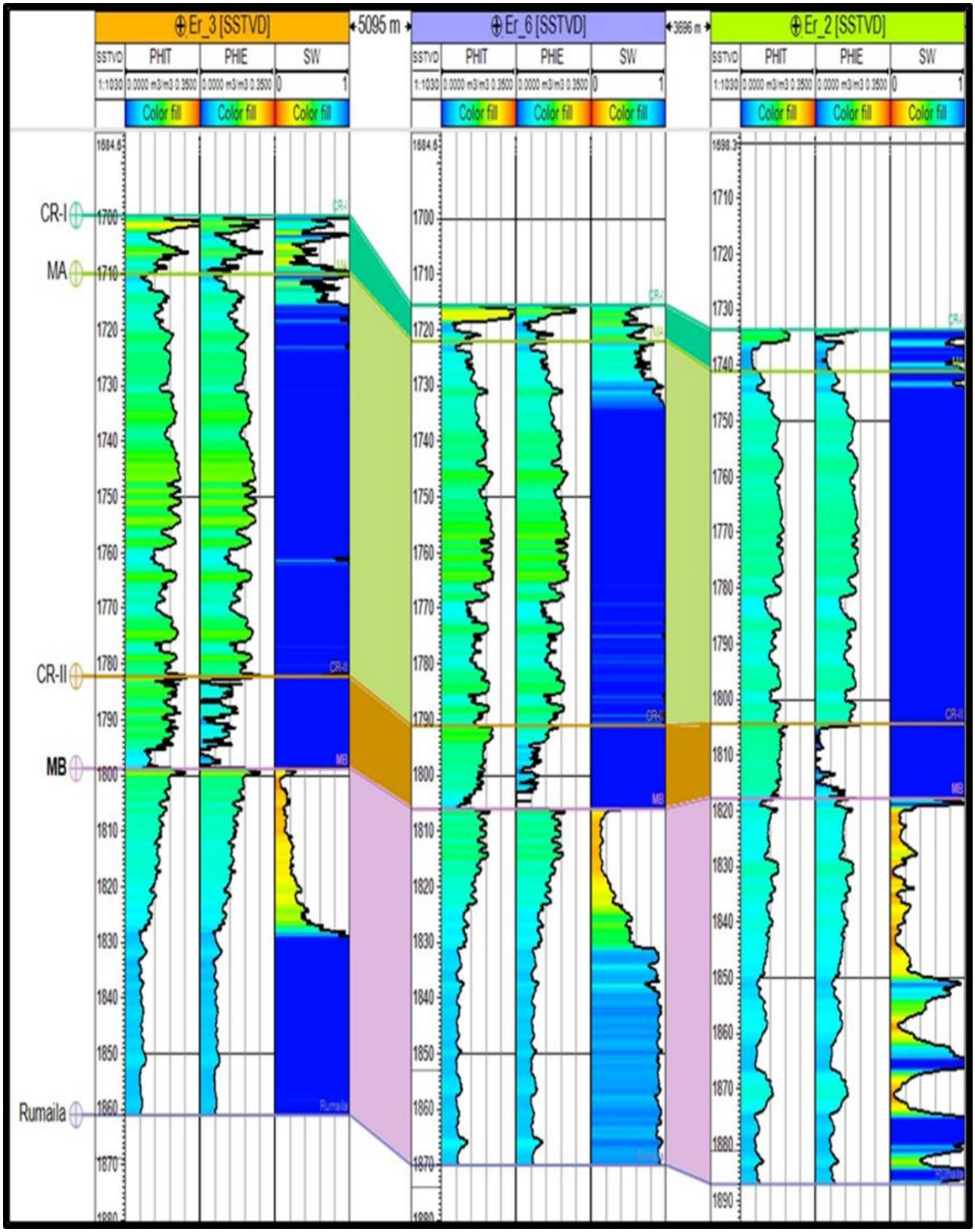

Figure (5-2) Vertical Cross section in direction N-S shows correlation of Mishrif Formation in Eridu oilfield in wells (ER-2, ER-3 and ER-6).

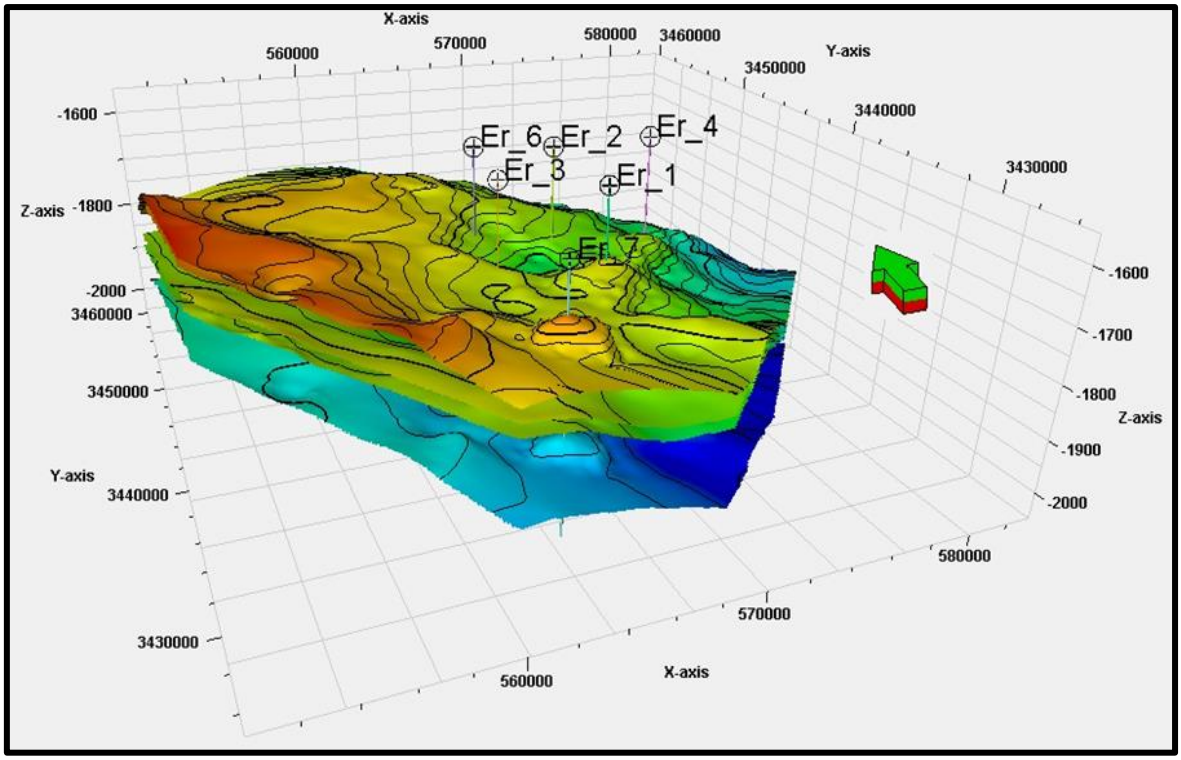

Figure (5-3) Structure modeling of Mishrif Formation in Eridu oilfield.

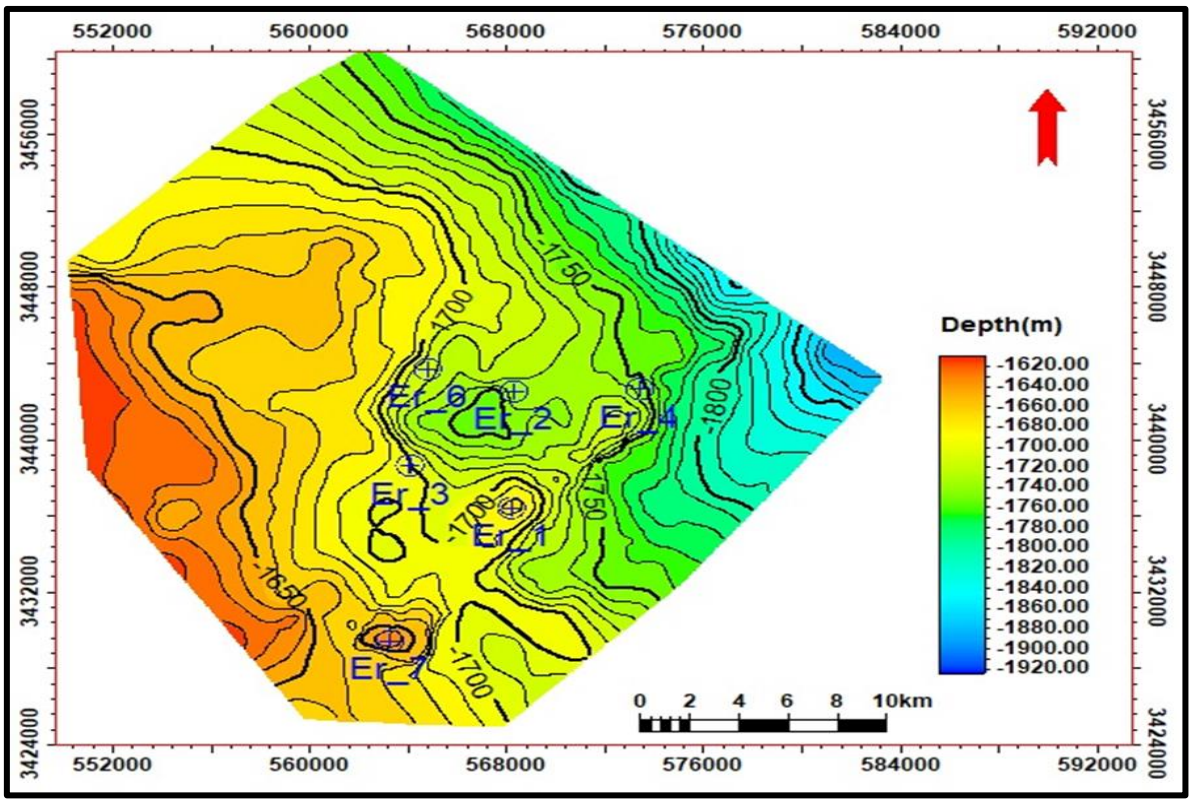

Figure (5-4) Structure map for top Mishrif Formation (CR-I) in Eridu oil field.

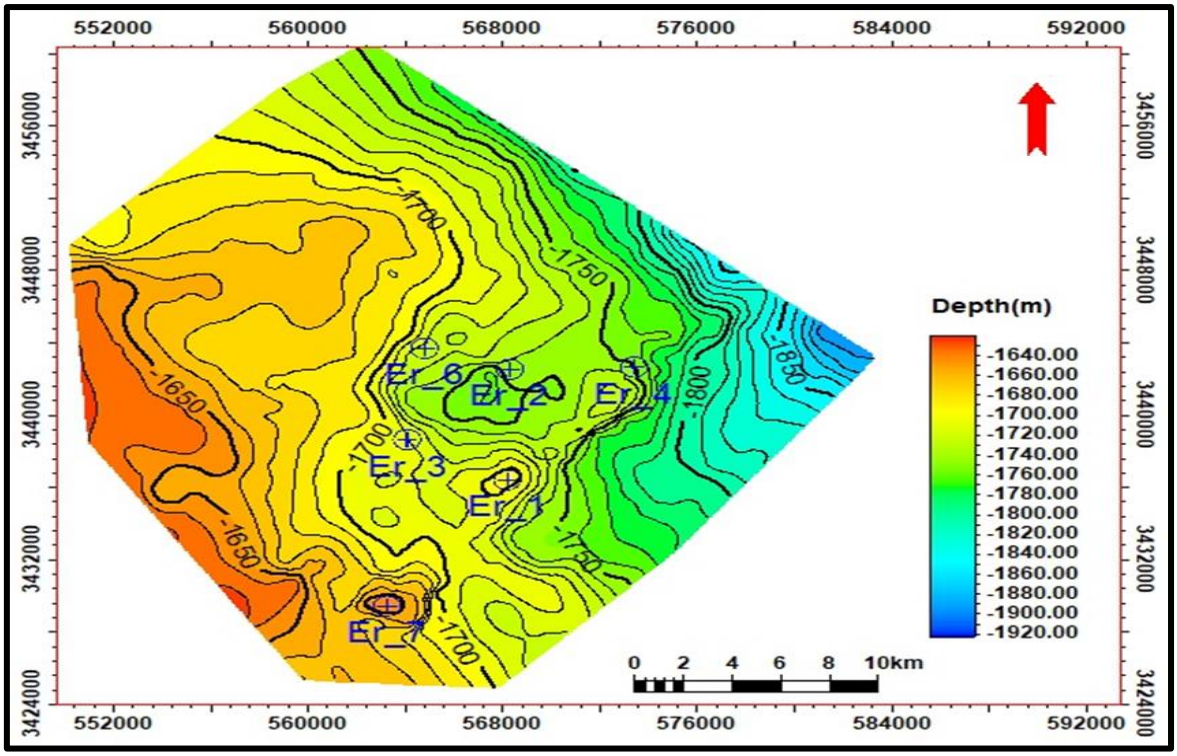

Figure (5-5) Structure map for top Mishrif Formation (MA) in Eridu oilfield.

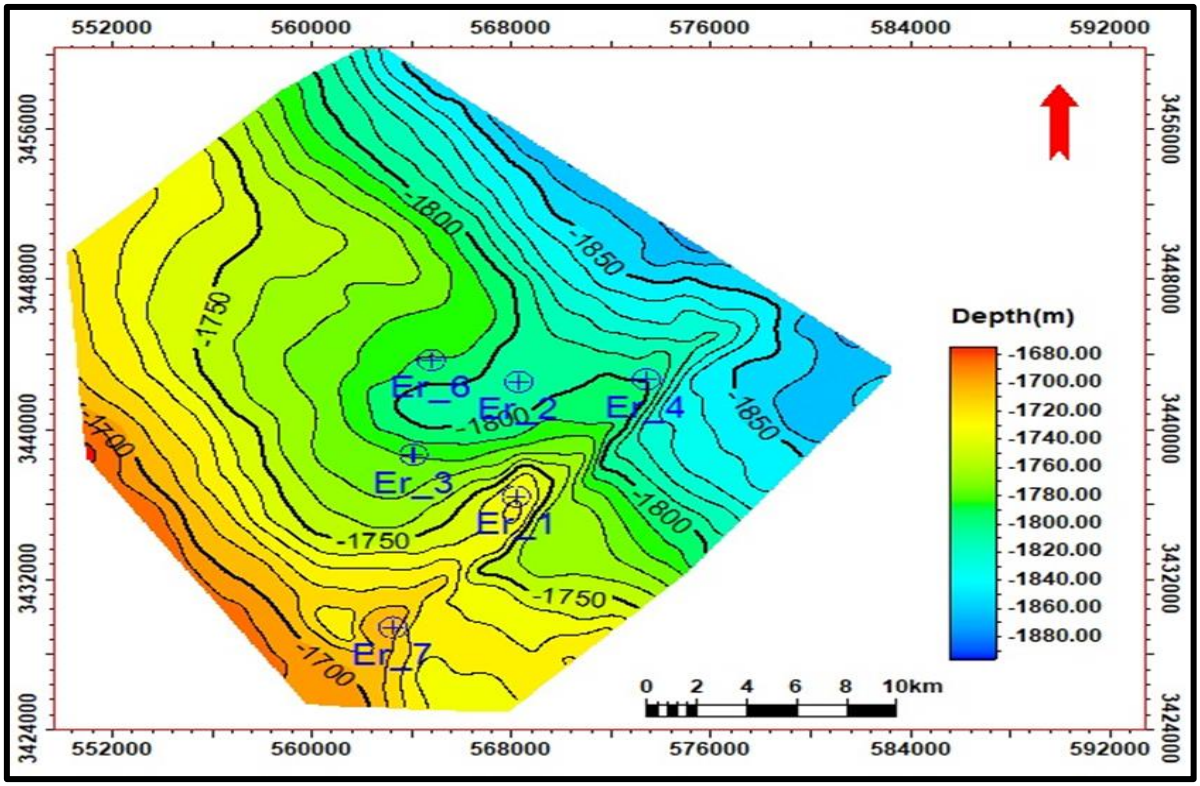

Figure (5-6) Structure map for top Mishrif Formation (CR-II) in Eridu oil field.

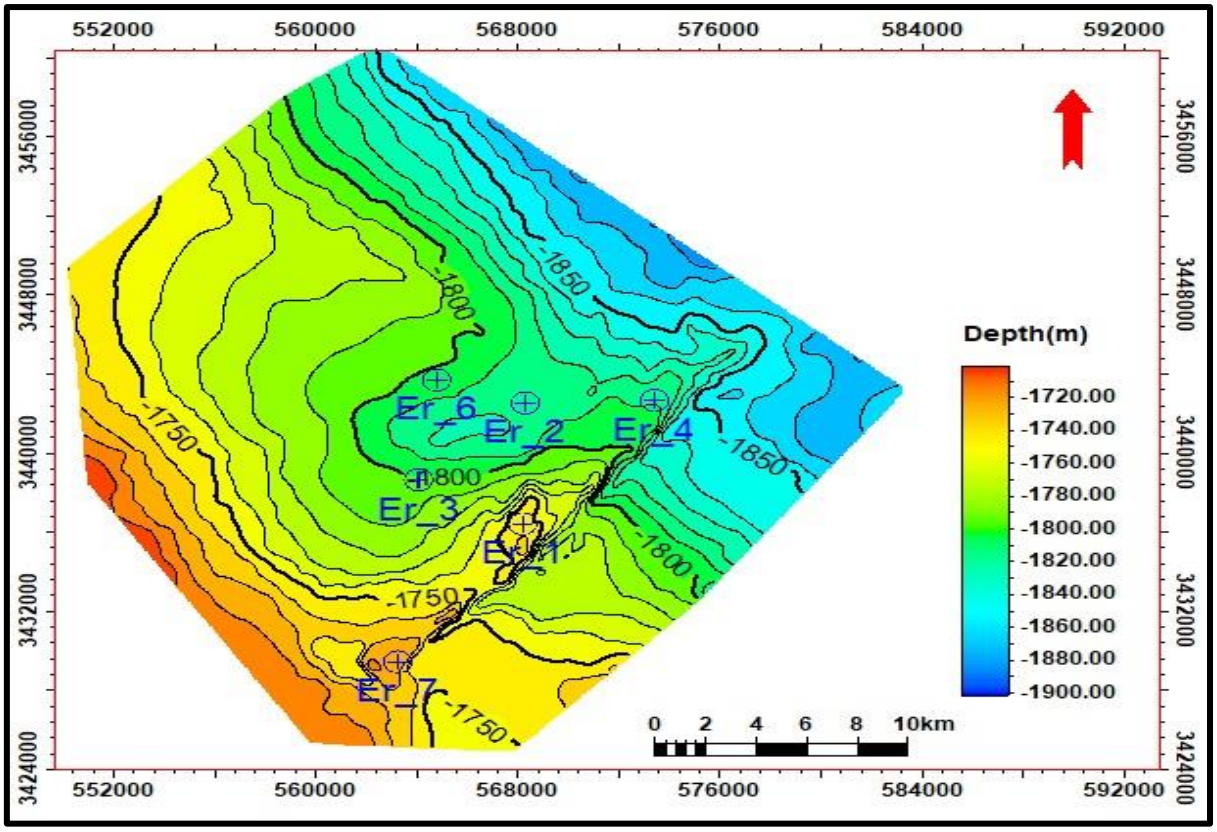

Figure (5-7) Structure map for top Mishrif Formation (MB) in Eridu oilfield.

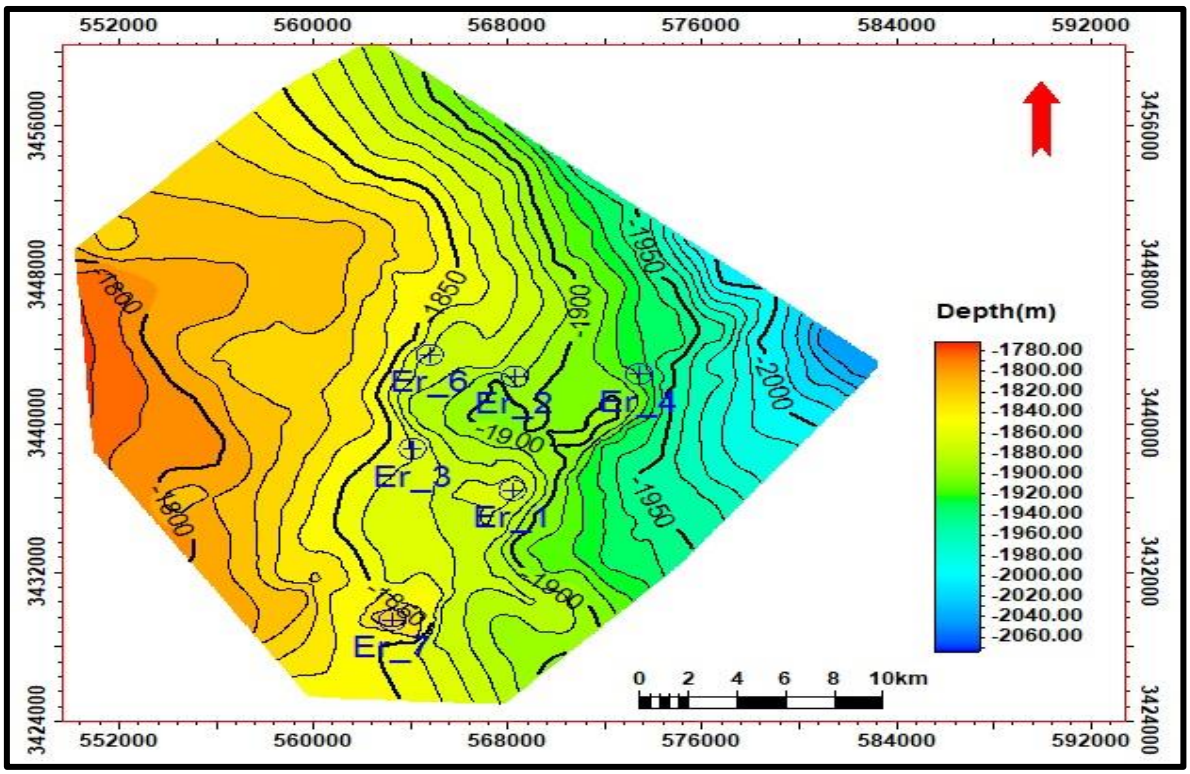

Figure (5-8) Structure map for top Rumaila formation in Eridu oil field.

5.7 Pillar Gridding

To make a 3D structure, the procedure known as pillar gridding is used to produce a surface for (x, y, and z) locations. Top, middle, and base skeleton grids are used to illustrate the skeleton. These skeletons were joined together at places, which made their locations clear.

Building a 3D grid is the initial step in the construction of a 3D model. A grid cell is introduced for each box of grids. Each grid cell's reservoir characteristics, also known as cell properties, such as porosity and rock type, were completed. The majority of the 3D gridding employed in the structural model is made up of several cubic cells that are stratified along faults and lined up with horizons. (Jean-Claude Dulac,2008)

A 3D grid model has been constructed Mishrif Formation by using (100×100 m) on x, and y-axis pillar gridding increasing in order to construct a structure for a 3D grid. Figure (5-9) displays a 3D pillar gridding skeleton for Mishrif formation.

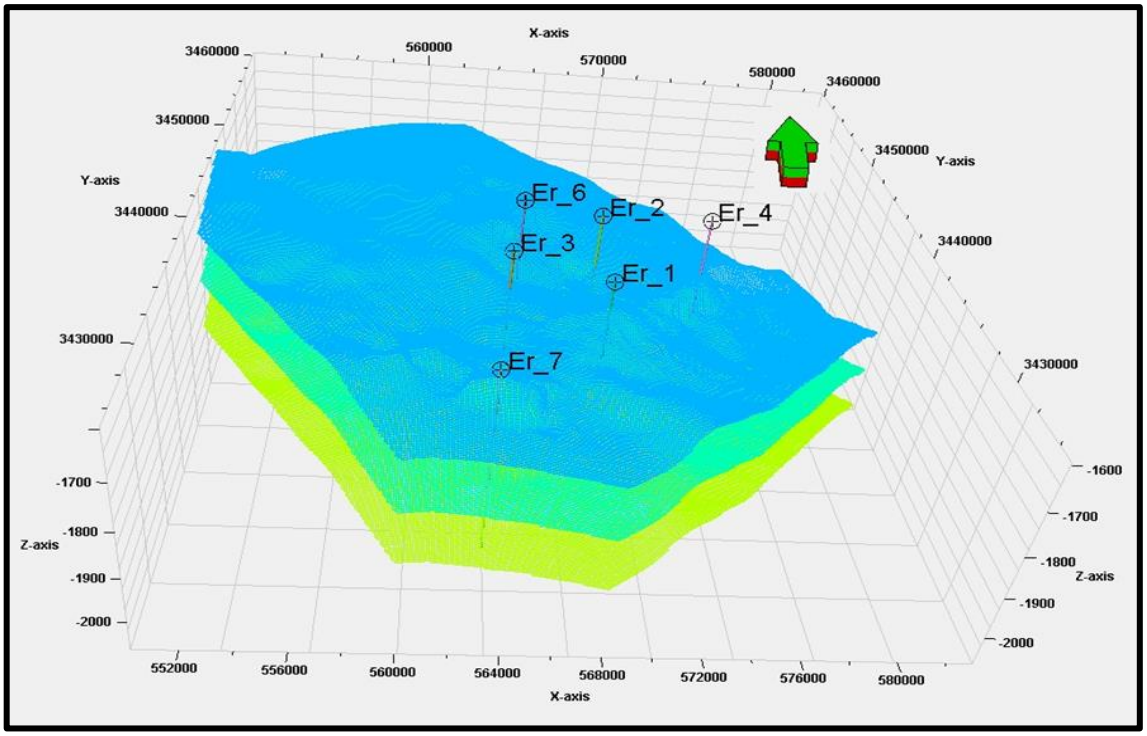

Figure (5-9) The Skeletons of Mishrif Formation in Eridu field.

5.8 Make Horizons and Zones

The horizontal plane means the boundary, which is made up of two distinct top zones or beds. In a 3D grid, the method of making the horizon is utilized to introduce layers in the vertical direction. Real 3D statistical methods portrayed layer surfaces as 2D while preserving the structure's well tops and well picks in place. All crossing locations between the horizon and the 3D pillar grid are known as points after establishing the horizon. (Morten Bendiksen,2013). Depending on geologic unit for Mishrif Formation in Eridu oilfield, there are five horizons have been built in structural model.

The next step in selecting the vertical resolution of the 3D grid is the create zones procedure. Zones are formed between each horizon by this technique. By including thickness information in the form of isochrones, constant thickness, and percentages, zones may be introduced to the model. As demonstrated in 3D view figure (5-11) and intersection view figure, well points may also be used to connect top constructions to well picks or to simply measure the thickness from top horizon to bottom one (5-10).

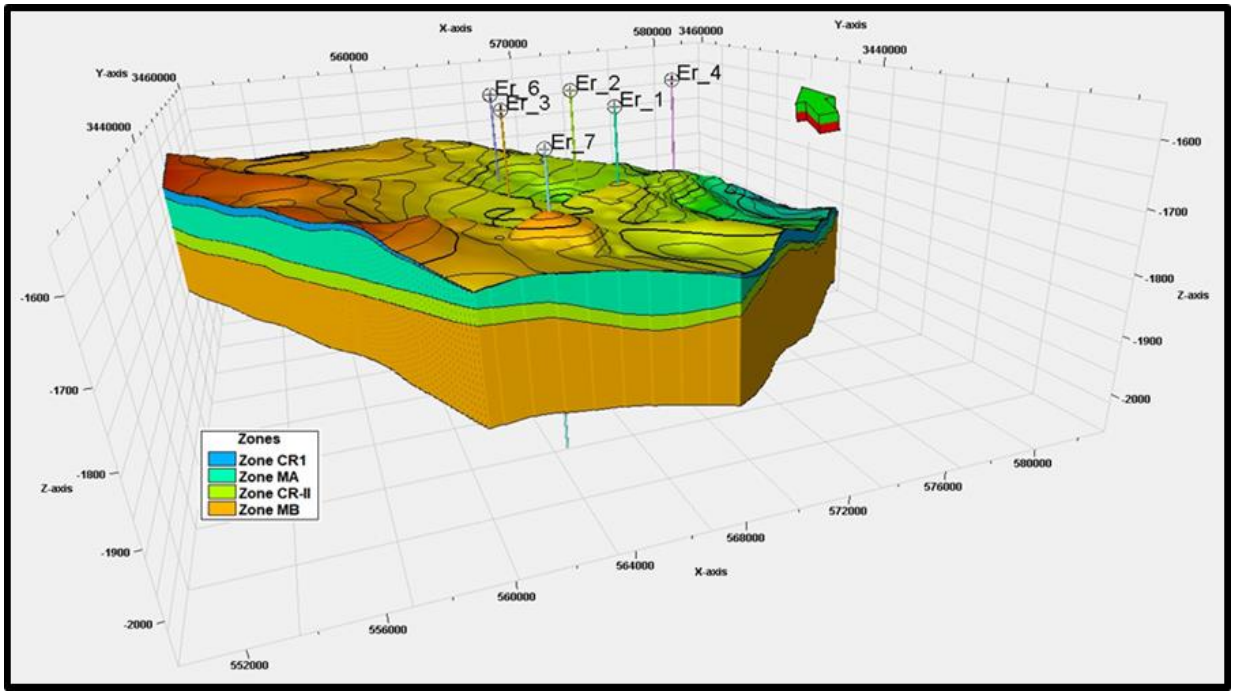

Figure (5-10) shows the top horizon and zones of Mishrif Formation in Eridu oilfield.

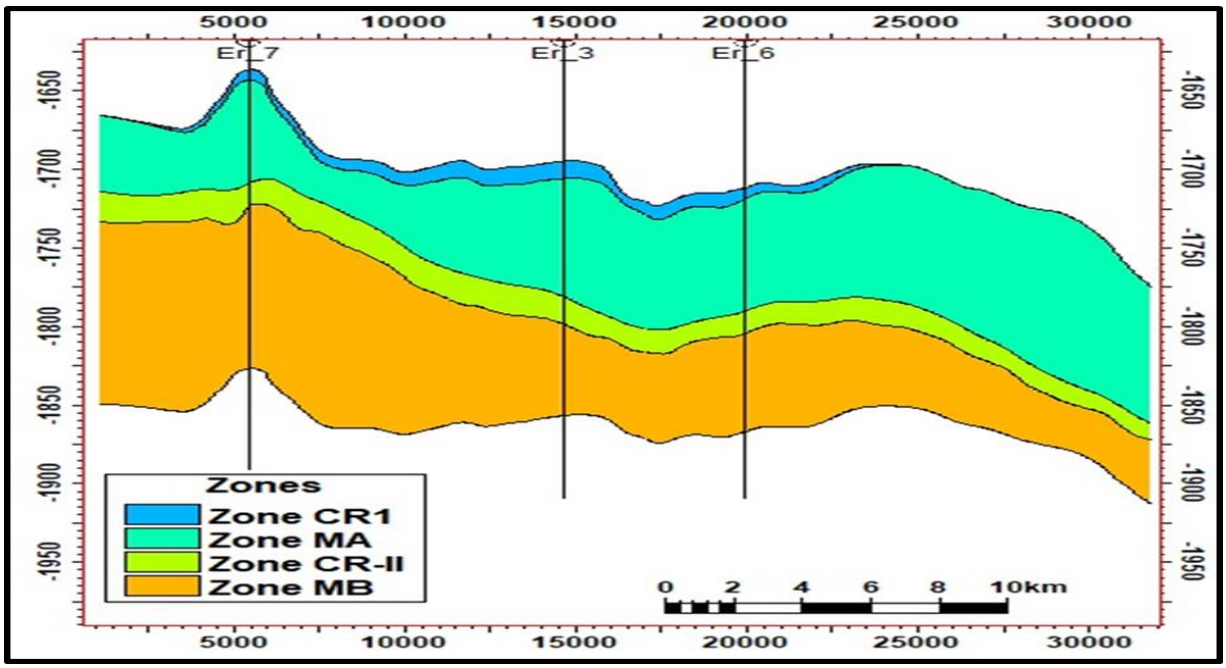

Figure (5-11) Intersection of 3D structure model which illustrate thicknesses of zones of Mishrif Formation in Eridu oilfield in wells (ER-7, ER-3 and ER-6).

5.9 Layering

The primary horizon of the 3D grid cell in the pillar gridding has numerous vertical levels. Each unit's reservoir parameters, like as porosity, were specified. These characteristics are thought to be crucial for estimate and fluid flow calculations. Depending on the quantity or thickness of cell layers, the final two steps making the horizon and layering can be utilized to introduce the choice of vertical direction in a 3D grid. Grid cells may be used to identify the top and bottom of geological units, and well tops that must be depicted in well sections can also be found there. (Al-Hajeri,2009)

Mishrif Formation units in Eridu oilfield have been divided into many layers depending on reservoir properties and unit thickness. Figure (5-12) illustrates layers of each zones Mishrif Formation reservoir. MB unit it is best geological

unit divided more than once as compared other units due to have good Petrophysical properties which explained in table (5-2).

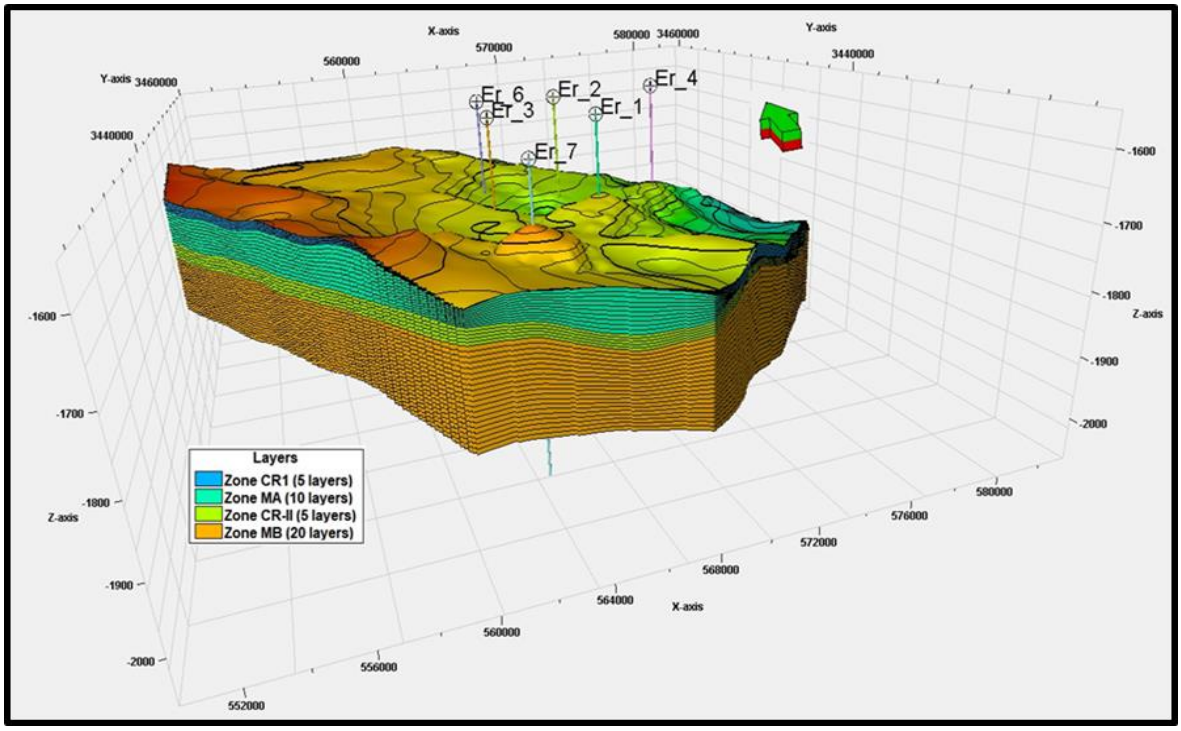

Figure (5-12) Layering division for each unit of Mishrif Formation in Eridu oilfield.

Table (5-2) Number of layers and average thickness for each unites of reservoir of Mishrif Formation in Eridu oilfield.

Zones	No. of Layers	Average Thickness(m)
CR1	5	8.9
MA	10	62.37
CR2	5	15.75
MB	20	76

5.10 The Scale up of Well Log

Scale up of well log is a technique of average values of well log in grid cell by employing statistical methodologies. Each cell 3D grid is perforated by number of wells.

For each Petrophysical property, each cell has a value of 1. Only the grid cells with the given value are shown in the final 3D grid results. Scaled-up well logs from this procedure can be applied to petrophysical modeling. For modeling reservoir characteristics, the region is divided into a 3D grid. The density of samples obtained from logs is often substantially lower than the size of grid cells. Any modeling procedure that relies on well log data should be scaled up so that it can produce 3D grids with precise dimensions. (Servet Unalmiser *et, al* ,1998).

There are a lot of statistical techniques used to scale up well log such as (harmonic, arithmetic average and geometric) methods. Average Petrophysical such as, porosity, and water saturation value which scaled up by arithmetic average. Figure (5-13) shows (PHIT, PHIE and SW) predicate are scaled up for (ER-1) and other wells were shows in appendix A.

5.11 Quality Control

When the well logs have been scaled up, a delicate and required operation has been carried out in order to visualize Units of the Mishrif have been captured. This technique is dependent on layering, which defines layer thickness.

If the layer thickness is too thin, it's possible that too much data will be lost. Thus, modifications for layer thickness are required. Comparison of the histogram window's scaled-up log data with the original log data. Clarity characteristics of the histogram are scaled up to the original log data. Figures (5-14), (5-15) and (5-16) show histogram for total porosity, effective porosity and water saturation.

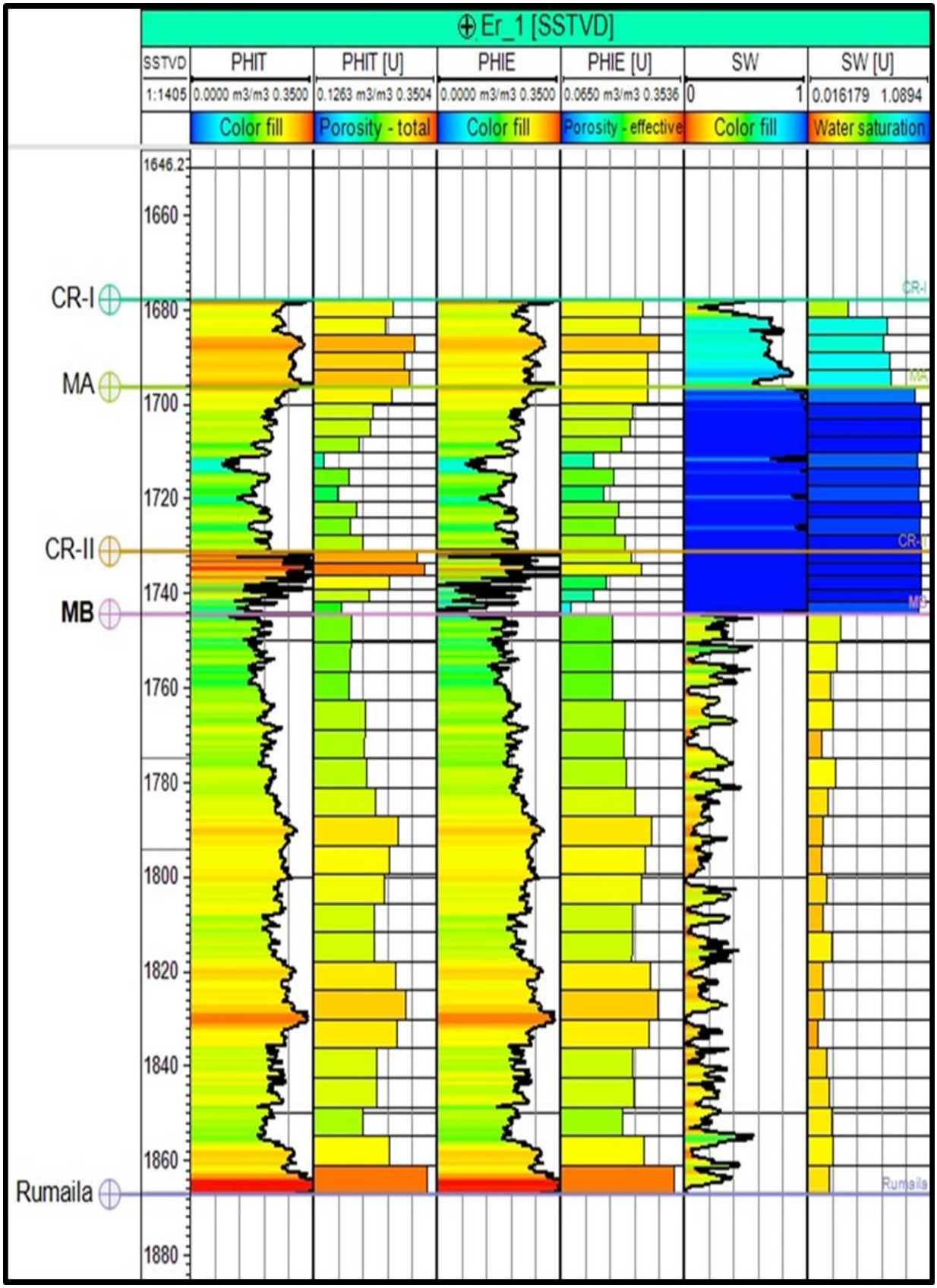

Figure (5-13) Scale up for Mishrif Formation in Eridu oilfield in wells (ER-1).

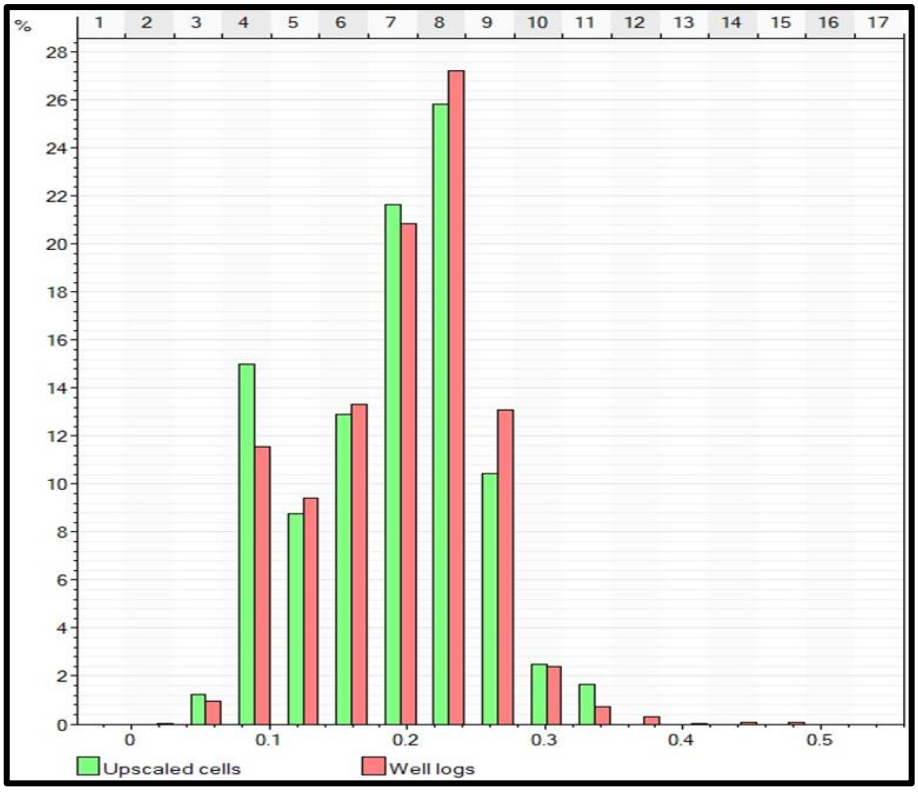

Figure (5-14) Quality histogram for PHIT of Mishrif Formation in Eridu oilfield.

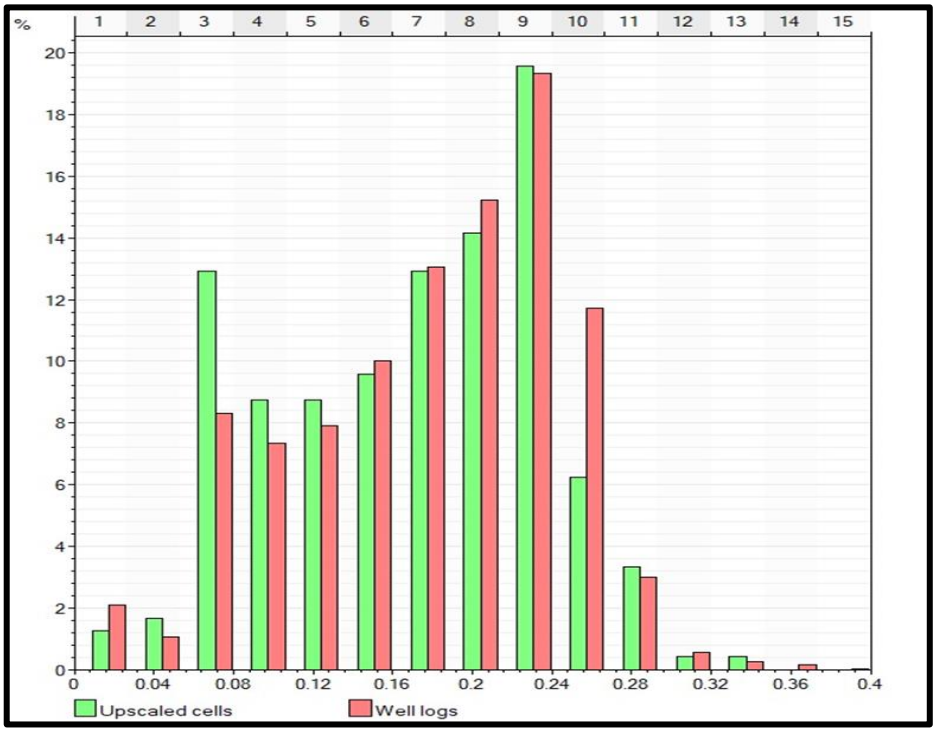

Figure (5-15) Quality histogram for PHIE of Mishrif Formation in Eridu oilfield.

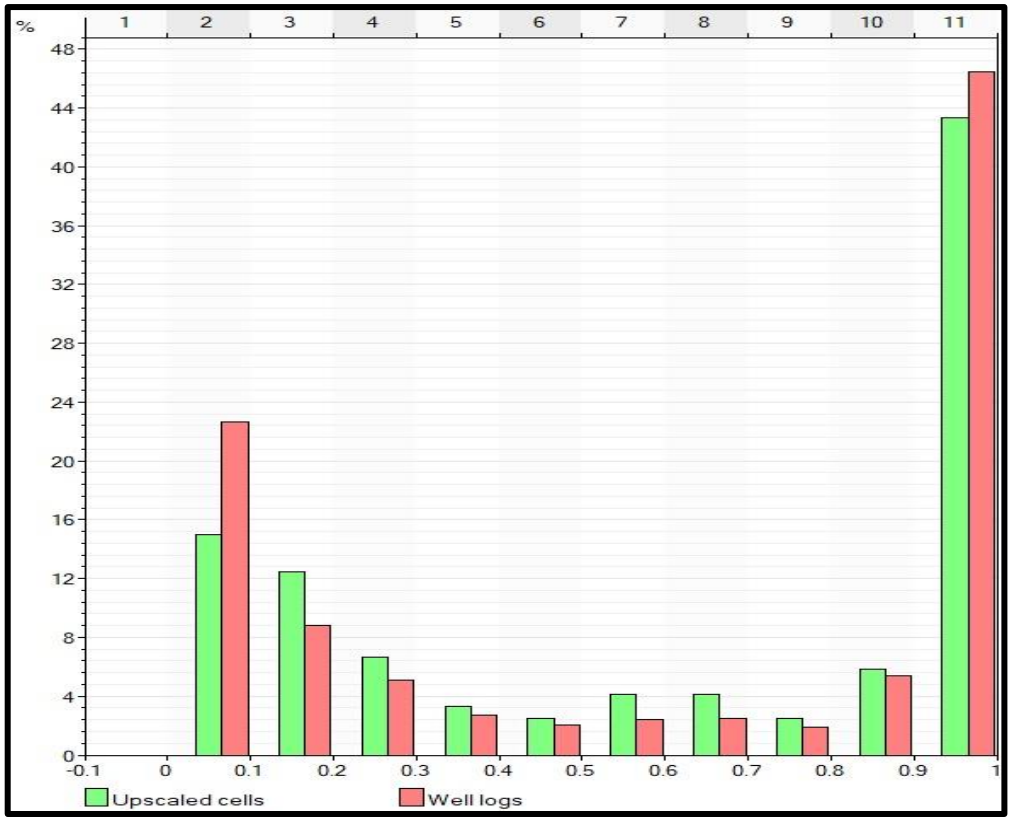

Figure (5-16) Quality histogram for SW of Mishrif Formation in Eridu oilfield.

Generally, these properties in Mishrif units shows good sampling after upscaling where each percent of unit are very close to well log value except some Sharp value of well log so the upscaling process made it with the general trend of unit properties.

5.12 Petrophysical Model

The process of giving each cell of the 3D grid a petrophysical property value (such as porosity, etc.) is known as petrophysical property modeling. For simulating the distribution of petrophysical attributes in a reservoir model, Petrel ve.18 provides a number of methods. Geostatistical techniques were used to create the Petrophysics model (Schlumberger, 2010, b).

The Petrophysics models include:

5.12.1 Porosity Model

Based on the density and neutron porosity log findings that were adjusted for and evaluated using the Tichloge ve. 15 software, a porosity model was constructed. A statistical approach that matches the volume of available data was the statistical sequential simulation technique (Schlumberger, 2010, b).

In this study, two type of porosity has been calculated (total and effective porosity (PHIT and PHIE). From porosity model the following conclusions can be shown:

- The PHIT model generally shows a high porosity reaches 33% specially in section of wells ER-7, ER-1, ER-4 while other had low porosity overall wells of ER-6, ER-2, ER-3. The PHIE model gives a high porosity up to 30% in the same trend line, in the other direction also its percent lower than this range.
- The PHIT of the unit MB reaches 32% in well ER-1 at the middle of the unit. The porosity decreased at the top of same well and reach 15%, in well ER-7, its opposite and increased at the top to reach 26%.
- The PHIE of the unit MB reaches 28% in well ER-1 at the middle of the unit. The porosity decreased at the south-west to reach 23% in well ER-7, and decreased at the north-east to reach 25% in well ER-4, while the porosity decreased at the north to lower than 12% in well ER-6.

Figures (5-17 and 5-18) show the total and effective Porosity 3D model respectively for Mishrif Formation in the Eridu field. Figure (5-19 and 5-20) shows intersection of the PHIT and PHIE along the direction of ER-7-ER-1-ER-4 while other section direction is in appendix A. Figures (5-21,5-22) are showing the porosity model for MB unit the other units shown in appendix A. Histogram window has been applied to recognize Petrophysical properties of

original log data and up scaling log data in order to check accuracy of the final 3D porosity model (PHIT and PHIE) shown in figure (5-23 and 5-24)

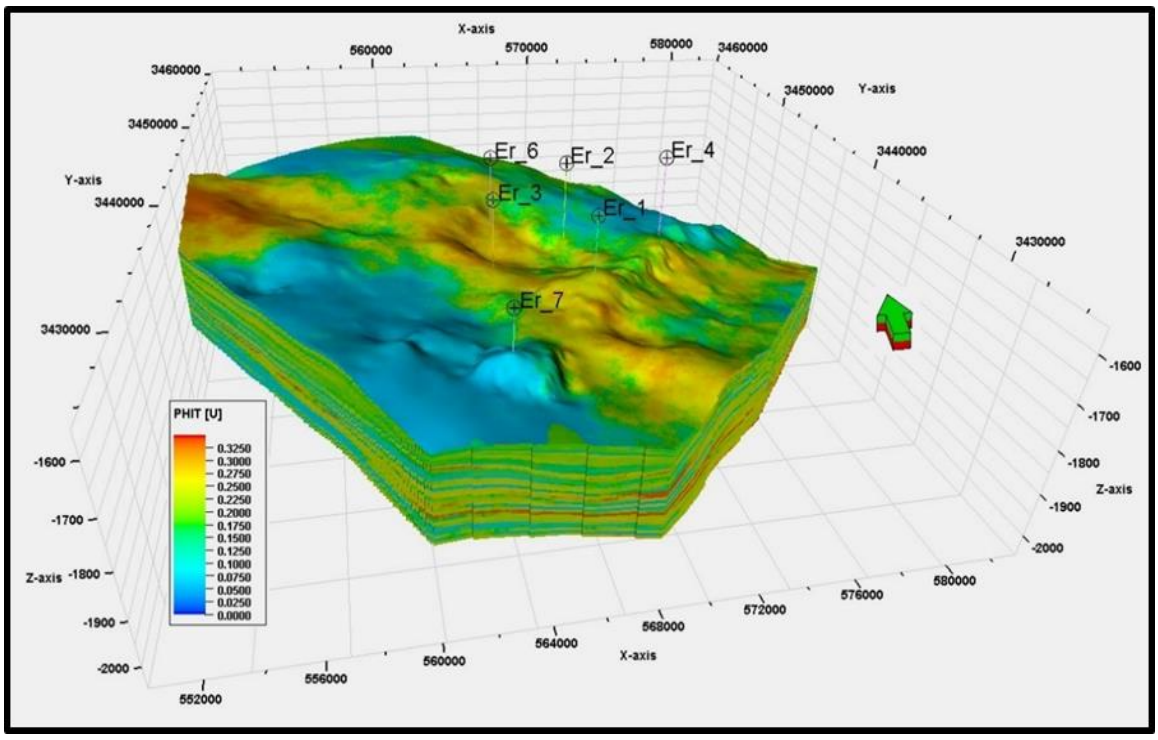

Figure (5-17) Total porosity of Mishrif Formation in Eridu oilfield.

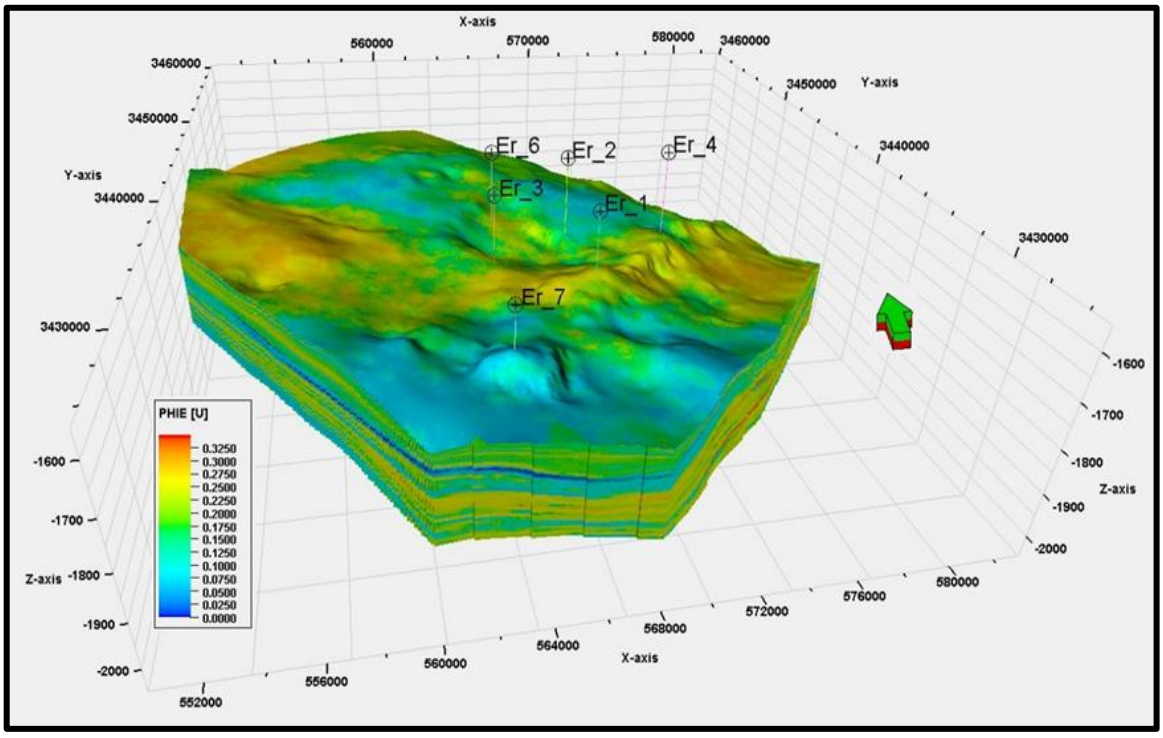

Figure (5-18) Effective porosity of Mishrif Formation in Eridu oilfield.

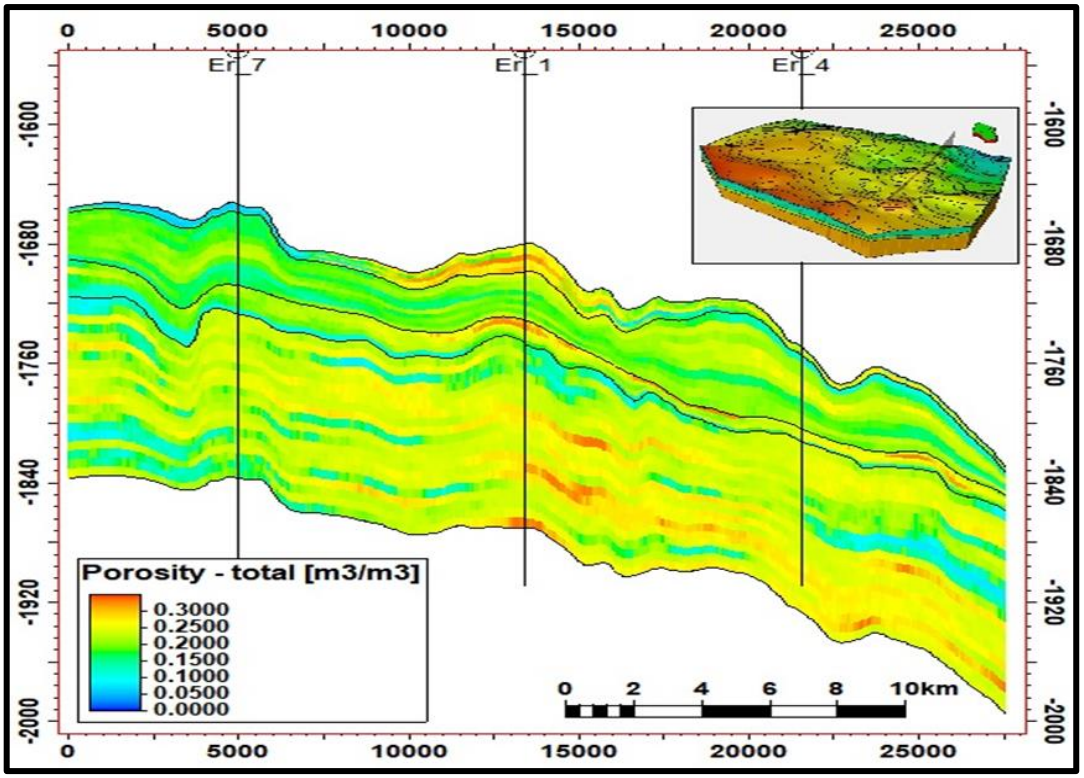

Figure (5-19) Total porosity intersection line of Mishrif Formation in Eridu oilfield in wells ER-7, ER-1 and ER-4.

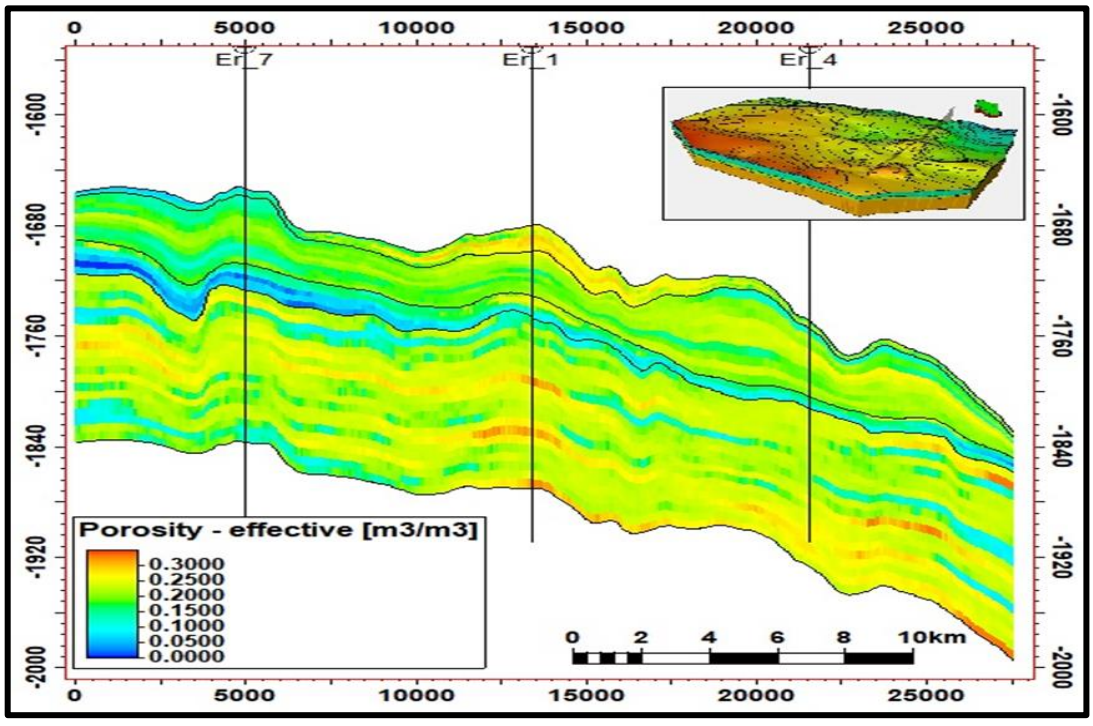

Figure (5-20) Effective porosity intersection line of Mishrif Formation in Eridu oilfield in wells ER-7, ER-1 and ER-4.

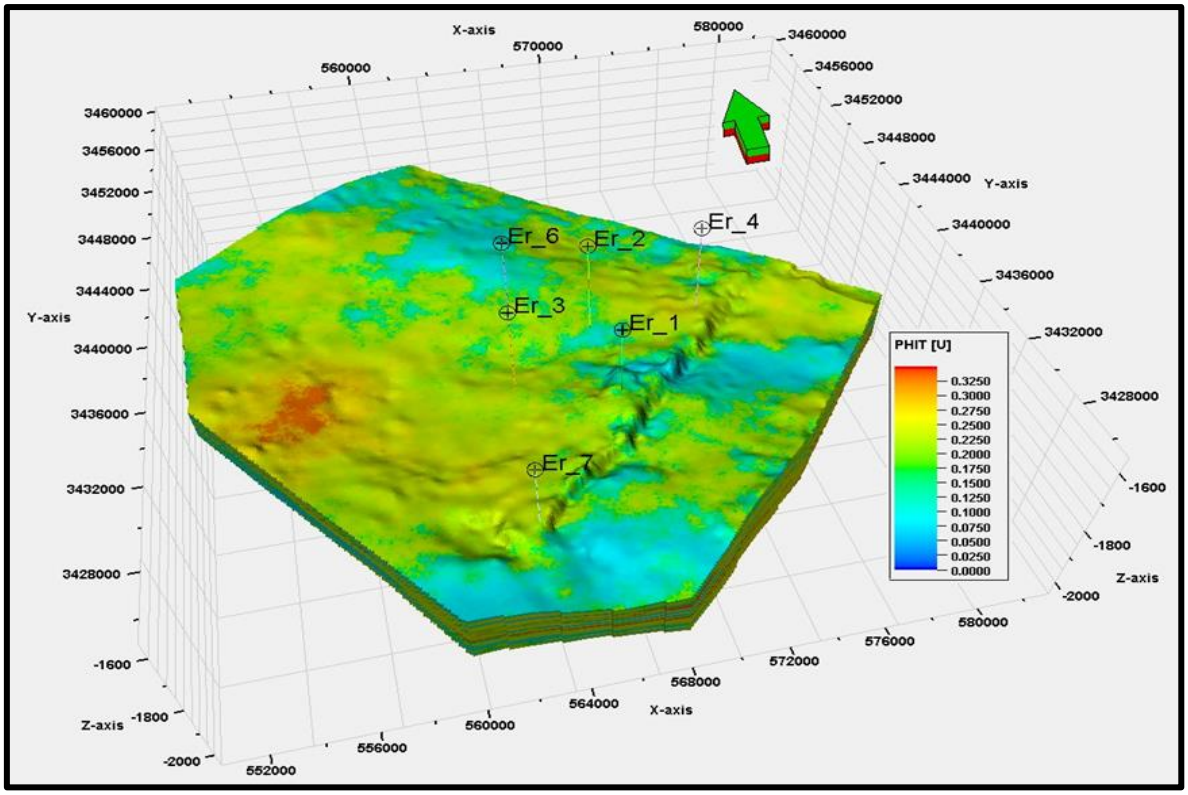

Figure (5-21) Total porosity for MB unit in Eridu oilfield.

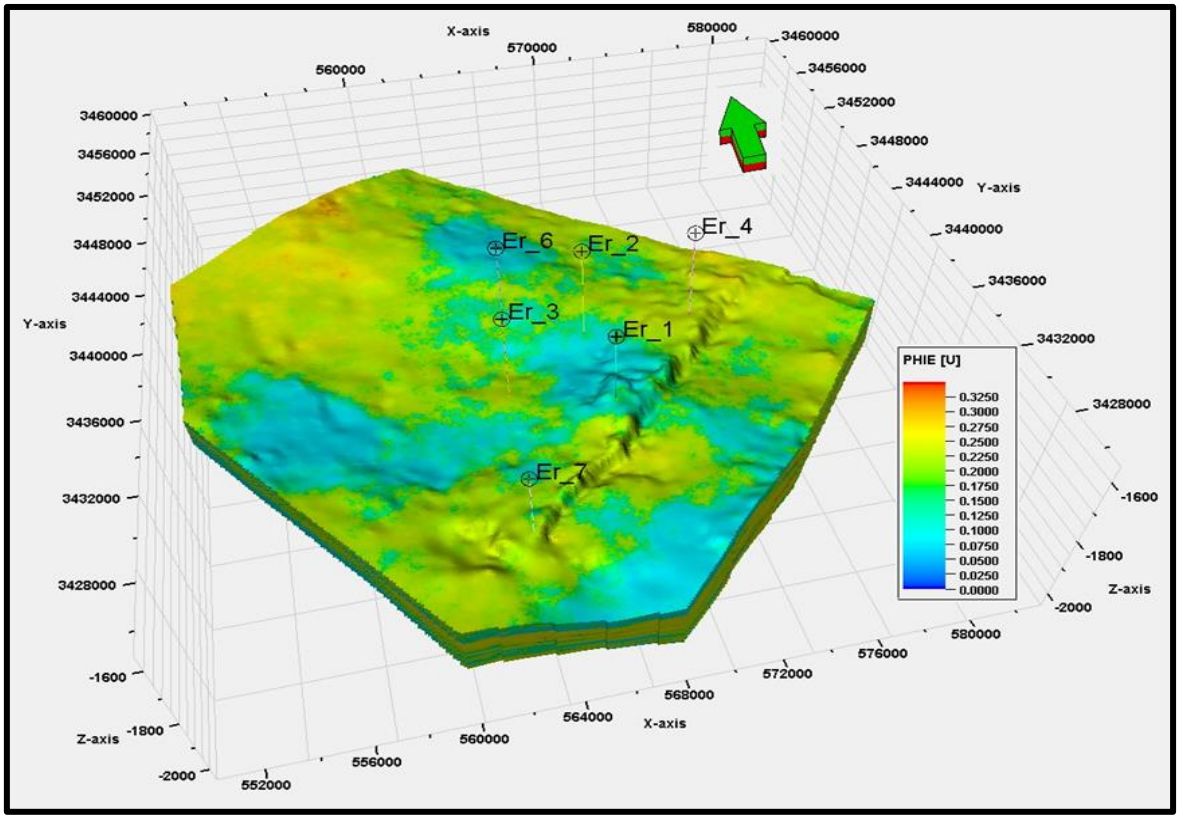

Figure (5-22) Effective porosity for MB unit in Eridu oilfield.

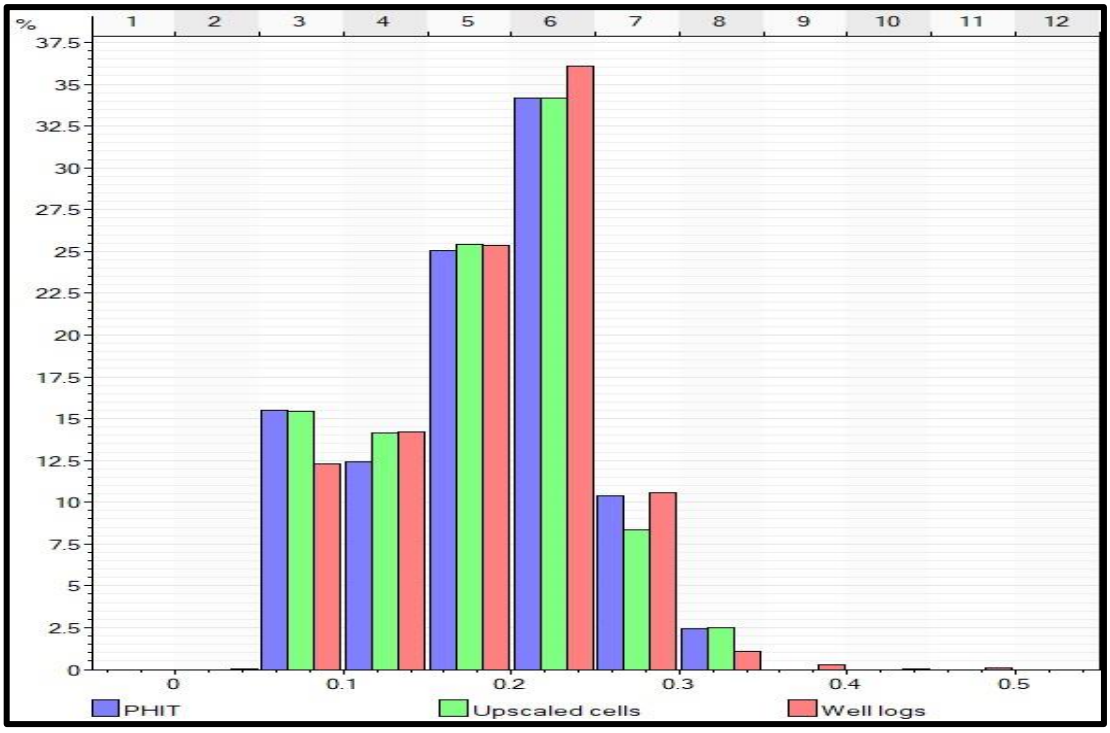

Figure (5-23) Histogram plot for total porosity of Mishrif Formation in Eridu oilfield.

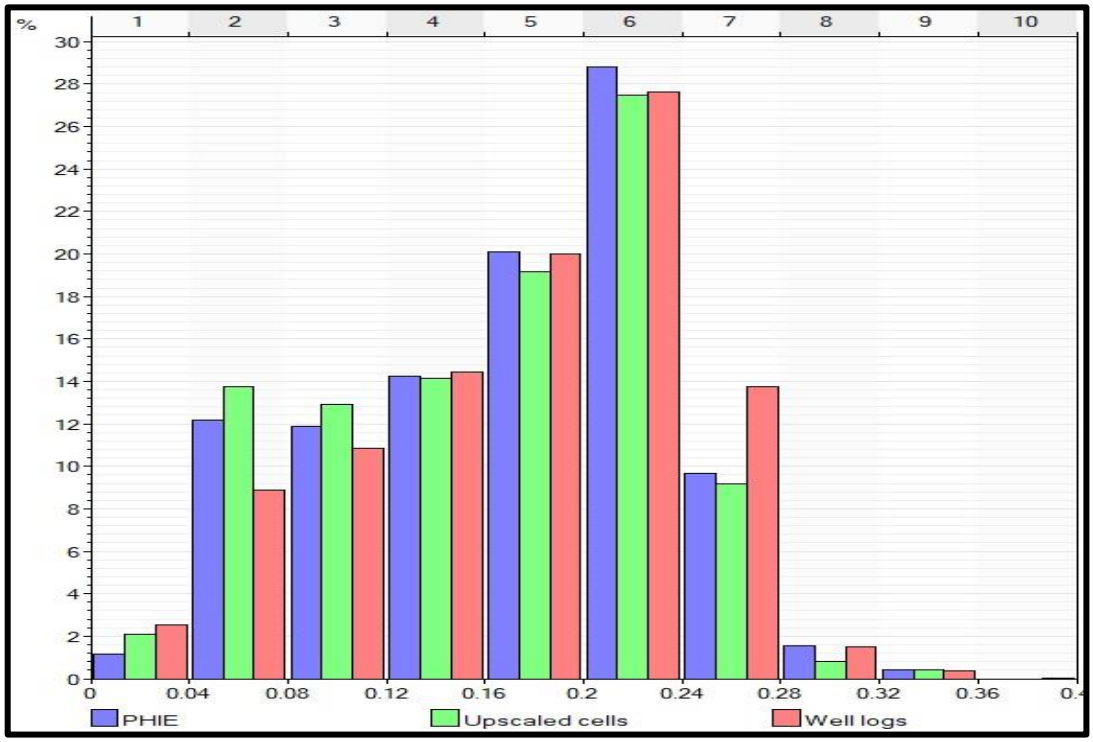

Figure (5-24) Histogram plot for effective porosity of Mishrif Formation in Eridu oilfield.

5.12.2 Water Saturation Model

The water saturation model was constructed using the same geostatistical methodology as in the porosity model. Each unit of the Mishrif Formation in the Eridu oilfield has a water saturation model constructed after the scale-up of water saturation that exports from Tichloge ve.15 software.

- The CR-II unit's water saturation ranges from 75% to 55%, particularly at the upper section of the structure high in well ER-1, and that range is mostly due to various types of clay minerals.
- In contrast to other units in the Eridu oilfield, the MA and CR-II units are distinguished by high water saturation levels that exceed 100%. Nevertheless, certain MA units in wells ER-7 and ER-4 had water saturation levels of less than 70%, which indicates that they did not exhibit any hydrocarbon.
- The Rudest build up with a very high rate forming a high structure and good hydrocarbon caused the water saturation in the MB unit to decrease to less than 10% in intersection direction SW-NE along ER-7, ER-1, ER-4 while in other will location specifically ER-2, ER-3, ER-6 reach up to 80% in some layers due to the shoal environment.

The Mishrif Formation's final water saturation model for the Eridu field is shown in Figures (5-25). Figures (5-26, 5-27) depict the water saturation section in the well's ER-7, ER-1, ER-4 and ER-7, ER-3, ER-6 directions. Appendix A depicts other directions. Figure (5-28) shows histogram window which has been applied to recognize water saturation of original log data and up scaling log data in order to check accuracy of the final 3D SW model. Unit MB in the Mishrif Formation of the Eridu field is shown to be water saturated in Figure (5-29), and appendix A contains the remaining units.

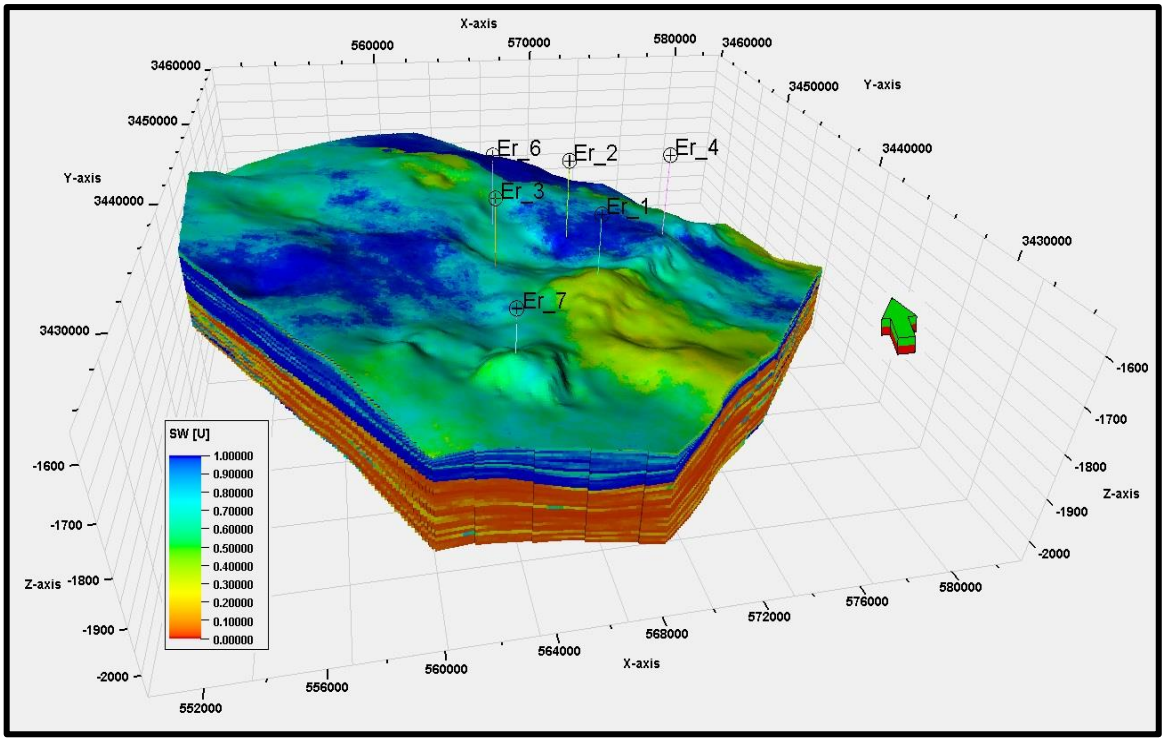

Figure (5-25) Water saturation of Mishrif Formation in Eridu oil field.

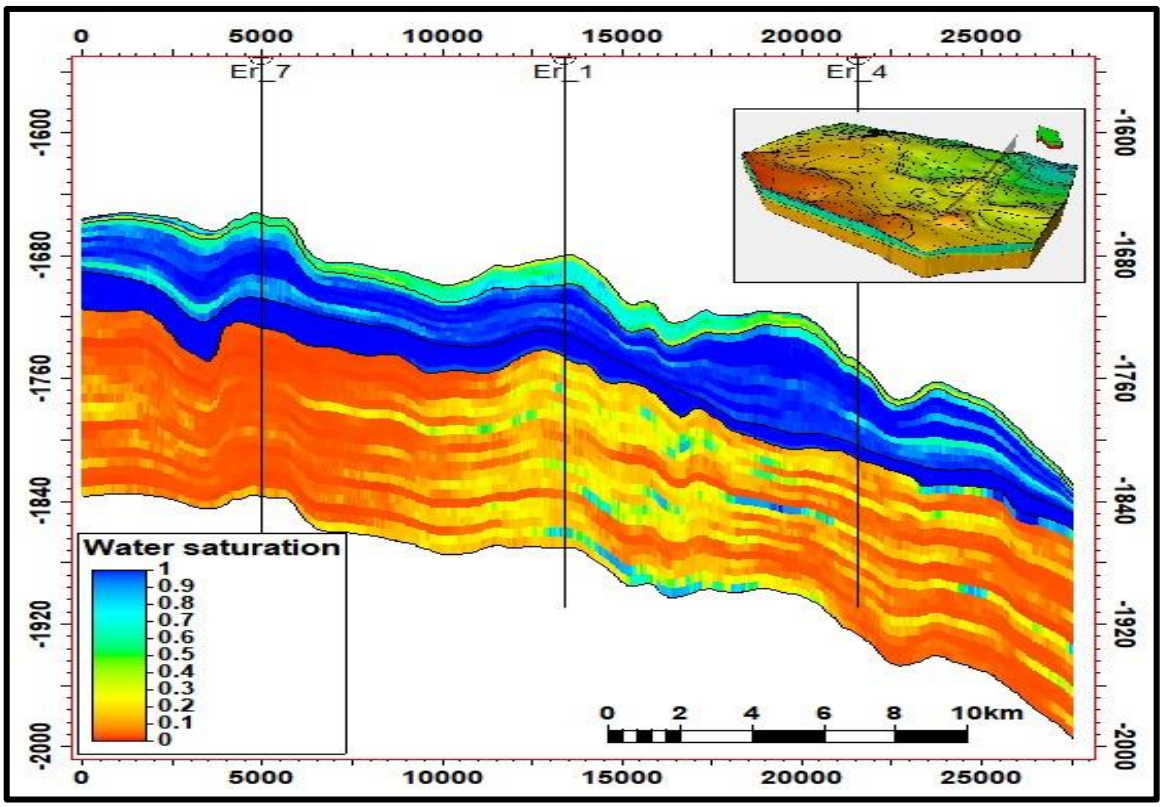

Figure (5-26) Water saturation intersection line on wells ER-7, ER-1 and ER-4.

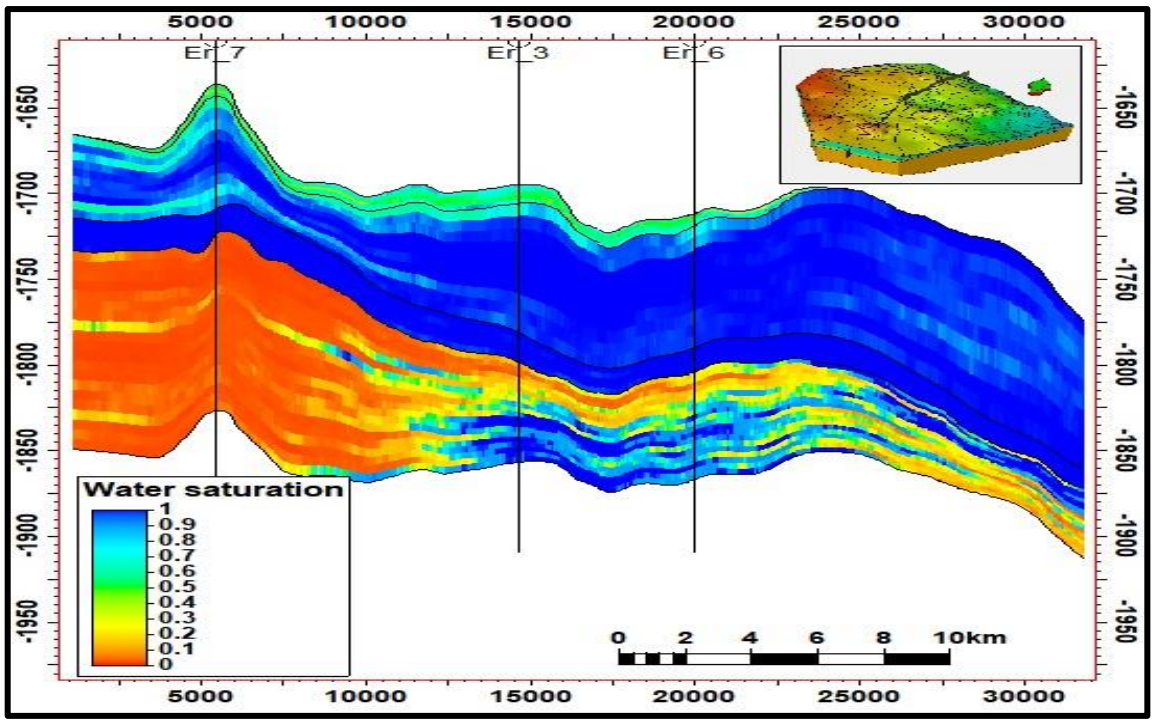

Figure (5-27) Water saturation intersection line on wells ER-7, ER-3 and ER-6.

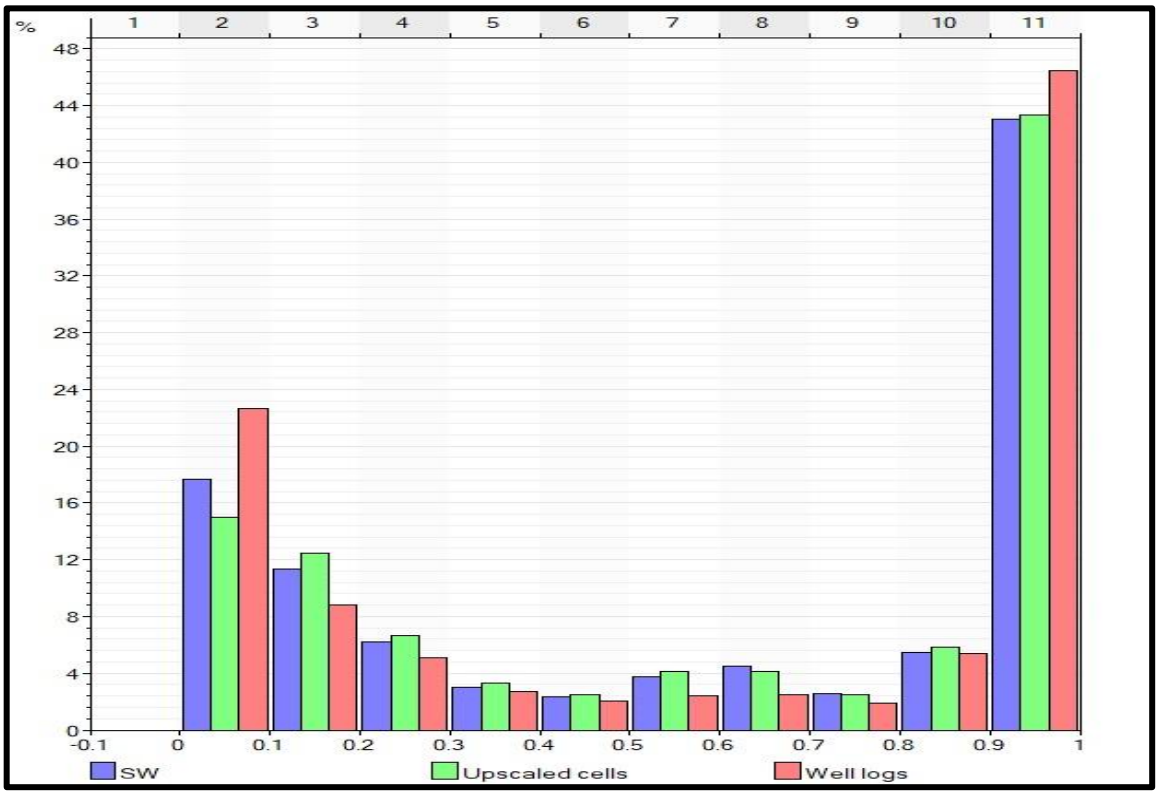

Figure (5-28) Histogram plot for water saturation of Mishrif Formation in Eridu field.

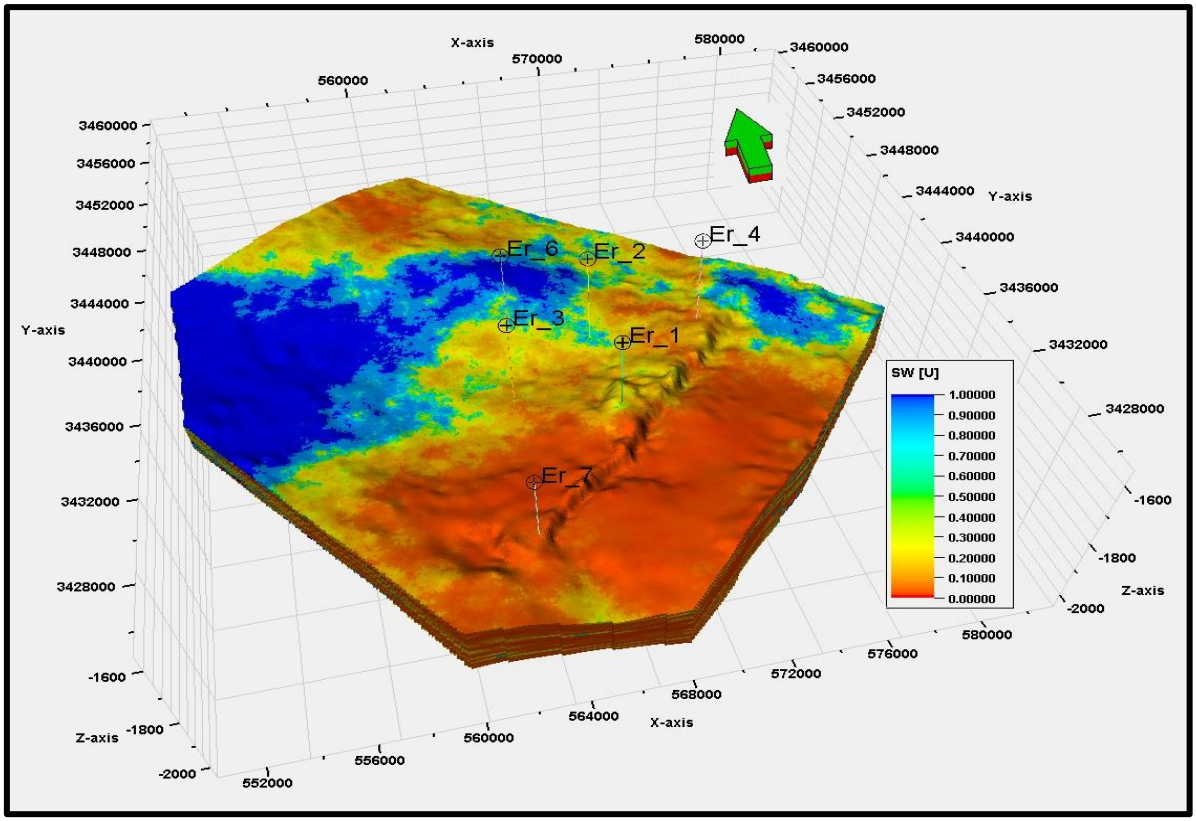

Figure (5-29) Water saturation for MB unit in Eridu oil field.

5.12.2 Facies and Environmental Model

Facies modeling is distributing discrete Facies throughout the model grid. Normally, the user will have upscaled well logs with discrete properties in the model grid, and possibly defined trends within the reservoir, by analyzing this data (Schlumberger, 2010, b)

Mishrif is divided into 5 depositional environments according to the thin sections, logs interpretation those environments are deep marine, shallow open marine, shoal, restricted marine and rudist Biostrum were generally interpreted for each well.

In this study, the 3D depositional model of Mishrif Formation was constructed from study of microfacies and sedimentary environments for ER-1 ,2and3 as obtained in chapter two.

The 3D environment model of the Mishrif Formation has been built by studying the microfacies for ER-1,2 and 3 and examining the available thin section as well as the logs data.

The facies model subdivides units of Mishrif as follow:

- CR-I unit consist of deep marine environment which represents a cap rock that has no oil bearing or shows.
- MA unit mainly of shallow open marine with some facies of shoal and restricted marine, this unit has poor petrophysical properties such as effective porosity and oil shows with little oil show in shoal layer.
- CR-II unit also consist of open marine environment which cover the main reservoir unit and it represented as a key layer deposited in most of south Iraq oil field.
- Rudist Biostrum and shoal facies which have good reservoir properties represent the reservoir unit and oil bearing zones in MB unit specially in the trend of wells ER-1,7 and4 (Rudist buildup zone) while other facies of restricted and open shallow marine had some oil shows but it doesn't regard as oil bearing layer in the other well of the Eridu oilfield.

Figure (5-30) show the final Facies and Environmental model for Mishrif Formation. Figures (5-31- 5-32) show the Facies and Environmental map for MA and MB of Mishrif Formations the other unit are in Appendix A.

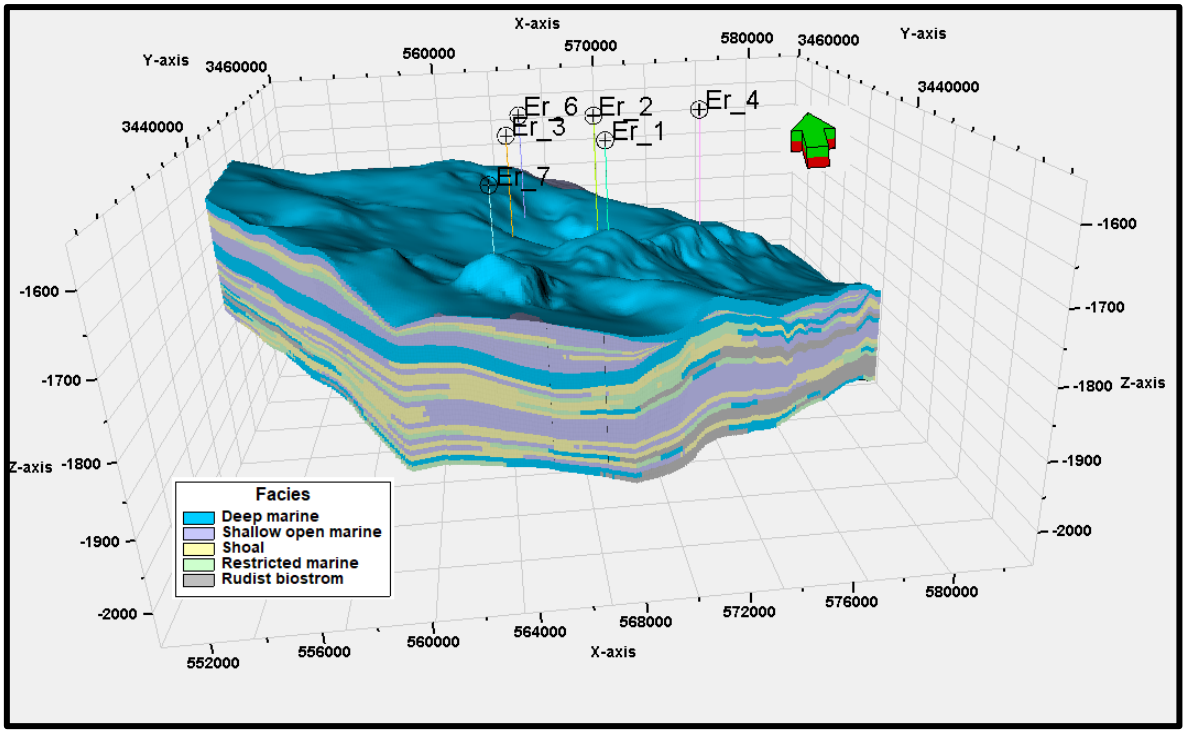

Figure (5-30) 3D view of Facies and Environmental distribution in Eridu oilfield.

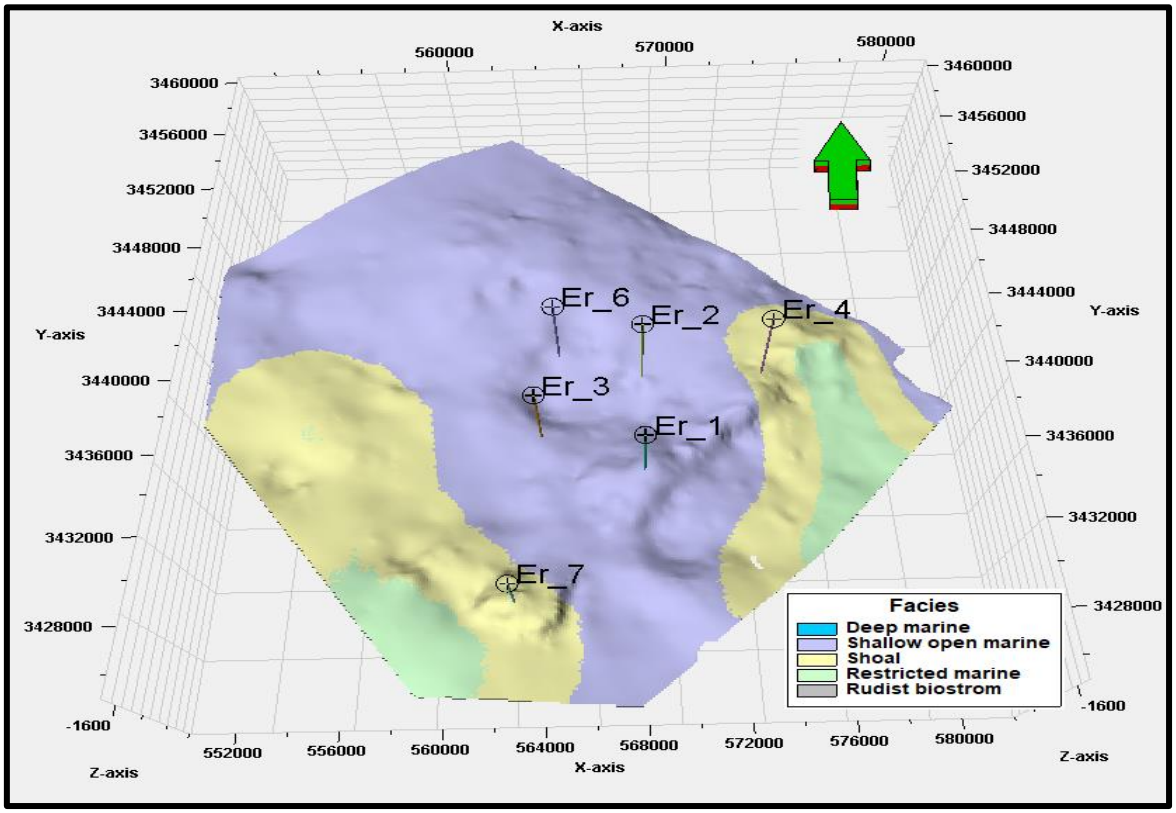

Figure (5-31) Facies and Environmental map of MA unit in Eridu oilfield.

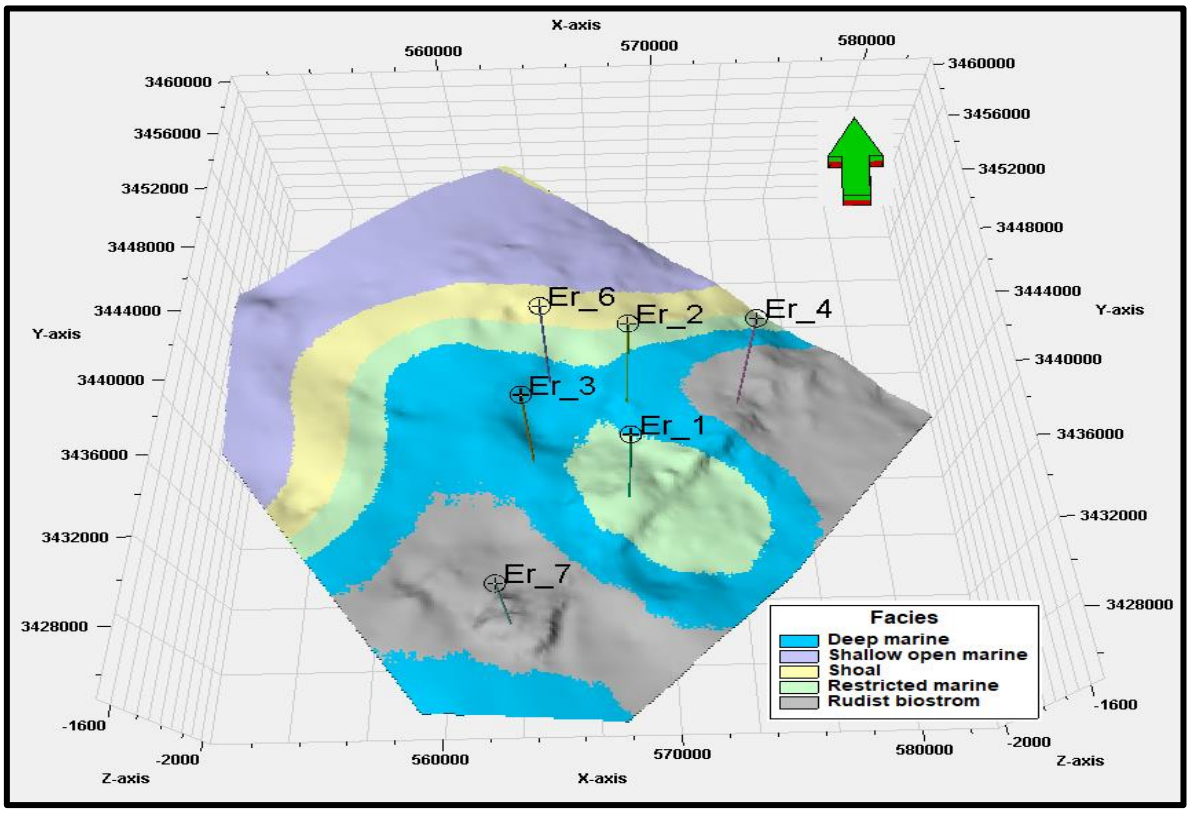

Figure (5-32) Facies and Environmental map of MB unit in Eridu oilfield.

Chapter Six

Conclusion and Recommendations

6.1 Conclusion

1. This study showed that the Mishrif Formation in Eridu oilfield consists of six major microfacies and ten secondary microfacies. They are Bioclastic Packstone, Rudstone, Boundstone large Rudist fragment, Plankton Foraminiferal Packstone, Bioclastic Wackestone to Packstone, Peloidal Packstone, Bioclastic Packstone to Grainstone, Peloidal to Bioclastic Packstone, Benthonic Foraminiferal Mudstone Packstone, Bioclastic Packstone to Grainstone, Peloidal to Bioclastic Packstone, Benthonic Foraminiferal Mudstone, and Rudist fragmented Mudstone. These microfacies were deposited in restricted, shoal, shallow open marine, rudist biostrum, and deep marine environments, which indicates a clear variation in sea level and tectonic activity that accompanied the sedimentation process.
2. Depending on the examination of the thin section and the interpretation of the behavior of the different logs, the Mishrif Formation was divided into four main units, which are the two reservoir units (MB, MA), the cover unit (CR 1) and the barrier unit (CR 2), where the covering unit deposited in the deep marine. The reservoir unit (MA) deposited in the shallow open marine, restricted marine and shoal, the unit (CR-II) deposited in the deep margin, while the main reservoir unit (MB) deposited in different environments that extended between rudist biostrum, restricted marine, shoal, shallow open marine and deep marine.
3. There are six diagenetic processes (Micritization, Dissolution, Compaction, Recrystallization, Dolomatiztion and Cementation) affected the rocks of the Mishrif formation, and the dissolution process had an important role in improving the reservoir specifications through what it consisted of different types of porosity, especially secondary porosity of a large type such as cavern, vugs growth framework, on the

other hand, the cementing process negatively affected the reservoir specifications by filling the porous spaces with cementitious materials.

4. From the Pota-Thor cross-plots for Mishrif Formation it is indicated that the main clay minerals are montmorillonite and illite-montmorillonite mixed layer clay, and chlorite.
5. Water saturation was calculated and show that water saturation increases in units (CRI, MA and CRII) and decrease in units (MB) which characterize good reservoir properties.
6. The residual hydrocarbon and movable hydrocarbon are few in the (CRI, CRII) units and are almost non-existent, while the (MA) unit contains few oil evidence, and for the (MB) unit, the value of the residual hydrocarbons is very high in the (7,1,4) wells, while the (6,2,3) wells contain oil, but at a lower rate from those wells, the percentage of water saturation is almost high in these wells.
7. For the Mishrif formations, five contour maps have been created. These units (CR-II, MA, CR-II, MB, and Rumaila) are based on the well tops of each well that was chosen in the Eridu oilfield. These structural maps depict a stratigraphic trap, or Rudest accumulation, particularly in the MB unit around the ER-7, ER-1, and ER-4 wells, with anticlines that have their axes in the same directions as the wells and the area's major slope running from west-southwest to north-east and east.
8. Each reservoir unit in Mishrif Formation has been divided into many layers depending on petrophysical properties and facies. CRI has been divided into 5 layers, MA has been divided into 10 layers, CRII has been divided into 5 layers and MB has been divided into 20 layers, because they are important layers with good reservoir properties.
9. Sequence stratigraphic analysis show there are five stratigraphic surfaces based on the abrupt changing in depositional environments, and intra-Mishrif four surfaces are maximum flooding surfaces which represents

the deepening up-ward association facies. Two major sequences (sequence I and sequence II) are identified based on the behaviors of facies association within sequence stratigraphic boundaries and TST and HST system tracts.

6.2 Recommendations

1. The study recommends providing core samples for wells that do not contain cores in order to study them in more detail from the lithological and petrophysical aspects.
2. New wells must be drilled in the northern dome of the field and drilled into the Mishrif Formation to cover this portion of the field in order to improve the accuracy of the formation evaluation.
3. Two and three dimensional seismic data are very important for building advanced geological models, so sufficient seismic geophysical studies must be provided to form a Mishrif Formation in the Eridu oilfield.

Reference

- Ahr, W.M, 2008. Geology of carbonate reservoirs: the identification, description, and characterization of hydrocarbon reservoirs in carbonate rocks. Texas A&M University. 277p.
- Al-Baldawi, B. A. (2020). Petrophysical Analysis of Well Logs for Asmari Reservoir in Abu Ghirab Oil Field, South Eastern Iraq. Iraqi Journal of Science, 2990-3001.
- Al-Hajeri, M. M., Al Saeed, M., Derks, J., Fuchs, T., Hantschel, T., Kauerauf, A., ... & Peters, K. (2009). Basin and petroleum system modeling. Oilfield Review, 21(2), 14-29.
- Al-K hafaji, Amer Jassim. (2015). The Mishrif, Yamama, and Nahr Umr reservoirs petroleum system analysis, Nasiriya oilfield, Southern Iraq. Arabian Journal of Geosciences, 8(2), 781–798.
- Almalik, M.S., Hamada, G.M. and Al-Awad, M.N., 2001. "Accuracy Analysis of Archie Parameter and Relevant Effect on Water Saturation Values", Saudi Arabia, SCA.
- Al-Mosawy, A.D.J., 2014. 3D integration geological modeling of Mishrif Formation in Halfaya oil field. M.Sc. Thesis, University of Baghdad,144p.
- Al-Naqib, K.M., 1967, Geology of the Arabian Peninsula, Southwestern Iraq, U.S. Geol. Survey Prof. paper, 560-G, P. 54.
- Alsultan, H.A.A., Maziqa, F.H.H., Al-Owaidi, M.R.A., 2022. A stratigraphic analysis of the Khasib, Tanuma and Sa'di formations in the Majnoon oil field, southern Iraq. Bulletin of the Geological Society of Malaysia, 73, 163 – 169.
- Aqrawi, A.A.M., J.C. Goff, A.D. Horbury, and F.N. Sadooni, 2010, The petroleum Geology of Iraq: Scientific press, 424p.

- Aqrawi, A.AM., Dhehni, G.A., Sherwani, G.H., and Kareem, B.M.M., 1998. Mid cretaceous Rudist-Bearing carbonate of the Mishrif Formation Journal Petroleum Geology, vol.21(1), p. 57-82.
- Archei, G.E., 1942. "Electrical Resistivity Log as and Aid in Determining Some Reservoir Characteristics," Trans., AIME.
- Asquith, G. B. and Krygowski, D., 2004, Basic Well Log Analysis, 2nd Edition: AAPG Methods in Exploration Series 16. Published by The American Association of Petroleum Geologists Tulsa, Oklahoma, 244p.
- Blatt, H., Middleton, G. and Murray, R., 1980. Origin of Sedimentary Rocks. Prentice – Hall, USA. 782 P.
- Boogs S. Jr., 2009. Petrology OF Sedimentary Rocks, second edition, Cambridge University Press, New York, 600p.
- Buday, T., 1980. The Regional Geology of Iraq. Vol.1: Stratigraphy and Paleogeography. Dar Al-Kutib Publishing house, University of Mousl, Iraq, 445p.
- Cannon, S., 2016. Petrophysics: A Practical Guide. John Wiley & Sons, Ltd Registered.
- Catuneanu, O. (2002). Sequence stratigraphy of clastic systems: concepts, merits, and pitfalls. Journal of African Earth Sciences, 35(1), 1-43.
- Chatton, M. and Hart, E., 1962. Review of the Cenomanian to Maastrichtian stratigraphy in Iraq, the Cenomanian cycle. Oil Exploration Company, Baghdad, Iraq (Internal Report).
- Choquette P.W. and Pray L.C., 1970. Geologic nomenclature and classification of porosity in sedimentary carbonates. AAPG. V.54, No.2, PP 207-250.

- Dan Hartmann J. and Edward Beaumont A.,1999. (Treatise of Petroleum Geology /Handbook of Petroleum Geology: Exploring for Oil and Gas Traps).
- Dandekar. A. Y., 2013. Petroleum reservoir rock and fluid properties. 2nd edition.
- Ditmar, V. and Iraqi-Soviet Team, 1980. Geological conditions and hydrocarbon prospects of the Republic of Iraq (Northern and Central parts). Manuscript report, INOC Library, Baghdad.
- Doyle, J. D., Sweet M. L.,1995. Three-Dimensional Distribution of Lithofacies, Bounding Surfaces, Porosity, and Permeability in a Fluvial Sandstone--Gypsy Sandstone of Northern Oklahoma, vol79, pp70-95
- Dunham R. J. 1962. Classification of carbonate rocks according to depositional texture: in Ham W. E. (ed), classification of rocks; a symposium, AAPG, No. 1, PP 108-121.
- Embry, AF, and Klovan, JE, 1971, A Late Devonian reef tract on Northeastern Banks Island, NWT: Canadian Petroleum Geology Bulletin, v. 19, p. 730-781.
- Emery, D. and Myers, K. (1996): Sequence Stratigraphy. Black Well Science- p.210.
- Ezekwe, N., 2011. Petroleum Reservoir Engineering Practice. Pearson Education Inc. Boston, USA. 768pp.
- Flugel, E. (2010) Microfacies of Carbonate Rocks, 2nd ed. SpringER-Verlag Berlin, Germany. 976 pp.
- Flugel, E., 1982. Microfacies analysis of limestones, SpringER-Verlag, Berlin, 663p.
- Flugel, E., 2004. Microfacies of Carbonate Rocks, analysis, Interpretation and Application. Springer Science+Business Media, Verlag Berlin Heidelberg. 976pp.

- Fouad, S. F. (2012). Tectonic Map of Iraq, scale 1: 1000 000, 3rd edit. GEOSURV, Baghdad, Iraq.
- Hilliburton, 2001. "Basic Petroleum Geology and Log Analysis".
- Hunt, J. M. (1996) Petroleum geochemistry and geology, 2nd edn, Freeman, New York, 743P.indicators: Geochimica et Cosmochimica Acta, v. 43, pp. 739-745.
- James, G. A., Wynd, J. g., 1965. Stratigraphic nomenclature of Iranian oil consortium agreement area: AAPG Bulletin, vol.49, pp 2182-2245.
- Jassim, S.Z. and Goff, J.C. (2006) Geology of Iraq, published, by Dolin, Prague and Moravian Museum, Brno (2006), 340p.
- Jervey, M.T., 1988. Quantitative geological modelling of siliciclastic rock sequences and their seismic expressions, in Wilgus, C.K., Hastings, B.S., Kendall, C.G.St.C., Posamentier, H.W., Ross, C.A., and van Wagoner, J.C. (eds.), Sae-level changes-an integrated approach. SEPM Spec.Publ.42, p.47-69.
- Kendall, A.C. and Tucker M. E. (1973). Radiaxial Fibrous Calcite: a replacement after acicular Carbonate. Sedimentology 20, 365 – 390.
- Kerans, C. and Tinker, C., 1997. Sequence stratigraphy and characterization of carbonate reservoirs. SEPM Short Course Notes, 40, 130 pp.
- Leverson, A.I., (1970) Geology of Petroleum vakilas and Feffer Simons Privale.
- Longman, M. W., 1980. Carbonate Digenetic Textures from near surface Digenetic Environment. AAPG. Bull., Vol. 64, NO. 4, PP. 461 – 487.
- Lucia F.J., 2007. Carbonate Reservoir Characterization. An Integrated Approach, Second Edition. SpringER-Verlag Berlin, Heidelberg. 336p.
- Mahdi, T. A., Aqrawi, A. A., Horbury, A. D., & Sherwani, G. H. (2013). Sedimentological characterization of the mid-Cretaceous

Mishrif reservoir in southern Mesopotamian Basin, Iraq. GeoArabia, 18(1), 139-174.

- Mitchum, R.M., Vail, P.R., and Sangree, J.B., 1977. Seismic stratigraphy and global changes of sea-level, part 6: Stratigraphic interpretation of seismic reflection patterns in depositional sequences, in Pyton, C.E. (ed.), Seismic stratigraphy-application to hydrocarbon exploration. AAPG Memoir 26, p.117-133.
- Pickett, G.R., 1966. Review of Current Techniques for Determination of Water Saturation from Logs. Journal of Petroleum Technology (JPT), pp: 1425-1433.
- Posamentier, H.W., Jervey, M.T., and Vail, P.R., 1988. Eustatic controls on clastic deposition II- coceptual framework, in Wilgus, C.K., Hastings, B.S., Kendall, C.G.St.C., Posamentier, H.W., Ross, C.A., and van Wagoner, J.C. (eds.), Sae-level changes- An integrated approach. SEPM Spec.Publ.42, p.125-154.
- Rabanit P. M. V., 1952. Rock units of Basrah area, BPC, unpublished report.
- Sarg, J. F. (1988): Carbonate sequence stratigraphy. In: sea level changes- An inegrated approach SEPM. Spec-pub., No. 42, pp. 155-181.
- Schlumberger, 1972. Log Interpretation charts, Houston, Schumberger well services, Inc., Vol.2.
- Schlumberger, 1989. "Log Interpretation Principles/Applications", Houston.
- Schlumberger, 1997. Interpretation Principles/Applications, Houston, Schlumberger Wireline and Testing.
- Schlumberger, 2008. "Petrel Manual and applications". introduction course Schlumberger, 72. Schlumberger, 2008. Petrel 50-334p.

- Scholle P. A. and UlmER-Scholle D. S., 2003, A Color Guide to the Petrography of Carbonate Rocks: Grains, textures, porosity, diagenesis, AAPG Memoir 77, Published by The American Association of Petroleum Geologists, Tulsa, Oklahoma, USA, 459pp.
- Scott, R.W., Franks, P.C., Stein, J.A., and Events, M.J., 1994. Graphic correlation tests the synchronous mid-Cretaceous depositional cycles: western interir and Gulf Coast, in Dolson, J.C. (ed.), Unconformity related hydrocarbons in sedimentary sequences. Rocky Montain Association Geologists, p.89-98.
- Selly, R. C., 1982. An introduction to Sedimentology. Academic Press Inc. (London) LTD. 408P.
- Sharland P. R., Archer R., Casey D. M., Davies R. B., Hall S. H., Heward A. P., Horrury A. D. and Simmons M. D., 2001. Arabian Plate Sequence Stratigraphy, GeoArabia Special Publication 2, Gulf PetroLink, Bahrain, 371 p.
- Stephen, K.D., Clark, J.D., Gardiner, A.R., 2001. Outcrop-based stochastic modeling of turbidite amalgamation and its effects on hydrocarbon recovery. Petroleum Geoscience, 7, 163–172.
- Taylar,1964. In Land 1967 Diagenesis of Skeletal Carbonates. J. Sed. Petr. Vol. 37, No. 3, pp. 914 – 930.
- Tiab, D., and Donaldson, E.C.,2004. Petrophysics, and Edition: Theory and Practice of Measuring Reservoir Rock and Fluid Transport Properties, Elsevier, Amsterdam, pp. 881
- Tucker M.E. and V.P. Wright, 1990. Carbonate sedimentology, Oxford, Blackwell scientific publications, Great Britain, 482p.
- Tucker, M.E., 1982. Sedimentary Petrology, An Introduction, Blackwell Scientific publications, 252P

- Van Bellen, R.C., H.V. Dunnington, Wetzel, R.and Morton, D. (1959) Lexique Stratigraphique International-Vol. III, Asie Fasc. 10a. Iraq, Paris. 333p.
- Van Wagoner, J. C., Posamentier, H. W., Mitchum, R. M., Vail, P.R., Sarg, J. F. loutit, T. S., and Hardenbol, J. (1988): An Over view of the fundamentals, in C. W. Wilgus et al., eds., sea level changes: an integrated approach, SEPM, special publication42-p-39-45.
- Wilber and Neumann, 1993. Effects of Submarine Cementation on Microfabrics and Physical Properties of Carbonate Slope Deposits, Northern Bahamas, pp 79-94.
- Wilson, J. L., 1975. Carbonate Facies in Geologic History. Springer Verlag, Berlin. 471p.
- Wyllie M. R. J., Gregory A. R., and Gardner G. H. F., 1958. An experimental investigation of the factors affecting elastic wave velocities in porous media: Geophysics, v. 23, p. 459–493

Appendix (A)

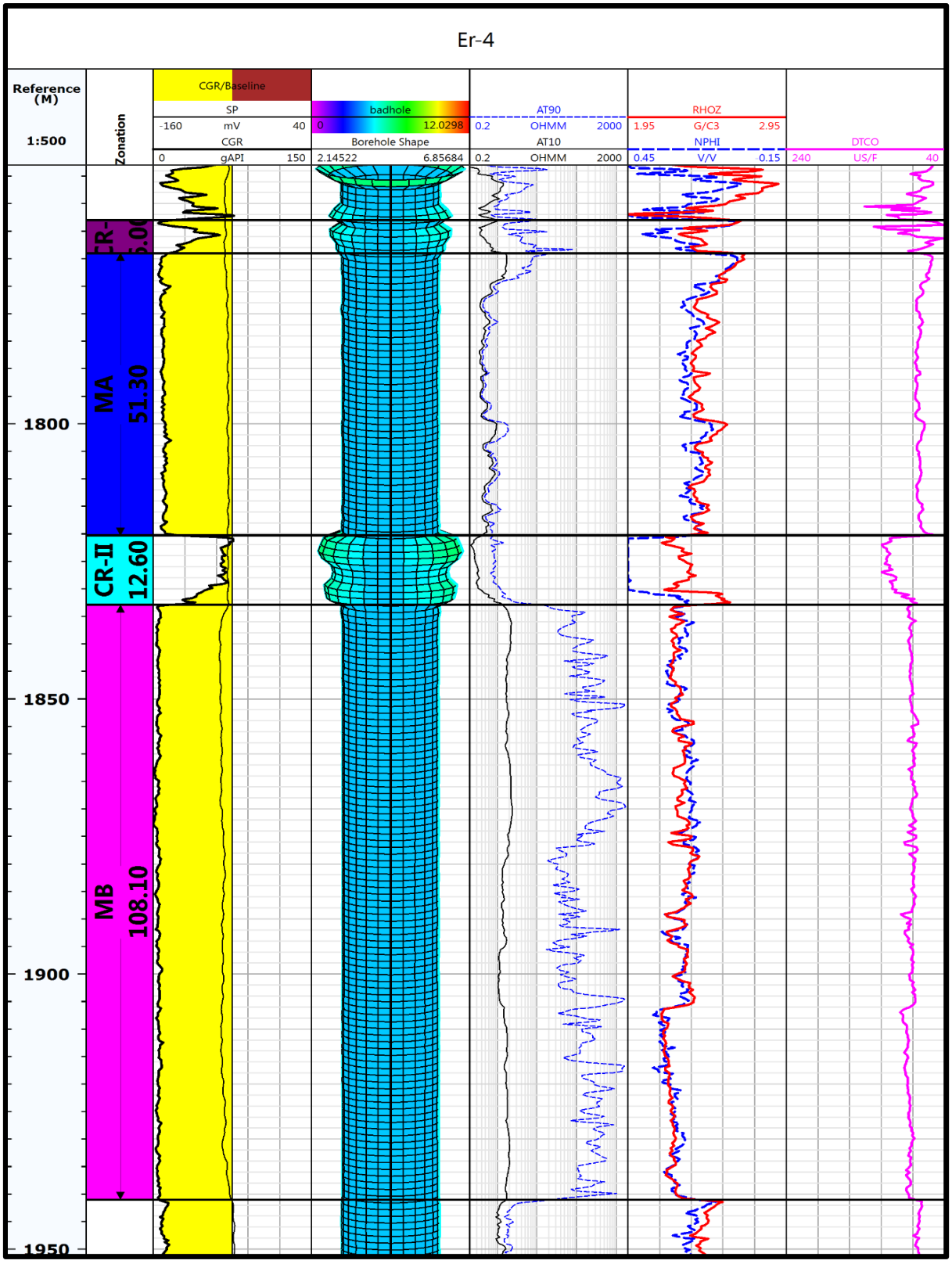

Figure (A,1) Qualitative interpretation of Mishrif Formation in the for well ER-4

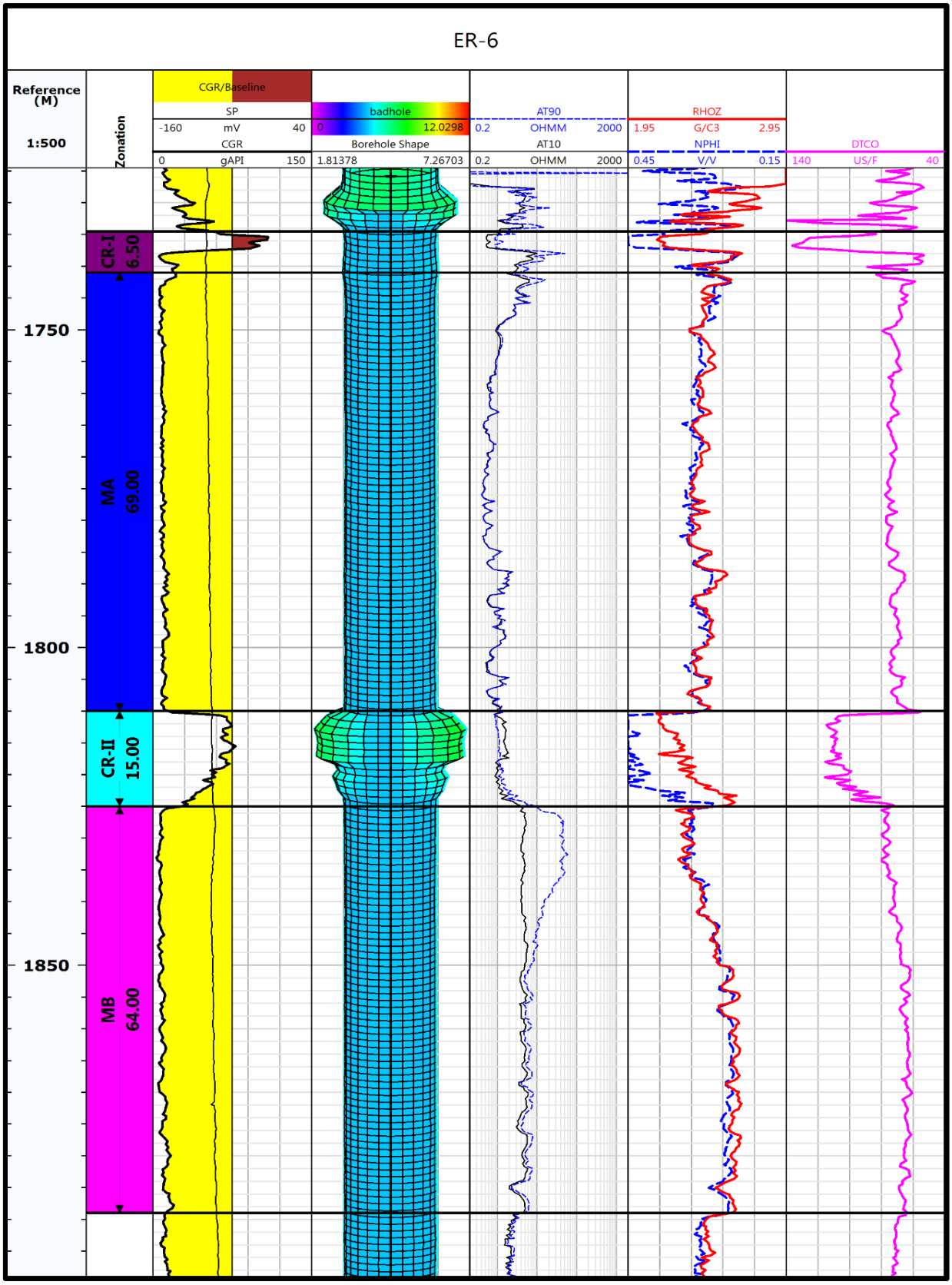

Figure (A,2) Qualitative interpretation of Mishrif Formation in the for well ER-6

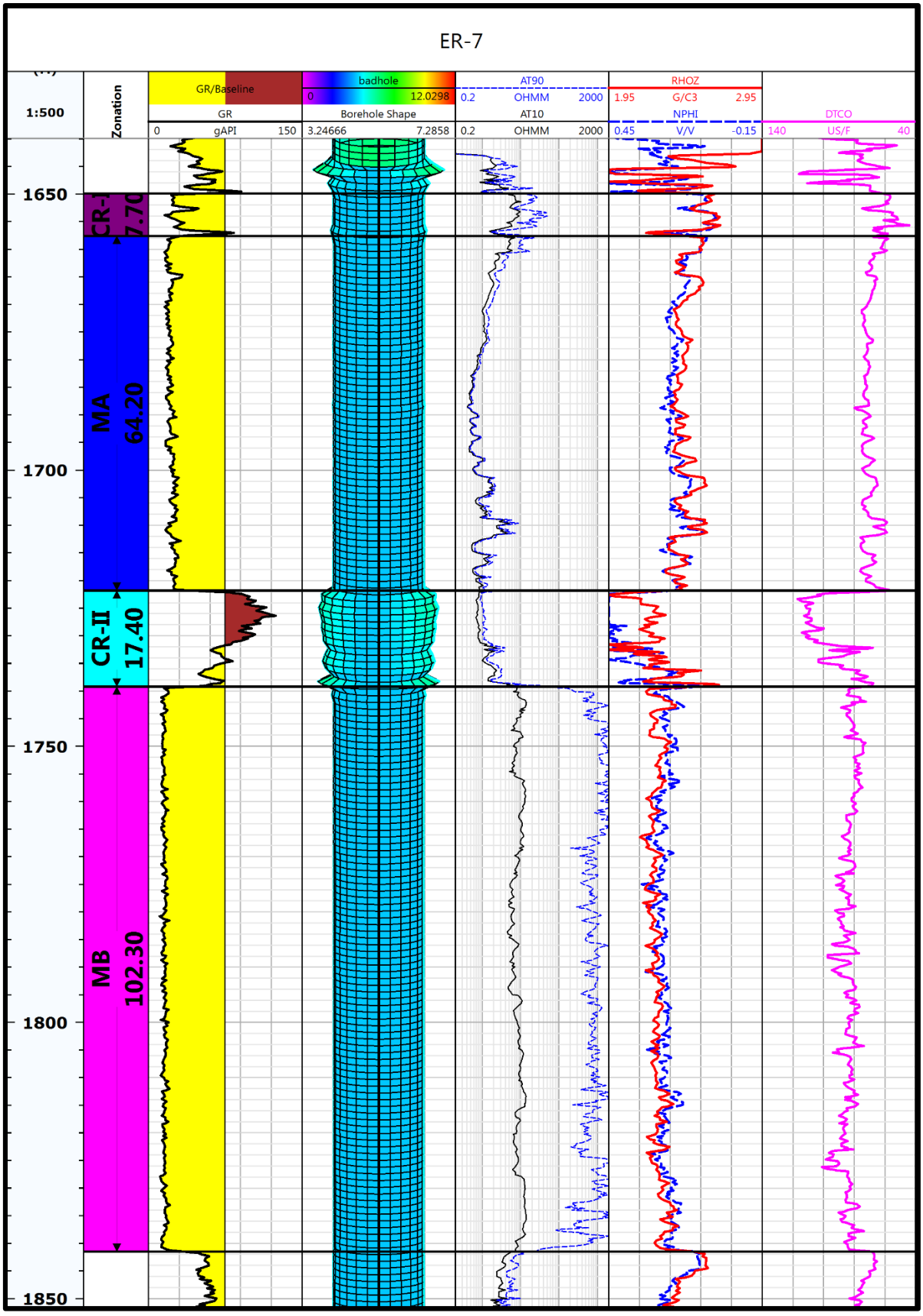

Figure (A,3) Qualitative interpretation of Mishrif Formation in the for well ER-7

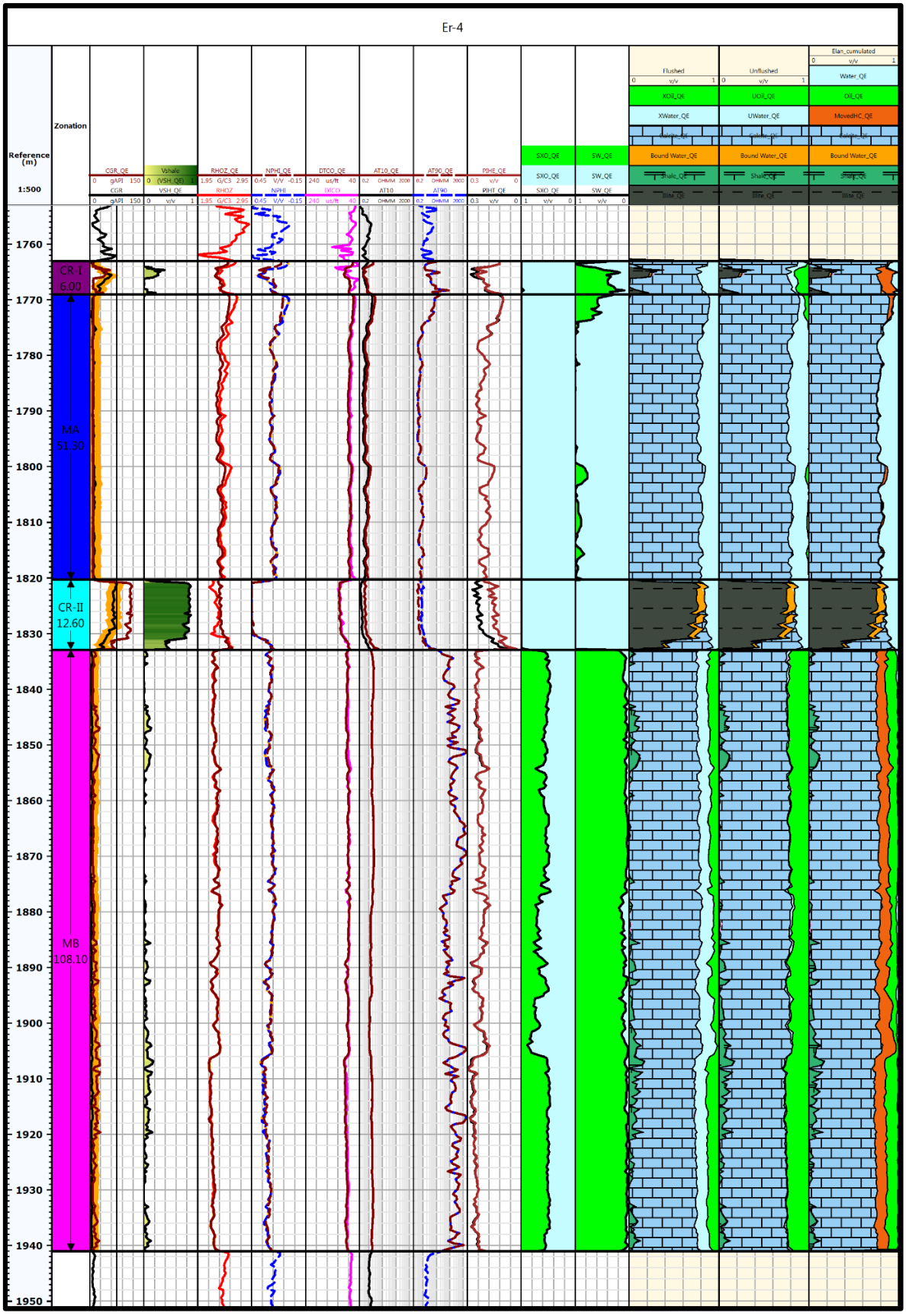

Figure (A,4) Petrophysical calculations for Mishrif Formation for well ER- 4

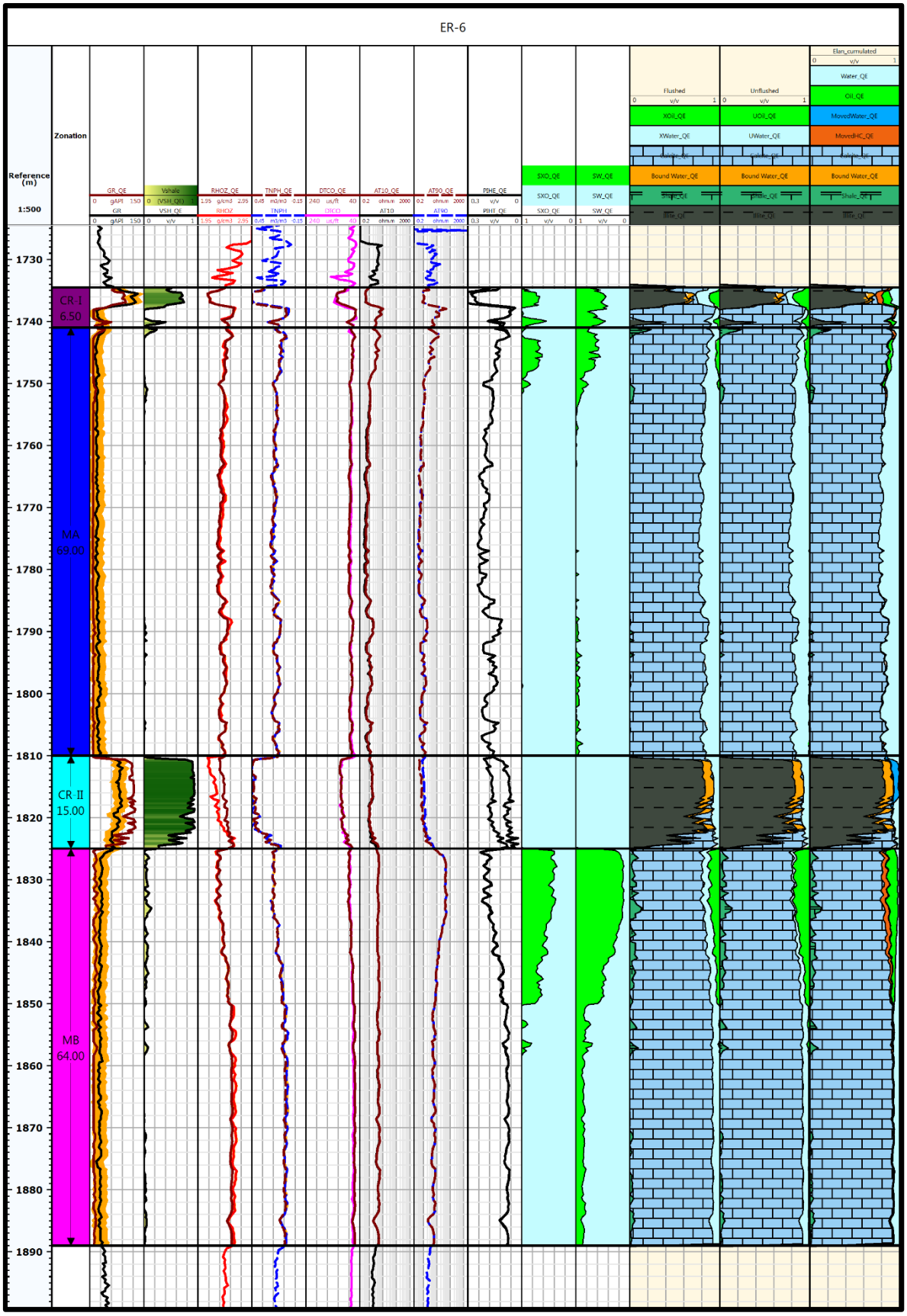

Figure (A,5) Petrophysical calculations for Mishrif Formation for well ER- 6

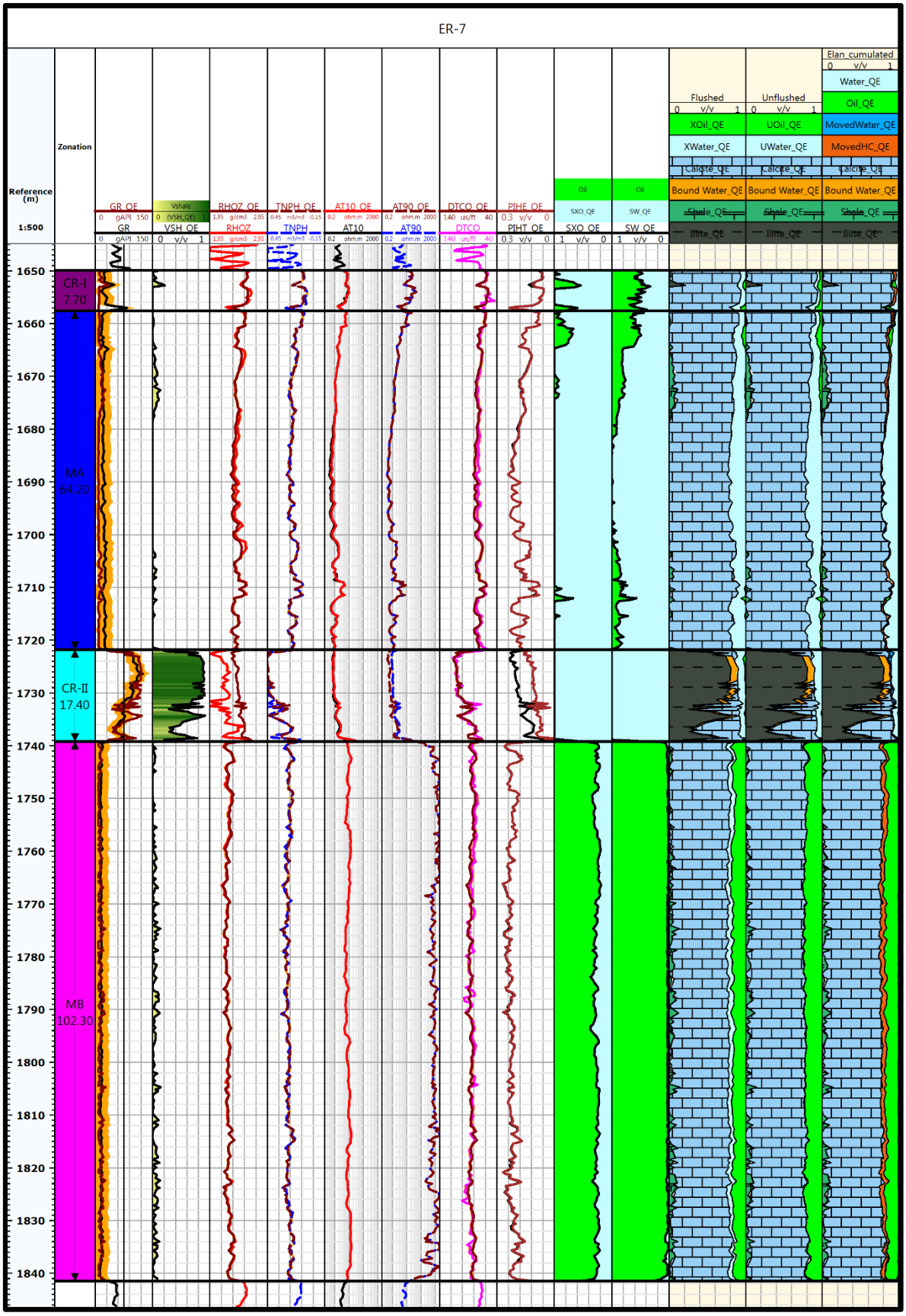

Figure (A,6) Petrophysical calculations for Mishrif Formation for well ER- 7

Appendix (A)

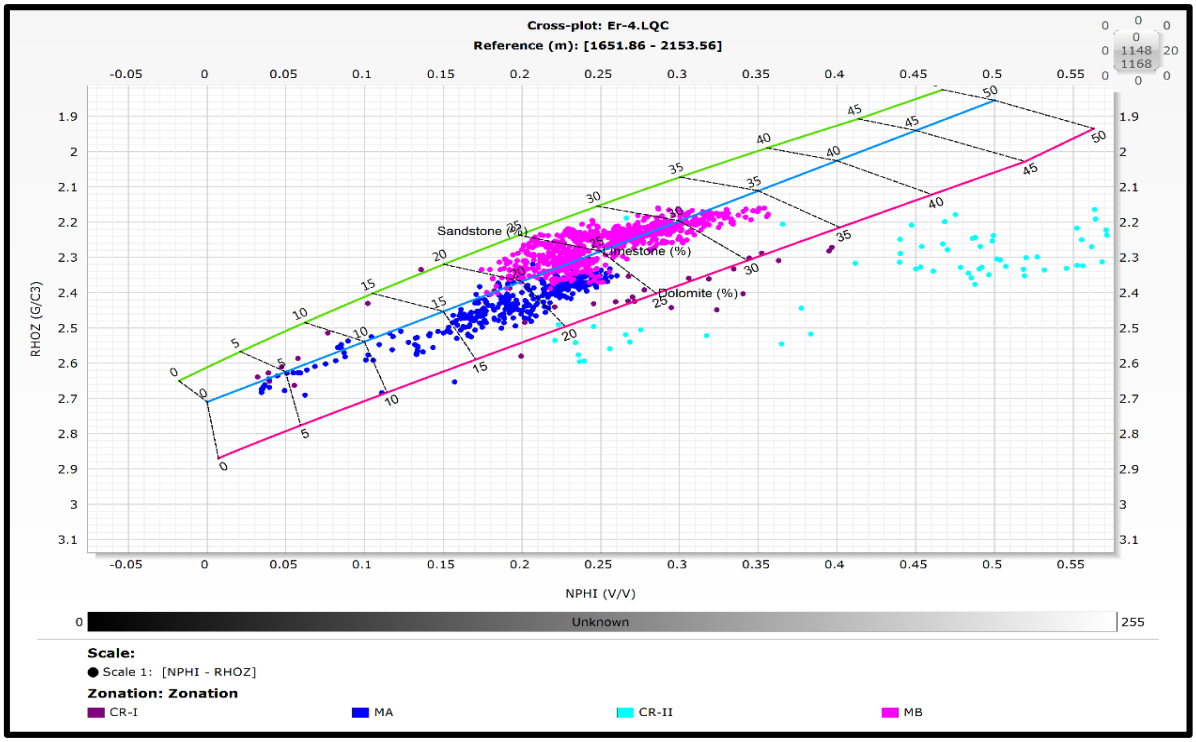

Figure (A,7) Shows the crossplot of Neutron porosity and Density porosity of Mishrif Formation in well ER-4

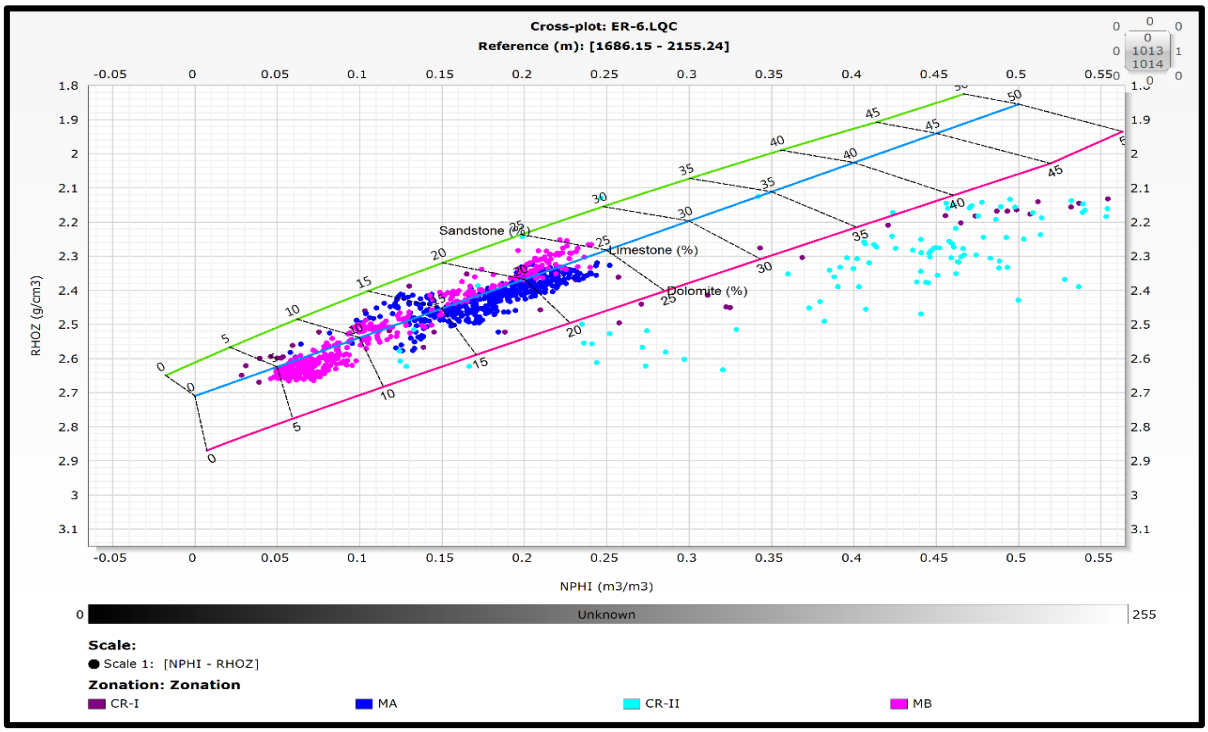

Figure (A,8) Shows the crossplot of Neutron porosity and Density porosity of Mishrif Formation in well ER-6

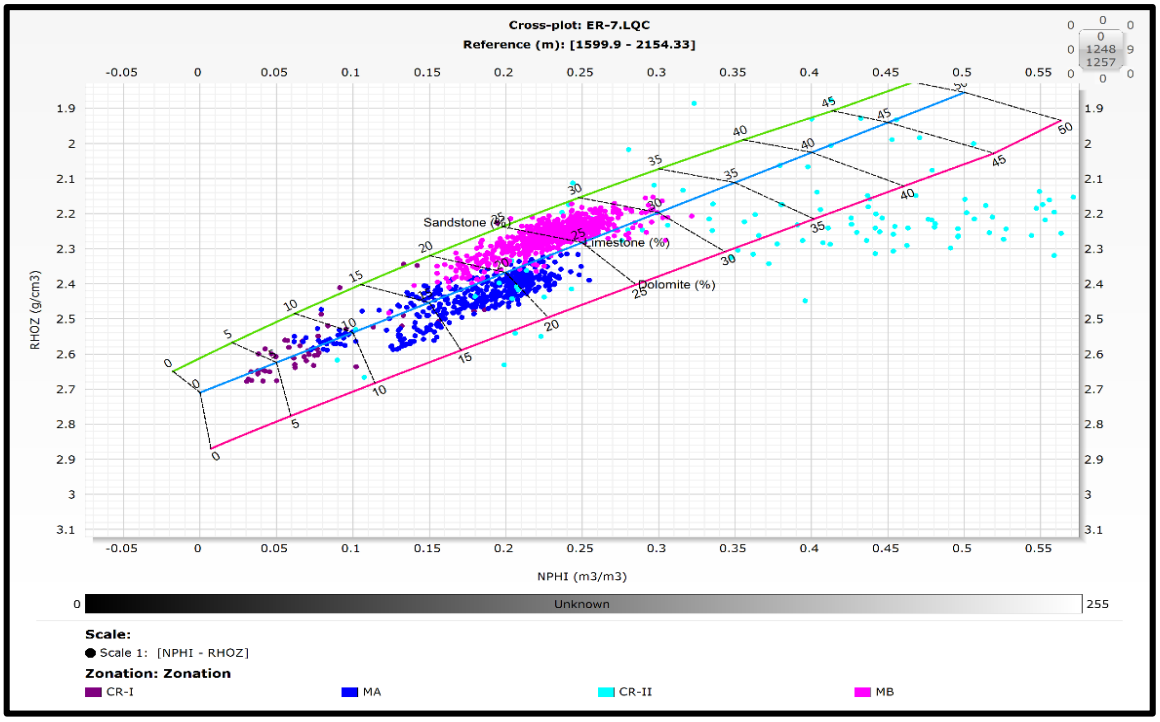

Figure (A,9) Shows the crossplot of Neutron porosity and Density porosity of Mishrif Formation in well ER-7

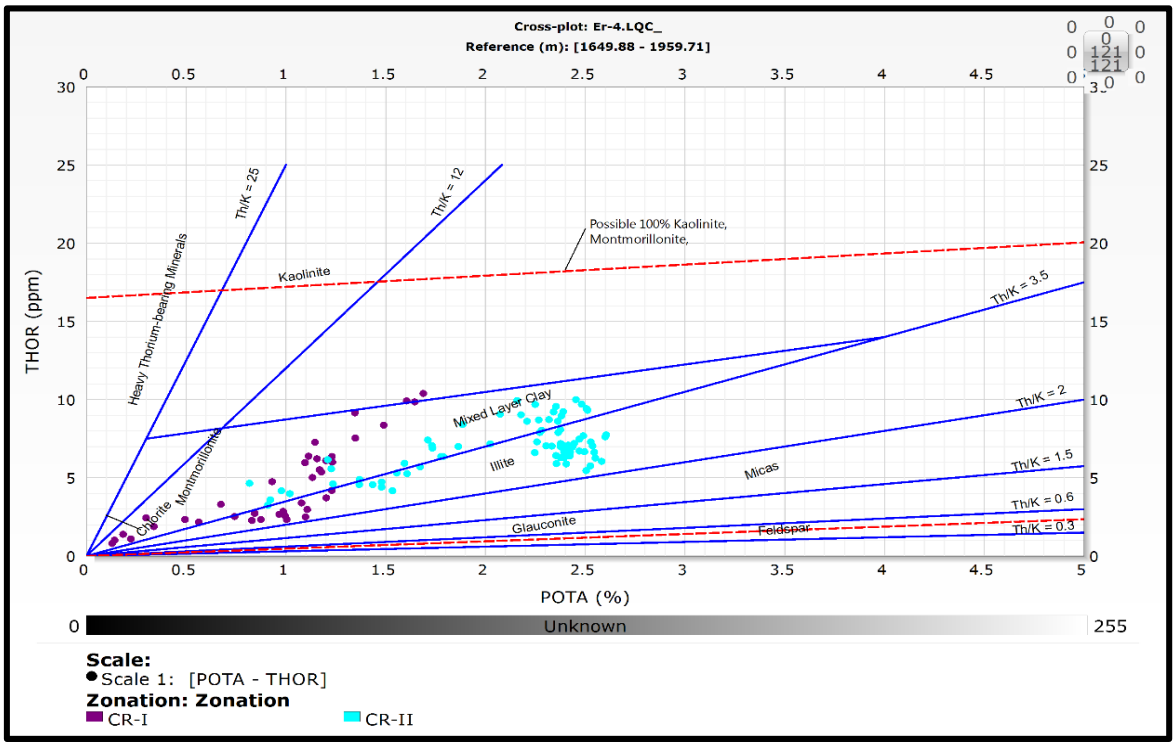

Figure (A,10) Shows the crossplot of POTA-THOR of Mishrif Formation in well ER-4

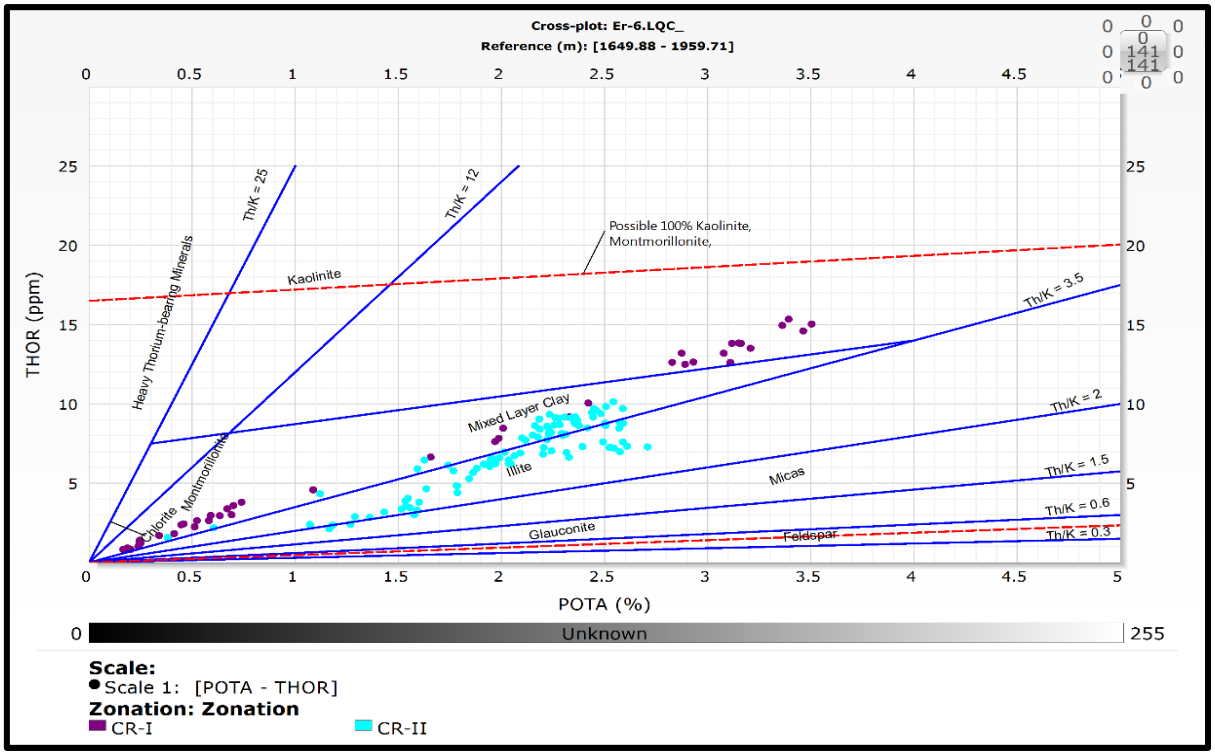

Figure (A,11) Shows the crossplot of POTA-THOR of Mishrif Formation in well ER-6

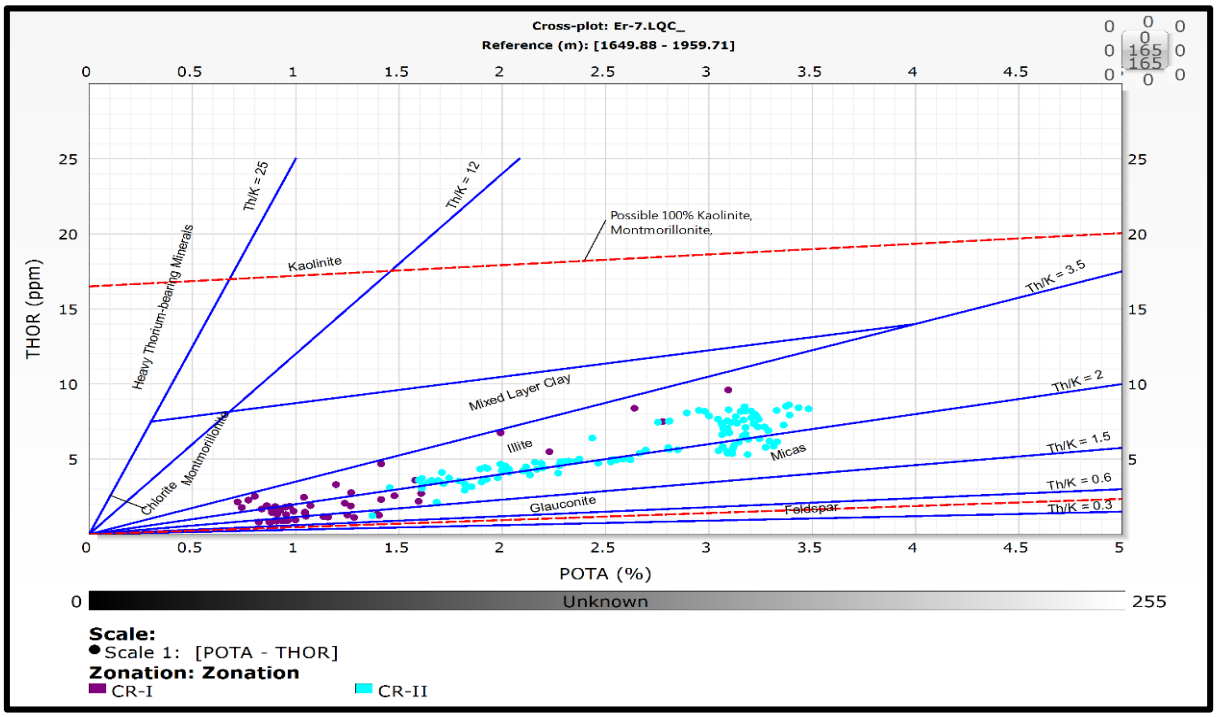

Figure (A,12) Shows the crossplot of POTA-THOR of Mishrif Formation in well ER-7

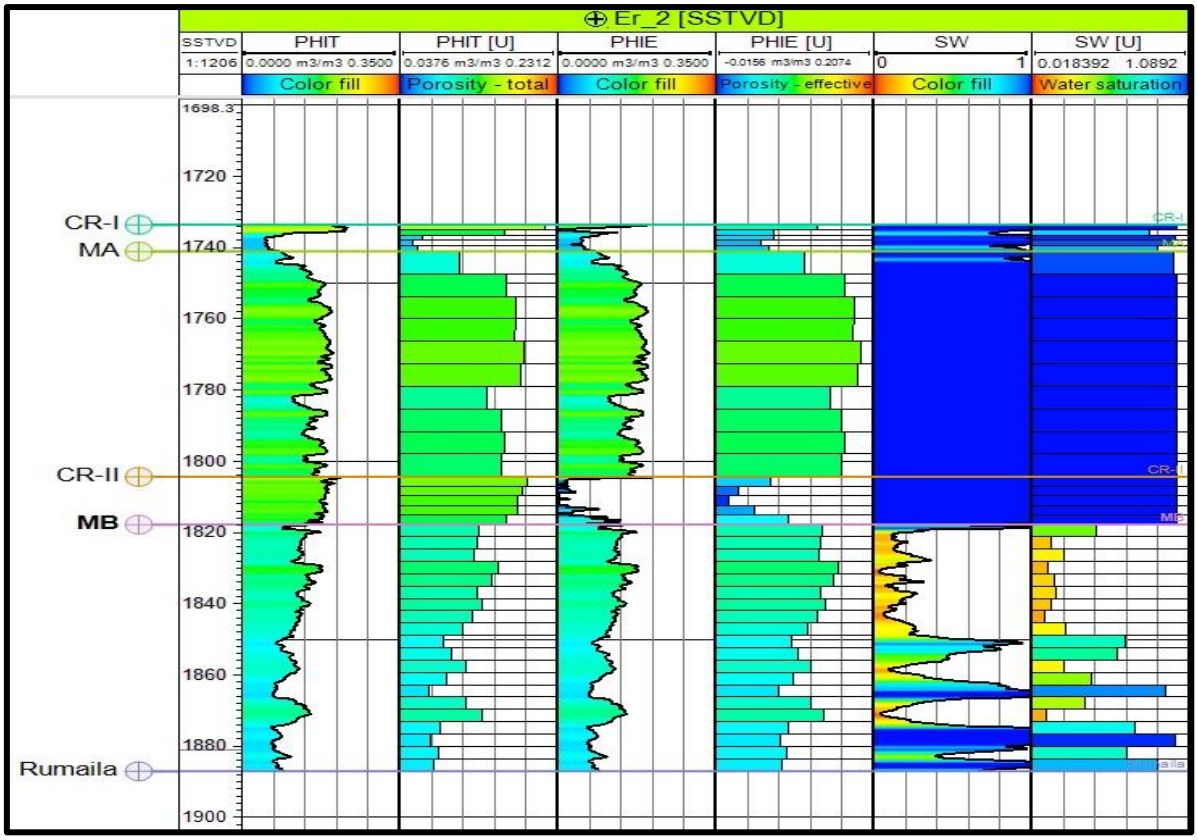

Figure (A,13) Scale up for Mishrif Formation in Eridu oilfield in well ER-2

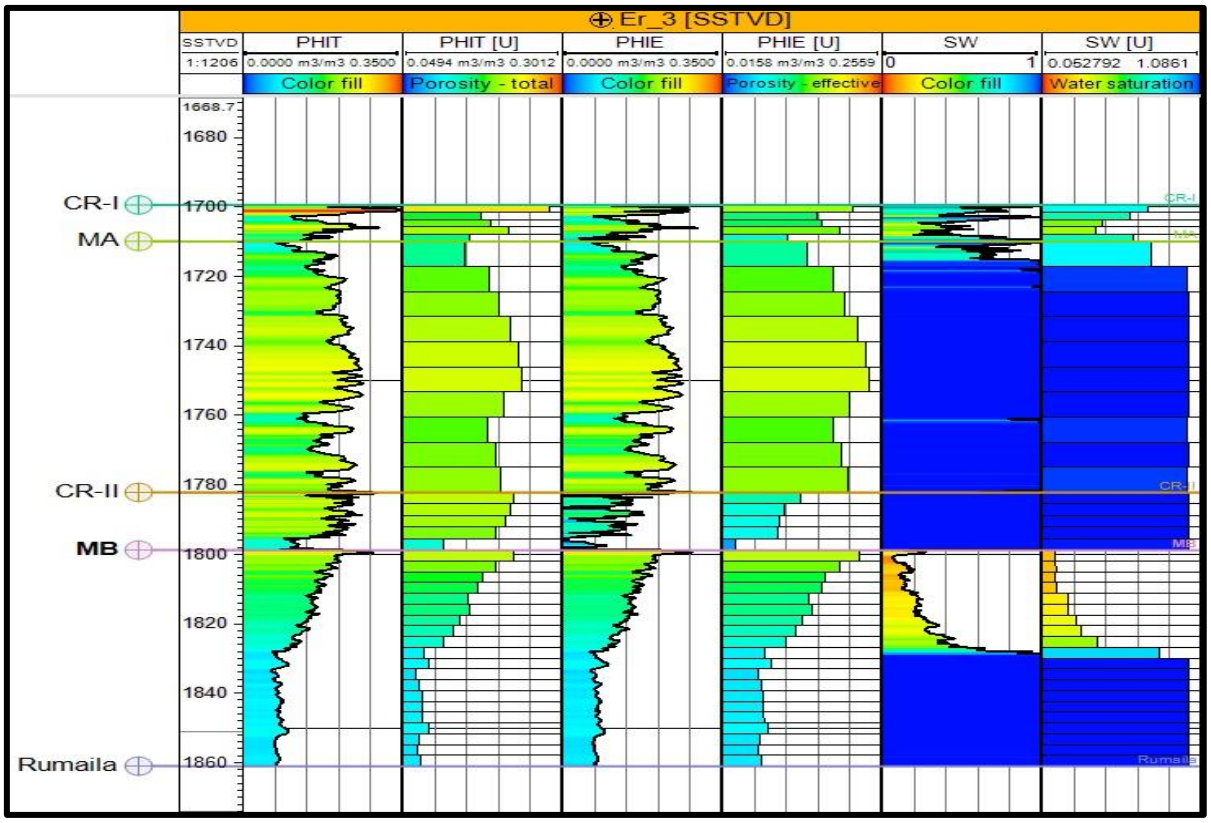

Figure (A,14) Scale up for Mishrif Formation in Eridu oilfield in well ER-3

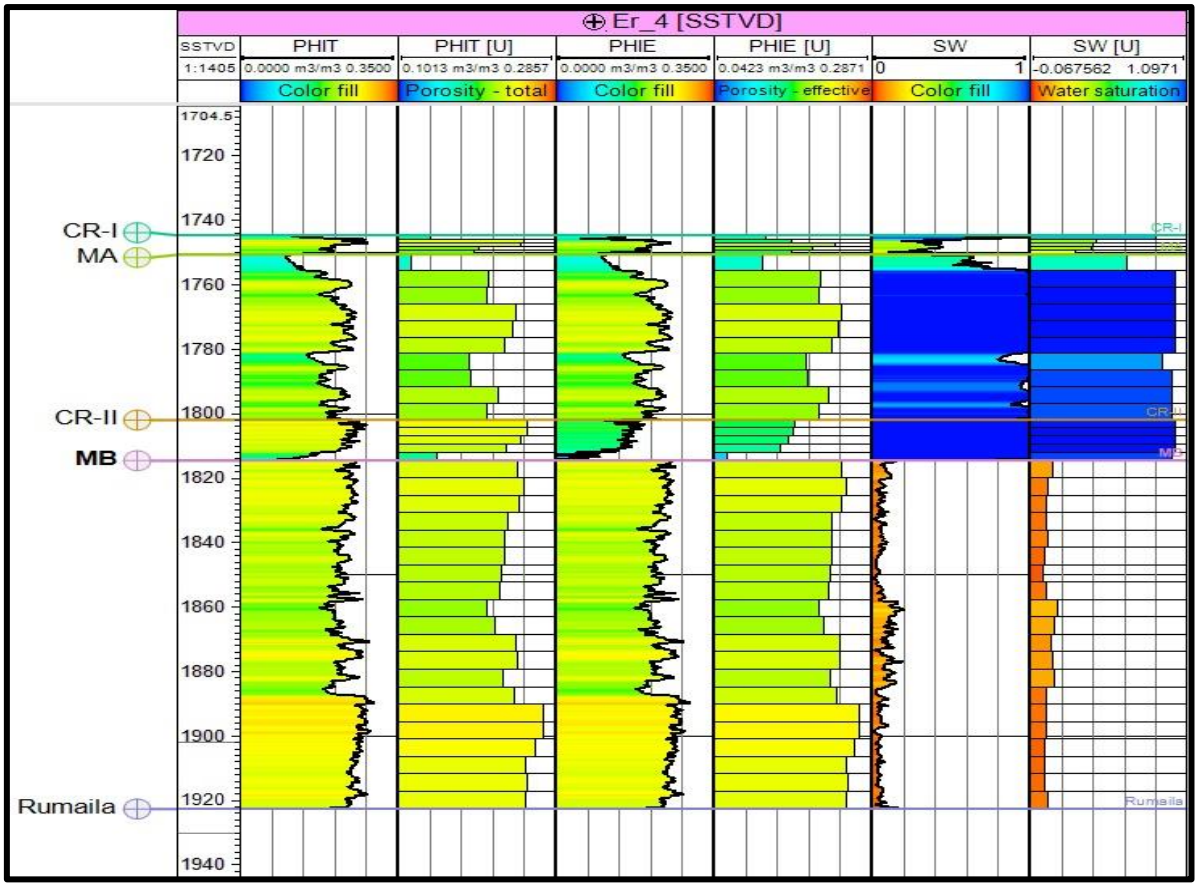

Figure (A,15) Scale up for Mishrif Formation in Eridu oilfield in well ER-4

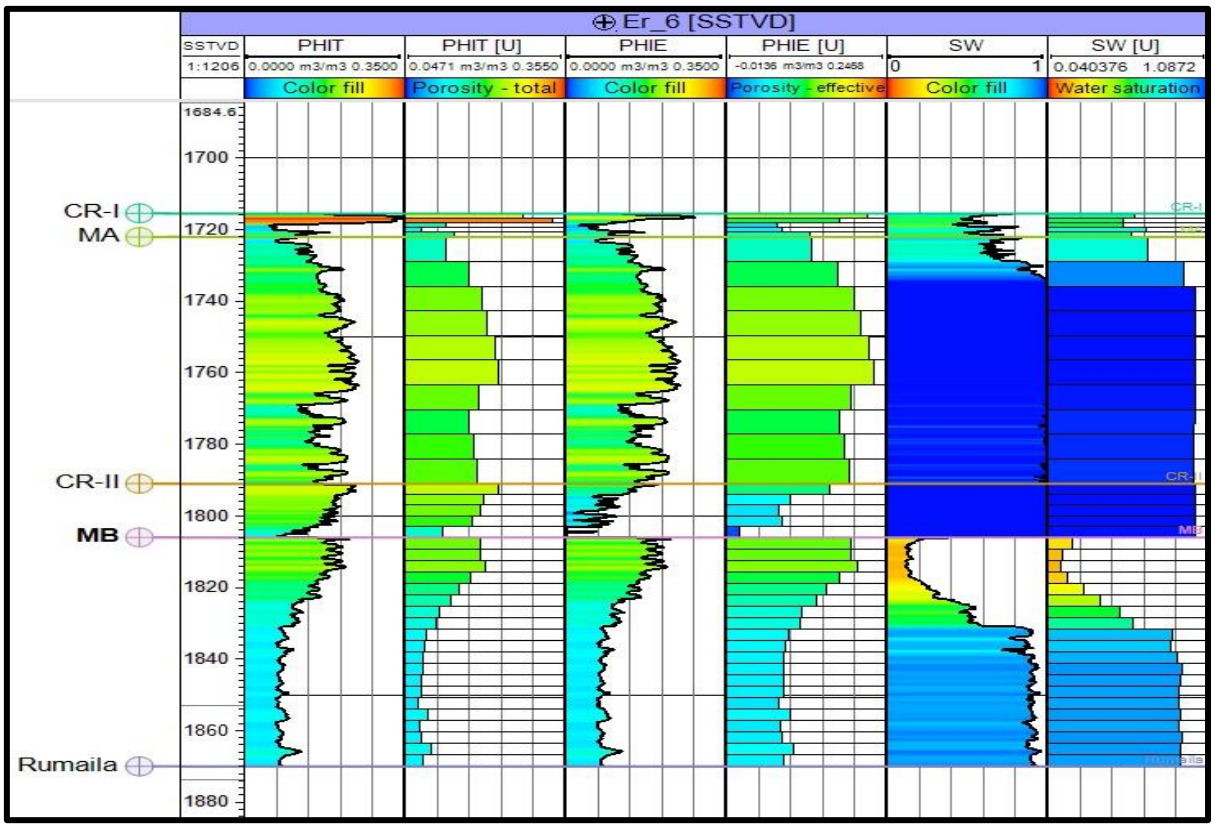

Figure (A,16) Scale up for Mishrif Formation in Eridu oilfield in well ER-6

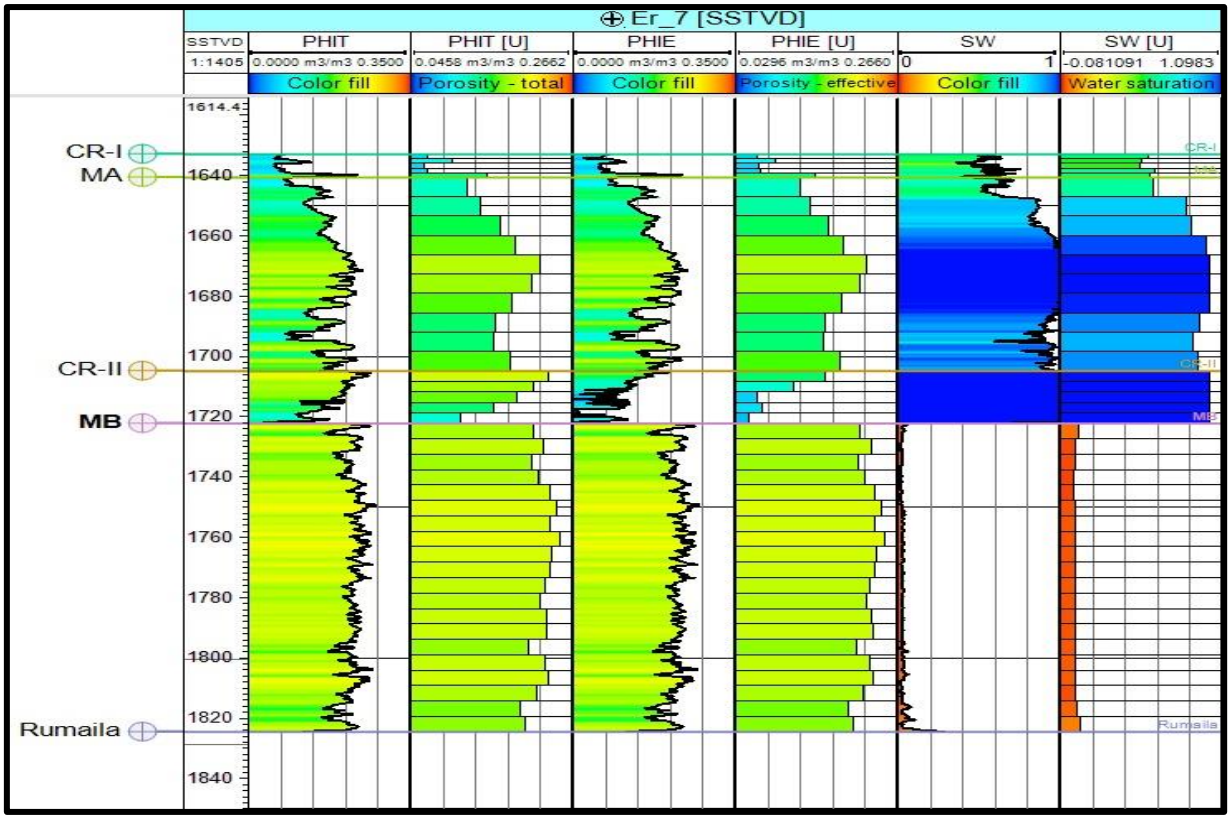

Figure (A,17) Scale up for Mishrif Formation in Eridu oilfield in well ER-7

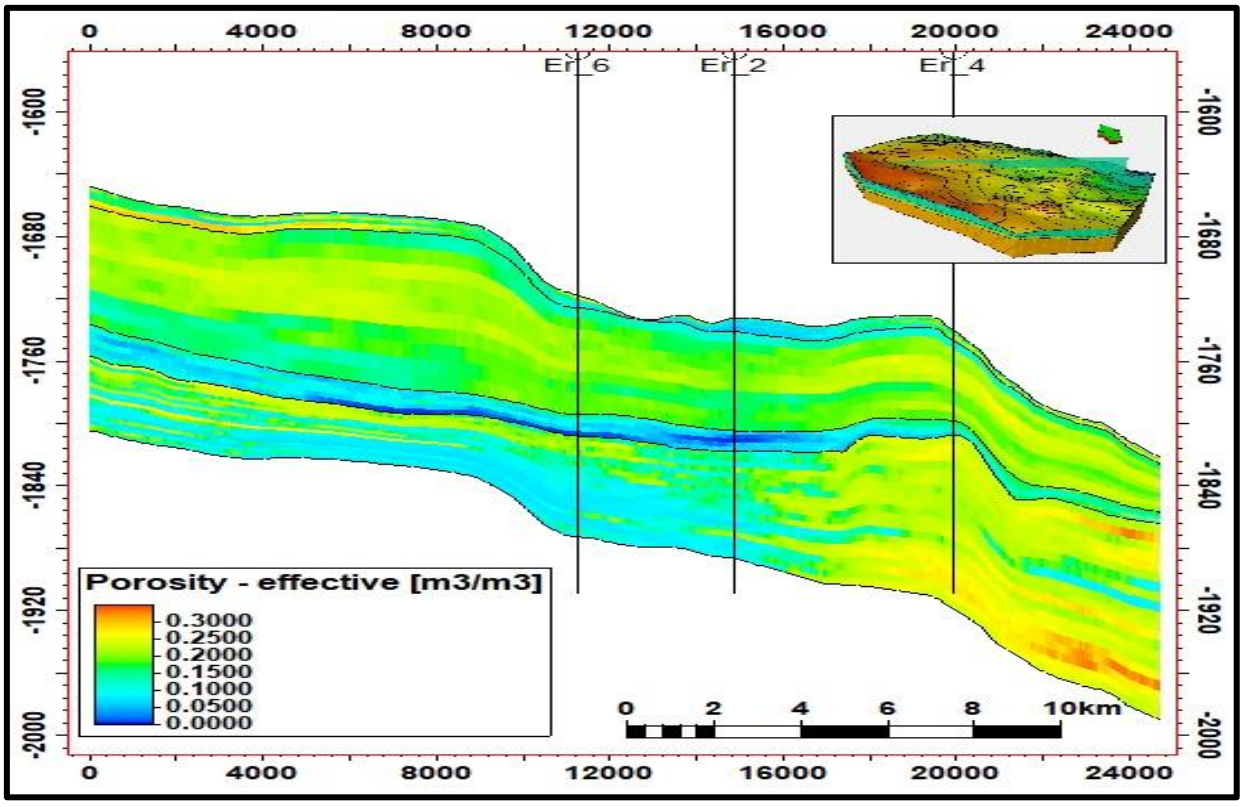

Figure (A,18) Effective porosity intersection line of Mishrif Formation in Eridu oilfield in wells ER-6, ER-2 and ER-4.

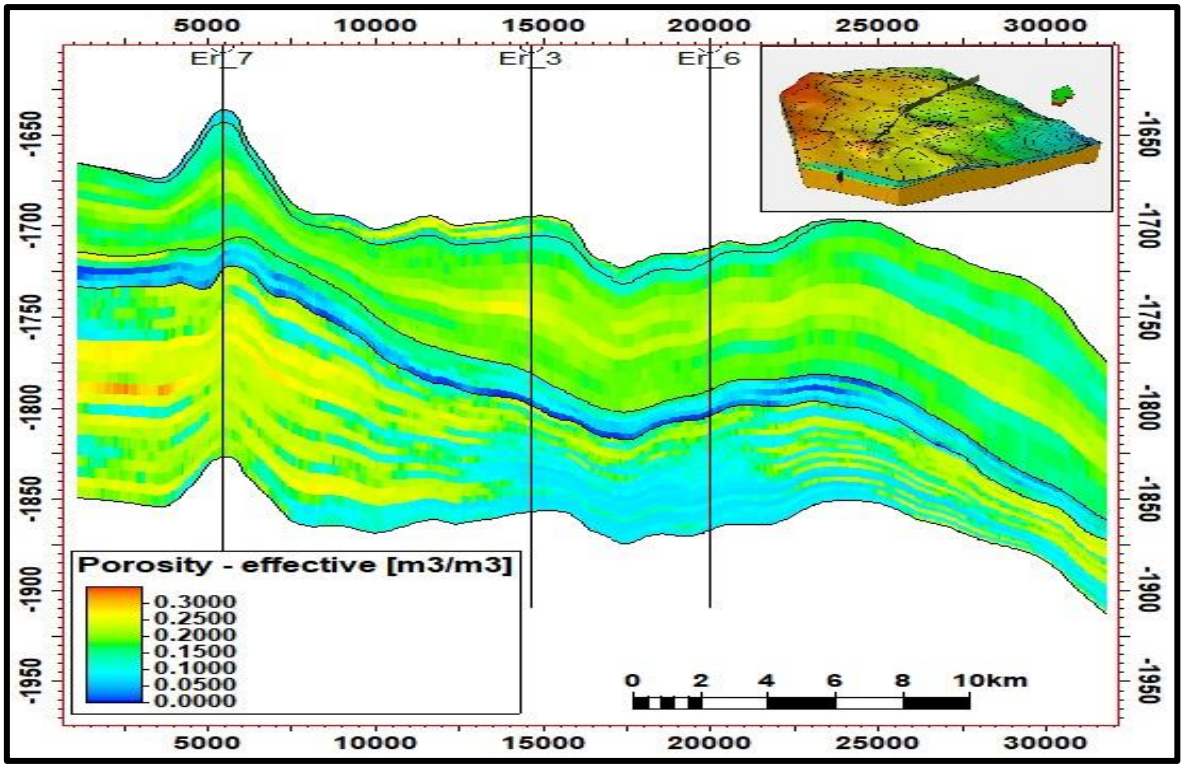

Figure (A,19) Effective porosity intersection line of Mishrif Formation in Eridu oilfield in wells ER-7, ER-3 and ER-6.

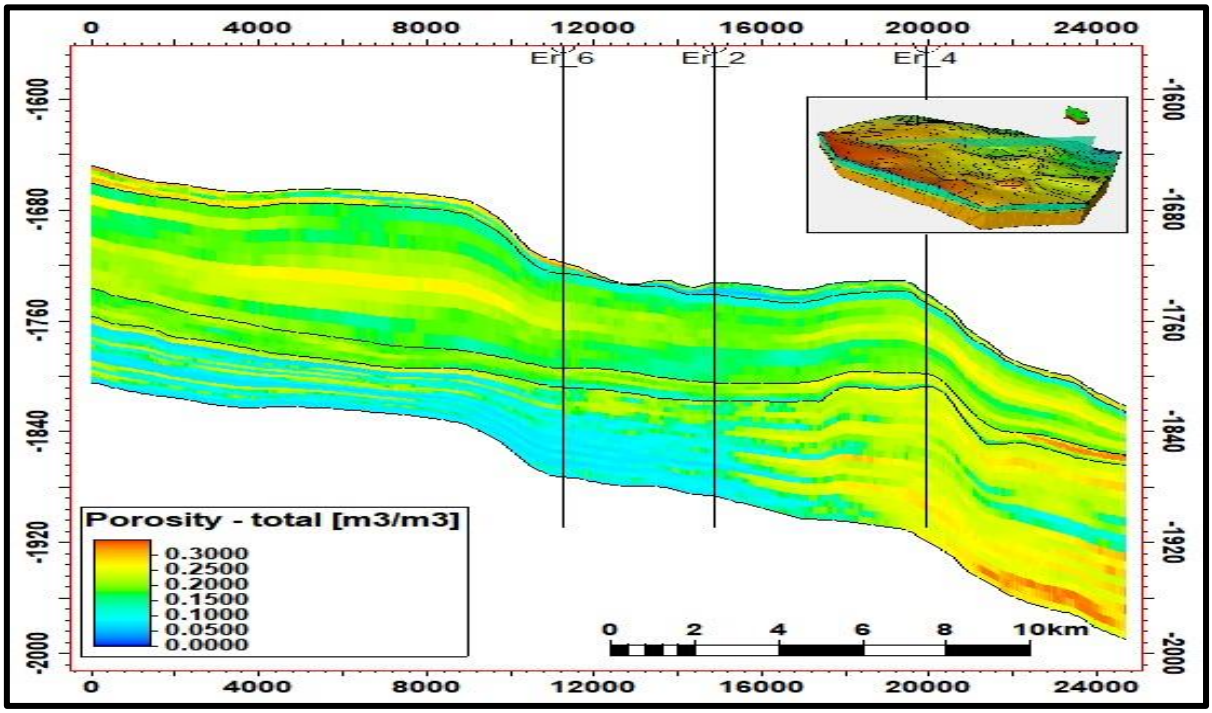

Figure (A,20) Total porosity intersection line of Mishrif Formation in Eridu oilfield in wells ER-6, ER-2 and ER-4.

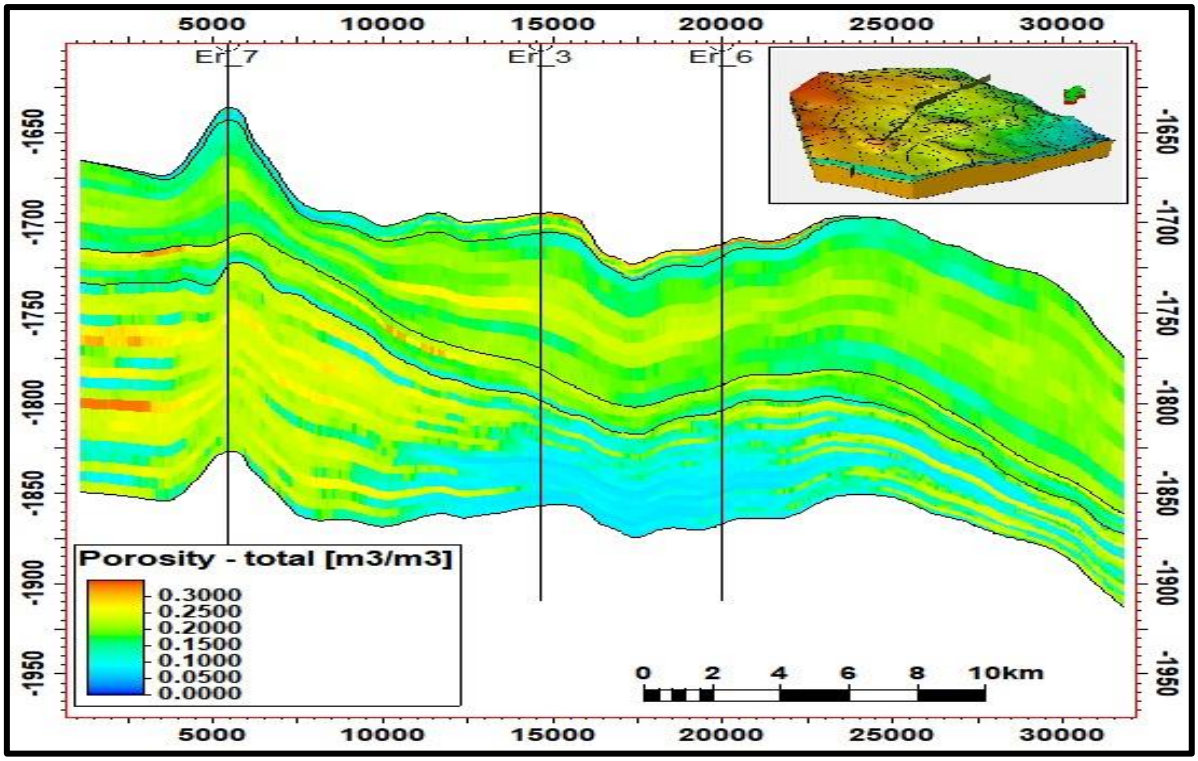

Figure (A,21) Total porosity intersection line of Mishrif Formation in Eridu oilfield in wells ER-7, ER-3 and ER-6.

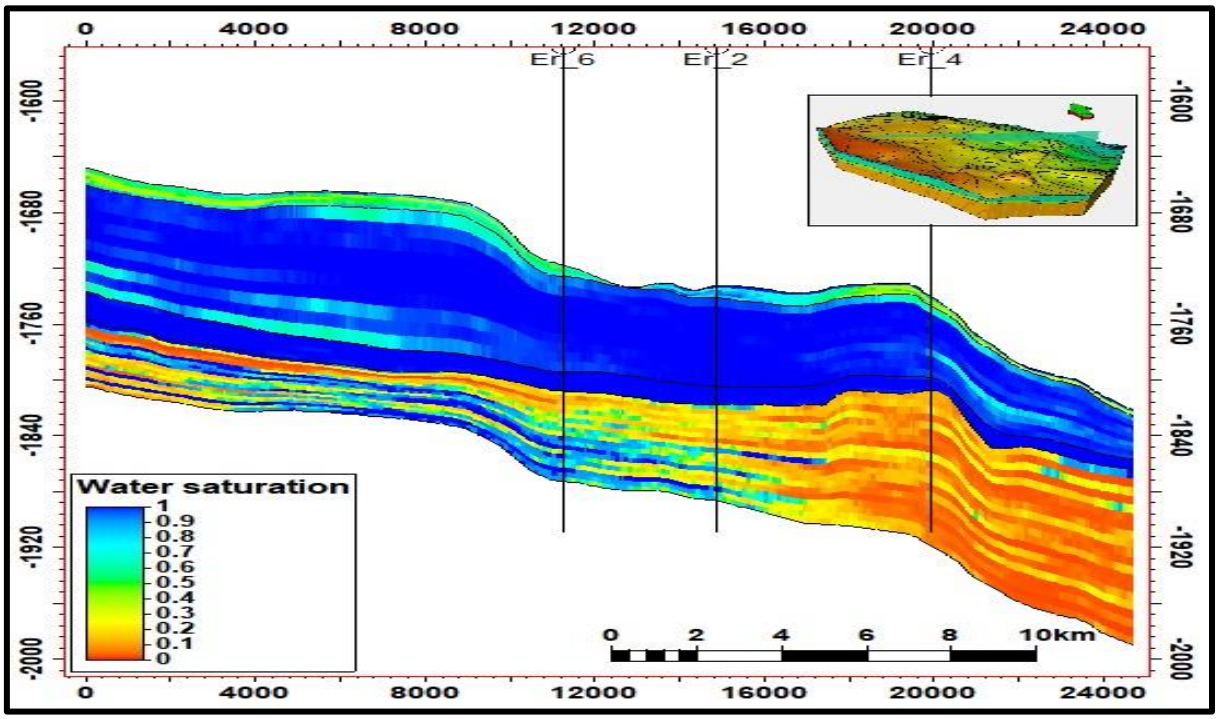

Figure (A,22) Water saturation intersection line of Mishrif Formation in Eridu oilfield in wells ER-6, ER-2 and ER-4.

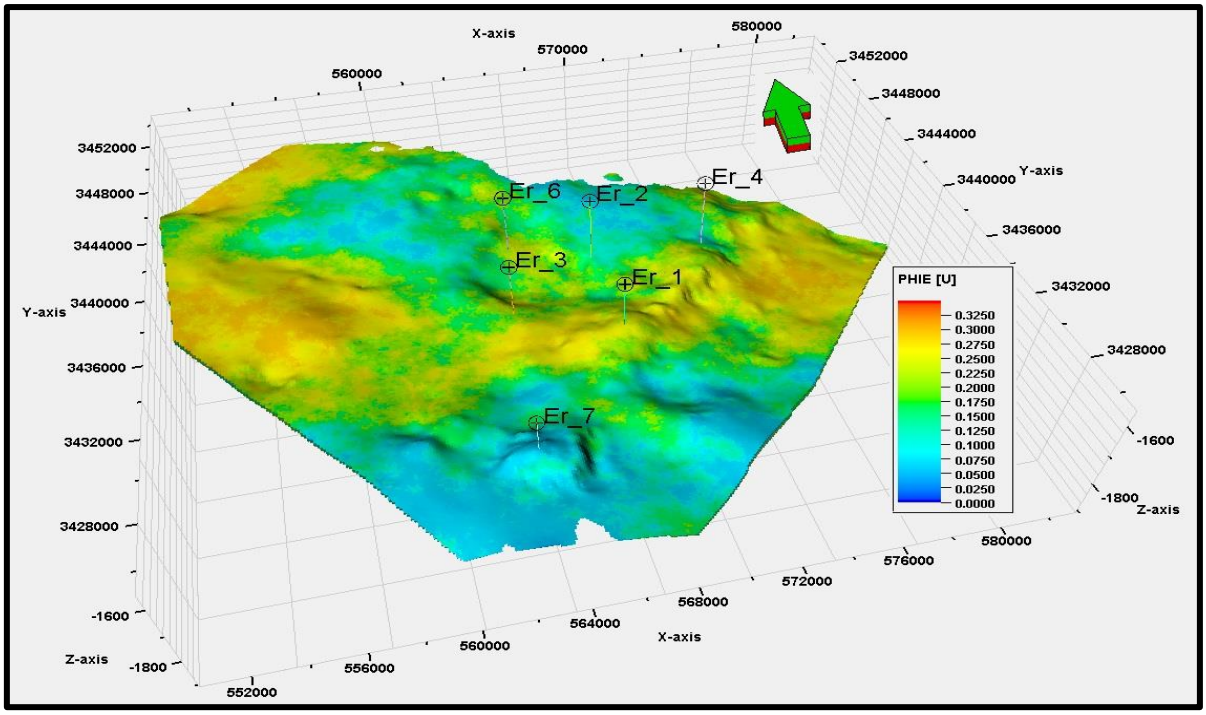

Figure (A,25) Effective porosity for CR-I unit of Mishrif Formation in Eridu oilfield.

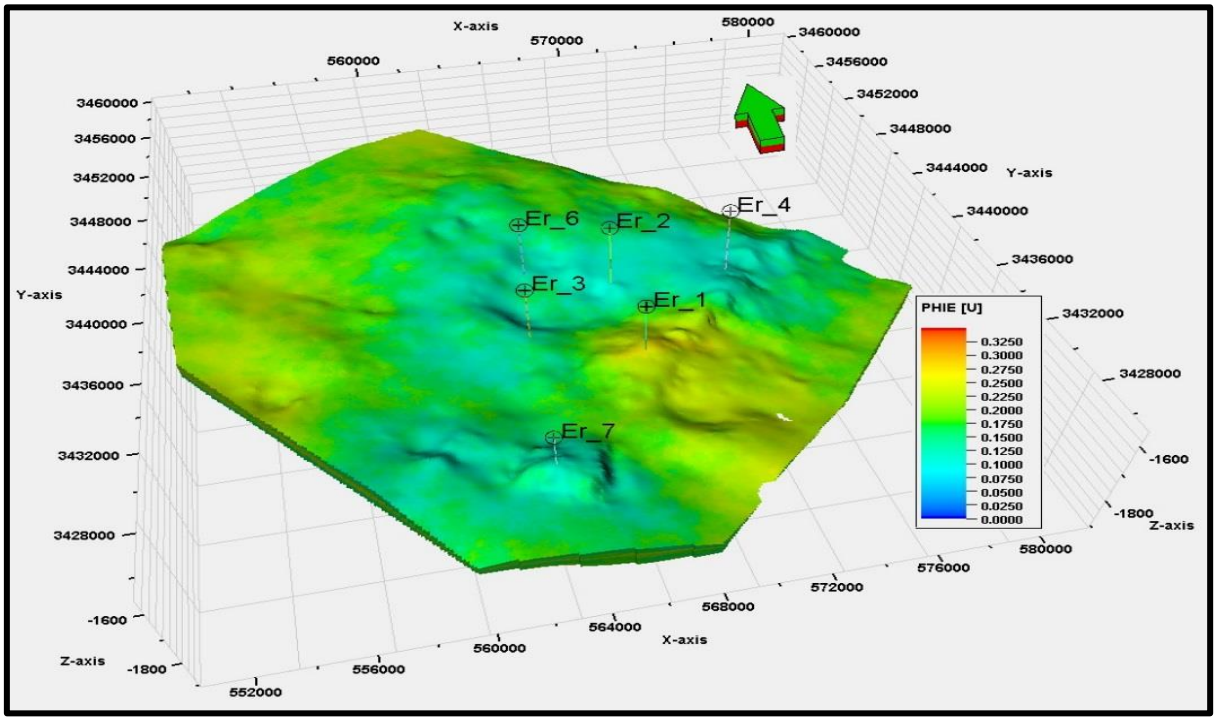

Figure (A,26) Effective porosity for MA unit of Mishrif Formation in Eridu oilfield.

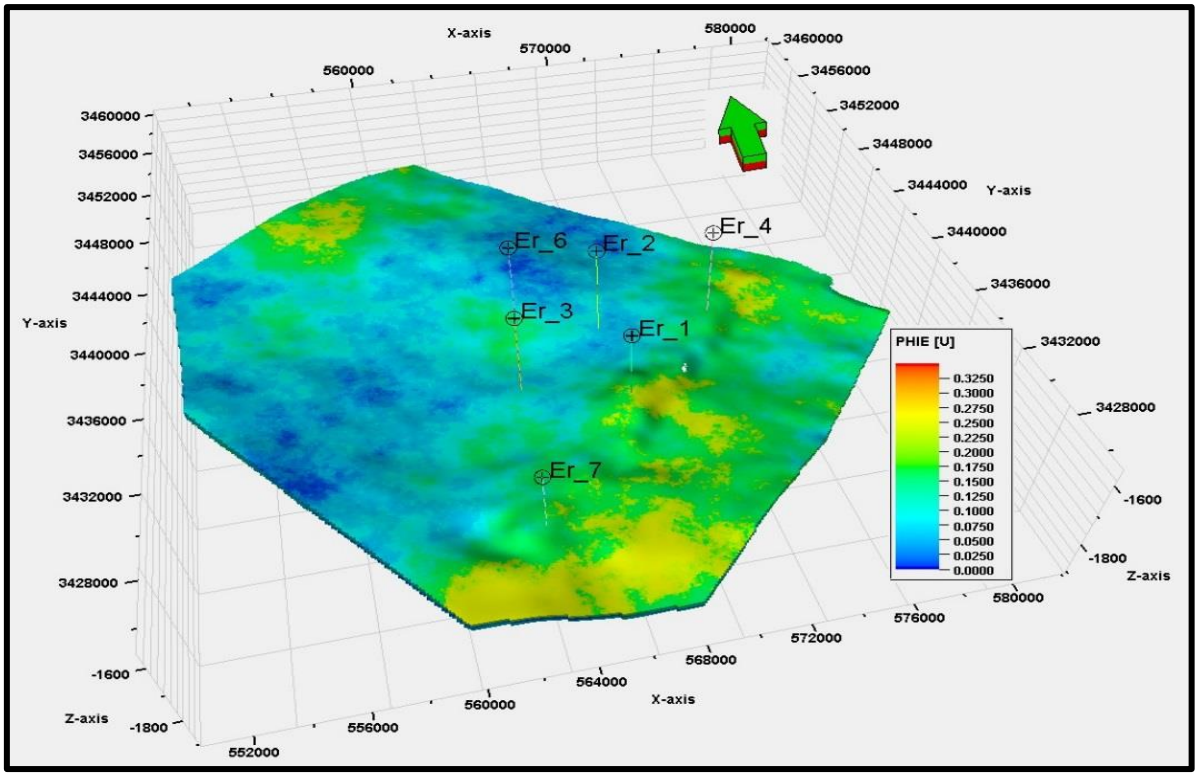

Figure (A,27) Effective porosity for CR-II unit of Mishrif Formation in Eridu oilfield.

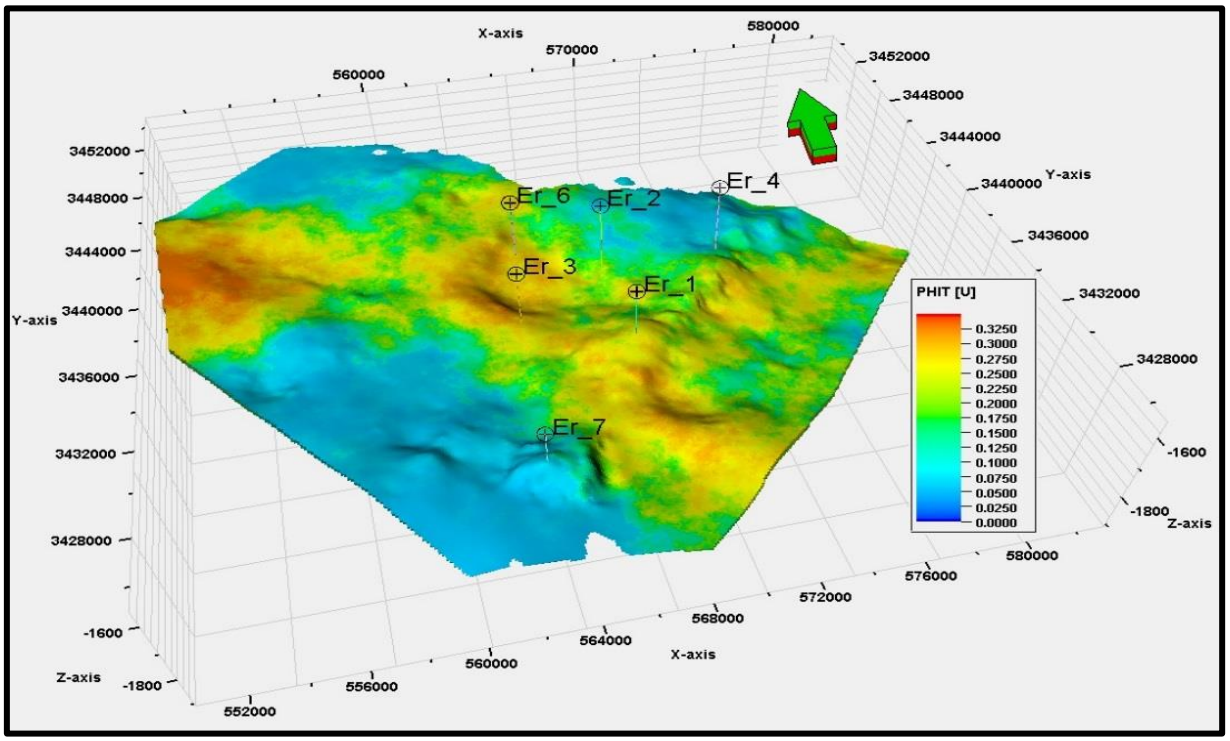

Figure (A,28) Total porosity for CR-I unit of Mishrif Formation in Eridu oilfield.

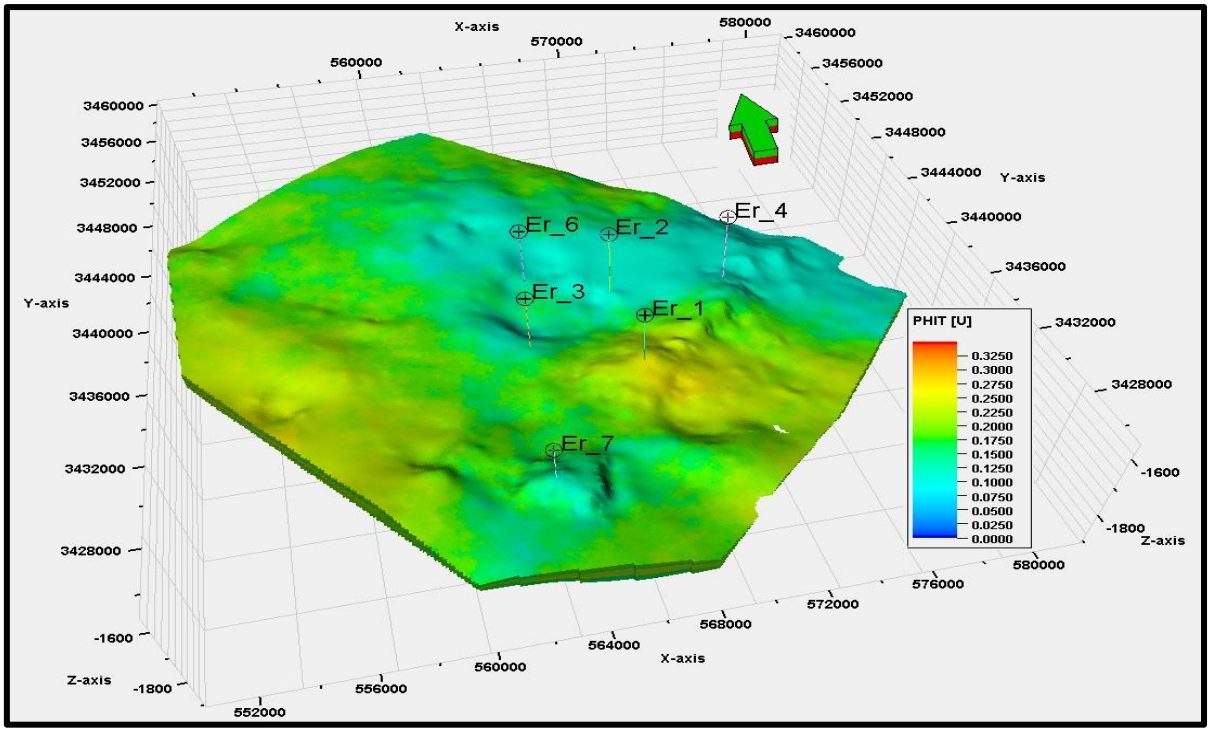

Figure (A,29) Total porosity for MA unit of Mishrif Formation in Eridu oilfield.

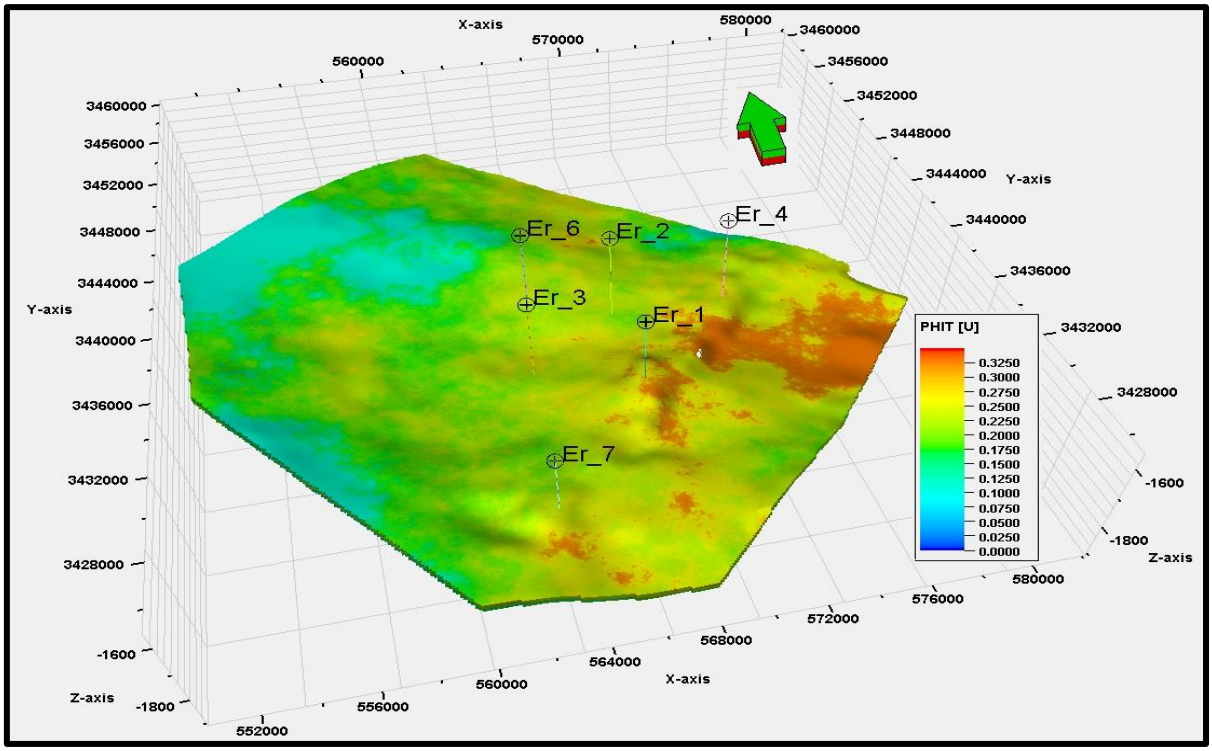

Figure (A,30) Total porosity for CR-II unit of Mishrif Formation in Eridu oilfield.

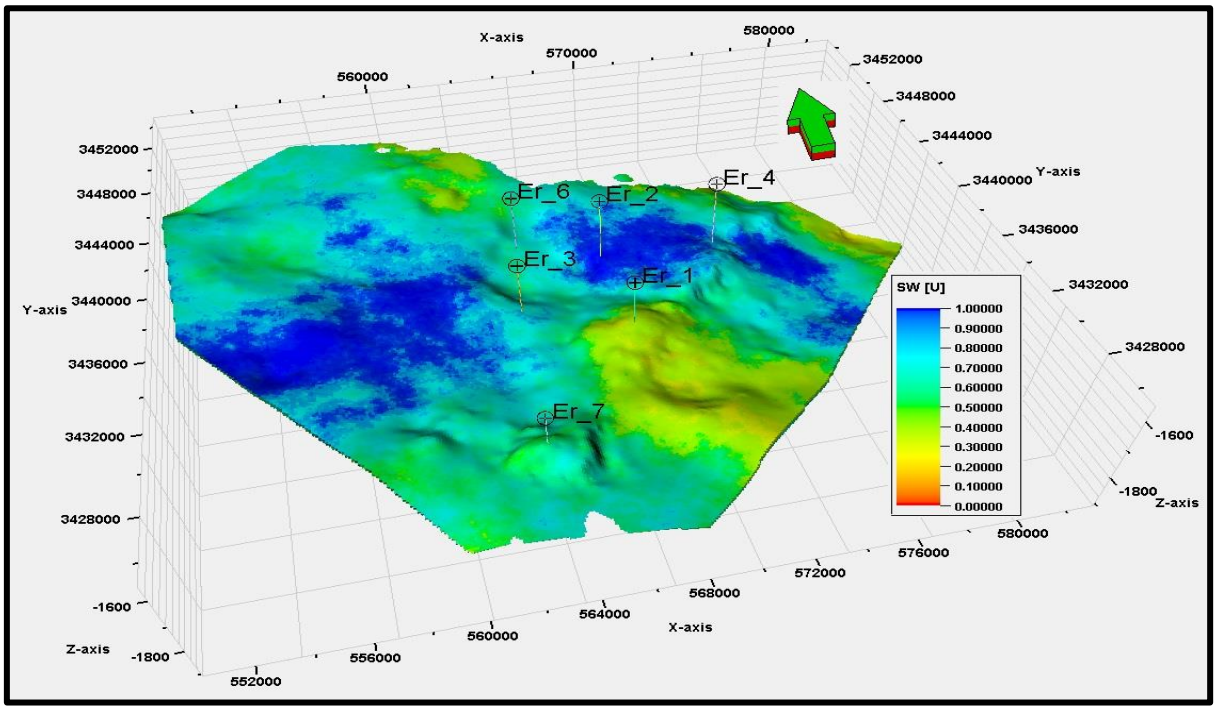

Figure (A,31) Water saturation for CR-I unit of Mishrif Formation in Eridu oilfield.

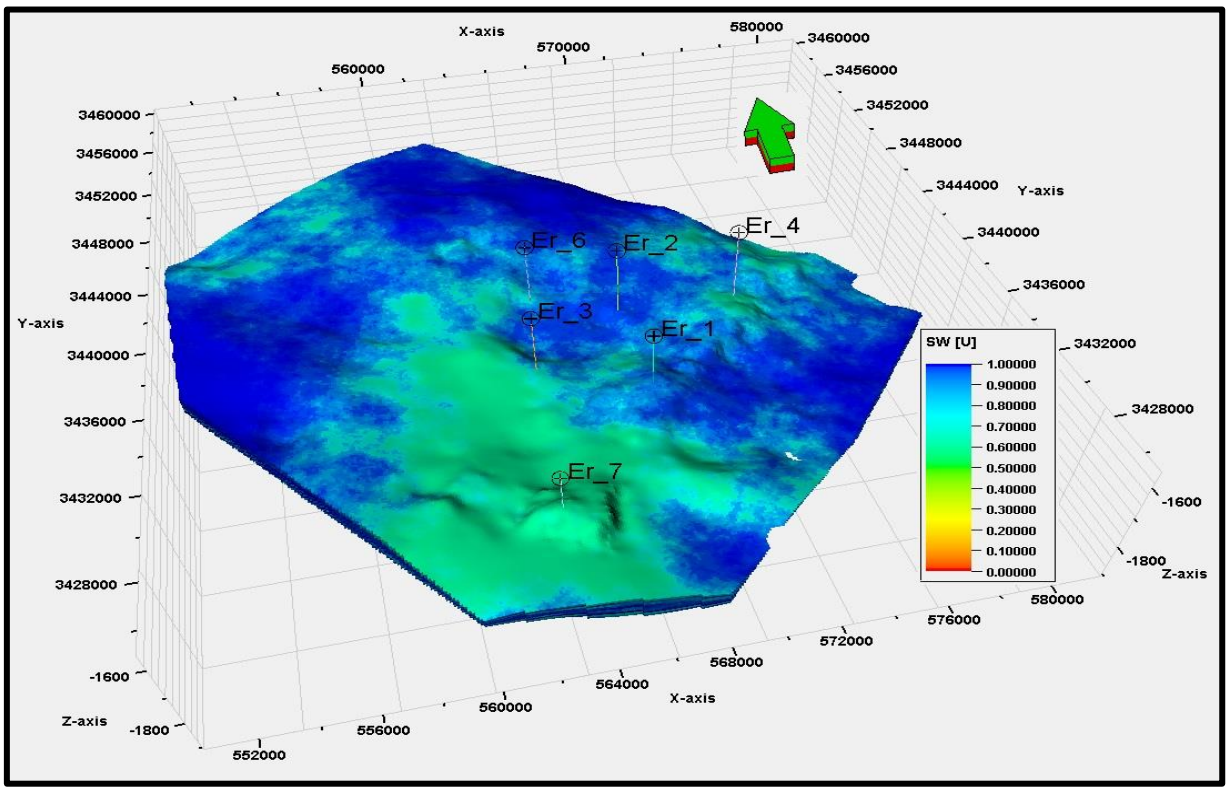

Figure (A,32) Water saturation for MA unit of Mishrif Formation in Eridu oilfield.

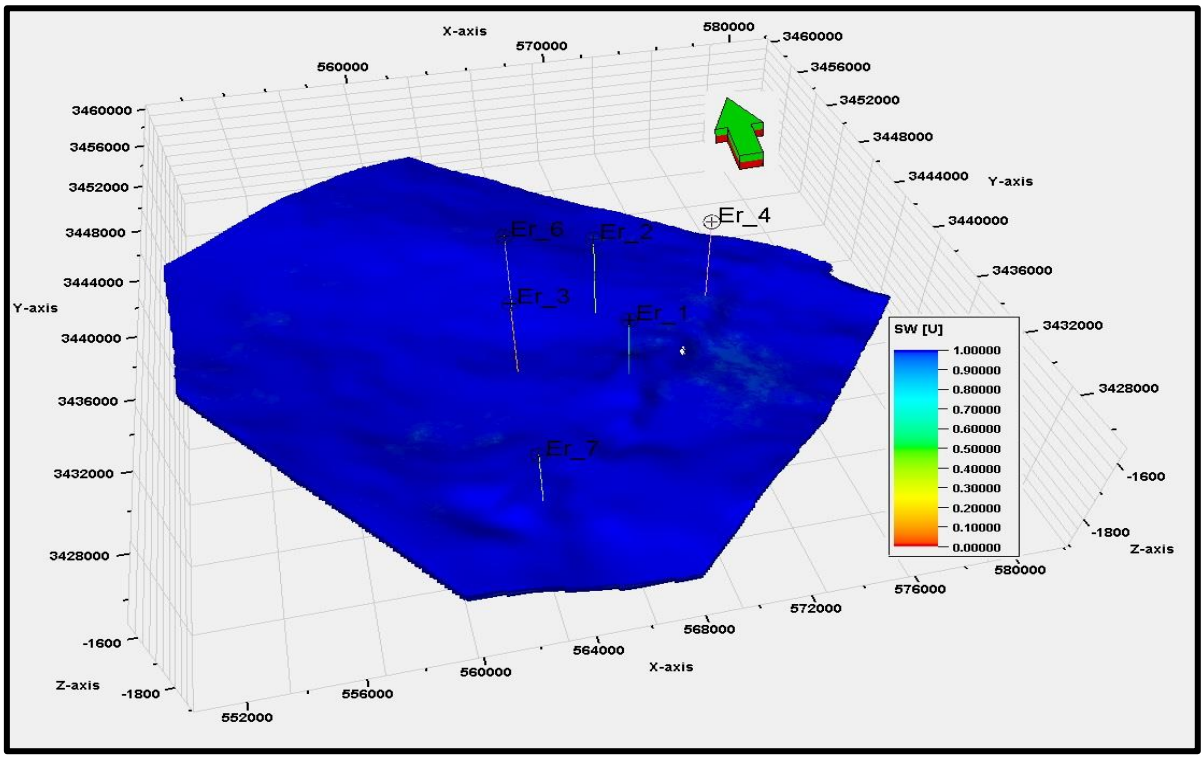

Figure (A,33) Water saturation for CR-II unit of Mishrif Formation in Eridu oilfield.

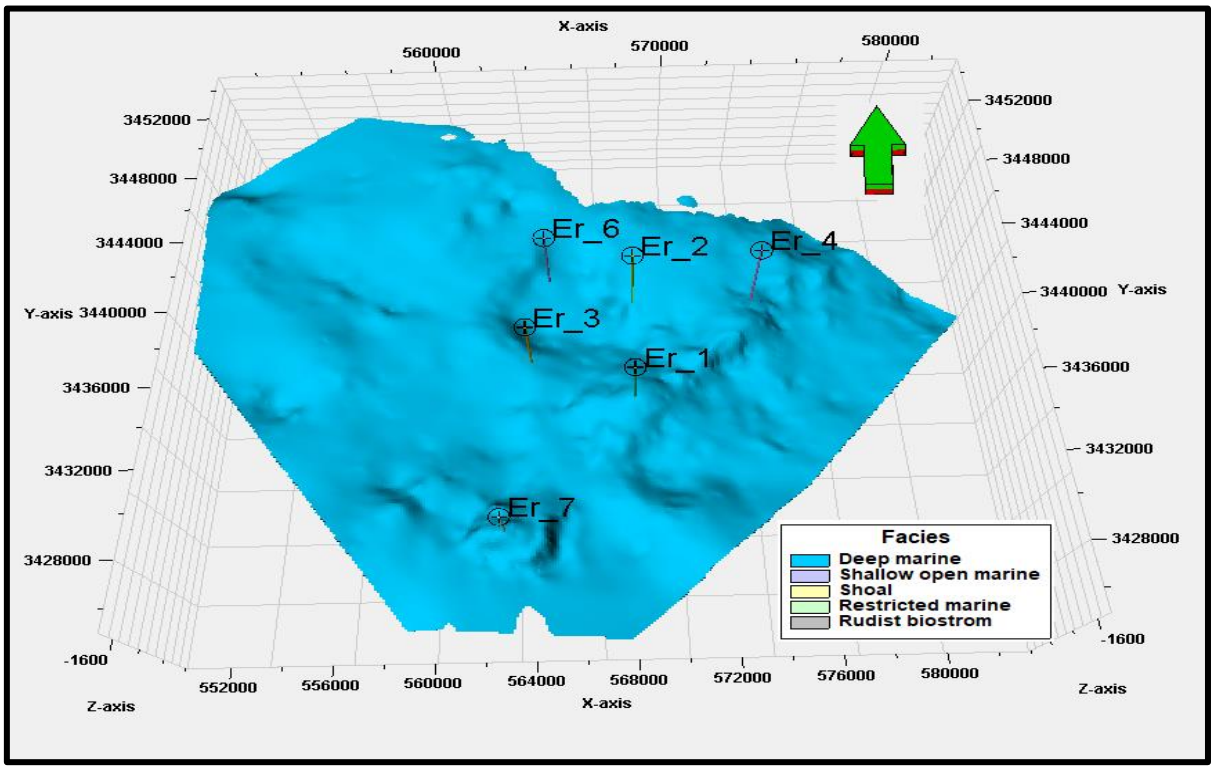

Figure (A,34) Facies model for CR-I unit of Mishrif Formation in Eridu oilfield.

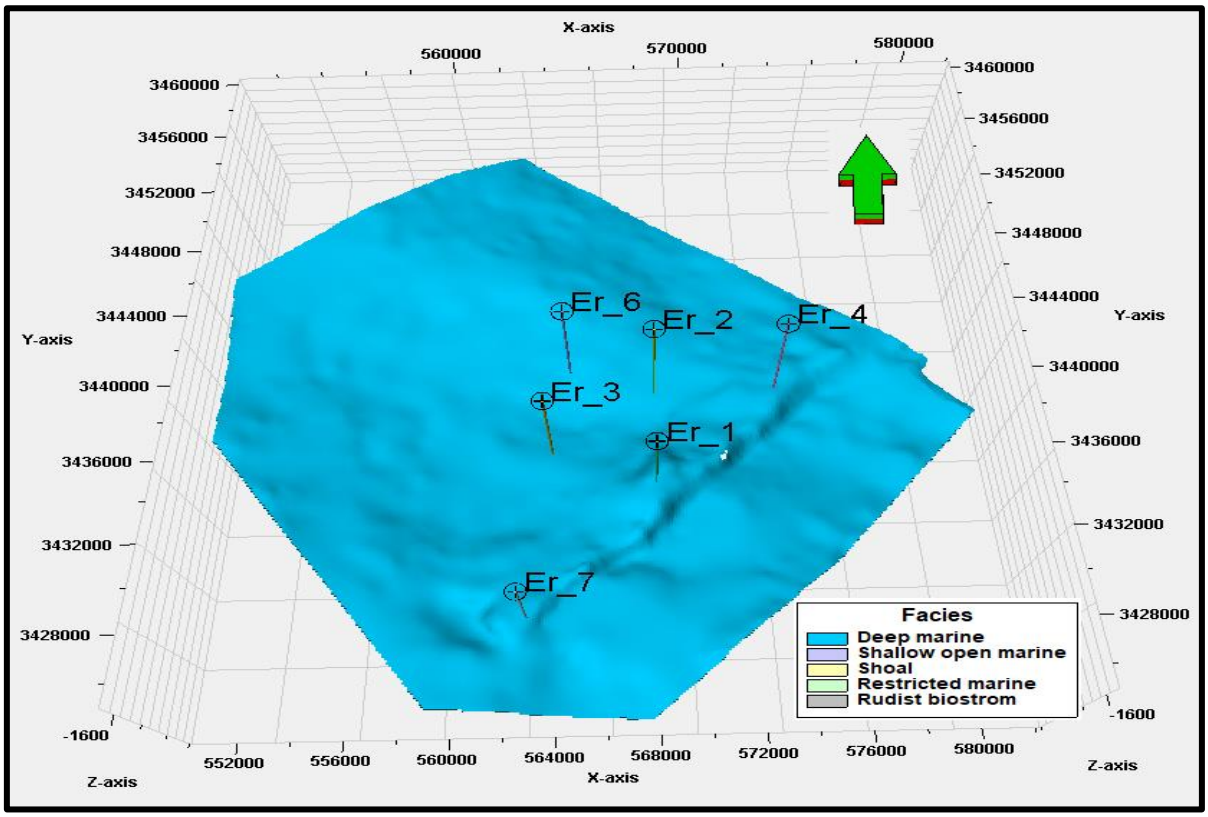

Figure (A,34) Facies model for CR-II unit of Mishrif Formation in Eridu oilfield.

المستخلص

تم اختيار ستة ابار نفطية في هذه الدراسة التي تضمنت تكوين مشرف في حقل اريدو النفطي (السينومينيان المتاخر-التورونيان المبكر) جنوب العراق والذي يعتبر من المكامن الرئيسية في الحقل لدراسة السحنات الدقيقة والعمليات التحويرية المؤثرة فيها والبيئات الترسيبية والأنواع المختلفة من المسامية وتقييم الخصائص البتروفيزيائية.

من خلال الفحص البتروغرافي تم تشخيص ستة سحنات رئيسة في تكوين مشرف تضمنت (سحنة الحجر الجيري الجيري الواكي، سحنة الحجر الجيري الجيري المرصوص، سحنة الحجر الجيري الجيري الحبيبي، سحنة الحجر الجيري الجيري المترابط، سحنة الحجر الجيري الجيري الطيني، سحنة الرودستون) اما السحنات الثانوية التي تم تشخيصها والتي كان عددها اثنتي عشر سحنة تضمنت (سحنة الحجر الجيري الطيني الحامة للمنخربات القاعية, سحنة الحجر الجيري الطيني – الواكي الحاملة لقع من الرودست, سحنة الحجر الجيري الطيني الحاملة للفتاتات الاحيائية ,سحنة الحجر الجيري الواكي الحاملة للفتات الاحيائية , سحنة الحجر الجيري الواكي- المرصوص المتحجرة, سحنة الحجر الجيري الواكي الحاملة للمنخربات الطافية,سحنة الحجر الجيري الواكي- المرصوص الحاملة للفتات الاحيائية,سحنة الحجر الجيري المرصوص الحاملة للمنخربات الطافية, سحنة الحجر الجيري المرصوص الحاملة للدمالق, سحنة الحجر الجيري المرصوص الحاملة للفتاتات الاحيائية بالإضافة الى الدمالق, سحنة الحجر الجيري المرصوص-الحبيبي الحاملة للفتاتات الاحيائية و سحنة الحجر الجيري الحبيبي الحاملة للدمالق) قد ترسبت هذه السحنات في مدى واسع من البيئات تضمنت (بيئة البحر المفتوح, بيئة الشعاب الرودستية, البيئة الضحضاحية و البيئة العميقة و البيئة البحرية المحصورة)

تم حساب ودراسة الخصائص البتروفيزيائية للتكوين (حجم السجيل، المسامية بأنواعها والتشبع المائي) باستعمال برنامج (Tichloge ve.15) باستخدام المجسات المتوفرة مثل (مجس اشعة كاما، مجس الكثافة، مجس النيوترون، مجس الجهد الذاتي، المجس الصوتي ومجسات المقاومة) فقد تم تقسيم تكوين مشرف الى أربعة وحدات من الأعلى الى الأسفل (CR-I,MA,CR-II and MB) حيث كانت الوحدات المكمنية ذات مسامية عالية في اغلب الابار تفصل بينهم صخور صلبة ذات مسامية قليلة اما بالنسبة للتشبع المائي فكانت نسبته عالية في الصخور الصلبة وكانت نسبة الهيدروكربونات المتبقية و المتحركة عالية في وحدة MB و لبعض الابار فقط و كانت قليلة في الوحدة المكمنية MA.

في هذه الدراسة تم رسم الخرائط التركيبية وبناء الموديل الجيولوجي ثلاثي الابعاد لتوزيع الخصائص البتروفيزيائية التي تضمنت المسامية الكلية والمسامية الفعالة والتشبع المائي وكذلك توزيع السحنات

لتكوين المشرف تم كل ذلك باستعمال برنامج (Petrel ve.18) وتبين من خلال الموديل ان الخصائص البتروفيزيائية تتحسن في الابار الواقعة في اتجاه الابار (ER-1,4 and7) حيث تتحسن المواصفات السحنية ويكون التشبع النفطي عالي عند هذه الابار مقارنة بالإبار الأخرى للدراسة.

وفي نهاية الدراسة تم عمل تحليل طباقي على ضوء البيئات الرسوبية التي تم تمييزها من خلال معرفة السحنات الدقيقة للإبار التي تحتوي على لباب صخري حيث تم تمييز خمسة دورات رسوبية وهي (A,B,C,D. E) وتم تحديد تتابعين رئيسيين (SB1,SB2) بناءً على سلوكيات ارتباط السحنات ضمن حدود طبقات التتابع ومسارات (HST and TST

وزارة التعليم العالي والبحث العلمي
جامعة بابل
كلية العلوم
قسم علم الأرض التطبيقي

التحليل البتروفيزيائي والطباقي لتكوين مشرف في حقل اريدو النفطي جنوب العراق

رسالة مقدمة
الى مجلس كلية العلوم جامعة بابل
كجزء من متطلبات درجة الماجستير علوم
في علم الأرض

من قبل

شهد ليث عباس سعيد

بكالوريوس علم الأرض التطبيقي (٢٠٢٠)

بأشراف

أ.د عامر عطية لفتة الخالدي **أ.د حامد علي احمد السلطان**

١٤٤٤ هـ ٢٠٢٣م